




Universitat Autònoma de Barcelona

ADVERTIMENT. L'accés als continguts d'aquesta tesi queda condicionat a l'acceptació de les condicions d'ús establertes per la següent llicència Creative Commons:  http://cat.creativecommons.org/?page_id=184

ADVERTENCIA. El acceso a los contenidos de esta tesis queda condicionado a la aceptación de las condiciones de uso establecidas por la siguiente licencia Creative Commons:  <http://es.creativecommons.org/blog/licencias/>

WARNING. The access to the contents of this doctoral thesis it is limited to the acceptance of the use conditions set by the following Creative Commons license:  <https://creativecommons.org/licenses/?lang=en>



Renormalons, power corrections, Borel summation and hyperasymptotics

$$\sum_{n=0}^{\infty} (-1)^n = \frac{1}{2}$$

Author: Xabier Lobregat

Supervisor: Prof. Antonio Miguel Pineda Ruiz

A thesis submitted for the degree of

Ph.D. in physics

Bellaterra 2021

Un auteur ne nuit jamais tant à ses lecteurs que
quand il dissimule une difficulté.

Évariste Galois

Abbreviations

QCD Quantum chromodynamics

QED Quantum electrodynamics

HQET Heavy quark effective theory

NRQCD Non relativistic QCD

pNRQCD Potential non relativistic QCD

OPE Operator product expansion

PV Principal value

RG Renormalization group

EFT Effective field theory

LL Leading log

NLL Next-to leading log

NNLL Next-to-next-to leading log

NNNLL Next-to-next-to-next-to leading log

IR Infrared

UV Ultraviolet

RHS Right hand side

LHS Left hand side

LO Leading order

NLO Next-to leading order

NNLO Next-to-next-to leading order

NNNLO Next-to-next-to-next-to leading order

MC Monte Carlo

NSPT Numerical stochastic perturbation theory

Publications

Refereed articles

- **HQET renormalization group improved Lagrangian at $\mathcal{O}(1/m^3)$ with leading logarithmic accuracy: Spin-dependent case**
X. Lobregat, D. Moreno, R. Petrossian-Byrne
Phys. Rev. D **97**, 054018 (2018)
arXiv:1802.07767 [hep-ph]
- **Supersymptotic and hyperasymptotic approximation to the operator product expansion**
C. Ayala, X. Lobregat, A. Pineda
Phys. Rev. D **99**, 074019 (2019)
arXiv:1902.07736 [hep-th]
- **Hyperasymptotic approximation to the top, bottom and charm pole mass**
C. Ayala, X. Lobregat, A. Pineda
Phys. Rev. D **101**, 034002 (2020)
arXiv:1909.01370 [hep-ph]
- **Determination of $\alpha(M_z)$ from an hyperasymptotic approximation to the energy of a static quark-antiquark pair**
C. Ayala, X. Lobregat, A. Pineda
JHEP 09 (2020) 016
arXiv:2005.12301 [hep-ph]
- **Hyperasymptotic approximation to the plaquette and determination of the gluon condensate**
C. Ayala, X. Lobregat, A. Pineda
JHEP 12 (2020) 093
arXiv:2009.01285 [hep-ph]

Conference proceedings

- **Hyperasymptotic approximation to the operator product expansion**
C. Ayala, X. Lobregat, A. Pineda
QCD 19 Montpellier (France)
Nucl.Part.Phys.Proc. 309-311 (2020) 77-86
arXiv:1910.04090 [hep-ph]

Abstract

Perturbative series in QCD are expected to be divergent asymptotic expansions, and therefore, there is an intrinsic fuzzyness to the information that can be extracted from them. Consequently, many summation schemes can be defined to assign them a reasonable finite number, each with its advantages and disadvantages. This discussion is particularly relevant when one considers OPEs, where non-perturbative corrections are considered on top of a perturbative expansion. These non-perturbative corrections will intimately depend on how the divergent perturbative expansion is regulated.

In this dissertation, one summation scheme to regulate divergent series is explored: Borel summation with the PV prescription. Two different avenues to estimate the Borel sum from truncated versions of the perturbative expansions are presented. These methods are then applied to obtain the gluon condensate from the OPE of the plaquette, and the HQET power correction $\bar{\Lambda}$, both from the lattice and B physics. We also obtain a value for the QCD strong coupling $\alpha(M_z)$ from lattice data of the singlet static quark-antiquark energy making use of PV Borel sums.

Contents

1	Divergent series, asymptotic expansions and Borel summation	1
1.1	Introduction	1
1.2	Asymptotic expansions	2
1.3	Borel summation	4
1.4	Directional Borel sums, the discontinuity function and the principal value Borel sum	8
1.5	The large order behavior of perturbation theory	9
1.6	Superasymptotics	12
2	Renormalons	17
2.1	A first glimpse on renormalons	18
2.2	The u plane and the t plane	19
2.3	The Borel transform of the QCD singlet static potential in the large β_0 approximation	20
2.4	The Borel transform of the pole mass in the large β_0 approximation	22
2.5	The operator product expansion	23
2.6	The OPE and renormalons	25
2.7	Fixing the condensates from the OPE	29
3	Approximating the PV Borel sum: Method 1	31
3.1	Dingle's terminants	31
3.2	Examples	33
3.2.1	The Stieltjes function	33
3.2.2	A branch cut singularity in the Borel plane	34
3.2.3	The double Stieltjes function	34
3.3	Beyond the leading terminant	35
3.4	The hyperasymptotic expansion	36
3.4.1	The double Stieltjes function revisited	38
3.5	Terminants in QCD	40
3.6	The QCD singlet static potential in the large β_0 approximation	43
3.7	The pole mass in the large β_0 approximation	50

4	Approximating the PV Borel sum: Method 2	57
4.1	The method	58
4.1.1	Beyond one loop running in Eq. (4.19)	62
4.2	The QCD singlet static potential in the large β_0 approximation	62
4.2.1	Alternative method	64
4.3	The pole mass in the large β_0 approximation	67
4.4	Qualitative comparison with Method 1	68
5	Hyperasymptotics of the average plaquette and the gluon condensate	71
5.1	Gauge fields in the lattice, the plaquette and the Wilson action	71
5.2	The average plaquette and the gluon condensate	73
5.3	The hyperasymptotic expansion of the average plaquette	76
5.4	Error sources	78
5.5	The fits	82
5.5.1	Order $(0, N_P(4))$	82
5.5.2	Order $(4, 0)$	83
5.5.3	Order $(4, N')$	85
5.6	Some plots on the asymptotics of the series of the average plaquette	85
5.7	Final remarks	85
6	Hyperasymptotics of the heavy quark pole mass and $\bar{\Lambda}$	91
6.1	$\bar{\Lambda}_{PV}(n_f = 3)$ from B physics in the \overline{MS} scheme	91
6.1.1	Comparison with other works	94
6.1.1.1	The RS mass	94
6.1.1.2	The BR mass	95
6.1.1.3	The MRS mass	96
6.1.1.4	Determinations of $\bar{\Lambda}$	97
6.2	$\bar{\Lambda}_{PV}(n_f = 0)$ from the lattice scheme	97
6.2.1	The Polyakov loop and δm	98
6.2.2	Hyperasymptotics of δm_{PV}	98
6.2.3	Fits of $\bar{\Lambda}_{PV}$	99
6.2.4	Renormalon dominance and the beta function coefficients in the lattice	101
6.2.5	Fits in the \overline{MS} scheme	102
6.3	The PV Borel sum of the top quark pole mass	103
6.3.1	About the pole mass ambiguity	103
6.3.2	Decoupling and running	104
6.3.3	$ d = 2$ renormalons?	110

7	Hyperasymptotics of the static quark antiquark energy and $\alpha(M_z)$	113
7.1	Introduction	113
7.2	The singlet static energy and the multipole expansion	114
7.3	The singlet static potential	115
7.3.1	Resumming ultrasoft logarithms in the static potential	116
7.4	The ultrasoft energy	118
7.4.1	Expanding ΔV and V_A in δE_{us}	119
7.5	Cancellation of ν_{us} in $E(r)$	119
7.6	The singlet static energy revisited	120
7.7	Getting rid of the $u = 1/2$ renormalon	120
7.8	Taking an r derivative in $E(r)$	121
7.9	Hyperasymptotics and \mathcal{F}	123
7.10	The normalization of the $u = 3/2$ renormalon	124
7.11	The lattice data	126
7.12	The expressions that go on the fits	127
7.13	Central value results	128
7.13.1	Dependence on ν_s	132
7.13.2	Dependence on ν_{us}	134
7.13.3	Dependence on Z_3^F	135
7.13.4	Other estimates of higher order contributions	135
7.13.5	Dependence on r_{ref}	136
7.14	Final numbers	136
7.15	Comparison with fixed order computations	137
7.16	What if $\nu_s = \text{constant}$?	138
7.17	A nonperturbative $\frac{d}{dr}\delta E_{\text{us}}$	139
7.18	Comparison with earlier work	140
7.19	Final remarks	141
	Conclusions	143
A	The large β_0 approximation	145
B	Renormalization scale and scheme invariance of the PV Borel sum of an observable	149
B.1	On the renormalization scale dependence of perturbative expansions of observables	149
B.2	Renormalization scale invariance of the PV Borel sum	150
B.3	Renormalization scheme invariance of the PV Borel sum	153
C	The computation of $\Delta\Omega$	157
C.1	The IR case	157
C.1.1	An alternative method	159
C.2	The UV case	159

D	Further contributions from the Borel plane in Method 2	161
D.1	Subleading contributions from the leading IR renormalon	161
D.2	The analytic part of $\hat{R}(t)$	162
D.3	UV renormalons	162
D.4	Subleading IR renormalons	163
E	The computation of v_2	165
E.1	The $d = 1$, $\Delta = 1$ and $N = N_S$ case	165
E.1.1	The $\log N_S$ term	166
E.1.2	Wick rotating Ξ	167
E.1.2.1	The path C_ϵ	168
E.1.2.2	The path C_δ	168
E.1.2.3	The path C_R	168
E.1.2.4	The path C_I	168
E.1.2.5	Final result for Ξ	169
E.1.3	Wick rotating Φ	169
E.1.3.1	The path C_I	169
E.1.3.2	The path C	169
E.1.3.3	The path C_δ	169
E.1.3.4	Final result for Φ	170
E.1.4	Final result	170
E.2	The $d = 1$, $\Delta = 1 - c'\alpha(1/r)$ and $N = N_A$ case	170
E.2.1	Wick rotation	171
E.2.1.1	The path C_ϵ	172
E.2.1.2	The path C_R	172
E.2.1.3	The path C_δ	172
E.2.1.4	The path C_I	173
E.2.1.5	Final result for Υ	173
E.2.2	The $r \sim 0$ asymptotics	173
F	The pole mass of a quark	177
F.1	The bottom quark pole mass	177
F.2	Massive bottom and charm effects in the top quark pole mass	178
G	pNRQCD	181
H	The r derivative of the singlet static energy with $\nu_s = \frac{x_s}{r}$ and $\nu_{us} = x_{us} \frac{C_A \alpha(\nu_s)}{2r}$	183
	Bibliography	185

Chapter 1

Divergent series, asymptotic expansions and Borel summation

1.1 Introduction

Divergent series are the invention of the devil,
and it is shameful to base on them any
demonstration whatsoever.

Niels Henrik Abel

As Abel's quote suggests, divergent series have a history of suspicion surrounding them. When one first learns about infinite series, it is customary to spend a fair amount of time on convergence criteria and on computing convergence radii. It is then not without irony, how many of the most useful expansions that one encounters happen to be divergent, a fact that is very often not pointed out. Stirling's approximation to the factorial features a classical example. The well-known $n! \approx (2\pi n)^{1/2}(n/e)^n$ formula is nothing but the LO of the Stirling series

$$n! = (2\pi n)^{1/2} \left(\frac{n}{e}\right)^n \left\{ 1 + \frac{1}{12n} + \frac{1}{288n^2} - \frac{139}{51840n^3} - \frac{571}{2488320n^4} + \dots \right\}. \quad (1.1)$$

As illustrated in Figure 1.1, for a fixed value of n the expansion above will keep converging to the true value as we add more terms in the series, up until a point where it will start to diverge¹. This behavior of converging at first, only to end up diverging, is the hallmark of the so called *asymptotic expansions*, of which the Stirling series is but an example. We will see that asymptotic expansions give information about the behavior of a function when a variable tends to a certain value, but regardless of this, are not required to ultimately converge. Nonetheless, they remain useful in practice since by truncating them before they blow up, we can extract valuable information.

This discussion is particularly relevant for quantum field theories. The lack of analytic tools to deal with them in the non-perturbative regime has given perturbation theory an importance that cannot be overstated. Quite interestingly, and perhaps at first surprisingly, perturbative expansions in field theory are expected² to be divergent. The first person to appreciate that in QED perturbative expansions were very likely to be divergent was Freeman Dyson [1]. An account of this story by Dyson himself can be found here <https://www.youtube.com/watch?v=g2xLZ1z093g>.

In spite of all this, the fact that perturbative expansions in field theory have been so successful in accounting for experimental data clearly suggests that they are far from being useless expansions that add up to infinity.

¹The order in $1/n$ where the series starts to diverge depends on the value of n , for higher n more terms in the series can be kept.

²We use the word *expected* because there is no rigorous proof of this fact for non-trivial theories such as QCD.

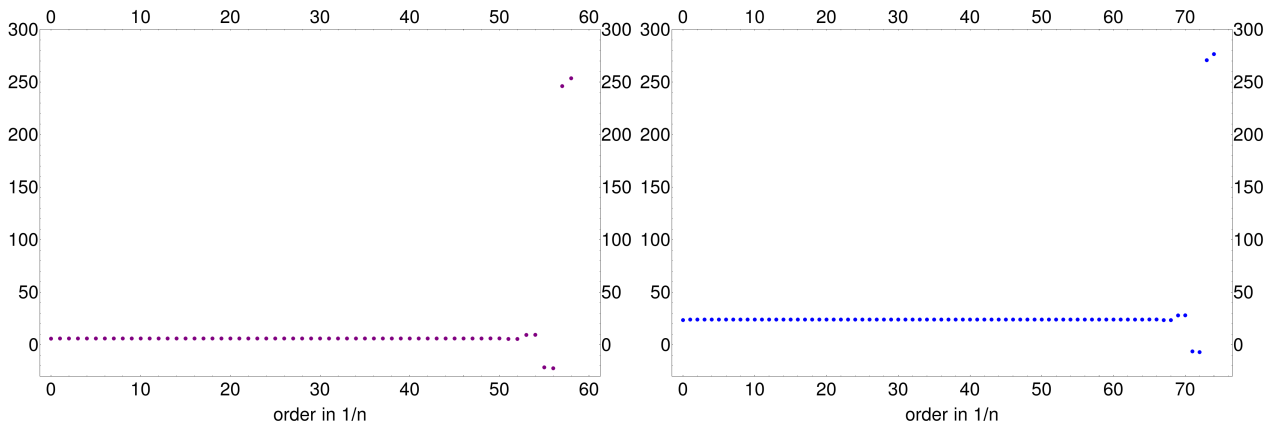


Figure 1.1: **Left panel** Eq. (1.1) with $n = 3$. **Right panel** Eq. (1.1) with $n = 4$. The horizontal axis displays the last order in $1/n$ kept inside braces in Eq. (1.1). In both cases, we see that at high orders the series begins to diverge.

Therefore, it is expected that, just like the Stirling series, these expansions are at least asymptotic expansions. Asymptotic expansions will play a very prominent role in this thesis, which is why we will precisely define this term in the next section.

1.2 Asymptotic expansions

The³ intuitive idea behind asymptotic expansions goes along these lines. Let us have a function f defined in some subset D of the complex plane that includes a point α_0 . Let f be analytic in D . Expanding this function in a Taylor expansion around α_0

$$f(\alpha) = \sum_{n=0}^N \frac{1}{n!} \frac{d^n}{d\alpha^n} f(\alpha) \Big|_{\alpha=\alpha_0} \times (\alpha - \alpha_0)^n + R_N(\alpha). \quad (1.2)$$

The error function $R_N(\alpha)$ satisfies that it goes to zero for a fixed N as $\alpha \rightarrow \alpha_0$. It also satisfies that $R_N(\alpha)$ goes to zero as $N \rightarrow \infty$ for values of α inside the convergence radius of the series above. If on the other hand, we had an asymptotic expansion of a function f , the error function would still go to zero for fixed N as $\alpha \rightarrow \alpha_0$, but this need not be the case for *fixed* α as $N \rightarrow \infty$. Therefore, asymptotic expansions can yield accurate predictions if truncated, but in general are not guaranteed to converge.

We will now rigorously define them. In order to properly be able to do that, we first need to introduce a few building blocks. As a starter, we need to define the so called *little-oh* notation. Let $f(\alpha)$ and $g(\alpha)$ be two complex valued functions defined in some subset D of the complex plane, whose closure contains a point α_0 (that is α_0 is a limit point of D). Then

$$f(\alpha) = o(g(\alpha)), \quad (1.3)$$

as $\alpha \rightarrow \alpha_0$ from D , if for any $\epsilon > 0$ there is a $\delta > 0$ such that

$$|f(\alpha)| \leq \epsilon |g(\alpha)|, \quad (1.4)$$

for α in D satisfying $0 < |\alpha - \alpha_0| < \delta$. That is, we can always find a region around α_0 which is contained in D , such that f is smaller in absolute value than *any* multiple of g . For instance, let n and m be integers satisfying

³This section is mainly based on [2].

$n > m$, then $\alpha^n = o(\alpha^m)$ as $\alpha \rightarrow 0$. We can also state an analogous definition at infinity. Let $f(\alpha)$ and $g(\alpha)$ be two complex valued functions defined in an unbounded subset D of the complex plane. Then

$$f(\alpha) = o(g(\alpha)) , \quad (1.5)$$

as $\alpha \rightarrow \infty$ from D , if for any $\epsilon > 0$ there is a $M > 0$ such that

$$|f(\alpha)| \leq \epsilon |g(\alpha)| , \quad (1.6)$$

for α in D satisfying $|\alpha| > M$. That is, we can always find a region in D with points α that are sufficiently far from the origin so that f is smaller in absolute value than *any* multiple of g . For instance, let m, n be integers satisfying $n > m$, then $\alpha^m = o(\alpha^n)$ for $\alpha \rightarrow \infty$.

Closely related to the little-oh notation, we have the *big-oh* notation. Whereas in the former case we demanded $|f(\alpha)| \leq \epsilon |g(\alpha)|$ for any $\epsilon > 0$, for the big-oh we will just require for there to be some $\epsilon > 0$ with an associated $\delta > 0$. We write this as

$$f(\alpha) = \mathcal{O}(g(\alpha)) , \quad (1.7)$$

as $\alpha \rightarrow \alpha_0$ from D . An analogous definition can be given at infinity.

We now need to define *asymptotic sequences*. Let $\{\phi_n(\alpha)\}_{n=0}^{\infty}$ be a sequence of complex functions defined on some subset D of the complex plane whose closure contains a point α_0 . This sequence is called an asymptotic sequence as $\alpha \rightarrow \alpha_0$ from D if whenever $n > m$, we have that

$$\phi_n(\alpha) = o(\phi_m(\alpha)) , \quad (1.8)$$

as $\alpha \rightarrow \alpha_0$ from D . That is, loosely speaking, we see that the functions on the sequence get smaller and smaller the further we go on the sequence. With obvious modifications, we can also define an analogous version when $\alpha \rightarrow \infty$. In perturbative QCD, we will mainly be concerned with the asymptotic sequence $\{\alpha^n\}_{n=0}^{\infty}$ as $\alpha \rightarrow 0$.

We are now in a position to state the definition of an asymptotic expansion. Let $\{\phi_n(\alpha)\}_{n=0}^{\infty}$ be an asymptotic sequence as $\alpha \rightarrow \alpha_0$ from some D . Let $f(\alpha)$ be a complex function defined on D . Let $\{a_n\}_{n=0}^{\infty}$ be a sequence of complex numbers. Let

$$f(\alpha) - \sum_{n=0}^N a_n \phi_n(\alpha) = o(\phi_N(\alpha)) , \quad (1.9)$$

or equivalently

$$f(\alpha) - \sum_{n=0}^N a_n \phi_n(\alpha) = \mathcal{O}(\phi_{N+1}(\alpha)) , \quad (1.10)$$

as $\alpha \rightarrow \alpha_0$ from D for each integer $N > 0$. Then, the formal series

$$\sum_{n=0}^{\infty} a_n \phi_n(\alpha) , \quad (1.11)$$

is said to be an asymptotic expansion of f as $\alpha \rightarrow \alpha_0$ from D . This is typically denoted as

$$f(\alpha) \sim \sum_{n=0}^{\infty} a_n \phi_n(\alpha) . \quad (1.12)$$

With obvious changes, an analogous version at infinity can be given. The term *formal series* has been used to denote Eq. (1.11) because the series displayed there in general need not be convergent. We will in the following section say a few more things about formal series. There are some important facts about asymptotic expansions that are useful to keep in mind:

- a) A function $f(\alpha)$ can have several asymptotic expansions with respect to different asymptotic sequences. In practice though, we will not care about this much since, as we have already mentioned, in perturbative QCD we will mainly be concerned with the asymptotic sequence $\{\alpha^n\}_{n=0}^\infty$.
- b) If a function has an asymptotic expansion to a given asymptotic sequence, then this expansion is unique.
- c) Two different functions can both have the same asymptotic expansion.

This last one is easy to illustrate. Let us have some function f defined around the origin with the asymptotic expansion

$$f(\alpha) \sim \sum_{n=0}^{\infty} a_n \alpha^n. \quad (1.13)$$

Then, we will also have

$$f(\alpha) + e^{-1/\alpha} \sim \sum_{n=0}^{\infty} a_n \alpha^n, \quad (1.14)$$

that is, the new non-analytic term $e^{-1/\alpha}$ is not seen by a small α expansion. There is one last interesting property we want to highlight:

- d) Let us have an asymptotic sequence $\{\phi_n(\alpha)\}_{n=0}^\infty$ as $\alpha \rightarrow \alpha_0$ from D . Let us consider an *arbitrary* sequence of complex numbers $\{a_n\}_{n=0}^\infty$. Then, there will exist at least one function $f(\alpha)$ defined for $\alpha \in D$ with $\alpha \neq \alpha_0$ such that

$$f(\alpha) \sim \sum_{n=0}^{\infty} a_n \phi_n(\alpha), \quad (1.15)$$

that is, given an asymptotic sequence and any sequence of complex numbers, without setting any constraint to how wildly they may grow with n , there is always a function to which the formal series above will be asymptotic.

1.3 Borel summation

In this section⁴, we will introduce Borel summation, and we will see its connection to asymptotic expansions. Let us consider the series that appears in the cover of this thesis

$$\sum_{n=0}^{\infty} (-1)^n. \quad (1.16)$$

This series oscillates indefinitely between 0 and 1, and it is clear that it does not converge to a sum in the conventional sense of the word. Nevertheless, we could try to bypass this issue by defining a generalized sum that may indeed assign a finite number for a conventionally divergent series. Let us call s to this would be sum

$$s = \sum_{n=0}^{\infty} (-1)^n. \quad (1.17)$$

Notice that in the equation above, the symbol $=$ is meant to imply equality with respect to our generalized concept of sum. We could ask to this generalized sum to reasonably satisfy the following properties⁵

⁴This section draws mainly from [3, 4].

⁵These constraints seem reasonable for the concept of a generalized sum, and many summation methods satisfy them, but not all summation methods satisfy them all. For more details see [4]. For instance, Borel summation (which will be our focus) satisfies the first three but not necessarily the last.

1. If $\sum_{n=0}^{\infty} a_n = s$, then $\sum_{n=0}^{\infty} ka_n = ks$.
2. If $\sum_{n=0}^{\infty} a_n = s$ and $\sum_{n=0}^{\infty} b_n = t$, then $\sum_{n=0}^{\infty} (a_n + b_n) = s + t$.
3. If $\sum_{n=1}^{\infty} a_n = s - a_0$, then $\sum_{n=0}^{\infty} a_n = s$.
4. If $\sum_{n=0}^{\infty} a_n = s$, then $\sum_{n=1}^{\infty} a_n = s - a_0$.

Then, by virtue of property 1 above

$$\sum_{n=0}^{\infty} -1 \times (-1)^n = -s. \quad (1.18)$$

By performing a simple summation index redefinition

$$-s = \sum_{n=0}^{\infty} -1 \times (-1)^n = \sum_{n=1}^{\infty} (-1)^n. \quad (1.19)$$

From property (3)

$$\sum_{n=0}^{\infty} (-1)^n = \sum_{n=1}^{\infty} (-1)^n + 1 = -s + 1, \quad (1.20)$$

but the LHS above is the original series, and therefore

$$s = -s + 1 \implies s = 1/2, \quad (1.21)$$

and we see that our generalized sum for the series in Eq. (1.16) is $s = 1/2$. In this simple example, the knowledge of some properties that we have asked s to satisfy has been enough to obtain a generalized sum for the series in question, without actually defining the summation procedure, but for more complicated divergent series things are not that simple. There are many summation methods for divergent series that allow us to assign a finite number to them that satisfies some properties that are reasonable for the concept of a generalized sum, and that in addition, reproduce the usual sum for convergent infinite series. A thorough exposition can be found in [4].

In this thesis, we will be concerned with Borel summation. We will define Borel summation on formal series, so before defining it, we will mention a few elementary remarks on formal series, and then we will go on to define Borel summation and its relation to asymptotic expansions. The space of all formal complex power series series in α is denoted by

$$\mathbb{C}[[\alpha]] = \left\{ \sum_{n=0}^{\infty} a_n \alpha^n, \text{ for any } a_0, a_1, \dots \in \mathbb{C} \right\}. \quad (1.22)$$

This set is a complex vector space, with addition of two formal series defined in the following way

$$\sum_{n=0}^{\infty} a_n \alpha^n + \sum_{n=0}^{\infty} b_n \alpha^n \equiv \sum_{n=0}^{\infty} (a_n + b_n) \alpha^n. \quad (1.23)$$

The product of a formal series in $\mathbb{C}[[\alpha]]$ with a complex number is done by multiplying each element in the series by the complex number

$$k \sum_{n=0}^{\infty} a_n \alpha^n \equiv \sum_{n=0}^{\infty} ka_n \alpha^n. \quad (1.24)$$

It also makes sense to multiply two formal series by the so called Cauchy product

$$\left(\sum_{n=0}^{\infty} a_n \alpha^n \right) \cdot \left(\sum_{n=0}^{\infty} b_n \alpha^n \right) \equiv \sum_{n=0}^{\infty} c_n \alpha^n, \quad (1.25)$$

where $c_n = \sum_{p+q=n} a_p b_q$, which actually makes $\mathbb{C}[[\alpha]]$ into an algebra. We emphasize that when doing algebra with formal series, the $=$ symbol does not indicate numerical equality (as in general these series need not be convergent), but rather, equality of all the coefficients of the series on the RHS and on the LHS with respect to the algebraic rules defined above. We will typically work with formal series without a constant term⁶. The space of all such formal series is called $\alpha\mathbb{C}[[\alpha]]$. Let R be a formal power series without a constant term

$$R \equiv \sum_{n=0}^{\infty} r_n \alpha^{n+1}. \quad (1.26)$$

We can then define the Borel transform \hat{R} of the power series in equation (1.20) as the following power series

$$\hat{R}(t) = \sum_{n=0}^{\infty} \frac{r_n}{n!} t^n, \quad (1.27)$$

where t is a complex variable. In mathematical jargon, we would say that the Borel transform is a linear isomorphism between $\alpha\mathbb{C}[[\alpha]]$ and $\mathbb{C}[[t]]$. Some remarks on notation. In the QCD literature it is customary to denote the Borel transform of R as $B[R](t)$. In most of this thesis⁷, we will use the more minimalistic notation found for instance in [3], and denote the Borel transform of the formal series R simply by a hat $\hat{R}(t)$.

It can be proven that the Borel transform has an infinite radius of convergence, and defines an entire function of bounded exponential type (that is, that there exist $A, c > 0$ such that $|\hat{R}(t)| \leq Ae^{c|t|}$ for all $t \in \mathbb{C}$) if and only if $|r_n| \leq Ac^n$ (which actually notice that implies that R is convergent with a radius of convergence of $1/c$). We state this fact for completeness, as the series we will find in QCD are not expected to grow at most as c^n , but rather as $c^n n!$.

These formal series that grow at most factorially are called 1-Gevrey formal series. Being more precise, let $R = \sum_{n=0}^{\infty} r_n \alpha^{n+1}$. This series is called a 1-Gevrey formal series if there exist $A, c > 0$, such that $|r_n| \leq Ac^n n!$. It can then be proven⁸ that \hat{R} has a finite radius of convergence of $1/c$. The reverse also holds, that is, Borel transforms with finite radius of convergence correspond to 1-Gevrey formal series⁹. It can be seen that the set of all 1-Gevrey formal series makes up a vector space on its own.

In order to define the Borel sum of R , one then consider the analytic continuation \hat{R}_{an} in some region of the complex t plane of \hat{R} . For 1-Gevrey formal series, this function is in general expected to have singularities in the t plane. By an abuse of notation, it is common practice to also call the analytically continued Borel transform the Borel transform, and to even use the same symbol \hat{R} to denote it. Usually, one can unambiguously deduce from the context to which object we are referring to, so we will also interchangeably refer to both the power series in Eq. (1.27) and to its analytic continuation as the Borel transform.

⁶There is no loss of generality here since, if we indeed had a series with a constant term, we could always leave it out and consider Borel summation in the series that begins at order α . Nevertheless, if for whatever reason we insist on working with series with a constant term, this can be done. See for instance [3].

⁷There is one caveat that should be mentioned. In section 2.2, we will see that in the QCD literature it is common to work in the complex u plane defined by Eq. (2.15), and thus, we will denote a slightly altered version of Eq. (1.27) with $B(u)$.

⁸Just take the ratio test: $\lim_{n \rightarrow \infty} \left| \frac{r_{n+1}/(n+1)!t^{n+1}}{r_n/n!t^n} \right| = c|t| < 1 \implies |t| < 1/c$.

⁹Assume the opposite, that is, assume $\hat{R}(t) = \sum_{n=0}^{\infty} \frac{r_n}{n!} t^n$ has a finite radius of convergence, and that there is no $A, c > 0$ such that $|r_n| \leq Ac^n n!$. Then, for any and all $A, c > 0$, the fixed order term of the series of the Borel transform satisfies $|\frac{r_n}{n!} t^n| > Ac^n |t|^n$. Let us pick a t inside the radius of convergence, and let us also pick $c > |t|$. Then, for $n \rightarrow \infty$, $|\frac{r_n}{n!} t^n| > Ac^n |t|^n$ implies that the (absolute value of the) fixed order term of the series of the Borel transform goes to infinity, which contradicts that t lies inside the radius of convergence.

The *Borel sum* of the formal series R is then defined as the Laplace transform of the analytically continued Borel transform

$$R_{\text{BS}} \equiv \int_0^\infty dt e^{-t/\alpha} \hat{R}(t). \quad (1.28)$$

Recall that the Laplace transform above is well defined if \hat{R} is continuous in \mathbb{R}^+ and if

$$|\hat{R}(t)| \leq Ae^{\omega t}, \quad \text{for } t \geq 1, \quad (1.29)$$

for some $A > 0$ and $\omega \in \mathbb{R}$. Then, the Borel sum is analytic in the complex α plane in the region $\{\alpha \in \mathbb{C} : \text{Re}(1/\alpha) > \omega\}$. Now comes the important statement: it can be seen that the original formal series R is an asymptotic expansion¹⁰ of $R_{\text{BS}}(\alpha)$ as $\alpha \rightarrow 0$.

$$R_{\text{BS}}(\alpha) \sim \sum_{n=0}^{\infty} r_n \alpha^{n+1}. \quad (1.30)$$

This is just Watson's lemma for the case of the Borel sum. Thus, we see that by starting off with a formal series, we construct a function, the Borel sum, such that the original formal series is an asymptotic expansion of this function. Borel summation [5] is a well known method¹¹ to sum divergent series. It satisfies properties 1,2 and 3 of the beginning of this section, but not the fourth [4]. Moreover, it can be seen that if R converges, we have that $R = R_{\text{BS}}$, a property known as regularity of the summation method [4].

A heuristic argument motivating the connection between the Borel sum and the formal series R is that if one inserts the Borel transform written as a power expansion in t as in Eq. (1.27), and commutes with impunity sum and integral (even though we may be integrating outside the radius of convergence of the power series), the original formal series R is recovered

$$\int_0^\infty dt e^{-t/\alpha} \sum_{n=0}^{\infty} \frac{r_n}{n!} t^n \rightarrow \sum_{n=0}^{\infty} \frac{r_n}{n!} \int_0^\infty dt e^{-t/\alpha} t^n = \sum_{n=0}^{\infty} r_n \alpha^{n+1}. \quad (1.31)$$

To illustrate the method, let's consider again the series of the beginning of this section Eq. (1.16)

$$R = \sum_{n=0}^{\infty} (-1)^n. \quad (1.32)$$

The Borel transform is clearly¹² (we may consider the series above as a power series with $\alpha = 1$).

$$\hat{R}(t) = \sum_{n=0}^{\infty} \frac{(-1)^n}{n!} t^n = e^{-t}. \quad (1.33)$$

Therefore, the Borel sum is

$$R_{\text{BS}} = \int_0^\infty dt e^{-t} e^{-t} = \frac{1}{2}, \quad (1.34)$$

which is the same sum we obtained before¹³.

¹⁰In this case, $\{\alpha^n\}_{n=0}^\infty$ is the asymptotic sequence considered, and D is the set where the Borel sum has been said to be analytic.

¹¹In fact, there are two methods to sum divergent series due to Borel, the one we have just mentioned which is known as the integral summation method, and a so-called exponential summation method. Nevertheless, it can be seen that the integral method is stronger in the sense that both methods agree on the sum whenever a formal series is summable by the two methods, but the integral method can sum all the functions the exponential method can and more. For more details see [4].

¹²Notice that the Borel transform is entire and of bounded exponential type, but there is no contradiction with the fact that R above is divergent. In this example $R = \sum_{n=0}^\infty (-1)^n \alpha^{n+1}$ which is convergent only for $\alpha < 1$, and we are considering the $\alpha = 1$ case.

¹³This hardly comes as a surprise, as the method of Borel summation satisfies properties 1 and 3 of the beginning of this section which have allowed us deduce the value $1/2$.

1.4 Directional Borel sums, the discontinuity function and the principal value Borel sum

In the previous section¹⁴, we have introduced Borel sums as a summation method for divergent series. This procedure involves an integral in the positive real line. Unfortunately, in QCD one expects to find singularities in the integration path of Eq. (1.28) [7], and one cannot perform the integral present in the Laplace transform of the analytically continued Borel transform. To circumvent this problem, other paths of integration where the Borel transform doesn't have singularities are considered. This leads us to define the *lateral Borel sums* as

$$R_{\pm} \equiv \int_{C_{\pm}} dt e^{-t/\alpha} \hat{R}(t) = e^{\pm i\eta} \int_0^{\infty} dx e^{-\frac{x e^{\pm i\eta}}{\alpha}} \hat{R}(x e^{\pm i\eta}), \quad (1.35)$$

where the paths of integration C_{\pm} are parametrized by $t = x e^{\pm i\eta}$. Even if all the coefficients r_n of the original formal series of Eq. (1.26) are real, lateral Borel sums are in general complex. Actually, R_+ and R_- only differ by an imaginary part that has a different sign for each lateral Borel sum (when $\eta \rightarrow 0$). This imaginary part that would be absent in a Borel sum along the positive real line is what sometimes is called the *ambiguity* of the formal series R . The idea is that in the presence of singularities in the integration path, we can only define the Borel sum up to this ambiguous term, that makes the Borel sum itself ambiguous. We can isolate this imaginary part by taking the difference of both lateral sums

$$\text{disc}(R) \equiv \lim_{\eta \rightarrow 0^+} \left\{ \int_{C_+} dt e^{-t/\alpha} \hat{R}(t) - \int_{C_-} dt e^{-t/\alpha} \hat{R}(t) \right\}. \quad (1.36)$$

The function $\text{disc}(R)$ above is called *the discontinuity function*. This function is a non-analytic exponentially suppressed function in α . The strength of the suppression is related to the location of the singularity of \hat{R} that is closest to the origin in the t plane. For instance, if $t = A$ where $A > 0$

$$\text{disc}(R) = e^{-\frac{A}{\alpha}} \times (\dots). \quad (1.37)$$

We will see in Eq. (2.91) an example of a discontinuity function for the case of a branch point singularity in the Borel plane. The non analytic term $e^{-\frac{A}{\alpha}}$ is reminiscent of a non-perturbative term which hints to a connection between perturbative and non-perturbative sectors. This connection is captured in the resurgent approach to field theory, which we will very briefly mention in section 2.6.

Coming back to physics for a while, let's consider the perturbative expansion of the QCD singlet static potential, whose Borel transform's singularity that happens to be closest to the origin is located at¹⁵ [8]

$$t = \frac{2\pi}{\beta_0}, \quad (1.38)$$

where β_0 is the first coefficient of the perturbative expansion of the beta function. In this thesis, we follow the convention

$$\mu \frac{d}{d\mu} \alpha(\mu) = \beta(\alpha) = -2\alpha(\mu) \sum_{j=0}^{\infty} \frac{\beta_j}{(4\pi)^{j+1}} \alpha^{j+1}(\mu), \quad (1.39)$$

where in particular, $\beta_0 = 11 - \frac{2}{3}n_f$ and $\beta_1 = 102 - \frac{38}{3}n_f$. Then, the discontinuity function is

$$\text{disc}(R) = e^{-\frac{2\pi}{\beta_0\alpha}} \times (\dots) = \Lambda_{\text{QCD}} \times (\dots), \quad (1.40)$$

¹⁴This section draws mainly from [6].

¹⁵We will see this proven in the large β_0 approximation in section 2.3.

which is what prompts the often mentioned statement that the ambiguity of the Borel sum of the static potential is of order Λ_{QCD} .

Since both lateral Borel sums differ by an imaginary constant, we can define a real term by taking the averaged sum of both. This is the *principal value* Borel sum (PV Borel sum for short)

$$R_{\text{PV}} \equiv \frac{1}{2} \lim_{\eta \rightarrow 0^+} \left\{ \int_{C_+} dt e^{-t/\alpha} \hat{R}(t) + \int_{C_-} dt e^{-t/\alpha} \hat{R}(t) \right\}. \quad (1.41)$$

We will also sometimes use the notation

$$R_{\text{PV}} \equiv \text{PV} \int_0^\infty dt e^{-t/\alpha} \hat{R}(t), \quad (1.42)$$

or

$$R_{\text{PV}} \equiv \text{PV} \sum_{n=0}^{\infty} r_n \alpha^{n+1}. \quad (1.43)$$

This object will have a very prominent role in this thesis. We will further on see two methods to compute it from truncated versions of Eq. (1.26), and use it for various purposes in subsequent chapters. We will see in Appendix B that by assuming some properties of \hat{R}_{an} , the PV Borel sum of a formal series that is formally renormalization scale and scheme independent is renormalization scale and scheme independent. This is in contrast to what happens to truncated versions of Eq. (1.26), which (when truncated at order $\alpha^N(\mu)$) have a $\mathcal{O}(\alpha^{N+1}(\mu))$ dependence in the scale and the scheme (for more details see Appendix B).

1.5 The large order behavior of perturbation theory

In the previous section, we have seen that in general we expect singularities in the Borel transforms of perturbative expansions in QCD. In this section, we will see that the large order behavior of the coefficients r_n of Eq. (1.26) is intimately related to singularities in the t plane of the Borel transform in Eq. (1.27).

This idea stems from an old theorem by Darboux [9] that links the large order behavior of the coefficients of the Taylor expansion of a function that is analytic around the origin with its singularities in the complex plane. This theorem can be applied to 1-Gevrey divergent series, once one realizes their Borel transforms do have a finite radius of convergence, which allows us to apply the theorem to their coefficients, which are straightforwardly related to the coefficients of the original series by a factorial [10].

Let us be more explicit. Let us consider a complex function f defined in some subset of the complex plane that is analytic in an open ball around the origin, but that has singularities in the complex plane. The singularity that lies closest to the origin will be called t_i . Let the Taylor expansion around $t = 0$ of f be

$$f(t) = \sum_{n=0}^{\infty} a_n t^n. \quad (1.44)$$

Now, let's consider another function g that has the same singularity at t_i in the sense that $f - g$ is not singular at this point. Let the Taylor expansion around $t = 0$ of g be

$$g(t) = \sum_{n=0}^{\infty} b_n t^n. \quad (1.45)$$

Then, it can be proven that [11]

$$a_n = b_n + o(|t_i|^{-n}). \quad (1.46)$$

Thus, we see that the large n behavior of the coefficients a_n is dictated by the coefficients b_n of the Taylor expansion of g . We will apply this method to the Borel transform Eq. (1.27) of the formal series Eq. (1.26), so that $f = \hat{R}$. Then, one would have

$$a_n = \frac{r_n}{n!}, \quad (1.47)$$

and by Eq. (1.46), we can easily obtain the large n behavior of r_n . In this thesis, we will be concerned with Borel transforms whose behavior around its singularities located at the points t_i is of the form

$$\hat{R}_{\text{sing}}(t) = Z \frac{1}{(1-t/t_i)^s} \sum_{j=0}^{\infty} w_j (1-t/t_i)^j, \quad (1.48)$$

for some Z, w_j, s . Therefore, our choice for g will simply be

$$g(t) = Z \frac{1}{(1-t/t_i)^s} \sum_{j=0}^{\infty} w_j (1-t/t_i)^j. \quad (1.49)$$

The form b_n takes for such a g is readily obtained by noticing that at $t = 0$, we can Taylor expand

$$\frac{(1-t/t_i)^j}{(1-t/t_i)^s} = \sum_{n=0}^{\infty} \frac{\Gamma(n+s-j)}{\Gamma(s-j)\Gamma(n+1)} \frac{1}{t_i^n} t^n. \quad (1.50)$$

This immediately leads to

$$b_n = Z \frac{1}{t_i^n} \sum_{j=0}^{\infty} w_j \frac{\Gamma(n+s-j)}{\Gamma(s-j)\Gamma(n+1)}. \quad (1.51)$$

It can be easily seen that each subsequent term in the j expansion above goes like n^{-j} , and is thus, less and less important for large n . In order to make this explicit, we just have to factor out¹⁶ the gamma function in Eq. (1.51)

$$b_n = Z \frac{1}{t_i^n} \frac{\Gamma(n+s)}{\Gamma(s)\Gamma(n+1)} \sum_{j=0}^{\infty} w_j \prod_{k=1}^j \frac{(s-k)}{(n+s-k)}. \quad (1.52)$$

At long last, combining Eqs. (1.47) and (1.46) with Eqs. (1.51) and (1.52)

$$r_n \rightarrow Z \frac{1}{t_i^n} \sum_{j=0}^{\infty} w_j \frac{\Gamma(n+s-j)}{\Gamma(s-j)}, \quad (1.53)$$

or alternatively

$$r_n \rightarrow Z \frac{1}{t_i^n} \frac{\Gamma(n+s)}{\Gamma(s)} \sum_{j=0}^{\infty} w_j \prod_{k=1}^j \frac{(s-k)}{(n+s-k)}. \quad (1.54)$$

Notice that the closer the singularity lies in the Borel plane, its contribution to the large n asymptotics of r_n will be more important (as long as s doesn't change the picture of course) due to the $1/t_i^n$ suppression. Nonetheless, it must be mentioned that, even though the former statement is true as $n \rightarrow \infty$, in some cases it is possible that the residue Z of some singularities to be suppressed (or enhanced) for whatever reason, and that it may happen that a singularity that lies further from the origin dominates a singularity that lies closer, for some values of n where naively¹⁷ you would expect this not to be the case. We will see this happening in section 3.7 for the pole mass in the large β_0 approximation.

So far, we have computed the large order behavior of the coefficients of a formal series whose leading singularity in the Borel plane is given by Eq. (1.48), but no mention to physics has been done. In QCD, we will expect this

¹⁶Keep in mind that $\prod_a^b(\dots) = 1$ if $b < a$.

¹⁷Using the arguments we will review in section 1.6.

behavior in the Borel plane, so the results of Eqs. (1.53) and (1.54) still apply, but there is an additional feature that deserves mention. Let us consider the formal series computed using perturbative QCD of a quantity that has zero mass dimensions (for instance, if we had the QCD static potential V in mind, we would consider rV)

$$R = \sum_{n=0}^{\infty} r_n(\mu) \alpha^{n+1}(\mu), \quad (1.55)$$

where we have made explicit the dependence on μ , the renormalization scale. We will now prove that if the large order asymptotics of $r_n(\mu)$ for $\mu = Q$, where Q is some external scale¹⁸, is given by Eqs. (1.53) and (1.54), then for arbitrary μ we need to perform the replacement

$$Z \rightarrow Z \left(\frac{\mu}{Q} \right)^d, \quad (1.56)$$

where the singularity in the t plane of the Borel transform of Eq. (1.55) is located at $t_i = \frac{2\pi d}{\beta_0}$. At this point, d can be an arbitrary complex number, but in the next chapter, we will see that in fact, we will be interested in positive and negative integer values. We will later call the constant Z the normalization of the renormalon. Let us consider first the formal series in Eq. (1.55), where the renormalization scale takes the value $\mu = Q$.

$$R = \sum_{n=0}^{\infty} r_n(Q) \alpha^{n+1}(Q). \quad (1.57)$$

As we have said, we assume the singularity of the Borel transform of the series above to be located at $t_i = \frac{2\pi d}{\beta_0}$, and to be given by Eq. (1.48). Therefore, the large order asymptotics of the coefficients of the series above is simply given by either Eq. (1.53) or Eq. (1.54). Keeping this in mind, we consider the relation between $\alpha(Q)$ and $\alpha(\mu)$

$$\alpha(Q) = \frac{\alpha(\mu)}{1 + \alpha(\mu) \frac{\beta_0}{2\pi} \log \left(\frac{Q}{\mu} \right)}, \quad (1.58)$$

where we have considered the one loop relation for simplicity. Making use of the equation above, we re-expand Eq. (1.57) in terms of $\alpha(\mu)$

$$\sum_{n=0}^{\infty} r_n(\mu) \alpha^{n+1}(\mu) = \sum_{n=0}^{\infty} r_n(Q) \frac{\alpha^{n+1}(\mu)}{\left(1 + \alpha(\mu) \frac{\beta_0}{2\pi} \log \left(\frac{Q}{\mu} \right) \right)^{n+1}} \quad (1.59)$$

$$= \sum_{n=0}^{\infty} \sum_{m=0}^{\infty} r_n(Q) \binom{-n-1}{m} \frac{\beta_0^m}{(2\pi)^m} \log^m \left(\frac{Q}{\mu} \right) \alpha^{n+m+1}(\mu). \quad (1.60)$$

where $\binom{a}{b}$ is a binomial coefficient¹⁹. Changing the summation index above to $j = n + m$, and renaming after $j \rightarrow n$, we get

$$\sum_{n=0}^{\infty} r_n(\mu) \alpha^{n+1}(\mu) = \sum_{n=0}^{\infty} \sum_{m=0}^n r_{n-m}(Q) \binom{-n-1+m}{m} \frac{\beta_0^m}{(2\pi)^m} \log^m \left(\frac{Q}{\mu} \right) \alpha^{n+1}(\mu), \quad (1.61)$$

where we have defined $r_{\text{negative}} \equiv 0$. Thus, we can write

$$r_n(\mu) = \sum_{m=0}^n r_{n-m}(Q) \binom{-n-1+m}{m} \frac{\beta_0^m}{(2\pi)^m} \log^m \left(\frac{Q}{\mu} \right). \quad (1.62)$$

¹⁸For example, typically $Q = 1/r$ for the static potential.

¹⁹The binomial formula for negative exponents is defined by $\binom{-N}{k} = (-1)^k \binom{N+k-1}{k}$, with $N > 0$ and $k \geq 0$, where $\binom{a}{b} = \frac{a!}{b!(a-b)!}$ for $a, b \geq 0$.

We are interested in the large n asymptotics of the equation above. In order to obtain that, we will substitute the large order behavior of the coefficients $r_j(Q)$ that we already know from Eqs. (1.53) and (1.54). Thus, we get

$$r_n^{(\text{as})}(\mu) = Z \frac{1}{t_i^n} \sum_{j=0}^{\infty} w_j \frac{1}{\Gamma(s-j)} \sum_{m=0}^n \Gamma(n-m+s-j) \binom{-n-1+m}{m} d^m \log^m \left(\frac{Q}{\mu} \right). \quad (1.63)$$

Noting

$$\Gamma(n-m+s-j) = \Gamma(n+s-j) \prod_{l=1}^m \frac{1}{n+s-j-l}, \quad (1.64)$$

we can further write

$$r_n^{(\text{as})}(\mu) = Z \frac{1}{t_i^n} \sum_{j=0}^{\infty} w_j \frac{\Gamma(n+s-j)}{\Gamma(s-j)} \sum_{m=0}^n d^m \log^m \left(\frac{Q}{\mu} \right) \binom{-n-1+m}{m} \prod_{l=1}^m \frac{1}{n+s-j-l}. \quad (1.65)$$

Expanding for large n

$$\binom{-n-1+m}{m} \prod_{l=1}^m \frac{1}{n+s-j-l} = \frac{(-1)^m}{m!} + \mathcal{O}(n^{-1}), \quad (1.66)$$

we see that Eq. (1.65) becomes

$$r_n^{(\text{as})}(\mu) = Z \frac{1}{t_i^n} \sum_{j=0}^{\infty} w_j \frac{\Gamma(n+s-j)}{\Gamma(s-j)} \sum_{m=0}^n \left\{ \frac{\left[-d \log \left(\frac{Q}{\mu} \right) \right]^m}{m!} + \mathcal{O}(n^{-1}) \right\}. \quad (1.67)$$

Thus, we see that when we consider the large n asymptotics of the expression above, the logs add up to an exponential, so for $n \sim \infty$ we write

$$r_n^{(\text{as})}(\mu) = Z \left(\frac{\mu}{Q} \right)^d \frac{1}{t_i^n} \sum_{j=0}^{\infty} w_j \frac{\Gamma(n+s-j)}{\Gamma(s-j)}. \quad (1.68)$$

The equation above is the generalization of Eq. (1.53) for arbitrary μ . We can also write Eq. (1.54) for a general value of μ in a similar fashion

$$r_n^{(\text{as})}(\mu) = Z \left(\frac{\mu}{Q} \right)^d \frac{1}{t_i^n} \frac{\Gamma(n+s)}{\Gamma(s)} \sum_{j=0}^{\infty} w_j \prod_{k=1}^j \frac{(s-k)}{(n+s-k)}. \quad (1.69)$$

As it has already been mentioned, we will later be interested in singularities in the t plane parametrized by positive and negative integer values of d . The ones with positive (negative) d will be called IR (UV) renormalons. It is worth noticing that for IR renormalons, we will have the factor

$$\left(\frac{\mu}{Q} \right)^{|d|}, \quad (1.70)$$

whereas for UV renormalons, we will instead have

$$\left(\frac{Q}{\mu} \right)^{|d|}. \quad (1.71)$$

1.6 Supersymptotics

Let us consider again the formal series

$$R = \sum_{n=0}^{\infty} r_n \alpha^{n+1}, \quad (1.72)$$

and let's assume that it is asymptotic to some function $f(\alpha) \sim \sum_{n=0}^{\infty} r_n \alpha^{n+1}$ for $\alpha \rightarrow 0$. It has already been stated that for a fixed truncation point, the truncated R series will converge to the value given by f for small values of α . One may wonder which is the best truncation point, so that, for a given fixed small value of α , the error committed is the smallest. In order to answer this, let us consider the (absolute value of the) fixed order term

$$|r_n \alpha^{n+1}|, \quad (1.73)$$

where r_n grows factorially in n . For a fixed small value of α , this fixed order term becomes smaller and smaller as n gets bigger due to the power suppression in α^{n+1} . However, eventually, no matter how small α may be, the factorial growth in r_n will overpower the power suppression, and the fixed order term will reach a minimum, and will boundlessly grow henceforth. This behavior can be illustrated in the simple example of the series

$$\sum_{n=0}^{\infty} (-1)^n n! \alpha^{n+1}. \quad (1.74)$$

This series is an asymptotic expansion of the function $\alpha S(\alpha)$ where

$$S(\alpha) \equiv \int_0^{\infty} dx e^{-x} \frac{1}{1 + \alpha x}, \quad (1.75)$$

is the Stieltjes function. Figure 1.2 depicts the behavior of the fixed order term for this series for $\alpha = 1/10$, as well as the behavior of the truncated series for various orders of truncation. As it can be seen, the fixed order term seems to converge around $n = 10$, and explodes a few orders later. The same behavior is exhibited by the truncated asymptotic expansion. The prediction becomes stable around the orders on which the fixed order term is minimal, and afterwards, the series diverges.

We also see in Figure 1.2 that the asymptotic series truncated at the orders on which the fixed order term is minimal in absolute value, yields a prediction that agrees quite well with the exact value (the dot dashed blue line in the right panel). Asymptotic expansions truncated at the minimal term are said to be *superasymptotic* [12, 13, 14]. The first thing one needs to notice is that the truncation point for a superasymptotic approximation is a blurry concept since, in general, there may be a few orders on which the minimal term is small and more or less of the same size, and there is no absolute rule that says which is the best. This behavior is clearly seen in Figure 1.2, where between $N = 7$ and $N = 12$ we have a plateau. Nevertheless, one can always obtain the order at which truncating the sum yields superasymptotic accuracy by simply minimizing the absolute value of the fixed order term in Eq. (1.73). For the series in Eq. (1.74), we have

$$\frac{d}{dN_{\star}} |(-1)^{N_{\star}} N_{\star}! \alpha^{N_{\star}+1}| = 0, \quad (1.76)$$

which implies

$$\psi(N_{\star} + 1) + \log \alpha = 0, \quad (1.77)$$

where ψ is the digamma function. This function has the following asymptotic expansion for large values of N_{\star}

$$\psi(N_{\star} + 1) = \log N_{\star} + \frac{1}{2N_{\star}} - \frac{1}{12N_{\star}^2} + \dots \quad (1.78)$$

Assuming N_{\star} is large enough, we can approximate Eq. (1.77) by

$$\log(N_{\star}) + \log \alpha = 0, \quad (1.79)$$

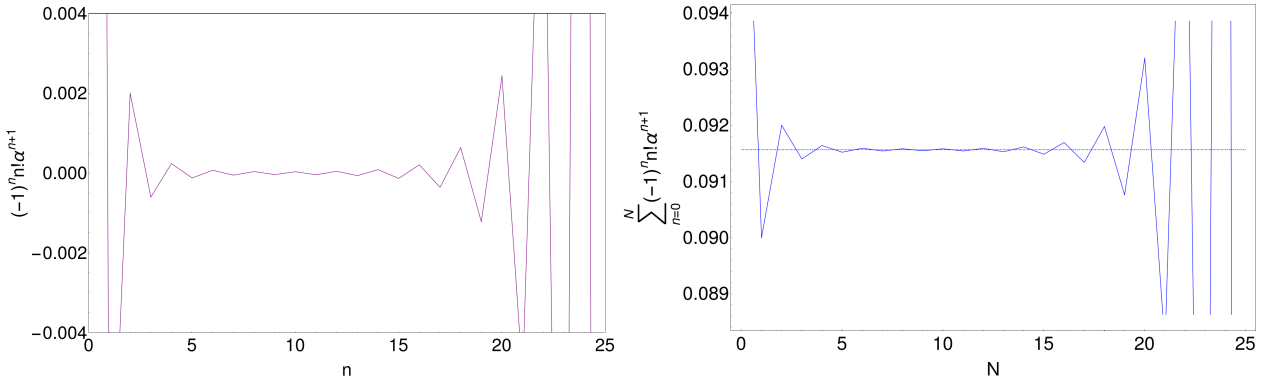


Figure 1.2: Plots with $\alpha = 1/10$. **Left panel:** $(-1)^n n! \alpha^{n+1}$ for various orders n . **Right panel:** $\sum_{n=0}^N (-1)^n n! \alpha^{n+1}$ for various truncation points N . The dot dashed blue line in the right panel is the exact value given by $\alpha S(\alpha)$.

which leads to

$$N_\star = \frac{1}{\alpha}. \quad (1.80)$$

For $\alpha = 1/10$, we see that the superasymptotic approximation is obtained around the order $N_\star = 10$, which agrees with what is displayed in Figure 1.2. We emphasize again that the value of N_\star above is not a well defined concept, and that we can truncate a few orders below or above that. This prompts the idea that, so to speak, the resolution of the asymptotic expansion is of the order of this minimal term, and that we can estimate the ambiguity due to the arbitrariness of the optimal truncation point by evaluating the fixed order term around the superasymptotic truncation point

$$\Delta \left(\sum_{n=0}^{N_\star} r_n \alpha^{n+1} \right) \equiv |r_{N_\star} \alpha^{N_\star+1}| \quad (1.81)$$

$$= N_\star! \alpha^{N_\star+1}. \quad (1.82)$$

Using the asymptotic expansion of the factorial of Eq. (1.1), we can obtain for large enough values of N_\star

$$\Delta \left(\sum_{n=0}^{N_\star} r_n \alpha^{n+1} \right) \approx (2\pi)^{1/2} \alpha^{1/2} e^{-\frac{1}{\alpha}}. \quad (1.83)$$

We obtain a non-analytic term that is reminiscent of the ambiguity of the Borel sum we have encountered before in Eq. (1.37). All of this seems to suggest that, no matter what we do to try to make sense of divergent asymptotic expansions, we will always encounter a source of ambiguity that will be non analytic and reminiscent of non-perturbative terms.

Needless to say, that the asymptotic series we have just considered is a very simple example, where we only have a sign alternating factorial. In general, the coefficients r_n of the series we will have in QCD will by far not be so simple. Nonetheless, assuming they are 1-Gevrey formal series, we still can say that, just as we have seen in the previous section, their large order behavior is again factorial (or being more precise, a gamma function as given by Eqs. (1.53) and (1.54)). Therefore, the qualitative behavior seen in the simple example of the asymptotic expansion of the Stieltjes function will take place in this scenario too. That is, the series will be at first dominated by the power suppression in α^{n+1} , and become smaller as n gets bigger, but eventually, the $\Gamma(n+s)$ in r_n will become the dominant term in r_n , and will overpower the power suppression making the series diverge.

Therefore, we can use the large n behavior of the coefficients r_n to obtain an estimate of the optimal superasymptotic truncation order for 1-Gevrey formal series, by repeating the same procedure as before, using the

leading term in Eq. (1.54) for r_n , and minimizing the absolute value of the fixed order term. This yields

$$\log\left(\frac{|t_i|}{\alpha}\right) - \psi(N_\star + s) = 0. \quad (1.84)$$

In this case, we have the following asymptotic expansion for the digamma function

$$\psi(N_\star + s) = \log N_\star + \frac{-1 + 2s}{2N_\star} + \frac{-1 + 6s - 6s^2}{12N_\star^2} + \dots, \quad (1.85)$$

so assuming again that N_\star is high enough to allow us reliably take the leading term in Eq. (1.85), we obtain from Eq. (1.84)

$$N_\star = \frac{|t_i|}{\alpha}. \quad (1.86)$$

In this thesis, we will use the relation given above between N_\star and α to superasymptotically truncate perturbative expansions. In general, it reproduces very well the order at which the fixed order term becomes minimal. Nevertheless, it should be emphasized that in order to obtain Eq. (1.86), we have assumed that at the order at which the fixed order term is minimal, r_{N_\star} to be given by its leading asymptotic expression given by Eq. (1.54). Thus, the precision of Eq. (1.86) at giving the optimal truncation point depends on how well r_{N_\star} is saturated by its asymptotic expression.

Just as we have done for the series of the Stieltjes function, estimating the ambiguity of the superasymptotic truncation by assuming r_{N_\star} to be saturated by its large N_\star behavior

$$\Delta\left(\sum_{n=0}^{N_\star} r_n \alpha^{n+1}\right) \equiv |r_{N_\star} \alpha^{N_\star+1}| \quad (1.87)$$

$$= \left|\frac{Z}{\Gamma(s)} \frac{1}{t_i^{N_\star}} \Gamma(N_\star + s) \alpha^{N_\star+1}\right|. \quad (1.88)$$

Using again the LO of the Stirling series to approximate the gamma function

$$\Delta\left(\sum_{n=0}^{N_\star} r_n \alpha^{n+1}\right) \approx \left|\frac{Z}{\Gamma(s)}\right| (2\pi)^{1/2} |t_i|^{1/2+s} \alpha^{1/2-s} e^{-\frac{|t_i|}{\alpha}}, \quad (1.89)$$

and yet again, a non analytic term in α appears.

Just as in section 1.4, let us again consider the case of the perturbative expansion of the QCD singlet static potential. We have already mentioned that the leading singularity in the Borel plane is located at $t = \frac{2\pi}{\beta_0}$. Thus, the superasymptotic approximation is obtained around the order

$$N_\star = \frac{2\pi}{\beta_0 \alpha}. \quad (1.90)$$

The ambiguity in the superasymptotic approximation is

$$e^{-\frac{2\pi}{\beta_0 \alpha}} \times (\dots) = \Lambda_{\text{QCD}} \times (\dots), \quad (1.91)$$

just as in Eq. (1.40).

Chapter 2

Renormalons

We have pointed out in the previous chapter that perturbative series in field theory are expected to be divergent. This divergence of perturbative expansions is not a phenomenon that is expected to happen only in quantum field theories, but it is more a feature that seems to follow perturbation theory wherever it goes¹. It also happens in quantum mechanics [17, 18, 19], in perturbative string theory [20], and even in more simple settings, such as field theory in 0 dimensions, where path integrals are just ordinary integrals, and in some examples you can actually compute the general form of the n -th order coefficient of the series, and the divergent nature of the expansion is explicitly seen. Let us for instance consider the partition function of zero dimensional Euclidean ϕ^4 theory defined on just a point

$$\mathcal{Z} = \frac{1}{(2\pi)^{1/2}} \int_{\mathbb{R}} d\phi e^{-\frac{1}{2}\phi^2 - \frac{\alpha}{4!}\phi^4}. \quad (2.1)$$

Expanding the integrand for small α , and commuting sum and integral, we find the following asymptotic expansion

$$\mathcal{Z} \sim \sum_{n=0}^{\infty} \frac{1}{\pi^{1/2}} \left(\frac{-1}{6}\right)^n \frac{\Gamma(2n+1/2)}{\Gamma(n+1)} \alpha^n. \quad (2.2)$$

Clearly, the factorials above will eventually beat the power suppression of α^n , no matter how small α is, and the series ultimately diverges.

We have seen in section 1.5 that the large order behavior of the coefficients of perturbative expansions are related to singularities on the Borel plane. The closer the singularity, the bigger its impact on the large n behavior. In quantum mechanics, this large order behavior is related to instanton singularities in the Borel plane², and is due to the proliferation of the number of Feynman diagrams [21]. There are other settings beyond quantum mechanics where the large order behavior of perturbation theory is still dominated by instantons. This seems to be the case too for super-renormalizable³ field theories [25, 26, 19, 27].

In renormalizable quantum field theories there is another source of divergence that is more important than instantons⁴: renormalons [7]. This divergence is not related to the existence of saddles in Euclidean actions, but rather, it is related to momenta integration regions in the computation of Feynman diagrams. We distinguish two types of renormalons, UV and IR. UV renormalons correspond to the UV part of Feynman diagrams, and IR renormalons correspond to the IR region of Feynman diagrams. Wording this differently, there would be no IR(UV)

¹See [15, 16] for a nice exposition of the divergent high order behavior of perturbation theory on various settings.

²For a heuristic argument for the relation between instantons and the Borel plane, see [7].

³The viewpoint presented is the usual lore, nevertheless, there are recent papers claiming renormalons in a super-renormalizable theory [22]. See also [23, 24] for renormalons in quantum mechanics.

⁴That is, they are closer to the origin in the Borel plane.

renormalon singularities in the Borel plane associated to perturbative expansions in renormalizable quantum field theories, if in the computation of the Feynman diagrams, we set an IR(UV) cutoff in the momentum integration.

In this thesis, we will be concerned with QCD, and therefore, the large order behavior of the series we will consider will be dominated by renormalons. In the next section, we use the large β_0 approximation (see Appendix A) to illustrate the relation between momenta integration regions for Feynman diagrams and singularities in the Borel plane.

2.1 A first glimpse on renormalons

We will make use of the framework of the large β_0 approximation in QCD to showcase how renormalons make their appearance. We review the large β_0 approximation to QCD in Appendix A. Let us consider an observable R in QCD. As it is explained in detail in Appendix A, the perturbative expansion associated to R in the large β_0 approximation is given by Eq. (A.15)

$$R_{\text{large } \beta_0} = \alpha(\mu) \sum_{n=0}^{\infty} \int_0^{\infty} dq F(q) \left\{ \frac{\beta_0 \alpha(\mu)}{4\pi} \log \left(\frac{\mu^2}{q^2} e^{-cx} \right) \right\}^n. \quad (2.3)$$

In the equation above, μ is the renormalization scale, and c_X is related to the renormalization scheme chosen and, for instance, in the $\overline{\text{MS}}$ scheme, we have $c_{\overline{\text{MS}}} = -5/3$. F will of course depend on the observable in question, and as seen in Eq. (A.11), it is related to the LO term in the perturbative expansion of R . The equation above features a momenta integral. We will show how the IR and the UV regions of this integral give rise to singularities in the Borel plane. Let us first consider the Borel transform of this series

$$\hat{R}_{\text{large } \beta_0}(t) = \sum_{n=0}^{\infty} \frac{1}{n!} \int_0^{\infty} dq F(q) \left\{ \frac{\beta_0 t}{4\pi} \log \left(\frac{\mu^2}{q^2} e^{-cx} \right) \right\}^n \quad (2.4)$$

$$= \int_0^{\infty} dq F(q) \sum_{n=0}^{\infty} \frac{1}{n!} \left\{ \frac{\beta_0 t}{4\pi} \log \left(\frac{\mu^2}{q^2} e^{-cx} \right) \right\}^n \quad (2.5)$$

$$= (\mu^2 e^{-cx})^{\frac{\beta_0 t}{4\pi}} \int_0^{\infty} dq F(q) \frac{1}{q^{\frac{\beta_0 t}{2\pi}}}. \quad (2.6)$$

Let's first worry about the IR part. In order to do this, we will introduce a cutoff λ in the integral

$$\hat{R}_{\text{large } \beta_0}^{\text{IR}}(t) \equiv (\mu^2 e^{-cx})^{\frac{\beta_0 t}{4\pi}} \int_0^{\lambda} dq F(q) \frac{1}{q^{\frac{\beta_0 t}{2\pi}}}. \quad (2.7)$$

Also, since we are dealing with the IR behavior of the integral, we are interested in the small q behavior of F , and therefore, we can perform a small q expansion

$$F(q) = \sum_{n=0}^{\infty} f_n q^n, \quad (2.8)$$

and hence⁵

$$\hat{R}_{\text{large } \beta_0}^{\text{IR}}(t) = (\mu^2 e^{-cx})^{\frac{\beta_0 t}{4\pi}} \sum_{n=0}^{\infty} f_n \int_0^{\lambda} dq q^{n - \frac{\beta_0 t}{2\pi}} \quad (2.9)$$

$$= \left(\frac{\mu^2}{\lambda^2} e^{-cx} \right)^{\frac{\beta_0 t}{4\pi}} \sum_{n=0}^{\infty} f_n \frac{\lambda^{1+n}}{1+n - \frac{\beta_0 t}{2\pi}}. \quad (2.10)$$

⁵The equality $\int_0^{\lambda} dq q^{n - \frac{\beta_0 t}{2\pi}} = \frac{\lambda^{1+n - \frac{\beta_0 t}{2\pi}}}{1+n - \frac{\beta_0 t}{2\pi}}$ is only true if $\text{Re}(n - \frac{\beta_0 t}{2\pi}) > -1$ which for low values of n can look like a problem. Nevertheless, notice that we can always compute the Borel transform for $t < 0$ values, for which the relation holds. Then, by analytic continuation, the expression obtained in Eq. (2.10) is true.

This is the expression we wanted to obtain. We see that we have singularities in the Borel plane located at $t = j \times \frac{2\pi}{\beta_0}$ for $j = 1, 2, 3, 4, 5, \dots$. These singularities are the IR renormalons. Since in QCD $\beta_0 > 0$, we see that they are located in the positive real line, and indeed, they pose a problem to Borel summation. Let us now come back to Eq. (2.6), and explore the UV region

$$\hat{R}_{\text{large } \beta_0}^{\text{UV}}(t) \equiv (\mu^2 e^{-cx})^{\frac{\beta_0 t}{4\pi}} \int_{\lambda}^{\infty} dq F(q) \frac{1}{q^{\frac{\beta_0 t}{2\pi}}}. \quad (2.11)$$

In this case, we will be dealing with the UV behavior of the integral, and hence, we will be interested in the large q behavior of F . Therefore, we will perform a large q expansion

$$F(q) = \sum_{n=2}^{\infty} f'_n \frac{1}{q^n}, \quad (2.12)$$

which leads to

$$\hat{R}_{\text{large } \beta_0}^{\text{UV}}(t) = (\mu^2 e^{-cx})^{\frac{\beta_0 t}{4\pi}} \sum_{n=0}^{\infty} f'_n \int_{\lambda}^{\infty} dq \frac{1}{q^{n+\frac{\beta_0 t}{2\pi}}} \quad (2.13)$$

$$= \left(\frac{\mu^2}{\lambda^2} e^{-cx} \right)^{\frac{\beta_0 t}{4\pi}} \sum_{n=0}^{\infty} f'_n \frac{\lambda^{1-n}}{-1+n+\frac{\beta_0 t}{2\pi}}. \quad (2.14)$$

Thus, we see that we have singularities at $t = -j \times \frac{2\pi}{\beta_0}$ for $j = 1, 2, 3, 4, 5, \dots$. These singularities are UV renormalons. Since in QCD $\beta_0 > 0$, we find that they are located at the negative real line.

2.2 The u plane and the t plane

Before going any further, it is worthwhile to make a remark on notation. There is a trend in the literature to, instead of working in the complex t plane, to work with the complex variable u where

$$u = \frac{\beta_0}{4\pi} t. \quad (2.15)$$

This is equivalent to considering formal series where the expansion parameter is $\frac{\beta_0 \alpha}{4\pi}$ instead of α . That is, instead of

$$R = \sum_{n=0}^{\infty} r_n \alpha^{n+1}, \quad (2.16)$$

we consider

$$R = \sum_{n=0}^{\infty} r_n \alpha^{n+1} \equiv \sum_{n=0}^{\infty} \rho_n \left(\frac{\beta_0 \alpha}{4\pi} \right)^{n+1}, \quad (2.17)$$

and take the Borel transform with respect to the expansion parameter $\frac{\beta_0 \alpha}{4\pi}$

$$B(u) \equiv \sum_{n=0}^{\infty} \frac{\rho_n}{n!} u^n. \quad (2.18)$$

Notice that $B(u)$ and $\hat{R}(t)$ are not the same object⁶, although they are trivially related. The expression for the Borel sum when working in the u plane is

$$\int_0^{\infty} du e^{-\frac{4\pi u}{\beta_0 \alpha}} B(u). \quad (2.19)$$

⁶To avoid any potential for ambiguity, in this thesis, we will use the symbol \hat{R} when we are working in the t plane, and the symbol B when we are working in the u plane. The reader is warned though, that in the literature, one may find B to denote either case.

Making this agree with the Borel sum we have been using in the t plane

$$\int_0^\infty du e^{-\frac{4\pi u}{\beta_0 \alpha}} B(u) = \int_0^\infty dt e^{-\frac{t}{\alpha} \hat{R}(t)}, \quad (2.20)$$

which implies

$$B(u) = \frac{4\pi}{\beta_0} \hat{R}(t = \frac{4\pi}{\beta_0} u), \quad (2.21)$$

$$\hat{R}(t) = \frac{\beta_0}{4\pi} B(u = \frac{\beta_0}{4\pi} t). \quad (2.22)$$

Despite both objects not being the same, we will denote them both as the Borel transform, and the context (and the notation) will make it clear to which we are referring to. We finish this section by mentioning that in the u plane, the IR and UV renormalons of the previous section are located at

$$u_{\text{renormalon}} = \pm j \times \frac{1}{2}, \quad (2.23)$$

that is, at positive and negative entire and semi entire values.

2.3 The Borel transform of the QCD singlet static potential in the large β_0 approximation

We will later use the QCD singlet static potential in the large β_0 approximation as a toy model, so we will review it in this section. Let us consider its perturbative expansion

$$V = \sum_{n=0}^{\infty} V_n \alpha^{n+1}. \quad (2.24)$$

The LO term is

$$V_{\text{LO}} \equiv V_0 \alpha = -\frac{C_F}{r} \alpha = \alpha \int_0^\infty dq \frac{-2C_F \sin(qr)}{\pi qr}, \quad (2.25)$$

where C_F is the Casimir of the fundamental representation of SU(3). Therefore, recalling Eq. (A.11), we have that

$$F(q) = \frac{-2C_F \sin(qr)}{\pi qr}. \quad (2.26)$$

Therefore, from Eq. (A.15), we find that the perturbative expansion of the singlet static potential in the large β_0 approximation is

$$V_{\text{large } \beta_0} = \frac{-2C_F \alpha(\mu)}{\pi} \sum_{n=0}^{\infty} \int_0^\infty dq \frac{\sin(qr)}{qr} \left\{ \frac{\beta_0 \alpha(\mu)}{4\pi} \log \left(\frac{\mu^2}{q^2} e^{-cx} \right) \right\}^n. \quad (2.27)$$

Let us consider its Borel transform. From Eq. (2.6), we can write

$$\hat{V}_{\text{large } \beta_0}(t) = \frac{-2C_F}{\pi} e^{-\frac{\beta_0 t}{4\pi} cx} \int_0^\infty dq \frac{\sin(qr)}{qr} \left(\frac{\mu}{q} \right)^{\frac{\beta_0 t}{2\pi}}. \quad (2.28)$$

Let's now notice [28]

$$\left(\frac{\mu}{q} \right)^w = \frac{1}{\Gamma(w)} \int_0^\infty dx x^{w-1} e^{-xq/\mu}, \quad (2.29)$$

so that

$$\hat{V}_{\text{large}\beta_0}(t) = \frac{-2C_F}{\pi} e^{-\frac{\beta_0 t}{4\pi} c_X} \int_0^\infty dq \frac{\sin(qr)}{qr} \frac{1}{\Gamma(\frac{\beta_0 t}{2\pi})} \int_0^\infty dx x^{\frac{\beta_0 t}{2\pi}-1} e^{-xq/\mu} \quad (2.30)$$

$$= \frac{-2C_F}{\pi} e^{-\frac{\beta_0 t}{4\pi} c_X} \frac{1}{\Gamma(\frac{\beta_0 t}{2\pi})} \int_0^\infty dx x^{\frac{\beta_0 t}{2\pi}-1} \int_0^\infty dq \frac{\sin(qr)}{qr} e^{-xq/\mu} \quad (2.31)$$

$$= \frac{-2C_F}{\pi r} e^{-\frac{\beta_0 t}{4\pi} c_X} \frac{1}{\Gamma(\frac{\beta_0 t}{2\pi})} \int_0^\infty dx x^{\frac{\beta_0 t}{2\pi}-1} \arctan\left(\frac{r\mu}{x}\right) \quad (2.32)$$

$$= \frac{-C_F}{r} e^{-\frac{\beta_0 t}{4\pi} c_X} (r\mu)^{\frac{\beta_0 t}{2\pi}} \frac{1}{\Gamma(\frac{\beta_0 t}{2\pi} + 1)} \sec\left(\frac{\beta_0 t}{4}\right), \quad (2.33)$$

and we obtain the expression for the Borel transform. Nevertheless, in the literature, it is customary to write this function in another way. In order to do that, we recall the trigonometric identity

$$\sec(z) = \frac{1}{\sin\left(\frac{\pi}{2} - z\right)}, \quad (2.34)$$

and Euler's reflection formula

$$\Gamma(1-z)\Gamma(z) = \frac{\pi}{\sin(\pi z)}, \quad (2.35)$$

which allow us to write Eq. (2.33) in the following way

$$\hat{V}_{\text{large}\beta_0}(t) = \frac{-C_F}{r\pi} e^{-\frac{\beta_0 t}{4\pi} c_X} (r\mu)^{\frac{\beta_0 t}{2\pi}} \frac{\Gamma\left(1/2 + \frac{\beta_0 t}{4\pi}\right) \Gamma\left(1/2 - \frac{\beta_0 t}{4\pi}\right)}{\Gamma\left(\frac{\beta_0 t}{2\pi} + 1\right)}. \quad (2.36)$$

Writing this Borel transform in the u plane

$$B(u) = \frac{-4C_F}{\beta_0 r} e^{-c_X u} (r\mu)^{2u} \frac{\Gamma(1/2 + u) \Gamma(1/2 - u)}{\Gamma(1 + 2u)}. \quad (2.37)$$

The above expression is the expression found in the original article [8] where this Borel transform was first computed. There is another, shorter way to write it. In order to compute it, we make use of the Legendre duplication formula

$$\Gamma(1/2 + u) = 2^{1-2u} \pi^{1/2} \frac{\Gamma(2u)}{\Gamma(u)}, \quad (2.38)$$

which leads to

$$B(u) = \frac{-4C_F \pi^{1/2}}{\beta_0 r} e^{-c_X u} \left(\frac{r^2 \mu^2}{4}\right)^u \frac{\Gamma(1/2 - u)}{\Gamma(1 + u)}, \quad (2.39)$$

or writing the Borel transform in the t plane

$$\hat{V}_{\text{large}\beta_0}(t(u)) = \frac{-C_F}{\pi^{1/2} r} e^{-c_X u} \left(\frac{r^2 \mu^2}{4}\right)^u \frac{\Gamma(1/2 - u)}{\Gamma(1 + u)}. \quad (2.40)$$

From the above equation, we find that this Borel transform has IR renormalons located at $u = \frac{2n+1}{2}$ for $n = 0, 1, 2, \dots$, that is, at half integer values $u = 1/2, 3/2, 5/2, \dots$. There are no UV renormalons. The Laurent expansion around the leading singularity $u = 1/2$ of Eq. (2.40) yields

$$\hat{V}_{\text{large}\beta_0}(t(u)) = \mu \frac{-2C_F}{\pi} e^{-c_X/2} \frac{1}{1-2u} + \dots, \quad (2.41)$$

where the dots denote analytic terms. It is customary to call to the residue of the pole the normalization of the $u = 1/2$ renormalon in the following way

$$Z_V^{\text{large}\beta_0} \equiv \frac{-2C_F}{\pi} e^{-c_X/2}. \quad (2.42)$$

Writing $V_{\text{large}\beta_0} \equiv \sum_{n=0}^{\infty} V_n \alpha^{n+1}$, the large n behavior associated to this $u = 1/2$ renormalon is

$$V_n^{(\text{as};u=1/2)} = \mu \frac{-4C_F}{\beta_0} e^{-c_X/2} \left(\frac{\beta_0}{2\pi}\right)^{n+1} n!. \quad (2.43)$$

It is worthwhile to point out that there is no r dependence on this renormalon. Furthermore, it is also interesting that, as we will see in the next section, the singularity in Eq. (2.41) coincides with the $u = 1/2$ singularity of the Borel transform of minus twice the pole masses, which makes the sum $V + 2m_{\text{OS}}$ devoid of the $u = 1/2$ renormalon [29]. The Laurent expansion of the Borel transform around $u = 3/2$ is

$$\hat{V}_{\text{large}\beta_0}(t(u)) = r^2 \mu^3 \frac{C_F}{9\pi} e^{-3c_X/2} \frac{1}{1 - \frac{2u}{3}} + \dots, \quad (2.44)$$

where the dots denote analytic terms. Thus, the subleading large order behavior associated to this singularity is

$$V_n^{(\text{as};u=3/2)} = r^2 \mu^3 \frac{2C_F}{3\beta_0} e^{-3c_X/2} \left(\frac{\beta_0}{6\pi}\right)^{n+1} n!. \quad (2.45)$$

We note that we can obtain similar formulas for all the singularities present in Eq. (2.40).

2.4 The Borel transform of the pole mass in the large β_0 approximation

After having dealt with the static potential in the large β_0 approximation, we will now review the pole mass, also in the large β_0 approximation. Let us consider \tilde{M} , the perturbative expansion of the pole mass $m_{\text{OS}}^{\text{large}\beta_0}$ minus the $\overline{\text{MS}}$ mass \bar{m} in the large β_0 approximation

$$\tilde{M} \equiv m_{\text{OS}}^{\text{large}\beta_0} - \bar{m} = \sum_{n=0}^{\infty} r_n \alpha^{n+1}. \quad (2.46)$$

The Borel transform in the $\overline{\text{MS}}$ scheme of the series above reads [30, 31, 32]

$$\hat{\tilde{M}}(t(u)) = \bar{m} \frac{C_F}{4\pi} \left[\left(\frac{\bar{m}^2}{\mu^2}\right)^{-u} e^{-c_{\overline{\text{MS}}}u} 6(1-u) \frac{\Gamma(u)\Gamma(1-2u)}{\Gamma(3-u)} - \frac{3}{u} + R(u) \right], \quad (2.47)$$

where $u = \frac{\beta_0}{4\pi} t$, and

$$R(u) = \sum_{n=1}^{\infty} \frac{1}{(n!)^2} \frac{d^n}{dz^n} G(z) \Big|_{z=0} u^{n-1} = -\frac{5}{2} + \frac{35}{24}u + \mathcal{O}(u^2), \quad (2.48)$$

$$G(u) = -\frac{1}{3}(3+2u) \frac{\Gamma(4+2u)}{\Gamma(1-u)\Gamma^2(2+u)\Gamma(3+u)}. \quad (2.49)$$

The formula for $R(u)$ above is only valid in the $\overline{\text{MS}}$ scheme. The Borel transform in Eq. (2.47) has singularities at the positive real line located at $u = 1/2, 3/2, 2, 5/2, 7/2, 9/2, \dots$, and at the negative real line at $u = -1, -2, -3, -4, \dots$, and thus, as opposed to what we had with the static potential, we have UV renormalons. The Laurent expansion around the leading singularity located at $u = 1/2$ is

$$\hat{\tilde{M}}(t(u)) = \mu \frac{C_F}{\pi} e^{-c_{\overline{\text{MS}}}/2} \frac{1}{1-2u} + \dots, \quad (2.50)$$

and we see that it is exactly $-1/2$ times the one we have in Eq. (2.41), and thus, as we have already mentioned, we see that the formal series $2m_{\text{OS}}^{\text{large}\beta_0} + V_{\text{large}\beta_0}$ has no renormalon at $u = 1/2$ [29].

2.5 The operator product expansion

The operator product expansion (OPE) and its relation with renormalons will be important for this thesis, so we will briefly review it in this section. The OPE was introduced by Wilson in [33] (see also [34]) as a conjecture for the short distance expansion of products of local operators. At first, it was rigorously proven to hold true in the framework of perturbation theory [35]. Afterwards, it was posited to also be valid beyond perturbation theory, and implemented in the famous QCD sum rules [36, 37, 38] (see also [39]). Being more precise, let $A(x)$ and $B(y)$ be local operators on some field theory, where with local what is meant is that they only depend on one spacetime point. Then, the idea is that we can write their operator product when $x \rightarrow y$ as a sum over all local operators \mathcal{O}_n

$$A(x)B(y) = \sum_n C_n^{AB}(x-y)\mathcal{O}_n(y) \quad \text{for } x \sim y. \quad (2.51)$$

The C_n^{AB} above are known as the *Wilson coefficients*, and due to translational symmetry, they depend only on the difference $x - y$. Typically, the Wilson coefficients will be singular for $x = y$, and in general, they will be distributions. Let d_A , d_B and $d_{\mathcal{O}_n}$ be the mass dimensions of the operators A , B and \mathcal{O}_n respectively. Then, naive dimensional arguments suggest that⁷

$$C_n^{AB}(x-y) \sim (x-y)^{d_{\mathcal{O}_n} - d_A - d_B}. \quad (2.52)$$

If we organize the sum in n in Eq. (2.51) according to the mass dimension of the operators \mathcal{O}_n , then Eq. (2.52) tells us that only the operators with lowest mass dimensions will be singular as $x \rightarrow y$.

Eq. (2.51) is meant to be understood as an operator equation, that is, it is valid when taken inside any two states $\langle \Psi | A(x)B(y) | \Phi \rangle$, and the beauty of it is that the Wilson coefficients will remain the same regardless of $\langle \Psi |$ and $| \Phi \rangle$. In this thesis, we will mainly be interested in vacuum expectation values

$$\langle \Omega | T\{A(x)B(y)\} | \Omega \rangle \equiv \langle A(x)B(y) \rangle, \quad (2.53)$$

where $|\Omega\rangle$ is the full vacuum of QCD. Thus, we write

$$\langle A(x)B(y) \rangle = \sum_{d=d_{\text{lowest}}}^{\infty} C_d^{AB}(x-y)\langle \mathcal{O}_d(y) \rangle \quad \text{for } x \sim y, \quad (2.54)$$

where we have now organized the operators in the sum according to their mass dimension, from lower to higher. Typically, the operator with lowest mass dimension will be the identity operator $\mathbb{1}$ with $d = 0$. It is worth mentioning that the vacuum expectation values $\langle \mathcal{O}_d(y) \rangle$ in Eq. (2.53) cancel in perturbation theory, except for the trivial operator, where we simply have $\langle \mathbb{1} \rangle = 1$. Furthermore, since we are considering vacuum expectation values in Eq. (2.54), only gauge invariant Poincaré scalar operators \mathcal{O}_d will survive. These are the first few vacuum expectation values in the OPE (also called the condensates) that we will have in QCD, ordered according to their mass dimension:

- for $d = 0$ the identity operator trivially leads to $\langle \mathbb{1} \rangle = 1$,
- for $d = 3$ the quark condensate $\langle \bar{q}^\alpha q^\alpha \rangle$,
- for $d = 4$ the gluon condensate $\langle G_{\mu\nu}^a G_{\mu\nu}^a \rangle$,

⁷Eq. (2.52) holds for free theories, but in general, renormalization slightly alters it.

- for $d = 5$ the quark gluon condensate $\langle \bar{q}^\alpha \sigma_{\mu\nu} t_{\alpha\beta}^a q^\beta G_{\mu\nu}^a \rangle$,
- for $d = 6$ the three gluon condensate $\langle f^{abc} G_{\mu\nu}^a G_{\nu\xi}^b G_{\xi\mu}^c \rangle$, and the four quark condensate $\langle \bar{q}^\alpha \Gamma_{\alpha\beta} q^\beta \bar{q}^\gamma \Gamma_{\gamma\delta} q^\delta \rangle$,

where a, b, c are SU(3) adjoint indexes, $\alpha, \beta, \gamma, \delta$ are SU(3) fundamental representation indexes, $t_{\alpha\beta}^a$ are the generators of SU(3) in the fundamental representation with the normalization $t_{\alpha\beta}^a t_{\beta\alpha}^b = 1/2 \times \delta^{ab}$, f^{abc} are the structure constants satisfying $[t^a, t^b] = i f^{abc} t^c$, and

$$\sigma_{\mu\nu} = \frac{i}{2} (\gamma_\mu \gamma_\nu - \gamma_\nu \gamma_\mu), \quad (2.55)$$

where γ_μ are the usual gamma matrices acting on spinors. We will not bother defining the Γ terms in the four quark condensate, as we will not use them. It is worth mentioning that there are no allowed operators with $d = 1$ or $d = 2$.

We haven't explicitly said it so far, but the terms in Eq. (2.54) depend on a factorization scale μ that separates long and short distance effects. Making this explicit

$$\langle A(x)B(y) \rangle = \sum_d C_d^{AB}(x-y, \mu) \langle \mathcal{O}_d(y, \mu) \rangle \quad \text{for } x \sim y. \quad (2.56)$$

The Wilson coefficients will contain the short distance behavior, and the condensates parametrize long distance effects. Thus, the Wilson coefficients can be approximated using perturbation theory, whereas for the condensates, a non-perturbative treatment is necessary. After renormalization, the condensates we have seen so far will, in general, depend on the scale μ . RG invariant versions can be defined [40, 41, 42]. For instance, for the quark and gluon condensate, we would have

$$\langle m \bar{q}^\alpha q^\alpha \rangle, \quad (2.57)$$

$$\frac{-2}{\beta_0} \left\langle \frac{\beta(\alpha)}{\alpha} G_{\mu\nu}^a G_{\mu\nu}^a \right\rangle, \quad (2.58)$$

where β is the beta function, and m is the quark mass. We finish by writing the Fourier transformed version of the OPE. Without loss of generality, we can consider the $y = 0$ case.

$$\langle A(x)B(0) \rangle = \sum_d C_d^{AB}(x, \mu) \langle \mathcal{O}_d(0, \mu) \rangle \quad \text{for } x \sim 0. \quad (2.59)$$

We can write a Fourier transformed version of Eq. (2.59)

$$\int d^4x e^{-iqx} \langle A(x)B(0) \rangle = \sum_d \langle \mathcal{O}_d(0, \mu) \rangle \int d^4x e^{-iqx} C_d^{AB}(x, \mu) \quad (2.60)$$

$$\equiv \sum_d \frac{1}{Q^d} \tilde{C}_d^{AB}(Q, \mu) \langle \mathcal{O}_d(0, \mu) \rangle, \quad (2.61)$$

where Q is Euclidean momenta, and we have factorized the Q^{-d} from the Wilson coefficients in momentum space. Just as the position space version works for $x \sim 0$, the Fourier transformed version is expected to be true for $Q \rightarrow \infty$.

2.6 The OPE and renormalons

In this section⁸, we will highlight the relation between renormalons and the OPE. Let us consider an OPE in momentum space of a dimensionless observable R (we skip the tilde in the Wilson coefficients on momentum space)

$$\langle R \rangle_{\text{OPE}} = \sum_{d=0}^{\infty} \frac{1}{Q^d} C_d^R(Q, \mu) \langle \mathcal{O}_d(0, \mu) \rangle. \quad (2.62)$$

The $d = 0$ operator will just be the identity operator, so we write

$$\langle R \rangle_{\text{OPE}} = C_0^R(Q, \mu) + \frac{1}{Q^{d_1}} C_{d_1}^R(Q, \mu) \langle \mathcal{O}_{d_1}(0, \mu) \rangle + \frac{1}{Q^{d_2}} C_{d_2}^R(Q, \mu) \langle \mathcal{O}_{d_2}(0, \mu) \rangle + \frac{1}{Q^{d_3}} C_{d_3}^R(Q, \mu) \langle \mathcal{O}_{d_3}(0, \mu) \rangle + \dots, \quad (2.63)$$

where d_i is the mass dimension of the operator \mathcal{O}_{d_i} , and d_1 is the lowest non-trivial one. As we have already mentioned, the Wilson coefficients are usually computed as power series expansions in the strong coupling

$$C_{d_i}^R(Q, \mu) = \sum_{n=-1}^{\infty} c_n^{(d_i)}(Q, \mu) \alpha^{n+1}(\mu), \quad (2.64)$$

where the series above is understood as a formal series that, in general, is expected to be divergent and asymptotic. Thus, the OPE takes the form

$$\langle R \rangle_{\text{OPE}} = \sum_{n=-1}^{\infty} c_n^{(0)}(Q, \mu) \alpha^{n+1}(\mu) + \frac{\langle \mathcal{O}_{d_1}(0, \mu) \rangle}{Q^{d_1}} \sum_{n=-1}^{\infty} c_n^{(d_1)}(Q, \mu) \alpha^{n+1}(\mu) + \dots. \quad (2.65)$$

We emphasize again that the series above are, in general, expected to be divergent and asymptotic. In practice, when implementing them, one has to choose a way to handle the divergent series, say by truncating them, or say by doing something else, for instance Borel summation. It is only after the specific way to regularize the perturbative sums has been stated, that one can give well defined numbers for each of the terms of the OPE. Note, however, that different regularizations of the perturbative sums will yield different numerical values, which will affect the values of the condensates. This is somewhat analogous to the freedom of scheme one has in the renormalization of the coupling constant.

There is a method that exploits these ideas to fix some coefficients of the Borel transform of the first series in the RHS of Eq. (2.65) in the vicinity of the closest IR renormalon. The idea is to compare the ambiguity of the first series in the RHS of Eq. (2.65) with the first condensate sector. In particular, we will see that this approach fixes the location of the first IR renormalon to be at $t = \frac{2\pi d_1}{\beta_0}$. Let us see how this works in more detail. We will use μ independent versions of the condensates by considering

$$\langle \bar{\mathcal{O}}_{d_i} \rangle \equiv \langle \mathcal{O}_{d_i}(0, \mu) \rangle \exp \left\{ \int_k^{\alpha(\mu)} d\alpha' \frac{\gamma_{\mathcal{O}_{d_i}}(\alpha')}{\beta(\alpha')} \right\}, \quad (2.66)$$

where k is an integration constant that will be irrelevant for us. Just as in Eq. (1.39), the beta function is

$$\mu \frac{d}{d\mu} \alpha(\mu) = \beta(\alpha(\mu)). \quad (2.67)$$

The anomalous dimension $\gamma_{\mathcal{O}_{d_i}}$ of the operator \mathcal{O}_{d_i} is defined in the following way

$$\mu \frac{d}{d\mu} \langle \mathcal{O}_{d_i}(0, \mu) \rangle \equiv -\gamma_{\mathcal{O}_{d_i}} \langle \mathcal{O}_{d_i}(0, \mu) \rangle, \quad (2.68)$$

⁸This section is based on [43, 44, 45, 46, 47, 48].

and

$$\gamma_{\mathcal{O}_{d_i}}(\alpha) = \sum_{k=1}^{\infty} \gamma_k^{(d_i)} \alpha^k. \quad (2.69)$$

It is easy to see using Eq. (2.68) and Leibniz's integral rule that

$$\mu \frac{d}{d\mu} \langle \bar{\mathcal{O}}_{d_i} \rangle = 0. \quad (2.70)$$

Also, we expect the condensate to be proportional to the QCD scale

$$\langle \bar{\mathcal{O}}_{d_i} \rangle = \# \Lambda_{\text{QCD}}^{d_i}, \quad (2.71)$$

and recall that we can write the small $\alpha(\mu)$ expansion of Λ_{QCD} by integrating the beta function in Eq. (1.39)

$$\Lambda_{\text{QCD}} = Q e^{\frac{-2\pi}{\beta_0 \alpha(Q)}} \left(\frac{\beta_0 \alpha(Q)}{4\pi} \right)^{-b} \exp \left\{ - \sum_{n=1}^{\infty} s_n \left(\frac{-b \beta_0 \alpha(Q)}{2\pi} \right)^n \right\}, \quad (2.72)$$

where we have defined

$$b \equiv \frac{\beta_1}{2\beta_0^2}, \quad (2.73)$$

$$s_1 \equiv \frac{\beta_1^2 - \beta_0 \beta_2}{2\beta_0^2 \beta_1}, \quad (2.74)$$

$$s_2 \equiv \frac{\beta_1^3 - 2\beta_0 \beta_1 \beta_2 + \beta_0^2 \beta_3}{4\beta_0^2 \beta_1^2}, \quad (2.75)$$

$$s_3 \equiv \frac{\beta_1^4 - 3\beta_0 \beta_1^2 \beta_2 + 2\beta_0^2 \beta_1 \beta_3 + \beta_0^2 \beta_2^2 - \beta_0^3 \beta_4}{6\beta_0^2 \beta_1^3}, \quad (2.76)$$

$$s_4 \equiv \frac{\beta_1^5 - 4\beta_0 \beta_1^3 \beta_2 + 3\beta_0^2 \beta_1^2 \beta_3 + 3\beta_0^2 \beta_1 \beta_2^2 - 2\beta_0^3 \beta_1 \beta_4 - 2\beta_0^3 \beta_2 \beta_3 + \beta_0^4 \beta_5}{8\beta_0^2 \beta_1^4}, \quad (2.77)$$

$$s_5 = \dots \quad (2.78)$$

All in all, a generic term of the OPE in Eq. (2.63) becomes

$$\frac{1}{Q^{d_i}} C_{d_i}^R(Q, \mu) \langle \mathcal{O}_{d_i}(Q, \mu) \rangle = \frac{1}{Q^{d_i}} C_{d_i}^R(Q, \mu) \exp \left\{ - \int_k^{\alpha(\mu)} d\alpha' \frac{\gamma_{\mathcal{O}_{d_i}}(\alpha')}{\beta(\alpha')} \right\} \langle \bar{\mathcal{O}}_{d_i} \rangle. \quad (2.79)$$

Let us now define

$$\bar{C}_{d_i}^R(Q) \equiv C_{d_i}^R(Q, \mu) \exp \left\{ - \int_k^{\alpha(\mu)} d\alpha' \frac{\gamma_{\mathcal{O}_{d_i}}(\alpha')}{\beta(\alpha')} \right\}, \quad (2.80)$$

and expand

$$\bar{C}_{d_i}^R(Q) = \bar{c}_{-1}^{(d_i)} \times \alpha^{\frac{2\pi\gamma_1^{(d_i)}}{\beta_0}}(Q) \left\{ 1 + \sum_{n=0}^{\infty} \bar{c}_n^{(d_i)} \alpha^{n+1}(Q) \right\}. \quad (2.81)$$

Notice that the coefficients $\bar{c}_n^{(d_i)}$ will mingle the coefficients β_n , $\gamma_n^{(d_i)}$ and those of the perturbative expansion of $C_{d_i}^R$. With these definitions, a generic term in the OPE becomes

$$\frac{1}{Q^{d_i}} C_{d_i}^R(Q, \mu) \langle \mathcal{O}_{d_i}(0, \mu) \rangle = \frac{1}{Q^{d_i}} \bar{C}_{d_i}^R(Q) \langle \bar{\mathcal{O}}_{d_i} \rangle, \quad (2.82)$$

which using Eq. (2.81), we write as

$$\frac{1}{Q^{d_i}} \bar{C}_{d_i}^R(Q) \langle \bar{\mathcal{O}}_{d_i} \rangle = \frac{\langle \bar{\mathcal{O}}_{d_i} \rangle}{Q^{d_i}} \bar{c}_{-1}^{(d_i)} \alpha^{\frac{2\pi\gamma_1^{(d_i)}}{\beta_0}}(Q) \left\{ 1 + \sum_{n=0}^{\infty} \bar{c}_n^{(d_i)} \alpha^{n+1}(Q) \right\}. \quad (2.83)$$

Using Eq. (2.72) to kick out the $1/Q^{d_i}$ dependence

$$\begin{aligned} \frac{1}{Q^{d_i}} \bar{C}_{d_i}^R(Q) \langle \bar{\mathcal{O}}_{d_i} \rangle &= \text{const} \times \left(\frac{\beta_0}{4\pi} \right)^{-bd_i} e^{\frac{-d_i 2\pi}{\beta_0 \alpha(Q)}} \alpha^{\frac{2\pi\gamma_i(d_i)}{\beta_0} - bd_i}(Q) \\ &\times \left\{ 1 + \sum_{n=0}^{\infty} \bar{c}_n^{(d_i)} \alpha^{n+1}(Q) \right\} \exp \left\{ - \sum_{n=1}^{\infty} s_n \left(\frac{-b\beta_0 \alpha(Q)}{2\pi} \right)^n \right\}^{d_i}, \end{aligned} \quad (2.84)$$

where $\text{const} \equiv \#c_{-1}^{(d_i)}$ is an irrelevant constant. Ignoring this constant, and all the other Q independent constants above, and expanding it all in $\alpha(Q)$

$$\frac{1}{Q^{d_i}} \bar{C}_{d_i}^R(Q) \langle \bar{\mathcal{O}}_{d_i} \rangle \sim e^{\frac{-d_i 2\pi}{\beta_0 \alpha(Q)}} \alpha^{\frac{2\pi\gamma_i(d_i)}{\beta_0} - bd_i}(Q) \left\{ 1 + \sum_{n=0}^{\infty} f_n^{(d_i)} \alpha^{n+1}(Q) \right\}, \quad (2.85)$$

where the constants $f_n^{(d_i)}$ combine the s_n and the $\bar{c}_n^{(d_i)}$. We will now consider the ambiguity associated to an IR renormalon⁹ located in $u = d/2$, and we will find out that the ambiguity associated to it will scale like $e^{\frac{-d2\pi}{\beta_0 \alpha(Q)}}$. We will then use this fact to fix some coefficients of the Borel transform in the vicinity to the aforementioned renormalon. Thus, let's consider the formal series¹⁰ of the first term on the RHS of Eq. (2.63)

$$C_0^R(Q) = \sum_{n=0}^{\infty} c_n^{(0)} \alpha^{n+1}(Q), \quad (2.86)$$

and its Borel transform

$$\hat{C}_0^R(t) = \sum_{n=0}^{\infty} \frac{c_n^{(0)}}{n!} t^n. \quad (2.87)$$

In the large β_0 examples we have considered so far, we have found renormalons to be poles in the complex plane. For real QCD, we will generalize this behavior to a branch cut singularity, so that for an IR renormalon located at $u = d/2$, we assume the behavior of the Borel transform around this singularity to be the one we have seen in section 1.5

$$\hat{C}_0^R(t(u)) = Z \frac{1}{(1 - 2u/d)^{1+l}} \sum_{j=0}^{\infty} w_j (1 - 2u/d)^j, \quad (2.88)$$

with $w_0 = 1$, and the rest of the coefficients w_j , l and Z are arbitrary. We have seen in section 1.4 that the ambiguity associated to the singularity above is related to the discontinuity function

$$\text{disc}(C_0^R) = \lim_{\eta \rightarrow 0^+} \left\{ \int_{C_+} dt e^{-t/\alpha(Q)} \hat{C}_0^R(t) - \int_{C_-} dt e^{-t/\alpha(Q)} \hat{C}_0^R(t) \right\}, \quad (2.89)$$

where C_{\pm} is parametrized by $t = xe^{\pm i\eta}$. These integrals yield

$$\text{disc}(C_0^R) = Z \left(\frac{2\pi d}{\beta_0} \right)^{1+l} 2i \sin(\pi[1+l]) \Gamma(-l) e^{\frac{-d2\pi}{\beta_0 \alpha(Q)}} \alpha^{-l}(Q) \sum_{n=0}^{\infty} \frac{\Gamma(n-l)}{\Gamma(-l)} \left(\frac{-\beta_0}{2\pi d} \right)^n w_n \alpha^n(Q), \quad (2.90)$$

where ignoring the constant factors, we obtain

$$\text{disc}(C_0^R) \sim e^{\frac{-d2\pi}{\beta_0 \alpha(Q)}} \alpha^{-l}(Q) \sum_{n=0}^{\infty} \frac{\Gamma(n-l)}{\Gamma(-l)} \left(\frac{-\beta_0}{2\pi d} \right)^n w_n \alpha^n(Q). \quad (2.91)$$

⁹Recall that, as we saw in section 1.5, the Borel transform around an UV renormalon located at $u = d/2$, where $d < 0$, will be proportional to $(Q/\mu)^{|d|}$. Then, the discontinuity function of Eq. (2.91) will schematically be $\sim Q^{|d|}/\mu^{2|d|} \Lambda_{\text{QCD}}^{|d|}$, as opposed to $\sim \Lambda_{\text{QCD}}^{|d|}/Q^{|d|}$ if we had an IR renormalon located at $u = |d|/2$, and thus, it cannot be absorbed in the condensates of the OPE whose terms are all powers of Λ_{QCD}/Q .

¹⁰We assume the $c_{-1}^{(0)}$ term to be zero.

Taking a look at Eq. (2.91) and Eq. (2.85), we notice that the parametric dependence in $\alpha(Q)$ is the same. Keeping this in mind, let us come back to Eq. (2.63)

$$\langle R \rangle_{\text{OPE}} = \sum_{n=0}^{\infty} c_n^{(0)} \alpha^{n+1} + \frac{1}{Q^{d_1}} C_{d_1}^R \langle \mathcal{O}_{d_1} \rangle + \frac{1}{Q^{d_2}} C_{d_2}^R \langle \mathcal{O}_{d_2} \rangle + \frac{1}{Q^{d_3}} C_{d_3}^R \langle \mathcal{O}_{d_3} \rangle + \dots \quad (2.92)$$

As we have just seen, the ambiguity associated to the leading IR renormalon of the series of the first term of the RHS above has a parametric dependence in $\alpha(Q)$ that is the same as that of the condensates. The heuristic idea then is that since the LHS of the equation above is meant to be a well defined object, then for the leading ambiguity of the perturbative series to be absorbed in the leading condensate $\langle \bar{\mathcal{O}}_{d_1} \rangle$. Thus, we need to equate the parametric dependence in $\alpha(Q)$ of Eqs. (2.91) and (2.85), yielding the relations

$$d = d_1, \quad (2.93)$$

$$l = db - \frac{2\pi\gamma_1^{(d_1)}}{\beta_0}, \quad (2.94)$$

$$w_1 = \frac{d}{bd\beta_0 - 2\pi\gamma_1^{(d_1)}} \{2\pi\bar{c}_0 + bd\beta_0 s_1\}, \quad (2.95)$$

$$w_2 = \frac{d^2}{2(bd\beta_0 - 2\pi\gamma_1^{(d_1)})(bd - 1)\beta_0 - 2\pi\gamma_1^{(d_1)}} \{8\pi^2\bar{c}_1 + 4bd\pi\beta_0 s_1 \bar{c}_0 + b^2 d \beta_0^2 (ds_1^2 - 2s_2)\}, \quad (2.96)$$

$$w_3 = \frac{-d^3}{6\beta_0^3(-bd + \frac{2\pi\gamma_1^{(d_1)}}{\beta_0} + 2)(-bd + \frac{2\pi\gamma_1^{(d_1)}}{\beta_0} + 1)(-bd + \frac{2\pi\gamma_1^{(d_1)}}{\beta_0})} \{48\pi^3\bar{c}_2 + 24bd\pi^2\beta_0 s_1 \bar{c}_1 \quad (2.97)$$

$$+ 6b^2 d \pi \beta_0^2 (ds_1^2 - 2s_2)\bar{c}_0 + b^3 d \beta_0^3 (d^2 s_1^3 - 6ds_1 s_2 + 6s_3)\}, \quad (2.98)$$

$$w_4 = \dots \quad (2.99)$$

In particular, we see that the location of the leading IR renormalon of the perturbative expansion is dictated by the mass dimensions of the leading condensate, and that the coefficients w_j parametrizing this singularity are given by the beta function coefficients and the coefficients of the Wilson coefficient. It is worth emphasizing that with this approach, we cannot fix the normalization of the renormalon Z of Eq. (2.88).

Before finishing this section, it is noteworthy pointing out the similarities between the procedure that has just been carried out, and resurgent transseries [49, 50, 51]. Roughly speaking, a transseries¹¹ is essentially an expansion in exponentials and powers of some parameter¹²

$$\sum_{m=0}^{\infty} e^{-\frac{a_m}{\alpha}} \sum_{n=0}^{\infty} r_n^{(m)} \alpha^{n+1}. \quad (2.100)$$

Let $a_0 = 0$ so that the first exponential sector above is just a perturbative expansion. Resurgence remarkably hypothesizes that the coefficients of the series of the various exponential sectors in the object above are deeply related, and that knowledge of the large order behavior of the coefficients $r_n^{(0)}$ in fact gives us knowledge on the coefficients $r_n^{(m)}$ of the rest of non-perturbative sectors. That is, perturbation theory seems to encode information of non-perturbative physics already(!), and its all hidden in its large order behavior. Moreover, each sector has a formal series that is in general divergent and whose sum is ambiguous, but these ambiguities can be made sense of when the whole transseries is considered. The connection with these ideas and the OPE comes from realizing that as we see in Eq. (2.85), a generic term in the OPE follows the schematic form displayed in the transseries

¹¹For a nice introduction to transseries see [52].

¹²In general, there can also be logarithms, and the functions that appear can have higher depth, that is, things like $e^{e^{-1/\alpha}}$ can appear.

above with various exponentially suppressed sectors. To name a few applications of resurgence in physics, we have quantum mechanics [53, 54, 55, 56, 57] and certain asymptotically free theories [58, 59, 60, 61]. For a perspective on resurgence and the OPE in supersymmetric theories see [62, 63].

2.7 Fixing the condensates from the OPE

Let us now consider again the OPE

$$\langle R \rangle_{\text{OPE}} = \sum_{n=0}^{\infty} c_n^{(0)}(Q, \mu) \alpha^{n+1}(\mu) + \frac{1}{Q^{d_1}} \bar{C}_{d_1}^R \langle \bar{\mathcal{O}}_{d_1} \rangle + \dots, \quad (2.101)$$

where we have only explicitly written the first condensate term. A major theme in the following chapters will be to use the equation above to fix the leading condensate. We will do this by writing

$$\langle \bar{\mathcal{O}}_{d_1} \rangle = Q^{d_1} \frac{1}{\bar{C}_{d_1}^R} \left\{ \langle R \rangle_{\text{OPE}} - \sum_{n=0}^{\infty} c_n^{(0)}(Q, \mu) \alpha^{n+1}(\mu) \right\} + \dots, \quad (2.102)$$

where we ignore the contributions of subleading terms in the OPE. As we have already emphasized many times, the various series in the equation above are divergent, and therefore, before making sense of the equation above, these need to be regularized. Consequently, the ambiguity on the method chosen to regularize them will translate itself on the condensate. For instance, we could simply truncate the various series above at order $\alpha^{N_{d_i}+1}$, and obtain for the condensate a value

$$\langle \bar{\mathcal{O}}_{d_1} \rangle_N \equiv Q^{d_1} \frac{1}{\bar{C}_{d_1}^R|_{N_{d_1}}} \left\{ \langle R \rangle_{\text{OPE}} - \sum_{n=0}^{N_0} c_n^{(0)}(Q, \mu) \alpha^{n+1}(\mu) \right\} + \dots. \quad (2.103)$$

One must keep in mind that since $\langle \bar{\mathcal{O}}_{d_1} \rangle_N$ is expected to scale as $\Lambda_{\text{QCD}}^{d_1}$, the series in braces above needs to be regularized with $\Lambda_{\text{QCD}}^{d_1}$ precision, because it is pointless to attempt to extract $\sim \Lambda_{\text{QCD}}^{d_1}$ terms from $\langle R \rangle_{\text{OPE}}$ if the Wilson coefficient of the trivial operator that we are subtracting to $\langle R \rangle_{\text{OPE}}$ itself doesn't have $\sim \Lambda_{\text{QCD}}^{d_1}$ precision. For instance, this is achieved if we truncate the series in braces above at the optimal truncation point as given in Eq. (1.86) dictated by the leading IR renormalon, which as we have seen in the previous section, will be located at $t = \frac{2\pi d_1}{\beta_0}$. It is worth pointing out that, as we have already mentioned, we can always keep one order more, or one order less around the optimal truncation point, and by doing this, the value of the condensate changes by terms that are of order $\Lambda_{\text{QCD}}^{d_1}$.

Truncation has the obvious advantage that one can always do it if one simply knows enough coefficients of the series. Nonetheless, truncation is not without its drawbacks. So far, we have assumed the various terms in the OPE to be formally μ independent, which implies

$$\mu \frac{d}{d\mu} \sum_{n=0}^{\infty} c_n^{(0)}(Q, \mu) \alpha^{n+1}(\mu) = 0, \quad (2.104)$$

order by order in $\alpha(\mu)$. Despite this, when one truncates the series above, there will always linger some residual $\mathcal{O}(\alpha^{N_0+2}(\mu))$ scale dependence (where we truncate at $\alpha^{N_0+1}(\mu)$), which will be carried to the condensate as defined in Eq. (2.103). In this thesis, we will use the PV Borel sum to regularize the formal series in braces¹³ in Eq. (2.102). As we show in Appendix B, assuming some properties for the analytically extended Borel transform of C_0^R , we can

¹³We will not worry much about the Wilson coefficient $\bar{C}_{d_1}^R$ because in the cases we will consider, the series will not be known to high enough orders to reach its asymptotic behavior, and in practice, we will just truncate it.

see that the PV Borel sum is renormalization scale and scheme independent. Thus, a condensate defined in the following way

$$\langle \bar{\mathcal{O}}_{d_1} \rangle_{\text{PV}} \equiv Q^{d_1} \frac{1}{\bar{C}_{d_1}^R |_{N_{d_1}}} \left\{ \langle R \rangle_{\text{OPE}} - \text{PV} \sum_{n=0}^{\infty} c_n^{(0)}(Q, \mu) \alpha^{n+1}(\mu) \right\} + \dots, \quad (2.105)$$

will be renormalization scale and scheme independent (up to subleading terms in the OPE).

The obvious drawback, of course, is that in order to compute the PV Borel sum, we need the Borel transform first, and this requires the knowledge of all the coefficients of the divergent series. Quite remarkably, it is possible to relate truncated formal series with their PV Borel sums. In this thesis, we will explore two avenues for that, which will be shown in the next two chapters. The first is based in the so called Dingle's theory of terminants [10], and the second draws from [64, 65, 66, 67].

Chapter 3

Approximating the PV Borel sum: Method 1

In this chapter, we review Dingle's method to obtain the PV Borel sum of a divergent series from truncated versions of it, and then apply it to some examples in the large β_0 approximation (see [68, 69, 70] for the original articles).

3.1 Dingle's terminants

In chapter 21 of his book [10], Dingle was concerned with the problem of extracting information from the remainder tail of a truncated divergent asymptotic expansion (which of course is also divergent), what he refers to as *terminating* a truncated series. Inspired by Borel summation, he proposed a method to assign a finite number to the remainder tail of a series, and called this object a *terminant*. Let's make all of this more precise. First of all, we should remind ourselves a feature of Borel summation. Let's consider a divergent asymptotic series and its Borel transform

$$R = \sum_{n=0}^{\infty} r_n \alpha^{n+1}, \quad (3.1)$$

$$\hat{R} = \sum_{n=0}^{\infty} \frac{r_n}{n!} t^n. \quad (3.2)$$

As we have already seen, if we introduce this object in a Laplace transform, ignoring the fact that we are considering the power series of the Borel transform outside its convergence radius, and commute sum and integral with impunity

$$\int_0^{\infty} dt e^{-t/\alpha} \sum_{n=0}^{\infty} \frac{r_n}{n!} t^n \rightarrow \sum_{n=0}^{\infty} \frac{r_n}{n!} \alpha^{n+1} \int_0^{\infty} dt e^{-t} t^n = \sum_{n=0}^{\infty} r_n \alpha^{n+1} = R, \quad (3.3)$$

we recover the original series. Let us now remark that the same can be achieved with a slight modification. We can define an analogue of the Borel transform of R changing slightly the factorial

$$\hat{R}' = \sum_{n=0}^{\infty} \frac{r_n}{\Gamma(n+1+\sigma)} t^n, \quad (3.4)$$

and modifying slightly the Laplace transform, introducing a factor $(t/\alpha)^\sigma$ to compensate

$$\int_0^{\infty} dt e^{-t/\alpha} (t/\alpha)^\sigma \sum_{n=0}^{\infty} \frac{r_n}{\Gamma(n+1+\sigma)} t^n, \quad (3.5)$$

such that, when we again commute integral and sum

$$\int_0^{\infty} dt e^{-t/\alpha} (t/\alpha)^\sigma \sum_{n=0}^{\infty} \frac{r_n}{\Gamma(n+1+\sigma)} t^n \rightarrow \sum_{n=0}^{\infty} \frac{r_n}{\Gamma(n+1+\sigma)} \alpha^{n+1} \int_0^{\infty} dt e^{-t} t^{n+\sigma} = \sum_{n=0}^{\infty} r_n \alpha^{n+1} = R, \quad (3.6)$$

we again obtain the original series. This change to the Borel sum might seem strange at this point, but the reason to consider it will be apparent soon. Keeping this in mind, let's consider a truncated divergent asymptotic series and its remainder

$$R = \sum_{n=0}^N r_n \alpha^{n+1} + \sum_{n=N+1}^{\infty} r_n \alpha^{n+1}. \quad (3.7)$$

As we have mentioned earlier, Dingle was concerned in trying to assign a value to the (divergent) remainder tail above. In order to do that, he applied the expression in Eq. (3.5) to the remainder tail. That is, he considered

$$\int_0^{\infty} dt e^{-t/\alpha} (t/\alpha)^{\sigma} \sum_{n=N+1}^{\infty} \frac{r_n}{\Gamma(n+1+\sigma)} t^n. \quad (3.8)$$

Dingle sought to apply the method to series that for large n diverged factorially, that is, $r_n \sim \Gamma(n+1+\sigma)$ for some σ , for large enough n . Now, since we are applying Eq. (3.8) to the remainder tail, r_n will be already well approximated by the leading asymptotic behavior, and we can substitute it above. Therefore, we see that in Eq. (3.8), we will basically have a geometric series and the reason for having introduced the σ in Eq. (3.5) is clear. Dingle considered both¹ fixed sign and sign alternating factorials $r_n^{(\text{as})} = K A^n \Gamma(n+1+\sigma)$ and $r_n^{(\text{as})} = (-1)^n K A^n \Gamma(n+1+\sigma)$, where we have added a power A^n to match precisely the type of behavior we have seen in Eq. (1.68). Let's first consider the fixed sign factorial. Introducing $r_n^{(\text{as})} = K A^n \Gamma(n+1+\sigma)$ in Eq. (3.8), we see that the analogue of the Borel transform becomes

$$K \sum_{n=N+1}^{\infty} A^n t^n = K A^{N+1} \frac{t^{N+1}}{1-At}. \quad (3.9)$$

The sum above is true if $|At| < 1$, but we generalize it to $\mathbb{C} - \{1/A\}$ by analytic continuation. Plugging it back in the expression of Eq. (3.8)

$$\frac{1}{\alpha^{\sigma}} K A^{N+1} \int_0^{\infty} dt e^{-t/\alpha} \frac{t^{N+1+\sigma}}{1-At}. \quad (3.10)$$

Now there is a catch. The integral above is ill defined, as there is a singularity on the integration path. Dingle proposed using the PV prescription to regulate it

$$T_+ \equiv \frac{1}{\alpha^{\sigma}} K A^{N+1} \text{PV} \int_0^{\infty} dt e^{-t/\alpha} \frac{t^{N+1+\sigma}}{1-At}. \quad (3.11)$$

The object above is what we will call a *terminant*. The subscript $+$ is meant to denote that the singularity in the t plane of the integrand is located at a positive value of t . We will generically denote a terminant with the symbol T , and sometimes add a subscript to specify some feature. It is worth mentioning that what Dingle called a terminant in chapter 21 of his book is slightly different to the object above. Quoting Dingle's book²: "Defining the terminant T_{Dingle} as the function which when multiplied by the $(N+1)$ -th term in an asymptotic series would correctly terminate that series...". That is

$$T = r_{N+1} \alpha^{N+1} T_{\text{Dingle}}, \quad (3.12)$$

where we truncate the series at order α^{N+1} , as we have done in Eq. (3.7). Had we had a sign alternating factorial, every step above could be repeated verbatim, except for the fact that we would not have a singularity in the

¹Actually, Dingle distinguishes other two cases where the series $\sum_n r_n \alpha^{n+1}$ has an index n that does not range in all the integers, but instead lacks every second term, just like the series expansions of the sine and the cosine. In any case, these cases will not be relevant for us.

²Page 404. We have adapted his notation to match ours. In particular, he considers asymptotic expansions at infinity and not at the origin, and he also includes a constant term (what for us would be $\sim \alpha^0$) in his series.

integration path, and the terminant would simply be

$$T_- \equiv (-1)^{N+1} \frac{1}{\alpha^\sigma} K A^{N+1} \int_0^\infty dt e^{-t/\alpha} \frac{t^{N+1+\sigma}}{1+At}. \quad (3.13)$$

The subscript $-$ denotes that the singularity of the integrand in the t plane is located at a negative t value. Summarizing, we consider a (factorially) divergent asymptotic series

$$R = \sum_{n=0}^{\infty} r_n \alpha^{n+1}, \quad (3.14)$$

we truncate it

$$R = \sum_{n=0}^N r_n \alpha^{n+1} + \sum_{n=N+1}^{\infty} r_n \alpha^{n+1}, \quad (3.15)$$

and we estimate the remainder series by the terminant T_i

$$\sum_{n=N+1}^{\infty} r_n \alpha^{n+1} \sim T_+ = \frac{1}{\alpha^\sigma} K A^{N+1} \text{PV} \int_0^\infty dt e^{-t/\alpha} \frac{t^{N+1+\sigma}}{1-At}, \quad (3.16)$$

or

$$\sum_{n=N+1}^{\infty} r_n \alpha^{n+1} \sim T_- = (-1)^{N+1} \frac{1}{\alpha^\sigma} K A^{N+1} \int_0^\infty dt e^{-t/\alpha} \frac{t^{N+1+\sigma}}{1+At}, \quad (3.17)$$

depending on whether the factorial is fixed or alternate signed. Therefore, the *terminated* series would be

$$\sum_{n=0}^N r_n \alpha^{n+1} + T. \quad (3.18)$$

We will see that this expression approximates the PV Borel sum of the original divergent series R .

3.2 Examples

3.2.1 The Stieltjes function

This is a very simple example where we will see that, in fact, adding Dingle's terminant will reproduce the original function *exactly*. Let us consider the Stieltjes function $S(\alpha)$ that we have already encountered in section 1.6

$$S(\alpha) \equiv \int_0^\infty dx e^{-x} \frac{1}{1+\alpha x}. \quad (3.19)$$

As we have already seen, $\alpha S(\alpha)$ has the following divergent asymptotic expansion

$$\alpha S(\alpha) \sim \sum_{n=0}^{\infty} (-1)^n n! \alpha^{n+1}, \quad (3.20)$$

that is, a simple sign alternating factorial. Therefore, from Eq. (3.17), the terminant is

$$T = (-1)^{N+1} \int_0^\infty dt e^{-t/\alpha} \frac{t^{N+1}}{1+t}, \quad (3.21)$$

and the terminated series is

$$\alpha S_{\text{terminated}}(\alpha) = \sum_{n=0}^N (-1)^n n! \alpha^{n+1} + (-1)^{N+1} \int_0^\infty dt e^{-t/\alpha} \frac{t^{N+1}}{1+t}. \quad (3.22)$$

Numerical evaluation of the terminated series vs. the exact Stieltjes function reveals exact agreement to any desired number of decimal places. This is just a consequence of the simplicity of the example. As it happens, the equation above is an exact one, as it can be seen from the relation

$$\frac{1}{1+\alpha x} = \sum_{n=0}^N (-1)^n (\alpha x)^n + \frac{(-\alpha x)^{N+1}}{1+\alpha x}, \quad (3.23)$$

that when inserted in Eq. (3.19), exactly reproduces Eq. (3.22). In general, things will not be so simple, and we will not obtain exact results.

3.2.2 A branch cut singularity in the Borel plane

The previous example is a very simple one, where we only have one singularity in the Borel plane (the Borel transform of Eq. (3.20) is just $\hat{R} = \frac{1}{1+t}$) which is a simple pole. As we have already discussed, in QCD, we typically expect singularities in the Borel plane to be of the form

$$\hat{R}(t) = \frac{1}{\left(1 - \frac{\beta_0}{2\pi}t\right)^{1+b}}, \quad (3.24)$$

where we have picked a singularity at $t = \frac{2\pi}{\beta_0}$. From Eq. (1.53), we know that the associated divergent series is

$$\sum_{n=0}^{\infty} \left(\frac{\beta_0}{2\pi}\right)^n \frac{\Gamma(n+1+b)}{\Gamma(1+b)} \alpha^{n+1}. \quad (3.25)$$

Therefore, from Eq. (3.16), the associated terminant is

$$T = \frac{1}{\alpha^b} \frac{1}{\Gamma(1+b)} \left(\frac{\beta_0}{2\pi}\right)^{N+1} \text{PV} \int_0^{\infty} dt e^{-t/\alpha} \frac{t^{N+1+b}}{1 - \frac{\beta_0}{2\pi}t}, \quad (3.26)$$

and the PV Borel sum of the series in Eq. (3.25) is

$$\text{PV} \int_0^{\infty} e^{-t/\alpha} \frac{1}{\left(1 - \frac{\beta_0}{2\pi}t\right)^{1+b}} = \sum_{n=0}^N \left(\frac{\beta_0}{2\pi}\right)^n \frac{\Gamma(n+1+b)}{\Gamma(1+b)} \alpha^{n+1} + T. \quad (3.27)$$

Indeed, numerical evaluation shows agreement. It is interesting noticing that on the LHS above, we have a branch cut singularity, whereas on the RHS, we take the PV over a simple pole.

3.2.3 The double Stieltjes function

We come back now to the Stieltjes functions with which we have dealt before, but with a slight twist that will let us highlight a few things. Let us consider the double Stieltjes function in the following way³

$$S_2(\alpha) \equiv S(\alpha) + S(\alpha/2). \quad (3.28)$$

where $S(\alpha)$ is the Stieltjes function. From the asymptotic expansion of the the Stieltjes function, we easily obtain the following asymptotic expansion

$$\alpha S_2(\alpha) \sim \sum_{n=0}^{\infty} (-1)^n n! \left\{1 + \frac{1}{2^n}\right\} \alpha^{n+1}. \quad (3.29)$$

Notice that the large n behavior of the coefficients of the expansion above is the *same* as for the Stieltjes function since the 1 inside braces above dominates over $1/2^n$. Consequently, the function can be terminated using the same terminant as for the Stieltjes function

$$\alpha S_{2;\text{terminated}}(\alpha) = \sum_{n=0}^N (-1)^n n! \left\{1 + \frac{1}{2^n}\right\} \alpha^{n+1} + (-1)^{N+1} \int_0^{\infty} dt e^{-t/\alpha} \frac{t^{N+1}}{1+t}. \quad (3.30)$$

³This example is drawn from [14].

Let us compare this expression against the exact result and the superasymptotic one. From Eq. (1.80), we know that the optimal truncation point for a series whose leading asymptotic behavior is $r_n^{(\text{as})} = (-1)^n n!$ is $N_* \sim 1/\alpha$. For $\alpha = 10^{-1}$, we have (we display 12 decimal places)

$$\alpha S_2(\alpha) = 0.187000424931, \quad (3.31)$$

$$\alpha S_{2;\text{superasymptotic}} = 0.187019023312, \quad (3.32)$$

$$\alpha S_{2;\text{terminated}} = 0.187000437252. \quad (3.33)$$

We see that the terminated expansion improves the result obtained by traditional asymptotics. Actually, we will now see that we can improve upon this by considering the contribution to the remainder tail of the series coming not only from the leading singularity in the Borel plane, but from the subleading ones as well.

3.3 Beyond the leading terminant

Let's get back to Eq. (3.8). So far, we have considered the contribution to r_n coming from the leading factorial divergence in r_n and associated to it a terminant. In general, we may have subleading factorial divergences as well. For instance, that is the case we had in Eq. (3.29). In general, in QCD, we expect a factorial divergence associated to each singularity in the Borel plane, where the ones closer to the origin give the leading behavior as $n \rightarrow \infty$. We will now include the contributions of this subleading terms. Being more precise, so far, we have considered a formal series R

$$R = \sum_{n=0}^{\infty} r_n \alpha^{n+1}, \quad (3.34)$$

we have superasymptotically truncated it

$$R = \sum_{n=0}^{N_{d_1}} r_n \alpha^{n+1} + \sum_{n=N_{d_1}+1}^{\infty} r_n \alpha^{n+1}, \quad (3.35)$$

we have estimated the contribution of the remainder tail of the leading factorial behavior in r_n with a terminant

$$\sum_{n=N_{d_1}+1}^{\infty} r_n^{(\text{as};d_1)} \alpha^{n+1} \sim T_{d_1}, \quad (3.36)$$

and then, written the following expression for the PV Borel sum of R

$$R_{\text{PV}} \approx \sum_{n=0}^{N_{d_1}} r_n \alpha^{n+1} + T_{d_1}, \quad (3.37)$$

where d_1 is meant to parametrize the location of the singularity in the Borel plane closest to the origin by

$$t_{d_i} = \frac{2\pi d_i}{\beta_0}. \quad (3.38)$$

Now, coming back to Eq. (3.35), we still have not accounted for most of what is in the remainder tail. In particular, the last term of the RHS below still has not been considered

$$R = \sum_{n=0}^{N_{d_1}} r_n \alpha^{n+1} + \sum_{n=N_{d_1}+1}^{\infty} r_n^{(\text{as};d_1)} \alpha^{n+1} + \sum_{n=N_{d_1}+1}^{\infty} (r_n - r_n^{(\text{as};d_1)}) \alpha^{n+1}. \quad (3.39)$$

The term

$$\sum_{n=N_{d_1}+1}^{\infty} (r_n - r_n^{(\text{as};d_1)}) \alpha^{n+1}, \quad (3.40)$$

will in general be a formal series that at some point will start to diverge as dictated by a subleading (we will assume for this section that we have many singularities in the Borel plane of \hat{R}) divergence in r_n that we call $r_n^{(\text{as}:d_2)}$. Thus, the situation is the same as we had initially, and we can truncate this series superasymptotically, and then associate a terminant to its leading divergence. That is, we write

$$R = \sum_{n=0}^{N_{d_1}} r_n \alpha^{n+1} + \sum_{n=N_{d_1}+1}^{\infty} r_n^{(\text{as}:d_1)} \alpha^{n+1} + \sum_{n=N_{d_1}+1}^{N_{d_2}} (r_n - r_n^{(\text{as}:d_1)}) \alpha^{n+1} \\ + \sum_{n=N_{d_2}+1}^{\infty} r_n^{(\text{as}:d_2)} \alpha^{n+1} + \sum_{n=N_{d_2}+1}^{\infty} (r_n - r_n^{(\text{as}:d_1)} - r_n^{(\text{as}:d_2)}) \alpha^{n+1}, \quad (3.41)$$

where N_{d_2} is the superasymptotic truncation point of the series $\sum_{n=N_{d_1}+1}^{\infty} (r_n - r_n^{(\text{as}:d_1)}) \alpha^{n+1}$. Then, just as in Eq. (3.36), we associate a terminant to the divergent tail associated to the subleading factorial divergence

$$\sum_{n=N_{d_2}+1}^{\infty} r_n^{(\text{as}:d_2)} \alpha^{n+1} \sim T_{d_2}, \quad (3.42)$$

just as we have done for the leading divergence. Of course, the values of K, A, N and σ in Eqs. (3.17) and (3.16) will be different compared to the terminant associated to the leading factorial divergence, and recall that from Eq. (1.54) $A = 1/t_i$, where t_i is the location in the Borel plane of the singularity associated to the factorial divergence we are considering. Thus, we write

$$R_{\text{PV}} = \sum_{n=0}^{N_{d_1}} r_n \alpha^{n+1} + T_{d_1} + \sum_{n=N_{d_1}+1}^{N_{d_2}} (r_n - r_n^{(\text{as}:d_1)}) \alpha^{n+1} + T_{d_2} + \sum_{n=N_{d_2}+1}^{\infty} (r_n - r_n^{(\text{as}:d_1)} - r_n^{(\text{as}:d_2)}) \alpha^{n+1}. \quad (3.43)$$

Of course, nothing stops us from systematically iterating this procedure, taking into account all the singularities in the Borel plane of \hat{R} by writing

$$R_{\text{PV}} = \sum_{i=0}^{\dots} \left\{ \sum_{n=N_{d_i}+1}^{N_{d_{i+1}}} (r_n - \sum_{j=1}^i r_n^{(\text{as}:d_j)}) \alpha^{n+1} + T_{d_{i+1}} \right\}, \quad (3.44)$$

where $N_{d_0} \equiv -1$, and d_i is meant to parametrize singularities in the Borel plane.

3.4 The hyperasymptotic expansion

Let's continue with Eq. (3.44). We have said that N_{d_1}, N_{d_2}, \dots are the orders around which the series

$$\sum_{n=N_{d_i}+1}^{\infty} (r_n - \sum_{j=1}^i r_n^{(\text{as}:d_j)}) \alpha^{n+1} \quad (3.45)$$

reaches the superasymptotic regime. Following Eq. (1.86), we will take these to be given by

$$N_{\text{P}}(d) \equiv \frac{2\pi|d|}{\beta_0 \alpha} (1 - c\alpha), \quad (3.46)$$

where the value of c is chosen as smallest as possible in absolute value, so that we do not deviate much from Eq. (1.86), while still making sure $N_{\text{P}}(d)$ is an integer for whatever value of α we are considering. We will now consider the expression in Eq. (3.44), but keeping only a few terms in the expansion, parametrized by the numbers D and N [69]. For $D = 0$, we have

$$R_{\text{PV}}^{(0,N)} \equiv \sum_{n=0}^N r_n \alpha^{n+1}, \quad (3.47)$$

and for $D > 0$

$$R_{\text{PV}}^{(D,N)} \equiv \sum_{|d| < D} S_{|d|} + \sum_{|d| \leq D} T_{|d|} + \sum_{n=N_{\text{P}}(D)+1}^{N_{\text{P}}(D)+N} (r_n - r_n^{(\text{as}:|d| \leq |D|)}) \alpha^{n+1}, \quad (3.48)$$

where the first two sums in the RHS above take all the values of d parametrizing singularities in the Borel plane of \hat{R} located at $\frac{2\pi d}{\beta_0}$, as well as the value $d = 0$. Notice that there may be more than one singularity for a $|d|$. For instance, for the case of the pole mass in the large β_0 approximation, we have seen in section 2.4 that we have singularities at $t = \pm \frac{8\pi}{\beta_0}$, and in this case, both would need to be considered. Furthermore, for $d = 0$, we write

$$S_0 \equiv \sum_{n=0}^{N_{\text{P}}(d_1)} r_n \alpha^{n+1}, \quad (3.49)$$

where d_1 parametrizes the singularity in the Borel plane of \hat{R} that lies closest to the origin. For $|d| > 0$

$$S_{|d|} \equiv \sum_{n=N_{\text{P}}(d)+1}^{N_{\text{P}}(d')} (r_n - r_n^{(\text{as}:|d| \leq |D|)}) \alpha^{n+1}, \quad (3.50)$$

where d' parametrizes the singularity in the Borel plane of \hat{R} that is next to $t = \frac{2\pi d}{\beta_0}$ in terms of distance to the origin, and we have that

$$r_n^{(\text{as}:|d| \leq |D|)} \equiv \sum_{|d|=|d_1|}^{|D|} r_n^{(\text{as}:|d|)}, \quad (3.51)$$

where $r_n^{(\text{as}:|d|)}$ is the large n factorial behavior of r_n associated to singularities located at $|t| = \frac{2\pi|d|}{\beta_0}$. We emphasize again that there may be more than one singularity with the same $|d|$, and in that case, the large n behavior associated to all of them has to be considered. Likewise, $T_{|d|}$ is meant to include all the terminants associated with singularities such that $|t| = \frac{2\pi|d|}{\beta_0}$, and in particular, we define $T_0 \equiv 0$.

Roughly speaking, D parametrizes the location of the last singularity in the Borel plane whose terminant is included in the expansion, and N tells us whether we add on top of this terminant, the series whose leading large order behavior is dictated by the singularity that is subleading to the one parametrized by D . In particular, we see that the order $(D = 0, N = N_{\text{P}}(d_1))$ gives us the superasymptotic approximation to R , and the order $(D = d_1, N = 0)$ includes the terminant associated to the leading singularity in the Borel plane on top of the superasymptotically truncated series.

The expression found in Eq. (3.47) or in Eq. (3.48) will be called throughout this thesis as the *hyperasymptotic expansion*. Hyperasymptotics [12, 13, 14] is a term denoting the improvement over a superasymptotically truncated asymptotic series using exponentially suppressed terms. It can be seen that each term in the hyperasymptotic expansion above follows this pattern of exponential suppression. We will see in the next section that the terminant T_d associated to a singularity in the Borel plane located at $t = \frac{2\pi d}{\beta_0}$, whose associated factorial divergence is $r_n^{(\text{as}:d)} = (\pm) K_d \left(\frac{\beta_0}{2\pi d} \right)^n \Gamma(n + 1 + \sigma_d)$ will have the following small α behavior

$$T_d \sim \alpha^{1/2 - \sigma_d} e^{-\frac{2\pi|d|}{\beta_0 \alpha}}, \quad (3.52)$$

so that the further away from the origin the singularity is located in the Borel plane, the more exponentially suppressed the associated terminant is. In order to obtain a rough estimate of the small α behavior of the series we add on top of the terminants, where the leading divergences of r_n are subtracted, such as the third term in the RHS of Eq. (3.43), let us consider a divergent expansion R whose Borel transform has many singularities in the

Borel plane. Let one of these singularities be parametrized by d_i , and let the next singularity in terms of distance with respect to the origin of the Borel plane be parametrized by d_f , that is, $|d_i| < |d_f|$. Then, the hyperasymptotic expansion would look

$$R_{\text{PV}} = \sum_{n=0}^{N_{\text{P}}(d_1)} r_n \alpha^{n+1} + T_{d_1} + \sum_{n=N_{\text{P}}(d_1)+1}^{N_{\text{P}}(d_2)} (r_n - r_n^{(\text{as}:d_1)}) \alpha^{n+1} \\ + \dots + T_{d_i} + \sum_{n=N_{\text{P}}(d_i)+1}^{N_{\text{P}}(d_f)} (r_n - r_n^{(\text{as}:d_1)} - \dots - r_n^{(\text{as}:d_i)}) \alpha^{n+1} + T_{d_f} + \dots \quad (3.53)$$

Let us roughly approximate

$$(r_n - r_n^{(\text{as}:d_1)} - \dots - r_n^{(\text{as}:d_i)}) \approx r_n^{(\text{as}:d_f)} = (\pm) K_{d_f} \left(\frac{\beta_0}{2\pi d_f} \right)^n \Gamma(n+1 + \sigma_{d_f}), \quad (3.54)$$

for some K_{d_f} and σ_{d_f} , and let us consider the absolute value of the fixed order term of the series in the second term of the second line in the RHS of Eq. (3.53) around $n = N_{\text{P}}(d_i) + 1$. Using Stirling's approximation for the gamma function, we can obtain the leading small α behavior

$$|r_{N_{\text{P}}(d_i)+1}^{(\text{as}:d_f)} \alpha^{N_{\text{P}}(d_i)+2}| \sim \alpha^{1/2 - \sigma_{d_f}} e^{\frac{-2\pi|d_i|}{\beta_0 \alpha} (1 + \log \frac{|d_f|}{|d_i|})}. \quad (3.55)$$

Since $|d_i| < |d_f|$, we see that

$$e^{\frac{-2\pi|d_i|}{\beta_0 \alpha}} < e^{\frac{-2\pi|d_i|}{\beta_0 \alpha} (1 + \log \frac{|d_f|}{|d_i|})} < e^{\frac{-2\pi|d_f|}{\beta_0 \alpha}}, \quad (3.56)$$

and therefore, the small α behavior of the second term on the second line on the RHS of Eq. (3.53) sits between that of T_{d_i} and T_{d_f} , and we have a hierarchy of exponentially suppressed terms in the hyperasymptotic expansion.

3.4.1 The double Stieltjes function revisited

Let us come back to the double Stieltjes function we have seen in subsection 3.2.1, and apply the ideas of the previous section. As we have seen in Eq. (3.30), we can write the terminated double Stieltjes function (times α) in the following way

$$\alpha S_{2,\text{terminated}}(\alpha) \equiv \alpha S_2^{(-\frac{\beta_0}{2\pi}, 0)}(\alpha) = \sum_{n=0}^{N_{\text{P}}(-\frac{\beta_0}{2\pi})} (-1)^n n! \left\{ 1 + \frac{1}{2^n} \right\} \alpha^{n+1} + (-1)^{N_{\text{P}}(-\frac{\beta_0}{2\pi})+1} \int_0^\infty dt e^{-t/\alpha} \frac{t^{N_{\text{P}}(-\frac{\beta_0}{2\pi})+1}}{1+t}, \quad (3.57)$$

that is, in the notation of the previous section, we have reached precision⁴ $(D, N) = (-\frac{\beta_0}{2\pi}, 0)$ in the hyperasymptotic expansion. The subleading singularity in the Borel plane is located at

$$t = -2 \implies d = -\frac{\beta_0}{\pi}, \quad (3.58)$$

and therefore, the next order in the hyperasymptotic expansion would be

$$\alpha S_2^{(-\frac{\beta_0}{2\pi}, N_{\text{P}}(-\frac{\beta_0}{2\pi}))}(\alpha) = \sum_{n=0}^{N_{\text{P}}(-\frac{\beta_0}{2\pi})} (-1)^n n! \left\{ 1 + \frac{1}{2^n} \right\} \alpha^{n+1} + (-1)^{N_{\text{P}}(-\frac{\beta_0}{2\pi})+1} \int_0^\infty dt e^{-t/\alpha} \frac{t^{N_{\text{P}}(-\frac{\beta_0}{2\pi})+1}}{1+t} \\ + \sum_{n=N_{\text{P}}(-\frac{\beta_0}{2\pi})+1}^{N_{\text{P}}(-\frac{\beta_0}{\pi})} (-1)^n n! \frac{1}{2^n} \alpha^{n+1}, \quad (3.59)$$

⁴Admittedly, the various β_0 and π factors look rather ugly here. Notice that the notation is tailored to QCD examples where renormalons are located at $t = \frac{2\pi d}{\beta_0}$, and all the awkward factors we have in this toy example simplify.

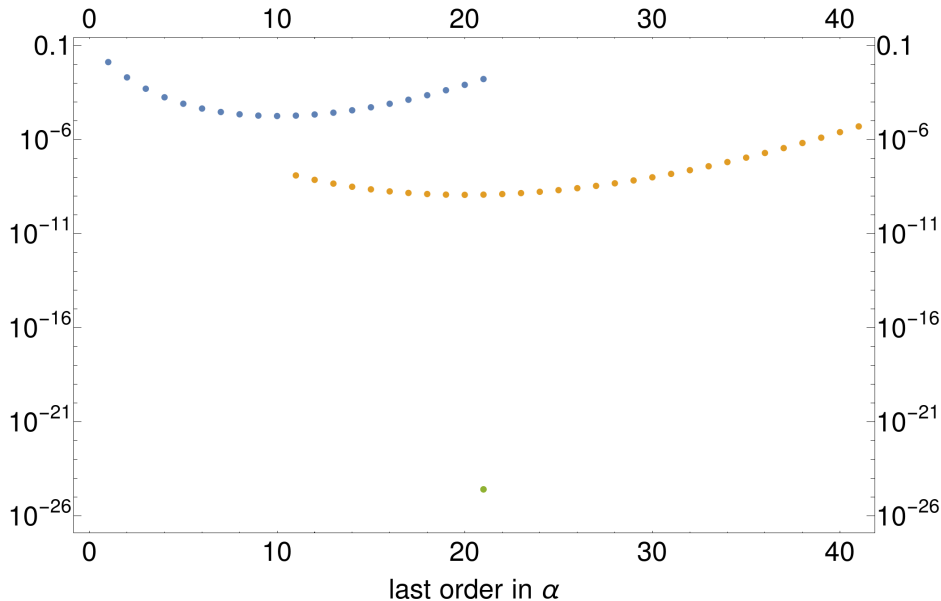


Figure 3.1: Comparison of the exact double Stieltjes function and the hyperasymptotic expansion for $\alpha = 1/10$ (notice that this implies $N_{\mathbb{P}}(-\frac{\beta_0}{2\pi}) = 10$). The blue dots denote $|S_2 - \sum_{n=0}^N (-1)^n n! (1 + \frac{1}{2^n}) \alpha^{n+1}|$. In the orange dots, we add the leading terminant, and we keep adding more terms of the second series, that is, $|S_2 - \sum_{n=0}^{10} (-1)^n n! (1 + \frac{1}{2^n}) \alpha^{n+1} - T_{-\frac{\beta_0}{2\pi}} - \sum_{n=10+1}^N (-1)^n n! \frac{1}{2^n} \alpha^{n+1}|$. For the green dot, we add the last terminant, that is, $|S_2 - \sum_{n=0}^{10} (-1)^n n! (1 + \frac{1}{2^n}) \alpha^{n+1} - T_{-\frac{\beta_0}{2\pi}} - \sum_{n=10+1}^{20} (-1)^n n! \frac{1}{2^n} \alpha^{n+1} - T_{-\frac{\beta_0}{\pi}}|$. The horizontal axis denotes the last order in α kept in series in the blue and orange dots, that is $N + 1$.

that is, we reach precision $(D, N) = (-\frac{\beta_0}{2\pi}, N_{\mathbb{P}}(-\frac{\beta_0}{2\pi}))$ in the hyperasymptotic expansion by adding the superasymptotically truncated series where the leading large n behavior associated to the leading terminant has been subtracted. We can improve upon this by adding the terminant associated to the $t = -2$ singularity

$$\begin{aligned} \alpha S_2^{(-\frac{\beta_0}{\pi}, 0)}(\alpha) &= \sum_{n=0}^{N_{\mathbb{P}}(-\frac{\beta_0}{2\pi})} (-1)^n n! \left\{ 1 + \frac{1}{2^n} \right\} \alpha^{n+1} + (-1)^{N_{\mathbb{P}}(-\frac{\beta_0}{2\pi})+1} \int_0^\infty dt e^{-t/\alpha} \frac{t^{N_{\mathbb{P}}(-\frac{\beta_0}{2\pi})+1}}{1+t} \\ &+ \sum_{n=N_{\mathbb{P}}(-\frac{\beta_0}{2\pi})+1}^{N_{\mathbb{P}}(-\frac{\beta_0}{\pi})} (-1)^n n! \frac{1}{2^n} \alpha^{n+1} + \left(-\frac{1}{2} \right)^{N_{\mathbb{P}}(-\frac{\beta_0}{\pi})+1} \int_0^\infty dt e^{-t/\alpha} \frac{t^{N_{\mathbb{P}}(-\frac{\beta_0}{\pi})+1}}{1+1/2t}, \end{aligned} \quad (3.60)$$

that is, we reach $(D, N) = (-\frac{\beta_0}{\pi}, 0)$ precision in the hyperasymptotic expansion. In Figure 3.1, we compare the exact double Stieltjes function versus the hyperasymptotic expansion. We see that by going further in the expansion, the accuracy is improved by orders of magnitude. It must be mentioned that, just as for the Stieltjes function, in this simple case, the hyperasymptotic expansion yields the exact result, and therefore, the green dot should be at 0. The fact that it is around 10^{-26} is due to the precision at which the numerical integrals in the expression of the double Stieltjes function, and the terminants have been implemented. This number can be made arbitrarily small by improving the implementation. In realistic QCD scenarios, things will not be so simple. In general, we will have an infinite tower of singularities in the Borel plane, all of which can in principle be taken into account.

In Figure 3.2, we show the behavior of the hyperasymptotic expansion for various values of α . In this figure, we observe the hierarchy of exponential suppression given in Eq. (3.56).

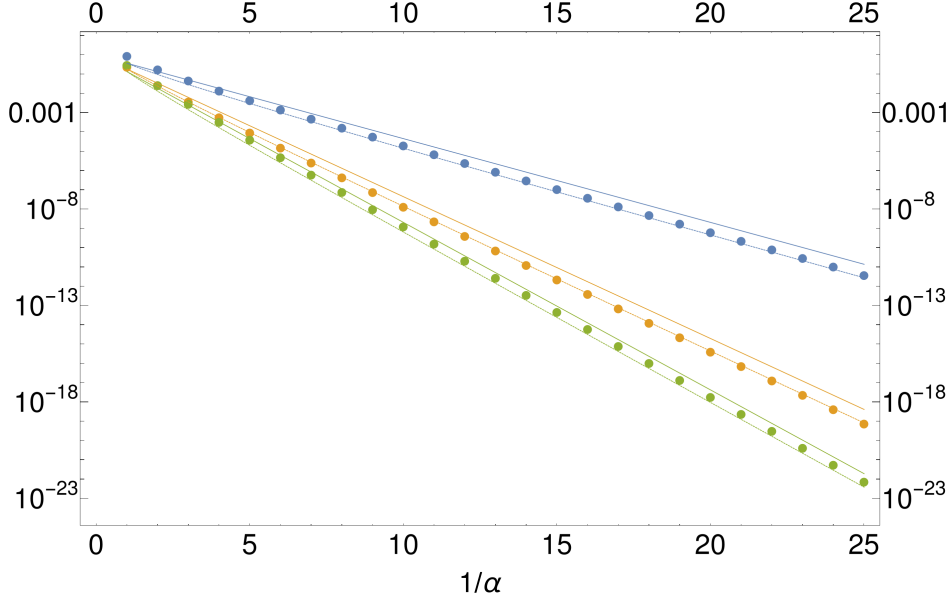


Figure 3.2: Comparison of the exact double Stieltjes function and the hyperasymptotic expansion at various orders for various values of α . The values of α have been chosen so that $N_{\text{P}}(-\frac{\beta_0}{2\pi})$ is integer, and $c = 0$ for all cases. Therefore, the horizontal axis plus 1 is the order in α at which the superasymptotic truncation is carried out. The blue dots denote $|S_2 - \sum_{n=0}^{N_{\text{P}}(-\frac{\beta_0}{2\pi})} (-1)^n n! (1 + \frac{1}{2^n}) \alpha^{n+1}|$. In the orange dots, we add the leading terminant, that is, $|S_2 - \sum_{n=0}^{N_{\text{P}}(-\frac{\beta_0}{2\pi})} (-1)^n n! (1 + \frac{1}{2^n}) \alpha^{n+1} - T_{-\frac{\beta_0}{2\pi}}|$. For the green dots, we have $|S_2 - \sum_{n=0}^{N_{\text{P}}(-\frac{\beta_0}{2\pi})} (-1)^n n! (1 + \frac{1}{2^n}) \alpha^{n+1} - T_{-\frac{\beta_0}{2\pi}} - \sum_{n=N_{\text{P}}(-\frac{\beta_0}{2\pi})+1}^{N_{\text{P}}(-\frac{\beta_0}{\pi})} (-1)^n n! \frac{1}{2^n} \alpha^{n+1}|$. The continuous blue lines are $e^{-\frac{1}{\alpha}}$ (blue), $e^{-\frac{1}{\alpha}(1+\log 2)}$ (orange) and $e^{-\frac{2}{\alpha}}$ (green). The dotted lines are the same functions multiplied by $\sqrt{\alpha}$.

3.5 Terminants in QCD

There is one last twist we need to take into account in order to apply the hyperasymptotic expansion to observables in QCD. Let us consider the perturbative expansion of an observable in QCD that has no mass dimensions

$$R = \sum_{n=0}^{\infty} r_n(\mu) \alpha^{n+1}(\mu). \quad (3.61)$$

So far, we have considered factorial divergences of the form

$$r_n^{(\text{as})} = (\pm) K A^n \Gamma(n+1+\sigma). \quad (3.62)$$

Nevertheless, we have seen in Eq. (1.68) (we write $s = l+1$ here) that in QCD one expects ($w_0 = 1$)

$$r_n^{(\text{as})}(\mu) = Z_d \left(\frac{\mu}{Q}\right)^d \left(\frac{\beta_0}{2\pi d}\right)^n \sum_{j=0}^{\infty} w_j \frac{\Gamma(n+1+l-j)}{\Gamma(1+l-j)} \quad (3.63)$$

to be the factorial divergence associated to a singularity in the Borel plane located at $t_d = \frac{2\pi d}{\beta_0}$

$$\Delta \hat{R}(t) = Z_d \left(\frac{\mu}{Q}\right)^d \frac{1}{\left(1 - \frac{\beta_0}{2\pi d} t\right)^{1+l}} \sum_{j=0}^{\infty} w_j \left(1 - \frac{\beta_0}{2\pi d} t\right)^j, \quad (3.64)$$

where notice that d can, in general, be complex. Therefore, as opposed to Eq. (3.62), one has an infinite sum of factorial divergences instead of just one. Nonetheless, it is easy to extend everything we have done so far for the realistic QCD case. Let us consider first the terminant associated to the $j = 0$ term above, and call it $\Delta\Omega(1)$. The

terminant associated to the $j = 1$ term in the sum in Eq. (3.63) is easy to write down, once one realizes that going from $j = 0$ to $j = 1$ is the same as performing $l \rightarrow l - 1$ inside the gamma functions, as well as $w_0 \rightarrow w_1$. Thus, the terminant associated to the $j = 1$ term is simply

$$w_1 \Delta\Omega(l - 1). \quad (3.65)$$

From all this, it is clear that the full terminant associated to the full divergence in Eq. (3.63) is

$$\Omega = \sum_{j=0}^{\infty} w_j \Delta\Omega(l - j). \quad (3.66)$$

We will use the symbol Ω to denote terminants associated to formal series that have no mass dimensions, that is, for instance, any terminant of the singlet static potential V would be denoted by T , and any terminant associated to rV by Ω . We will see by computing the small $\alpha(\mu)$ expansion of $\Delta\Omega(l)$ that each subsequent term in Eq. (3.66) is subleading compared to the previous one. We will now give explicit formulas for the small $\alpha(\mu)$ expansion of both $\Delta\Omega(l)$ and of Ω for IR and UV renormalons. We will start with the IR case. Let us consider the series in Eq. (3.61), and we assume the leading large n asymptotics of $r_n(\mu)$ to be dominated by a singularity in the Borel plane of \hat{R} given by

$$t = \frac{2\pi d}{\beta_0}, \quad (3.67)$$

where $d > 0$. We further assume l and the w_j coefficients of Eq. (3.63) to be determined by the procedure of section 2.6 assuming compliance with a condensate of dimension d , so that

$$r_n^{(\text{as})}(\mu) = Z_d \left(\frac{\mu}{Q}\right)^d \left(\frac{\beta_0}{2\pi d}\right)^n \sum_{j=0}^{\infty} w_j \frac{\Gamma(n+1+db-\gamma-j)}{\Gamma(1+db-\gamma-j)}, \quad (3.68)$$

where looking at Eq. (2.94), we have defined

$$\gamma \equiv \frac{2\pi\gamma_1^{(d)}}{\beta_0}, \quad (3.69)$$

for simplicity. Following the procedure outlined so far, we truncate the series in Eq. (3.61) at order $\alpha^{N_{\text{P}}(d)+1}(\mu)$, where N_{P} is given by Eq. (3.46) and the terminant associated to the $j = 0$ term in Eq. (3.63) related to aforementioned singularity is then given by Eq. (3.16)

$$\Delta\Omega_{\text{IR}}(l) \equiv Z_d \frac{\mu^d}{Q^d} \frac{1}{\Gamma(1+db-\gamma)} \left(\frac{\beta_0}{2\pi d}\right)^{N_{\text{P}}(d)+1} \alpha^{N_{\text{P}}(d)+2}(\mu) \text{PV} \int_0^{\infty} dx \frac{x^{db-\gamma+N_{\text{P}}(d)+1} e^{-x}}{1-x\frac{\beta_0\alpha(\mu)}{2\pi d}}, \quad (3.70)$$

where we remind that $l = db - \gamma$ and $w_0 = 1$. We can write the small $\alpha(\mu)$ expansion of the above equation in the following way (for details on the computation see Appendix C)

$$\begin{aligned} \Delta\Omega_{\text{IR}}(l) = & -Z_d \frac{\mu^d}{Q^d} \frac{1}{\Gamma(1+db-\gamma)} \left(\frac{2\pi d}{\beta_0}\right)^{db-\gamma+1} e^{\frac{-2\pi d}{\beta_0\alpha(\mu)}} \alpha^{1/2-db+\gamma}(\mu) \left\{ \frac{\beta_0^{1/2}}{d^{1/2}} \left[-\eta_c + \frac{1}{3} \right] \right. \\ & + \alpha(\mu) \frac{\beta_0^{3/2}}{\pi d^{3/2}} \left[-\frac{1}{12}\eta_c^3 + \frac{1}{24}\eta_c - \frac{1}{1080} \right] + \alpha^2(\mu) \frac{\beta_0^{5/2}}{\pi^2 d^{5/2}} \left[-\frac{1}{160}\eta_c^5 - \frac{1}{96}\eta_c^4 + \frac{1}{144}\eta_c^3 \right. \\ & \left. \left. + \frac{1}{96}\eta_c^2 - \frac{1}{640}\eta_c - \frac{25}{24192} \right] + \mathcal{O}(\alpha^3(\mu)) \right\}, \quad (3.71) \end{aligned}$$

where $\eta_c \equiv -db + \gamma + \frac{2\pi d}{\beta_0} c - 1$. From the above expression, we see that by performing $l \rightarrow l - 1$ in $\Delta\Omega_{\text{IR}}(l)$, we pick an extra $\alpha(\mu)$ from the $\alpha^{1/2-db+\gamma}(\mu)$ term that will make the $j = 1$ term in Eq. (3.66) subleading compared to the $j = 0$ term, or perhaps phrasing things better, only a finite amount of terms in Eq. (3.66) will contribute to each

order in $\alpha(\mu)$ in Ω_{IR} , so that knowing a finite amount of the coefficients w_j (as is the case in realistic scenarios), we can still obtain Ω_{IR} in a small $\alpha(\mu)$ expansion, and the higher the value of j in Eq. (3.66) the less important it is. By performing some algebra, we find that the small $\alpha(\mu)$ expansion of the full terminant is

$$\Omega_{\text{IR}} = K_{\text{IR}}^{(\text{P})} \frac{\mu^d}{Q^d} \left(\frac{\beta_0 \alpha(\mu)}{4\pi} \right)^{-db} e^{-\frac{2\pi d}{\beta_0 \alpha(\mu)}} \alpha^{1/2+\gamma}(\mu) \left(1 + \bar{K}_{\text{IR},1}^{(\text{P})} \alpha(\mu) + \bar{K}_{\text{IR},2}^{(\text{P})} \alpha^2(\mu) + \mathcal{O}(\alpha^3(\mu)) \right), \quad (3.72)$$

or in terms of Λ_{QCD}

$$\Omega_{\text{IR}} = K_{\text{IR}}^{(\text{P})} \frac{\Lambda_{\text{QCD}}^d}{Q^d} \alpha^{1/2+\gamma}(\mu) \left(1 + K_{\text{IR},1}^{(\text{P})} \alpha(\mu) + K_{\text{IR},2}^{(\text{P})} \alpha^2(\mu) + \mathcal{O}(\alpha^3(\mu)) \right), \quad (3.73)$$

where

$$K_{\text{IR}}^{(\text{P})} = \frac{-Z_d}{\Gamma(1+bd-\gamma)} \left(\frac{2\pi d}{\beta_0} \right)^{bd-\gamma+1} \left(\frac{\beta_0}{4\pi} \right)^{bd} \left(\frac{\beta_0}{d} \right)^{1/2} \left[-\eta_c + \frac{1}{3} \right], \quad (3.74)$$

$$\bar{K}_{\text{IR},1}^{(\text{P})} = \frac{\beta_0/(\pi d)}{-\eta_c + \frac{1}{3}} \left[-w_1(bd-\gamma) \left(\frac{1}{2}\eta_c + \frac{1}{3} \right) - \frac{1}{12}\eta_c^3 + \frac{1}{24}\eta_c - \frac{1}{1080} \right], \quad (3.75)$$

$$K_{\text{IR},1}^{(\text{P})} = \bar{K}_{\text{IR},1}^{(\text{P})} - \frac{b\beta_0 ds_1}{2\pi}, \quad (3.76)$$

$$\begin{aligned} \bar{K}_{\text{IR},2}^{(\text{P})} = & \frac{\beta_0^2/(\pi d)^2}{-\eta_c + \frac{1}{3}} \left[-w_2(bd-\gamma-1)(bd-\gamma) \left(\frac{1}{4}\eta_c + \frac{5}{12} \right) \right. \\ & + w_1(bd-\gamma) \left(-\frac{1}{24}\eta_c^3 - \frac{1}{8}\eta_c^2 - \frac{5}{48}\eta_c - \frac{23}{1080} \right) - \frac{1}{160}\eta_c^5 \\ & \left. - \frac{1}{96}\eta_c^4 + \frac{1}{144}\eta_c^3 + \frac{1}{96}\eta_c^2 - \frac{1}{640}\eta_c - \frac{25}{24192} \right], \end{aligned} \quad (3.77)$$

$$K_{2,\text{IR}}^{(\text{P})} = \frac{1}{8\pi^2} (8\pi^2 \bar{K}_{\text{IR},2}^{(\text{P})} - 4bd\pi s_1 \beta_0 \bar{K}_{\text{IR},1}^{(\text{P})} + b^2 d^2 s_1^2 \beta_0^2 + 2b^2 ds_2 \beta_0^2). \quad (3.78)$$

Let us now consider the case of an UV renormalon, that is, we consider a singularity in the Borel plane located at $t = \frac{-2\pi|d|}{\beta_0}$ where in this case $d < 0$. The Borel transform around this singularity behaves like

$$\Delta \hat{R}(t) = Z_d \frac{Q^{|d|}}{\mu^{|d|}} \frac{1}{\left(1 + \frac{\beta_0}{2\pi|d|} t\right)^{1+l'}} \sum_{j=0}^{\infty} w'_j \left(1 + \frac{\beta_0}{2\pi|d|} t\right)^j, \quad (3.79)$$

and the associated large order behavior of $r_n(\mu)$ is given by

$$r_n(\mu) \rightarrow (-1)^n Z_d \frac{Q^{|d|}}{\mu^{|d|}} \left(\frac{\beta_0}{2\pi|d|} \right)^n \sum_{j=0}^{\infty} w'_j \frac{\Gamma(n+1+l'-j)}{\Gamma(1+l'-j)}. \quad (3.80)$$

We distinguish the w_j and l we have fixed in the IR case in section 2.6, and the primed versions above. We will not encounter any UV renormalon in this thesis (except for the pole mass in the large β_0 approximation, where the Borel transform is known exactly, as we have seen in Eq. (2.47), and therefore, the terminant is exactly known anyway), so we will not bother about l' and w'_j . For more details, one can see [47]. Thus, from Eq. (3.17), we see that if we truncate the series at $\alpha^{N_{\text{P}}(d)+1}$, the terminant is

$$\Delta \Omega_{\text{UV}}(l') = (-1)^{N_{\text{P}}(d)+1} Z_d \frac{Q^{|d|}}{\mu^{|d|}} \frac{1}{\Gamma(l'+1)} \left(\frac{\beta_0}{2\pi|d|} \right)^{N_{\text{P}}(d)+1} \alpha^{N_{\text{P}}(d)+2}(\mu) \int_0^{\infty} dx \frac{e^{-x} x^{N_{\text{P}}(d)+1+l'}}{1 + \frac{x\beta_0\alpha(\mu)}{2\pi|d|}}. \quad (3.81)$$

The expression above can be written in a small $\alpha(\mu)$ expansion (see Appendix C for details)

$$\begin{aligned} \Delta \Omega_{\text{UV}}(l') = & (-1)^{N_{\text{P}}(d)+1} Z_d \frac{Q^{|d|}}{\mu^{|d|}} \frac{\pi^{1+l'} 2^{l'}}{\Gamma(l'+1)} \left(\frac{\beta_0}{|d|} \right)^{-l'-1/2} \alpha(\mu)^{1/2-l'} e^{-\frac{2\pi|d|}{\beta_0\alpha(\mu)}} \left\{ 1 + \frac{\alpha(\mu)}{\pi} \frac{\beta_0}{12|d|} [-1 + 3\eta_c^2] \right. \\ & \left. + \frac{\alpha^2(\mu)}{\pi^2} \frac{\beta_0^2}{1152|d|^2} \left[13 - 48\eta_c - 60\eta_c^2 + 48\eta_c^3 + 36\eta_c^4 \right] + \mathcal{O}(\alpha^3(\mu)) \right\}, \end{aligned} \quad (3.82)$$

where we now define $\eta_c \equiv -l' + \frac{2\pi|d|c}{\beta_0} - 1$. With this, we can compute the small $\alpha(\mu)$ expansion of the full terminant which is

$$\Omega_{\text{UV}} = K_{\text{UV}}^{(\text{P})} \frac{Q^{|d|}}{\mu^{|d|}} e^{\frac{-2\pi|d|}{\beta_0\alpha(\mu)}} \left(\frac{\beta_0\alpha(\mu)}{4\pi} \right)^{-l'} \alpha^{1/2}(\mu) \left\{ 1 + \bar{K}_{\text{UV},1}^{(\text{P})}\alpha(\mu) + \bar{K}_{\text{UV},2}^{(\text{P})}\alpha^2(\mu) + \mathcal{O}(\alpha^3(\mu)) \right\}, \quad (3.83)$$

where now

$$K_{\text{UV}}^{(\text{P})} = Z_d (-1)^{N_{\text{F}}(d)+1} \left(\frac{\beta_0}{\pi^2|d|} \right)^{-1/2} \frac{1}{\Gamma(l'+1)} \left(\frac{2}{|d|} \right)^{-l'}, \quad (3.84)$$

$$\bar{K}_{\text{UV},1}^{(\text{P})} = \left(\frac{2}{\pi} \right)^{1/2} \left(w_1' \frac{\beta_0 l'}{2\sqrt{2\pi}|d|} + \frac{\beta_0}{12|d|\sqrt{2\pi}} (-1 + 3\eta_c^2) \right), \quad (3.85)$$

$$\begin{aligned} \bar{K}_{\text{UV},2}^{(\text{P})} &= \left(\frac{2}{\pi} \right)^{1/2} \left(w_2' \frac{l'(l'-1)\beta_0^2}{4\sqrt{2}|d|^2\pi^{3/2}} + w_1' \frac{l'\beta_0^2(-1+3(\eta_c+1)^2)}{24\sqrt{2}|d|^2\pi^{3/2}} \right. \\ &\quad \left. + \frac{\beta_0^2}{1152|d|^2 2^{1/2}\pi^{3/2}} \left[13 - 48\eta_c - 60\eta_c^2 + 48\eta_c^3 + 36\eta_c^4 \right] \right). \end{aligned} \quad (3.86)$$

Before finishing this section, we take a small detour and, as an interesting aside, we mention that the expression for the terminants that we have obtained allows us to quantify the μ dependence of the truncated series

$$R_{\text{P}} \equiv \sum_{n=0}^{N_{\text{P}}(d)} r_n(\mu) \alpha^{n+1}(\mu), \quad (3.87)$$

where d parametrizes the location of the closest singularity to the origin in the Borel plane of \hat{R} . The hyperasymptotic expansion reads

$$R_{\text{PV}}(Q) = R_{\text{P}}(Q, \mu) + \Omega(\mu, Q) + \dots \quad (3.88)$$

Since the PV Borel sum is μ independent, the leading term in the μ derivative above will be given by just the terminant

$$\mu \frac{d}{d\mu} R_{\text{P}} = -\mu \frac{d}{d\mu} \Omega + \dots, \quad (3.89)$$

the dots containing terms exponentially more suppressed than the leading terminant. Therefore, plugging Eq. (3.73) (we just consider the IR case)

$$\begin{aligned} \mu \frac{d}{d\mu} R_{\text{P}} &= -K_{\text{IR}}^{(\text{P})} \left(\frac{\Lambda_{\text{QCD}}}{Q} \right)^d \alpha^{\frac{3}{2}+\gamma}(\mu) \left\{ -\frac{\beta_0}{4\pi} (1+2\gamma) \right. \\ &\quad \left. + \alpha(\mu) \frac{1}{16\pi^2} \left[-4K_{\text{IR},1}^{(\text{P})} \pi \beta_0 (3+2\gamma) - \beta_1 (1+2\gamma) \right] \right. \\ &\quad \left. + \alpha^2(\mu) \frac{1}{64\pi^3} \left[-16K_{\text{IR},2}^{(\text{P})} \pi^2 \beta_0 (2\gamma+5) - 4K_{\text{IR},1}^{(\text{P})} \pi \beta_1 (2\gamma+3) - \beta_2 (2\gamma+1) \right] + \mathcal{O}(\alpha^3(\mu)) \right\}. \end{aligned} \quad (3.90)$$

3.6 The QCD singlet static potential in the large β_0 approximation

After having seen the general case for a terminant associated to a branch point singularity on the Borel plane, we will now focus on a non-trivial, albeit simpler, QCD example: the singlet static potential in the large β_0 approximation. In this toy example, the analytically extended Borel transform is fully known, as we have seen in section 2.3, and hence, we can compute the PV Borel sum *exactly*. Consequently, we can test the hyperasymptotic expansion against the exact result, and see how well it performs.

We will now write down the form terminants take for this specific example. The first thing to keep in mind is that, as we have mentioned in section 2.3, all the singularities in the Borel plane lie on the positive real line. Furthermore,

all these singularities in the Borel plane happen to be simple poles, which simplifies the form terminants take since in Eq. (3.66), we will only have the $j = 0$ term, and thus, we will be able to know the terminant exactly. We will only consider the terminants associated to the $d = 1, 3, 5$ renormalons. Adapting Eq. (3.70) to this case, the (dimensionless) terminant associated to a singularity located at $t = \frac{2\pi d}{\beta_0}$ to be added on top of the series truncated at order $\alpha^{N_{\text{P}}(d)+1}$, whose large n behavior is dictated by the aforementioned singularity is

$$\Omega_d = Z_d(\mu r)^d \left(\frac{\beta_0}{2\pi d} \right)^{N_{\text{P}}(d)+1} \alpha^{N_{\text{P}}(d)+2}(\mu) \text{PV} \int_0^\infty dx \frac{x^{N_{\text{P}}(d)+1} e^{-x}}{1 - x \frac{\beta_0 \alpha(\mu)}{2\pi d}}, \quad (3.91)$$

and the dimensionful terminant T_d is, of course, just

$$T_d = \frac{1}{r} \Omega_d. \quad (3.92)$$

It is also instructive to consider its small $\alpha(\mu)$ expansion. Adapting Eq. (3.73)

$$\Omega_d = K_{\text{IR}}^{(\text{P})} (r \Lambda_{\text{QCD}})^d \alpha^{1/2}(\mu) \left\{ 1 + K_{\text{IR},1}^{(\text{P})} \alpha(\mu) + K_{\text{IR},2}^{(\text{P})} \alpha^2(\mu) + \mathcal{O}(\alpha^3(\mu)) \right\}, \quad (3.93)$$

where now

$$K_{\text{IR}}^{(\text{P})} = -Z_d \frac{2\pi d^{1/2}}{\beta_0^{1/2}} \left[-\eta_c + \frac{1}{3} \right], \quad (3.94)$$

$$K_{\text{IR},1}^{(\text{P})} = \frac{\beta_0/(\pi d)}{-\eta_c + \frac{1}{3}} \left[-\frac{1}{12} \eta_c^3 + \frac{1}{24} \eta_c - \frac{1}{1080} \right], \quad (3.95)$$

$$K_{\text{IR},2}^{(\text{P})} = \frac{\beta_0^2/(\pi d)^2}{-\eta_c + \frac{1}{3}} \left[-\frac{1}{160} \eta_c^5 - \frac{1}{96} \eta_c^4 + \frac{1}{144} \eta_c^3 + \frac{1}{96} \eta_c^2 - \frac{1}{640} \eta_c - \frac{25}{24192} \right], \quad (3.96)$$

and $\eta_c = \frac{2\pi d}{\beta_0} c - 1$. Note also that since in the large β_0 approximation, we only include β_0 in the running of the strong coupling, we have that $\Lambda_{\text{QCD}} = \mu e^{-2\pi/(\beta_0 \alpha(\mu))}$ exactly, and therefore, Eqs. (3.72) and (3.73) are the same. Eq. (3.91) is the expression that is used to generate all the plots that will be shown later, and is an exact expression for the terminant. Nevertheless, it is worthwhile to keep in mind that in realistic QCD examples, instead of simple poles in the Borel plane, we will have branch cuts, and we will need to consider the whole series in Eq. (3.66). Therefore, it is instructive to study how well the exact result is reproduced by the small α expansion of the terminant. This comparison is done for the terminant associated to the $u = 1/2$ renormalon in Table 3.1. We observe that the exact result is very well reproduced by the first terms of the expansion.

We will consider the case of the $\overline{\text{MS}}$ scheme and the lattice scheme, both with⁵ $n_f = 0$. Recall that, as we have seen in Eq. (A.15), in the large β_0 approximation, the scheme dependence is parametrized⁶ by c_X . For the $\overline{\text{MS}}$ scheme, we have $c_{\overline{\text{MS}}} = -5/3$. To fix c_{latt} , we have used the fact that $e^{-c_X/2} \Lambda_{\text{QCD}}^X$ is renormalization scheme independent [32]. This implies

$$c_{\text{latt}} = c_{\overline{\text{MS}}} + 2 \log \left(\frac{\Lambda_{\text{QCD}}^{\text{latt}}}{\Lambda_{\text{QCD}}^{\overline{\text{MS}}}} \right). \quad (3.97)$$

We will also need

$$\Lambda_{\text{QCD}}^{\overline{\text{MS}}} = e^{\frac{2\pi d_1}{\beta_0}} \Lambda_{\text{QCD}}^{\text{latt}}, \quad (3.98)$$

where

$$\alpha_{\overline{\text{MS}}}(\mu) = \alpha_{\text{latt}} \left\{ 1 + d_1 \alpha_{\text{latt}}(\mu) + \mathcal{O}(\alpha_{\text{latt}}^2(\mu)) \right\}, \quad (3.99)$$

⁵See [68] for an analysis also for $n_f = 3$.

⁶Do not confuse this c_X with c in Eq. (3.46).

$\overline{\text{MS}}\text{-Scheme } (n_f = 0)$					
r in r_0 units	c	$\frac{1}{r}\Omega_{\text{Exact}}$	$\left \frac{\Omega_{\text{LO}}}{\Omega_{\text{Exact}}} - 1\right \times 10^2$	$\left \frac{\Omega_{\text{NLO}}}{\Omega_{\text{Exact}}} - 1\right \times 10^3$	$\left \frac{\Omega_{\text{NNLO}}}{\Omega_{\text{Exact}}} - 1\right \times 10^4$
1.5	0.1786	8.3643	22.4162	47.5334	1969.2176
1.2	0.5693	2.9883	0.4033	24.9029	253.6241
1.0	0.8885	1.8767	3.9895	17.1315	24.5298
0.8	1.2791	1.1346	4.6169	3.8201	43.2013
0.6	0.0321	2.3128	5.1448	0.9797	9.6112
0.4	0.7419	1.2686	1.1501	2.5458	1.8752
0.2	0.2047	1.4294	1.5391	0.3529	1.5947
0.1	1.4182	0.5194	1.1653	0.2750	1.3679
0.01	0.1972	0.9148	0.6543	0.0730	0.1209
Lattice-Scheme $(n_f = 0)$					
r in r_0 units	c	$\frac{1}{r}\Omega_{\text{Exact}}$	$\left \frac{\Omega_{\text{LO}}}{\Omega_{\text{Exact}}} - 1\right \times 10^3$	$\left \frac{\Omega_{\text{NLO}}}{\Omega_{\text{Exact}}} - 1\right \times 10^4$	$\left \frac{\Omega_{\text{NNLO}}}{\Omega_{\text{Exact}}} - 1\right \times 10^5$
1.5	0.8101	0.7825	6.4931	4.4345	0.0788
1.2	1.2008	0.5624	9.5418	1.2988	4.3698
1.0	1.5200	0.3953	7.3017	3.2941	5.5745
0.8	0.1599	1.0434	9.3353	0.8118	2.3144
0.6	0.6636	0.7654	3.0040	2.8190	0.7265
0.4	1.3734	0.4195	7.0275	0.6984	2.6968
0.2	0.8362	0.6128	4.4603	1.7421	0.1626
0.1	0.2990	0.7906	3.4270	0.8249	0.6717
0.01	0.8287	0.4959	2.8716	0.7300	0.0478

Table 3.1: Values of the $d = 1$ terminant in r_0 units for the $n_f = 0$ singlet static potential in the large β_0 approximation. Ω_{Exact} corresponds to Eq. (3.91), and the LO, NLO and NNLO subscripts correspond to truncation orders inside brackets in Eq. (3.93), where the LO is just order α^0 , and so on. **Upper panel** computed in the $\overline{\text{MS}}$ scheme. **Lower panel** computed in the lattice scheme. Lattice seems to be better, but in both schemes the truncated version of the terminant approximates well the exact one.

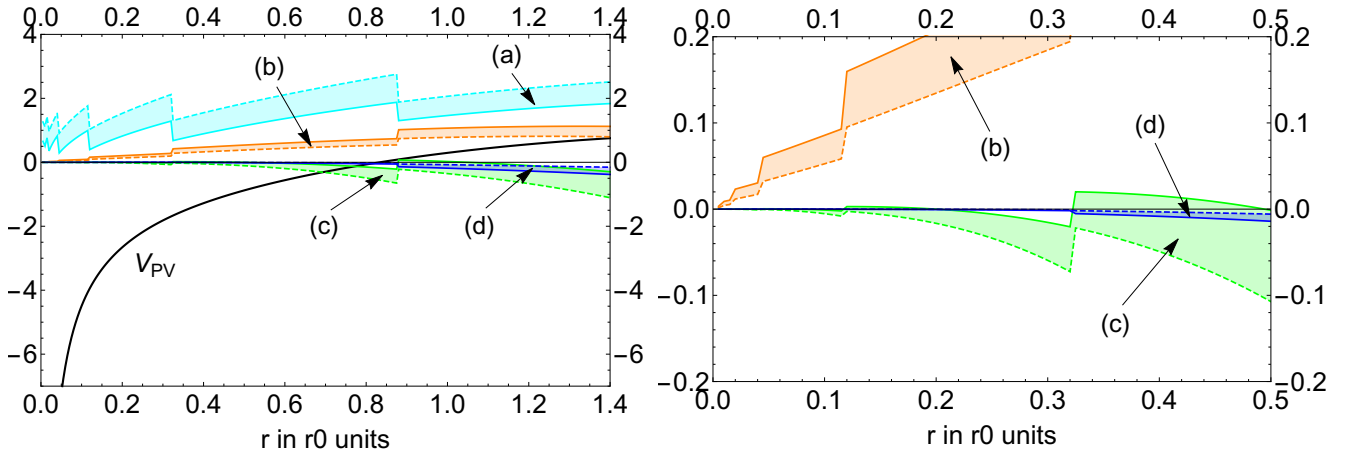


Figure 3.3: **Left panel:** We plot V_{PV} (black line) and the differences: (a) $V_{\text{PV}} - V_{\text{P}}$ (cyan), (b) $V_{\text{PV}} - V_{\text{P}} - T_1$ (orange), (c) $V_{\text{PV}} - V_{\text{P}} - T_1 - \sum_{n=N_{\text{P}}(1)+1}^{N_{\text{P}}(3)} (V_n - V_n^{(\text{as}:d=1)}) \alpha^{n+1}$ (green), and (d) $V_{\text{PV}} - V_{\text{P}} - T_1 - \sum_{n=N_{\text{P}}(1)+1}^{N_{\text{P}}(3)} (V_n - V_n^{(\text{as}:d=1)}) \alpha^{n+1} - T_3$ (blue) in the lattice scheme with $n_f = 0$ quark flavours. For each difference, the bands are generated by the difference of the prediction produced by the smallest (in absolute value) positive or negative values of c that yield integer values for N_{P} . **Right panel:** As in the left panel but with smaller vertical and horizontal range.

and [71, 72, 73] $d1 = 5.88359144663707(1)$. All of this then implies

$$c_{\text{latt}} = c_{\overline{\text{MS}}} - \frac{4\pi d_1}{\beta_0} \approx -8.38807. \quad (3.100)$$

Moreover, we remark that a change of the renormalization scheme of α in the large β_0 approximation is equivalent to a change of scale, that is, if we are in the, say, $\overline{\text{MS}}$ scheme with $\alpha_{\overline{\text{MS}}}(\mu_0)$, and then, we go to another renormalization scheme X of the strong coupling, we can have the same value of the strong coupling staying in the $\overline{\text{MS}}$ scheme and instead changing the scale to $\mu = \mu_0 \frac{\Lambda_{\overline{\text{MS}}}}{\Lambda_X}$. From Eq. (3.98), we see that for the lattice scheme we have $\mu = \mu_0 e^{\frac{2\pi d_1}{\beta_0}} \approx 29\mu_0$. In any case, we will fix the renormalization scale to $\mu = 1/r$ for both the lattice and the $\overline{\text{MS}}$ schemes. We will work in r_0 units ($r_0^{-1} \approx 400$ MeV) where we take $\Lambda_{\overline{\text{MS}}} = 0.602r_0^{-1} \approx 0.238\text{GeV}$ [74].

We will compare the exact value of the PV Borel sum of the static potential against the hyperasymptotic expansion. The first few orders read

$$V_{\text{PV}}^{\text{hyp}} = \sum_{n=0}^{N_{\text{P}}(d=1)} V_n \alpha^{n+1} + T_1 + \sum_{n=N_{\text{P}}(d=1)+1}^{N_{\text{P}}(d=3)} (V_n - V_n^{(\text{as}:d=1)}) \alpha^{n+1} + T_3 + \dots, \quad (3.101)$$

where V_n are the coefficients of the perturbative expansion of the singlet static potential in the large β_0 approximation $V = \sum_{n=0}^{\infty} V_n \alpha^{n+1}$. We will also define $V_{\text{P}} \equiv \sum_{n=0}^{N_{\text{P}}(1)} V_n \alpha^{n+1}$. We test the following stages of the hyperasymptotic expansion: $(D, N) \in \{(0, N_{\text{P}}(1)), (1, 0), (1, 2N_{\text{P}}(1)), (3, 0)\}$, that is, we evaluate:

- a) $V_{\text{PV}} - V_{\text{P}}$,
- b) $V_{\text{PV}} - V_{\text{P}} - T_1$,
- c) $V_{\text{PV}} - V_{\text{P}} - T_1 - \sum_{n=N_{\text{P}}(1)+1}^{N_{\text{P}}(3)} (V_n - V_n^{(\text{as}:d=1)}) \alpha^{n+1}$,
- d) $V_{\text{PV}} - V_{\text{P}} - T_1 - \sum_{n=N_{\text{P}}(1)+1}^{N_{\text{P}}(d=3)} (V_n - V_n^{(\text{as}:d=1)}) \alpha^{n+1} - T_3$.

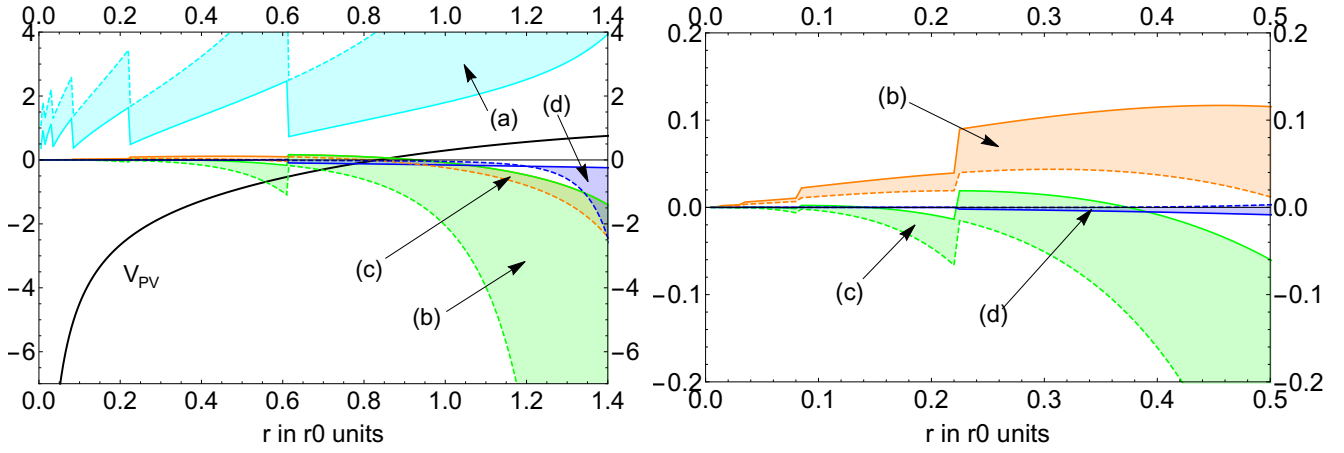


Figure 3.4: As in Figure 3.3 but in the $\overline{\text{MS}}$ scheme.

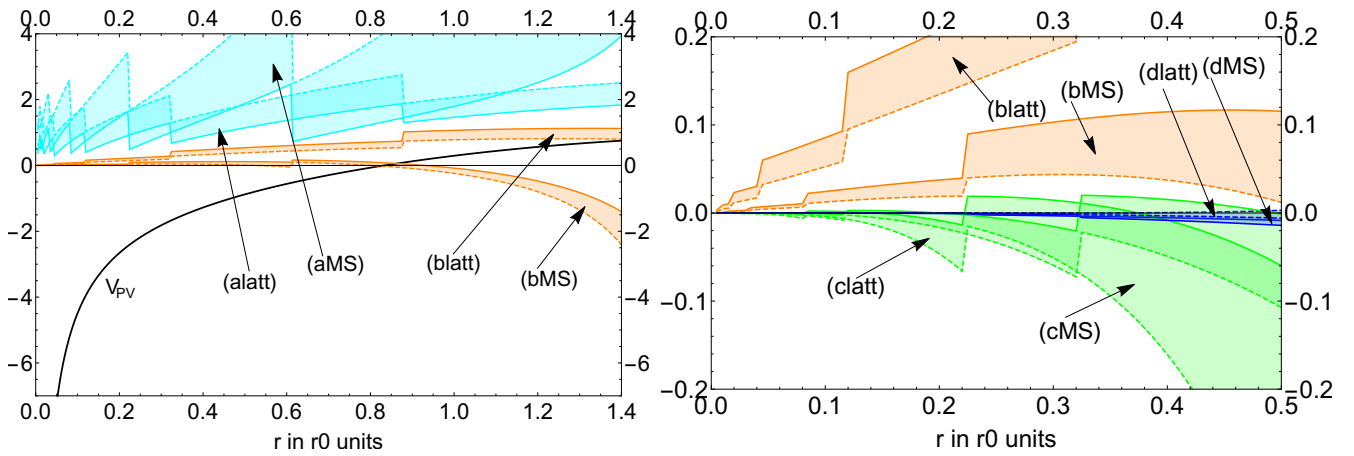


Figure 3.5: Comparison of lattice and $\overline{\text{MS}}$ scheme results for $n_f = 0$. **Left panel:** We plot V_{PV} and the differences: (a) $V_{\text{PV}} - V_{\text{P}}$ (cyan), and (b) $V_{\text{PV}} - V_{\text{P}} - T_1$ (orange). **Right panel:** Right panels of Figure 3.3 and Figure 3.4 combined.

We consider various values of r , and for each value we consider two values of c in Eq. (3.46), the positive and negative values of c that are smallest in absolute value. This way, for every value of r , and for every stage in the hyperasymptotic expansion, we have two points that form a band. The results are displayed in Figure 3.3, Figure 3.4, and Figure 3.5.

We observe a very nicely convergent pattern in all cases up to surprisingly large distances. The size of the band generated by the different values of c (in other words, the c dependence) decreases as we introduce more terms in the hyperasymptotic expansion, as we would expect. Let us now go order by order in the hyperasymptotic expansion. We observe that the r dependence of V_{PV} is basically eliminated in $V_{\text{PV}} - V_{\text{P}}$. This happens both in the lattice and $\overline{\text{MS}}$ scheme. The latter shows a stronger c dependence. This is to be expected since in the $\overline{\text{MS}}$ scheme α is bigger which makes the ambiguity in the truncation (that goes like $e^{\frac{-2\pi}{\beta_0\alpha}}$) bigger. As we can see in the left panel of Figure 3.5, both schemes yield consistent predictions for $V_{\text{PV}} - V_{\text{P}}$.

Let's now consider $V_{\text{PV}} - V_{\text{P}} - T_1$. Adding the new term gets us closer to zero than before. The width of the orange band is also considerably narrower than the cyan one. After the introduction of T_1 , the $\overline{\text{MS}}$ scheme yields more accurate results than the lattice scheme. Once $\sum_{n=N_{\text{P}}(d=1)+1}^{N_{\text{P}}(d=3)} (V_n - V_n^{(\text{as}:d=1)})\alpha^{n+1}$ is incorporated, most of the difference disappears although, the lattice scheme is marginally better. Nevertheless, after introducing T_3 , we get even closer to zero, and the $\overline{\text{MS}}$ becomes marginally better again. In any case, the difference between schemes gets smaller as we go further in the hyperasymptotic expansion.

An alternative interesting presentation of these results can be seen in Figure 3.6. Here, we take one particular value $r = 0.04 r_0 \approx 0.1 \text{ GeV}^{-1}$, and consider N_{P} values so that c is the smallest positive one ($N_{\text{P}}^{\overline{\text{MS}}}(1) = 3$ and $N_{\text{P}}^{\text{latt}}(1) = 7$). We then start by subtracting to V_{PV} the perturbative expansion at different orders (blue points) as specified in the horizontal axis. Eventually, we reach the superasymptotic regime, and at order $\alpha^{N_{\text{P}}(1)+1}$, we introduce the first terminant which greatly improves the convergence. Then, we proceed at incorporating term after term (yellow points) in $\sum_{n=N_{\text{P}}(1)+1}^{N_{\text{P}}(3)} (V_n - V_n^{(\text{as}:d=1)})\alpha^{n+1}$. Again, when the superasymptotic regime⁷ is reached, we introduce the second terminant (at the order $\alpha^{N_{\text{P}}(3)+1}$), and again, the precision is greatly improved. From this point on, we proceed in the same fashion (green points) subtracting the series whose leading large order asymptotics is dictated by the $u = 5/2$ renormalon.

We nicely see that, once reached the minimum, both lattice (empty circles) and $\overline{\text{MS}}$ (full circles) schemes yield similar precision, the only difference being that in the lattice scheme (which recall has a smaller $\alpha(1/r)$ for the same r) more terms of the perturbative expansions are needed to reach the same precision. From this, we could say that for the purpose of estimating the PV Borel sum, the smaller the renormalization scale μ the better, since we achieve the same precision with having to know less exact perturbative coefficients.

As a final plot, it is also interesting to display the hierarchy of exponentially suppressed sectors of the hyperasymptotic expansion depicted in Eq. (3.56) for this toy model. We do this⁸ in Figure 3.7, and the desired behavior is clearly displayed.

⁷Notice that the superasymptotic regime of the formal series $\sum_{n=N_{\text{P}}(d=1)+1}^{\infty} (V_n - V_n^{(\text{as}:d=1)})\alpha^{n+1}$, and of $\sum_{n=0}^{\infty} V_n\alpha^{n+1}$ are different things.

⁸This figure is for the case $n_f = 3$. We have employed $\Lambda_{\text{QCD}}^{\overline{\text{MS}}} = 0.174 \text{ GeV}$ so that $\alpha(M_\tau) \approx 0.3$.

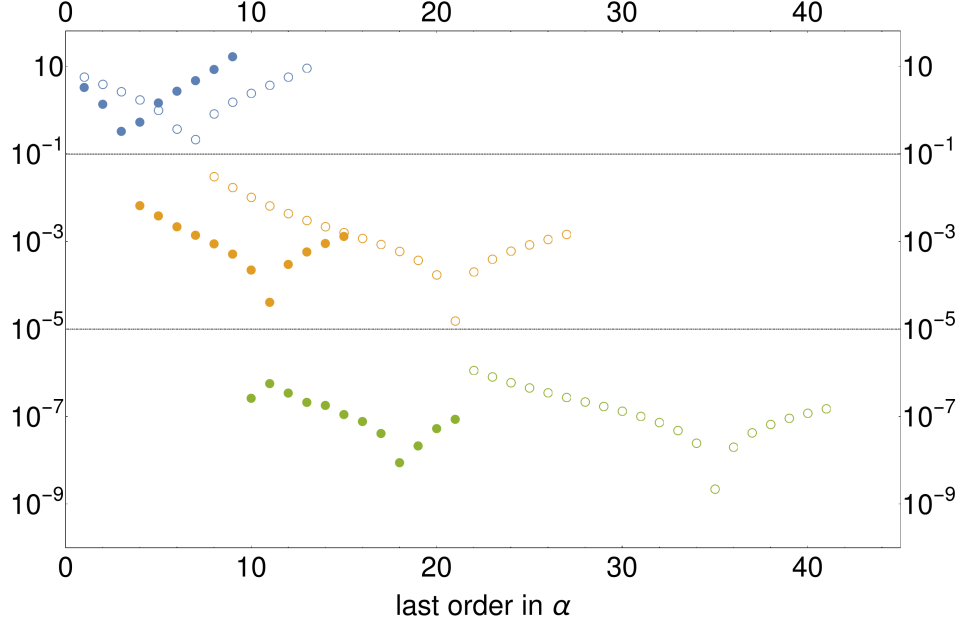


Figure 3.6: $|V_{\text{PV}} - V_{\text{PV}}^{\text{Hyperasymptotic}}|$ in r_0 units for $r = 0.04 r_0$. $N_{\text{P}}^{\overline{\text{MS}}}(1) = 3$ with $c = 1.2717$ and $N_{\text{P}}^{\text{latt}}(1) = 7$ with $c = 0.1524$. Full points have been computed in the $\overline{\text{MS}}$ scheme and empty points in the lattice scheme. Points above the horizontal line at 10^{-1} are $|V_{\text{PV}} - V_N|$ (in r_0 units) where V_N is the series of the static potential in the large β_0 approximation truncated at the order indicated in the horizontal axis. Points between the horizontal lines at 10^{-1} and 10^{-5} are $|V_{\text{PV}} - V_{\text{P}} - T_1 - \sum_{n=N_{\text{P}}(1)+1}^N (V_n - V_n^{(\text{as}:d=1)}) \alpha^{n+1}|$, where again α^{N+1} is dictated by the horizontal axis. Points below the horizontal line at 10^{-5} are $|V_{\text{PV}} - V_{\text{P}} - T_1 - \sum_{n=N_{\text{P}}(1)+1}^{N_{\text{P}}(3)} (V_n - V_n^{(\text{as}:d=1)}) \alpha^{n+1} - T_2 - \sum_{n=N_{\text{P}}(3)+1}^N (V_n - V_n^{(\text{as}:d=1)} - V_n^{(\text{as}:d=3)}) \alpha^{n+1}|$, where yet again α^{N+1} is dictated by the horizontal axis. Jumps correspond to the inclusion of the various terminants.

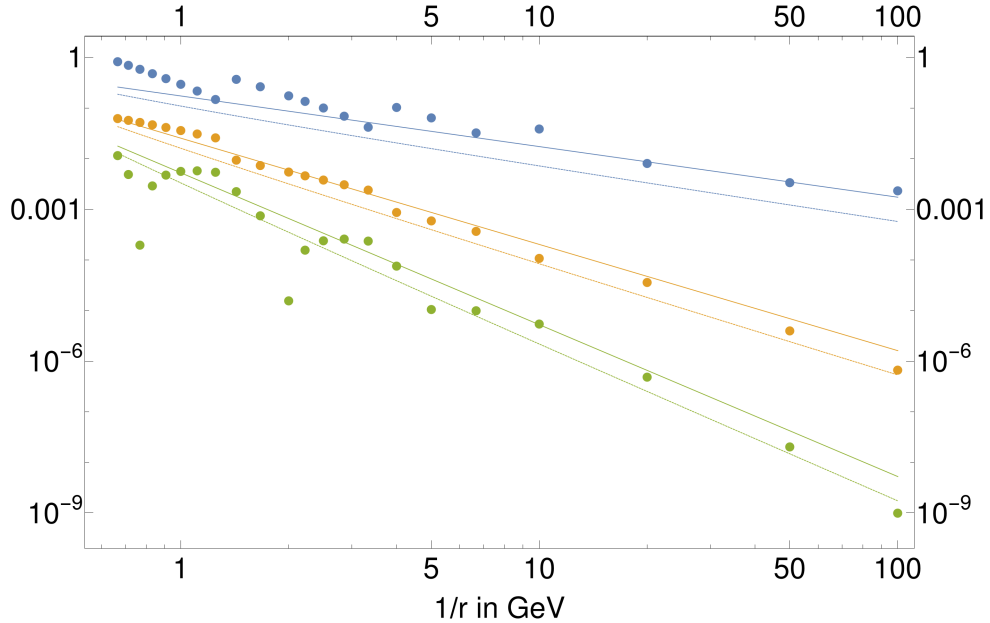


Figure 3.7: Blue points are $|r(V_{\text{PV}} - V_{\text{P}})|$, orange points are $|r(V_{\text{PV}} - V_{\text{P}}) - \Omega_1|$ and green points are $|r(V_{\text{PV}} - V_{\text{P}}) - \Omega_1 - r \sum_{n=N_{\text{P}}(1)+1}^{N_{\text{P}}(3)} (V_n - V_n^{(\text{as}:d=1)}) \alpha^{n+1}|$. They are plotted as functions of $1/r$ in logarithmic scale (which is equivalent to plotting them in terms of $1/\alpha$). In the notation (D, N) of Eq. (3.48), they correspond to $(0, N_{\text{P}}(1))$, $(1, 0)$ and $(1, 2N_{\text{P}}(1))$ respectively. The continuous lines are $e^{-\frac{2\pi}{\beta_0 \alpha}}$ (blue), $e^{-(1+\ln 3)\frac{2\pi}{\beta_0 \alpha}}$ (orange), $e^{-3\frac{2\pi}{\beta_0 \alpha}}$ (green). The dashed lines are the same functions multiplied by $\sqrt{\alpha}$. This factor $\sqrt{\alpha}$ is introduced in compliance with Eqs. (1.89) and (3.55), but is overall not too important. The computation has been done with $n_f = 3$, in the $\overline{\text{MS}}$ scheme, taking for each value of r the smallest positive value possible of c that yields integer values for N_{P} .

3.7 The pole mass in the large β_0 approximation

After having dealt with the static potential in the large β_0 approximation, we will now toy with the pole mass, also in the large β_0 approximation. The discussion will run parallel to the static potential, the main difference being that, just as we have seen in section 2.4, in addition to IR renormalons, the pole mass also has UV renormalons. The setup will be analogous to the static potential. We consider again⁹ $n_f = 0$ light quark flavors, the values of Λ_{QCD} used will be the same, and we will again consider the $\overline{\text{MS}}$ and the lattice schemes. Nevertheless, there is one caveat that we should mention regarding the schemes used. In Eq. (2.47), we have seen that the Borel transform of the pole mass depends on a function $R(u)$ that is given in Eq. (2.48), which has been computed in the $\overline{\text{MS}}$ scheme. Nonetheless, we will not be too bothered by this, and we will use the same function in the lattice scheme too. Strictly speaking, then, the object we compute in the lattice scheme is not the pole mass, but it will have the same singularity structure in the Borel plane. These singularities happen to be again simple poles, and therefore, we can obtain the exact terminant with just $\Delta\Omega$. Let us first write the case of the IR renormalons (which is analogous to what we have seen with V) located at $t_{\text{IR}} = \frac{2\pi d}{\beta_0}$, where $d > 0$, by adapting Eq. (3.70) to this case

$$\Omega_{d>0} = Z_d \frac{\mu^d}{\overline{m}^d} \left(\frac{\beta_0}{2\pi d} \right)^{N_{\text{P}}(d)+1} \alpha^{N_{\text{P}}(d)+2}(\mu) \text{PV} \int_0^\infty dx \frac{x^{N_{\text{P}}(d)+1} e^{-x}}{1 - x \frac{\beta_0 \alpha(\mu)}{2\pi d}}, \quad (3.102)$$

and of course, the dimensionful terminant is

$$T_{d>0} = \overline{m} \Omega_{d>0}. \quad (3.103)$$

Just like for the static potential, the exact expression above is what will be used to generate the figures. Nevertheless, it is instructive to also consider the small α expansion of the terminant. This is done by adapting Eq. (3.73) to this case

$$\Omega_{d>0} = K_{\text{IR}}^{(\text{P})} \frac{\Lambda_{\text{QCD}}^d}{\overline{m}^d} \alpha^{1/2}(\mu) \left\{ 1 + K_{\text{IR},1}^{(\text{P})} \alpha(\mu) + K_{\text{IR},2}^{(\text{P})} \alpha^2(\mu) + \mathcal{O}(\alpha^3(\mu)) \right\}, \quad (3.104)$$

where again

$$K_{\text{IR}}^{(\text{P})} = -Z_d \frac{2\pi d^{1/2}}{\beta_0^{1/2}} \left[-\eta_c + \frac{1}{3} \right], \quad (3.105)$$

$$K_{\text{IR},1}^{(\text{P})} = \frac{\beta_0/(\pi d)}{-\eta_c + \frac{1}{3}} \left[-\frac{1}{12} \eta_c^3 + \frac{1}{24} \eta_c - \frac{1}{1080} \right], \quad (3.106)$$

$$K_{\text{IR},2}^{(\text{P})} = \frac{\beta_0^2/(\pi d)^2}{-\eta_c + \frac{1}{3}} \left[-\frac{1}{160} \eta_c^5 - \frac{1}{96} \eta_c^4 + \frac{1}{144} \eta_c^3 + \frac{1}{96} \eta_c^2 - \frac{1}{640} \eta_c - \frac{25}{24192} \right], \quad (3.107)$$

and $\eta_c = \frac{2\pi d}{\beta_0} c - 1$. By adapting Eq. (3.81), the terminant associated to UV renormalons $t_{\text{UV}} = \frac{2\pi d}{\beta_0}$, where $d < 0$, takes the form

$$\Omega_{d<0} = (-1)^{N_{\text{P}}(d)+1} Z_d \frac{\overline{m}^{|d|}}{\mu^{|d|}} \left(\frac{\beta_0}{2\pi|d|} \right)^{N_{\text{P}}(d)+1} \alpha^{N_{\text{P}}(d)+2}(\mu) \int_0^\infty dx \frac{x^{N_{\text{P}}(d)+1} e^{-x}}{1 + x \frac{\beta_0 \alpha_X}{2\pi|d|}}. \quad (3.108)$$

The small α expansion of this terminant is obtained by adapting Eq. (3.83)

$$\Omega_{d<0} = K_{\text{UV}}^{(\text{P})} \frac{\overline{m}^{|d|}}{\mu^{2|d|}} \Lambda_{\text{QCD}}^{|d|} \alpha^{1/2}(\mu) \left\{ 1 + \bar{K}_{\text{UV},1}^{(\text{P})} \alpha(\mu) + \bar{K}_{\text{UV},2}^{(\text{P})} \alpha^2(\mu) + \mathcal{O}(\alpha^3(\mu)) \right\}, \quad (3.109)$$

⁹For an analysis of the $n_f = 3$ case (which is qualitatively the same as for $n_f = 0$) see [70].

where

$$K_{\text{UV}}^{(\text{P})} = Z_d(-1)^{N_{\text{P}}(d)+1} \left(\frac{\beta_0}{\pi^2 |d|} \right)^{-1/2}, \quad (3.110)$$

$$\bar{K}_{\text{UV},1}^{(\text{P})} = \left(\frac{2}{\pi} \right)^{1/2} \frac{\beta_0}{12|d|\sqrt{2\pi}} (-1 + 3\eta_c^2), \quad (3.111)$$

$$\bar{K}_{\text{UV},2}^{(\text{P})} = \left(\frac{2}{\pi} \right)^{1/2} \frac{\beta_0^2}{1152|d|2^{1/2}\pi^{3/2}} \left[13 - 48\eta_c - 60\eta_c^2 + 48\eta_c^3 + 36\eta_c^4 \right], \quad (3.112)$$

and $\eta_c = \frac{2\pi|d|c}{\beta_0} - 1$. As we have already mentioned, in what is to follow, we have used the exact expression for Ω_d . In full QCD we will not know the exact expressions, and therefore, it makes sense to study how well the exact result is reproduced by its small α expansion. Since the residue of the $d = 1$ renormalon of the pole mass is the residue of the $d = 1$ renormalon of the static potential divided by -2 [29], both terminants will be related by this factor -2 . Therefore, the results of Table 3.1 can be recycled with the trivial identification $r \rightarrow 1/\bar{m}$, and we see that the exact terminant is well approximated by its small α expansion. For Ω_{-2} , we compare in Table 3.2 the exact result and the truncated expansions for an illustrative set of values. We observe that the exact result is very well saturated by the first terms of the expansion.

$\overline{\text{MS}}\text{-Scheme } (n_f = 0)$						
\bar{m} in r_0^{-1}	c	$\bar{m}\Omega_{\text{Exact}}$	$\frac{\Omega_{\text{LO}}}{\Omega_{\text{Exact}}} - 1 \times 10^2$	$\frac{\Omega_{\text{NLO}}}{\Omega_{\text{Exact}}} - 1 \times 10^3$	$\frac{\Omega_{\text{NNLO}}}{\Omega_{\text{Exact}}} - 1 \times 10^4$	
0.6667	0.1786	0.2089	33.8725	147.6403	3372.6316	
0.8333	0.5693	0.0572	8.1940	93.6387	922.9926	
1	0.8885	0.0362	14.1752	45.6019	16.0275	
1.25	1.2791	0.0260	5.7282	13.6703	130.9304	
1.6667	0.0321	0.0199	12.0969	7.3724	12.2818	
2.5	0.7419	0.0094	4.9357	7.7804	6.5465	
5	0.2047	0.0042	2.9590	0.5254	4.8485	
10	1.4182	0.0018	0.2254	2.2970	2.3334	
100	0.1972	0.0001	1.2994	0.1190	0.3921	
$\text{Lattice-Scheme } (n_f = 0)$						
\bar{m} in r_0^{-1}	c	$\bar{m}\Omega_{\text{Exact}} \times 10^9$	$\frac{\Omega_{\text{LO}}}{\Omega_{\text{Exact}}} - 1 \times 10^3$	$\frac{\Omega_{\text{NLO}}}{\Omega_{\text{Exact}}} - 1 \times 10^4$	$\frac{\Omega_{\text{NNLO}}}{\Omega_{\text{Exact}}} - 1 \times 10^5$	
0.6667	0.8101	33.6426	23.0068	12.0234	0.0662	
0.8333	1.2008	26.3200	13.9400	5.2020	12.6514	
1	1.5200	21.9714	11.9588	13.8372	5.6692	
1.25	0.1599	17.2326	20.0735	0.3375	6.8312	
1.6667	0.6636	12.0608	15.0134	9.1011	3.3875	
2.5	1.3734	7.7980	1.2511	7.4890	5.3010	
5	0.8362	3.5950	14.9013	4.4611	0.5006	
10	0.2990	1.7262	4.2812	2.3903	2.5575	
100	0.8287	0.1453	9.6561	1.8908	0.1339	

Table 3.2: $\bar{m}\Omega_{-2}$ in the large β_0 approximation for $n_f = 0$ in r_0 units compared with truncated versions at different powers of α . Upper panel computed in the $\overline{\text{MS}}$ scheme. Lower panel in the lattice scheme. Lattice seems to be better, but both schemes yield very good convergence.

We are now in a position to compare the exact expression for the PV Borel sum of the pole mass

$$m_{\text{OS}}^{\text{PV}} = \bar{m} + \int_0^\infty dt e^{-t/\alpha(\mu)} \hat{M}(t), \quad (3.113)$$

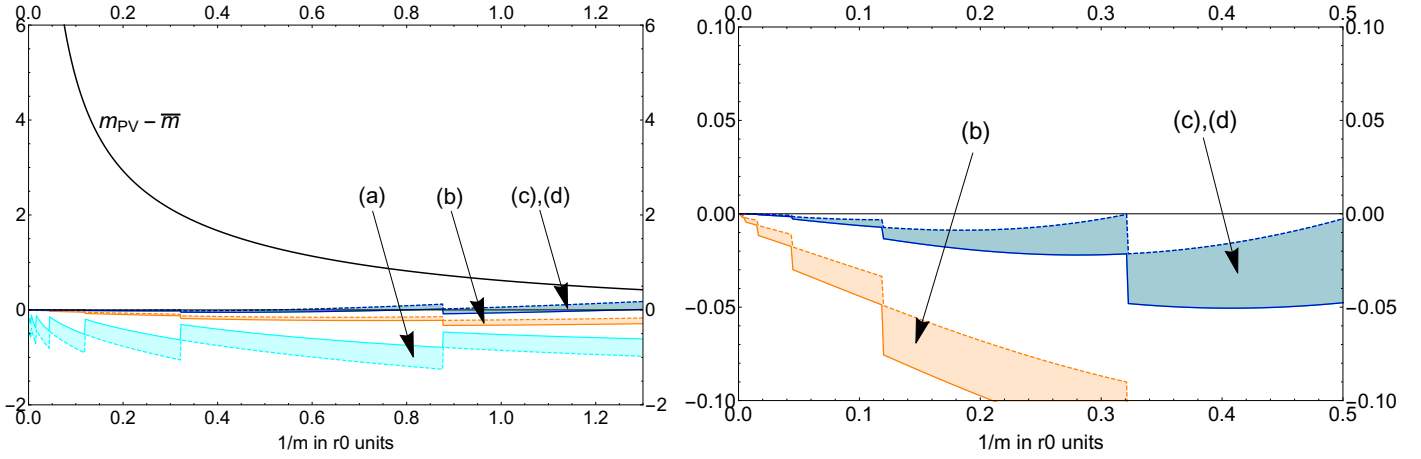


Figure 3.8: **Left panel:** We plot (in r_0 units) $m_{\text{OS}}^{\text{PV}} - \bar{m}$ (black line) and the differences: (a) $m_{\text{OS}}^{\text{PV}} - m_{\text{OS}}^{\text{P}}$ (cyan), (b) $m_{\text{OS}}^{\text{PV}} - m_{\text{OS}}^{\text{P}} - T_1$ (orange), (c) $m_{\text{OS}}^{\text{PV}} - m_{\text{OS}}^{\text{P}} - T_1 - \sum_{n=N_{\text{P}}(1)+1}^{N_{\text{P}}(-2)} (r_n - r_n^{(\text{as:d=1})}) \alpha^{n+1}$ (green), and (d) $m_{\text{OS}}^{\text{PV}} - m_{\text{OS}}^{\text{P}} - T_1 - \sum_{n=N_{\text{P}}(1)+1}^{N_{\text{P}}(-2)} (r_n - r_n^{(\text{as:d=1})}) \alpha^{n+1} - T_{-2}$ (blue) in the large β_0 approximation using the lattice scheme with $n_f = 0$ light quark flavours. The (c) and (d) bands are one on top of the other. **Right panel:** As in the left panel, but with a smaller vertical and horizontal ranges. The value of $N_{\text{P}}(1)$ depends on the scale $1/\bar{m}$ we use. For instance, for the positive c values we have: $N_{\text{P}}(1) = 9$ for $1/\bar{m} \in [0.003r_0, 0.0045r_0]$, $N_{\text{P}}(1) = 8$ for $1/\bar{m} \in [0.006r_0, 0.0015r_0]$, $N_{\text{P}}(1) = 7$ for $1/\bar{m} \in [0.0165r_0, 0.0435r_0]$, $N_{\text{P}}(1) = 6$ for $1/\bar{m} \in [0.045r_0, 0.01185r_0]$, $N_{\text{P}}(1) = 5$ for $1/\bar{m} \in [0.12r_0, 0.321r_0]$, $N_{\text{P}}(1) = 4$ for $1/\bar{m} \in [0.3225r_0, 0.876r_0]$ and $N_{\text{P}}(1) = 3$ for $1/\bar{m} \in [0.8775r_0, 1.299r_0]$.

where we recall that \hat{M} is given in Eq. (2.47), with its hyperasymptotic expansion. The first few orders read

$$m_{\text{OS}}^{\text{PV, hyp}} = \bar{m} + \sum_{n=0}^{N_{\text{P}}(1)} r_n \alpha^{n+1} + T_1 + \sum_{n=N_{\text{P}}(1)+1}^{N_{\text{P}}(-2)} (r_n - r_n^{(\text{as:d=1})}) \alpha^{n+1} + T_{-2} + \dots, \quad (3.114)$$

where the formal series of the pole mass is written $m_{\text{OS}} = \bar{m} + \sum_{n=0}^{\infty} r_n \alpha^{n+1}$, and we set throughout this section $\mu = \bar{m}$. In (D, N) notation, we will consider the orders $(D, N) \in \{(0, N_{\text{P}}(1)), (1, 0), (1, N_{\text{P}}(1)), (-2, 0)\}$, that is, we evaluate

- a) $m_{\text{OS}}^{\text{PV}} - m_{\text{OS}}^{\text{P}}$,
- b) $m_{\text{OS}}^{\text{PV}} - m_{\text{OS}}^{\text{P}} - T_1$,
- c) $m_{\text{OS}}^{\text{PV}} - m_{\text{OS}}^{\text{P}} - T_1 - \sum_{n=N_{\text{P}}(1)+1}^{N_{\text{P}}(-2)} (r_n - r_n^{(\text{as:d=1})}) \alpha^{n+1}$,
- d) $m_{\text{OS}}^{\text{PV}} - m_{\text{OS}}^{\text{P}} - T_1 - \sum_{n=N_{\text{P}}(1)+1}^{N_{\text{P}}(-2)} (r_n - r_n^{(\text{as:d=1})}) \alpha^{n+1} - T_{-2}$,

where we have defined the superasymptotically truncated pole mass

$$m_{\text{OS}}^{\text{P}} \equiv \bar{m} + \sum_{n=0}^{N_{\text{P}}(1)} r_n \alpha^{n+1}. \quad (3.115)$$

Analogously to what we had for the static potential, we again consider various values of \bar{m} , and for each value, we consider two values of c in Eq. (3.46), the positive and negative values that are smallest in absolute value and yield integer values of N_{P} . The results are displayed in Figure 3.8, Figure 3.9 and Figure 3.10.

Just as with the static potential, we observe a nicely convergent pattern in all cases down to surprisingly small scales. The main difference is that the second terminant T_{-2} , that is, the one associated to the first UV renormalon gives a very small contribution overall, in particular in the lattice scheme. This small contribution of the second

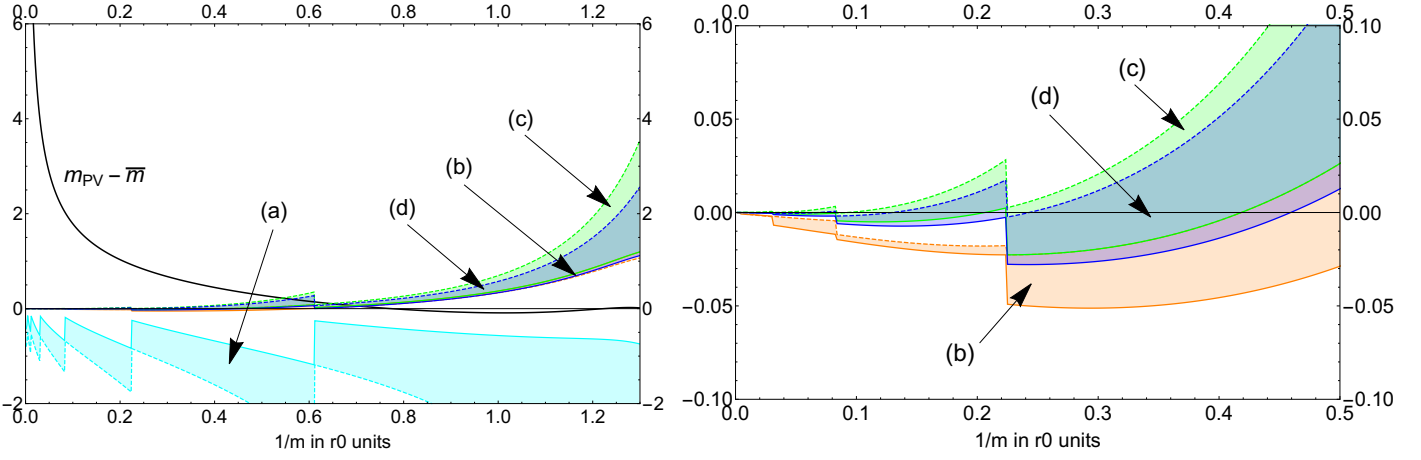


Figure 3.9: As in Figure 3.8, but in the $\overline{\text{MS}}$ scheme. The values of $N_{\text{P}}(1)$ for positive c are: $N_{\text{P}}(1) = 6$ for $1/m = 0.003r_0$, $N_{\text{P}}(1) = 5$ for $1/m \in [0.0045r_0, 0.0105r_0]$, $N_{\text{P}}(1) = 4$ for $1/m \in [0.012r_0, 0.03r_0]$, $N_{\text{P}}(1) = 3$ for $1/m \in [0.0315r_0, 0.0825r_0]$, $N_{\text{P}}(1) = 2$ for $1/m \in [0.084r_0, 0.2235r_0]$, $N_{\text{P}}(1) = 1$ for $1/m \in [0.225r_0, 0.6105r_0]$ and $N_{\text{P}}(1) = 0$ for $1/m \in [0.612r_0, 1.5r_0]$.

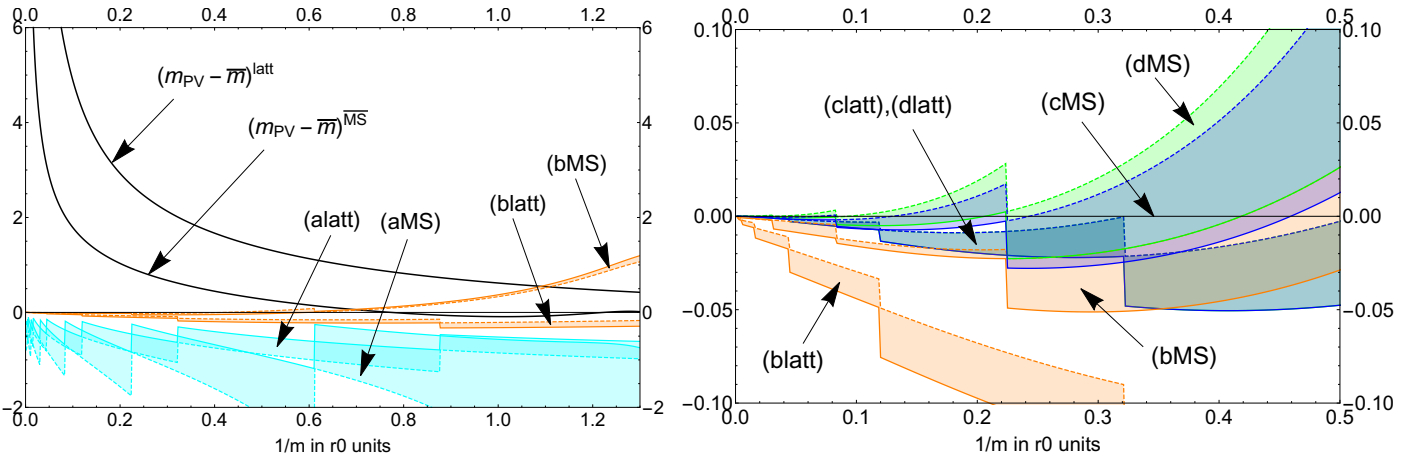


Figure 3.10: Comparison of lattice and $\overline{\text{MS}}$ scheme results for $n_f = 0$ obtained in Figs. Figure 3.8 and Figure 3.9. **Left panel:** We plot $m_{\text{OS}}^{\text{PV}} - \bar{m}$ and the differences: (a) $m_{\text{OS}}^{\text{PV}} - m_{\text{OS}}^{\text{P}}$, and (b) $m_{\text{OS}}^{\text{PV}} - m_{\text{OS}}^{\text{P}} - T_1$. **Right panel:** Lower panel Figs. 3.8 and 3.9 combined.

terminant is due to the fact that around the order $\alpha^{N_{\text{P}}(-2)+1}$, the series $\sum_{n=N_{\text{P}}(1)+1}^{\infty} (r_n - r_n^{(\text{as}:d=1)})\alpha^{n+1}$ is still not dominated by the $d = -2$ renormalon, and therefore, the optimal truncation formula we have obtained in Eq. (1.86) fails because to obtain it, we have assumed the series to be saturated by the renormalon around the truncation point. The reason is that, even though we would expect from Eq. (1.69) that, the further away from the origin a singularity in the Borel plane is located (for singularities with the same s , which since all of them are simple poles is the case), the smaller its contribution to the large n asymptotics to be, this can be spoiled if the residues Z_d of some singularities are very suppressed. This is indeed the case for UV renormalons in the pole mass. Notice that all singularities in the Borel plane of the pole mass stem from the following term in the Borel transform Eq. (2.47)

$$e^{-cxu} 6(1-u) \frac{\Gamma(u)\Gamma(1-2u)}{\Gamma(3-u)} - \frac{3}{u}. \quad (3.116)$$

Consequently, in the Laurent expansion of this term around the singularities located at $u = d/2$, they all pick a $e^{-cx d/2}$ factor. For the schemes we have considered $c_X < 0$, and therefore, for IR renormalons with $d > 0$, we have an exponential boost to Z_d , but for UV renormalons that have a negative d , we have an exponential suppression of Z_d . Because of this, it is possible for an IR renormalon that is further away from the origin than an UV one to dominate the coefficients, or at least to contribute quite sizably to them. This is exactly what happens with the $d = -2$ and $d = 3$ renormalons in the pole mass. This explains the modest contribution of the inclusion of T_{-2} in the hyperasymptotic series. The effect is more pronounced in the lattice scheme because c_{latt} is considerably bigger in absolute value than $c_{\overline{\text{MS}}}$. In any case, the convergence is still quite good, and the inclusion of the $d = 3$ terminant makes things even better as it is seen in Figure 3.11 .

Let us discuss the results in more detail. We first observe that the \overline{m} dependence of $m_{\text{OS}}^{\text{PV}}$ is basically eliminated in $m_{\text{OS}}^{\text{PV}} - m_{\text{OS}}^{\text{P}}$, as expected. This happens both in the lattice and $\overline{\text{MS}}$ scheme. The latter shows a stronger c dependence. This is to be expected, as in the $\overline{\text{MS}}$, we truncate at smaller orders which makes the truncation ambiguity bigger. As we can see in the left panel of Figure 3.10, both schemes yield consistent predictions for $m_{\text{OS}}^{\text{PV}} - m_{\text{OS}}^{\text{P}}$. We can draw some interesting observations out of this analysis. Since the lattice scheme works better than the $\overline{\text{MS}}$ scheme, specially for lower mass scales (and keeping in mind that, as we have said earlier, the lattice scheme can be considered the $\overline{\text{MS}}$ scheme with a larger renormalization scale μ), to evaluate $m_{\text{OS}}^{\text{PV}} - m_{\text{OS}}^{\text{P}}$ it seems that working with a larger renormalization scale may be better, at least if enough coefficients of the perturbative expansion can be obtained.

We now turn to $m_{\text{OS}}^{\text{PV}} - m_{\text{OS}}^{\text{P}} - T_1$. Adding the first terminant brings much better agreement with expectations, and we get closer to zero. After the introduction of T_1 , the $\overline{\text{MS}}$ scheme yields more accurate results than the lattice scheme. This can already be seen in the left panel of Figure 3.10, and in greater detail in the right panel of said figure. Once $\sum_{n=N_{\text{P}}(-2)}^{N_{\text{P}}(1)+1} (r_n - r_n^{(\text{as}:d=1)})\alpha^{n+1}$ is incorporated in the prediction, most of the difference between schemes disappears. As we have already discussed, the effect of introducing T_{-2} is very small, in particular in the lattice scheme. In any case, the difference between schemes gets smaller and smaller as we go to higher orders in the hyperasymptotic expansion, in particular at short distances. We also want to stress that this analysis opens the window to apply perturbation theory at rather large distances. Note that in the left panel plots in Figure 3.8, Figure 3.9, and Figure 3.10, we have gone to very large distances. It would be interesting to see if the same happens beyond the large β_0 approximation.

We can display the convergence in the same fashion it was done in Figure 3.6, by showing what happens order by order. In analogy with the plot of the static potential, where we took $r = 0.04 r_0$, we now take $\overline{m} = 25 r_0^{-1}$

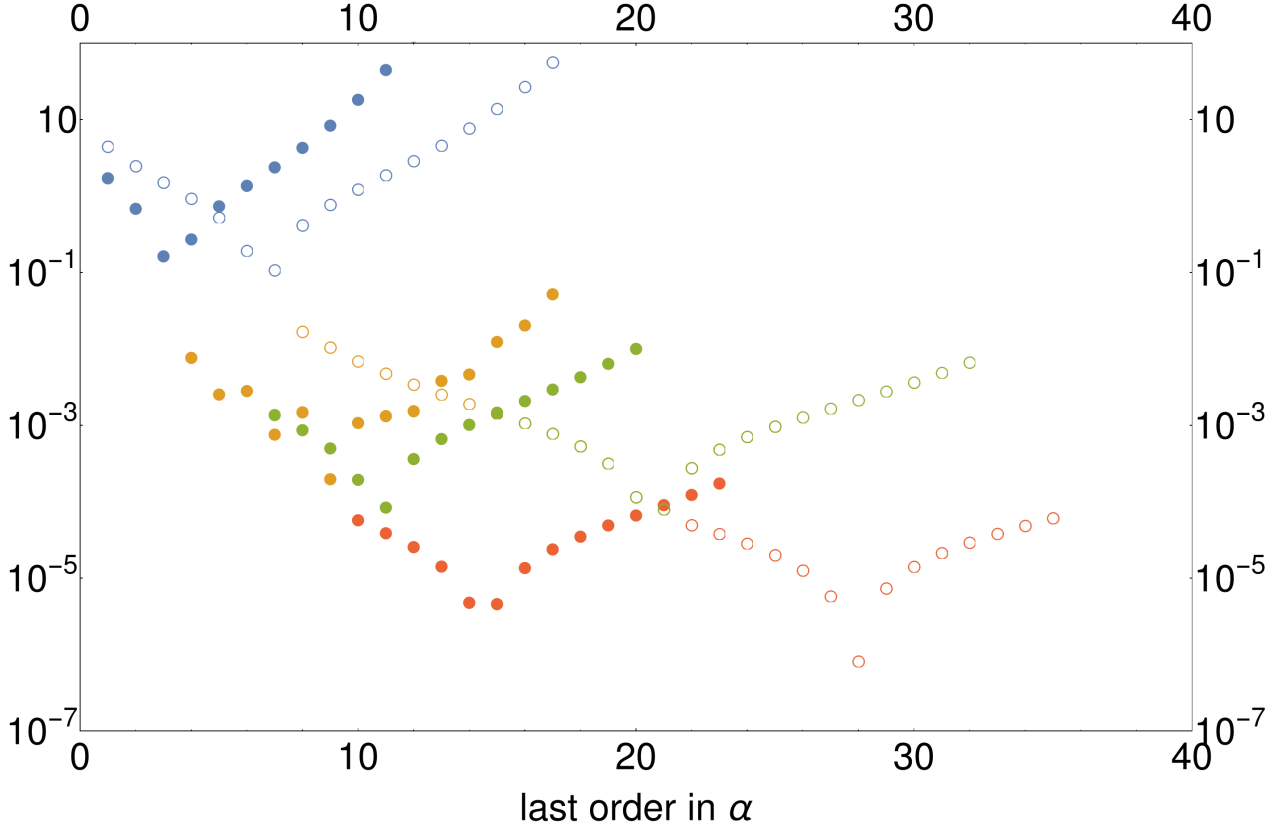


Figure 3.11: $|m_{\text{OS}}^{\text{PV}} - m_{\text{OS}}^{\text{PV,hyp}}|$ in r_0 units for $n_f = 0$ and $\bar{m} = 25 r_0^{-1}$. Full/Empty circles correspond to the $\overline{\text{MS}}$ /lattice scheme. We choose the smallest positive c that yields an integer value of N_{P} : $N_{\text{P}}^{\overline{\text{MS}}}(1) = 3$ with $c = 1.2717$ and $N_{\text{P}}^{\text{latt}}(1) = 7$ with $c = 0.1524$. Blue points are $|m_{\text{OS}}^{\text{PV}} - M_N|$, where the order at which the series of the pole mass is truncated α^{N+1} is specified in the horizontal axis. Orange points are $|m_{\text{OS}}^{\text{PV}} - m_{\text{OS}}^{\text{P}} - T_1 - \sum_{n=N_{\text{P}}(1)+1}^N (r_n - r_n^{(\text{as}:d=1)}) \alpha^{n+1}|$. Green points are $|m_{\text{OS}}^{\text{PV}} - m_{\text{OS}}^{\text{P}} - T_1 - \sum_{n=N_{\text{P}}(1)+1}^{N_{\text{P}}(-2)} (r_n - r_n^{(\text{as}:d=1)}) \alpha^{n+1} - T_{-2} - \sum_{n=N_{\text{P}}(-2)+1}^N (r_n - r_n^{(\text{as}:d=1)} - r_n^{(\text{as}:d=-2)}) \alpha^{n+1}|$. Red points are $|m_{\text{OS}}^{\text{PV}} - m_{\text{OS}}^{\text{P}} - T_1 - \sum_{n=N_{\text{P}}(1)+1}^{N_{\text{P}}(-2)} (r_n - r_n^{(\text{as}:d=1)}) \alpha^{n+1} - T_{-2} - \sum_{n=N_{\text{P}}(-2)+1}^{N_{\text{P}}(3)} (r_n - r_n^{(\text{as}:d=1)} - r_n^{(\text{as}:d=-2)}) \alpha^{n+1} - T_3 - \sum_{n=N_{\text{P}}(3)+1}^N (r_n - r_n^{(\text{as}:d=1)} - r_n^{(\text{as}:d=-2)} - r_n^{(\text{as}:d=3)}) \alpha^{n+1}|$. Notice that all terms have a series that is truncated at order α^{N+1} as specified in the horizontal axis. The jumps correspond to the inclusion of the various terminants.

and consider the N_{P} with the smallest positive c (notice that since $1/25 = 0.04$, the values of N_{P} and c will be the same here as we had in Figure 3.6: $N_{\text{P}}^{\overline{\text{MS}}}(1) = 3$ with $c = 1.2717$ and $N_{\text{P}}^{\text{latt}}(1) = 7$ with $c = 0.1524$). The numbers are shown in Figure 3.11. We find that the inclusion of the $d = 1$ terminant improves the convergence, and just as we have seen earlier, the $d = -2$ renormalon is barely visible, specially in the lattice where we see that the inclusion of the terminant does not seem to do much, and we have a seamless transition between the yellow and green points. Nevertheless, we also find that the inclusion of the $d = 3$ renormalon once again introduces a nice converging pattern. All of this is in agreement with the discussion we have had around Eq. (3.116), where we have remarked that UV renormalons are suppressed with respect to IR renormalons.

Just as we saw in Figure 3.6, both schemes yield similar precision, but in the lattice scheme (bigger scale μ) more terms of the perturbative expansions are needed to reach the same precision. One important lesson one may extrapolate from this exercise is that, if the number of perturbative coefficients is limited, the smaller the renormalization scale μ , the better since one can obtain much better precision for an equal number of perturbative coefficients.

Chapter 4

Approximating the PV Borel sum: Method 2

This chapter can be skipped on a first reading without losing continuity with the rest of the thesis. In the previous chapter, a method to systematically approximate the PV Borel sum of a formal series, making use of a truncated series and knowledge of the singularities in the Borel plane has been introduced. In this chapter, we will also relate the PV Borel sum with a truncated series, but in a different way. The method relies on an equation first written by Stevenson [64], and further polished on the works of Maxwell [75], Chyla and Burdick [65, 66], and Acoleyen and Verschelde [67]. The outline of the method is as follows: we will consider a formal series in perturbative QCD where the renormalization scale is fixed at a particular value $\mu = Q$

$$R = \sum_{n=0}^{\infty} r_n(\mu = Q) \alpha^{n+1}(\mu = Q). \quad (4.1)$$

Let's assume that the IR renormalon that lies closest to the origin in the Borel plane is located at

$$t = \frac{d_0 2\pi}{\beta_0}. \quad (4.2)$$

Then, from Eq. (1.86), we know the optimal truncation point is around

$$N_{\star} = \frac{d_0 2\pi}{\beta_0 \alpha(\mu)}. \quad (4.3)$$

We will run the renormalization scale in Eq. (4.1), and consider a slight variation of the equation above, where the truncation point and the scale at which the series will be evaluated will be correlated in the following way

$$R_{N_A} \equiv \sum_{n=0}^{N_A} r_n(\mu) \alpha^{n+1}(\mu), \quad (4.4)$$

where

$$N_A \equiv \frac{2\pi d_0}{\beta_0 \alpha(\mu)} (1 - c' \alpha(Q)), \quad (4.5)$$

and c' is some positive and small number. We will then consider the $N_A \rightarrow \infty$ limit of Eq. (4.4) (notice that this also implies $\mu \rightarrow \infty$)

$$\lim_{N_A \rightarrow \infty} R_{N_A}. \quad (4.6)$$

Quite surprisingly, the limit above yields a *finite* number(!), despite the fact that the series in Eq. (4.1) is divergent. That is, considering a particular correlation between the truncation order and the scale at which the renormalization

scale is evaluated as given by Eq. (4.5), we are able to obtain a convergent series which actually gives a sum when the whole infinite series is considered. In addition to this, we will see that this sum can be related with the PV Borel sum, using knowledge about the renormalon closest to the origin. Admittedly, the steps above look rather mysterious at this point, so we will review in the next section the rationale behind them. This chapter is based on [68].

4.1 The method

The origin of this discussion is a paper by Stevenson [64]. In this paper, the following sign alternating factorially divergent series was considered¹

$$R = \sum_{n=0}^{\infty} (-1)^n n! \alpha_0^{n+1}, \quad (4.7)$$

where α_0 is a small expansion parameter. Then, he considers the following equation

$$\alpha = \frac{\alpha_0}{1 + \tau \alpha_0}, \quad (4.8)$$

where τ is a real number, and re-expands the formal series above in the expansion parameter α

$$R = \sum_{n=0}^{\infty} (-1)^n n! \sum_{m=0}^n \frac{1}{m!} (-\tau)^m \alpha^{n+1}. \quad (4.9)$$

The inspiration for the transformation in Eq. (4.8) is the one loop relation between the coupling at some scale Q $\alpha_0 \equiv \alpha(Q)$ and the coupling at some other scale $\alpha(\mu)$

$$\alpha(\mu) = \frac{\alpha(Q)}{1 + \alpha(Q) \frac{\beta_0}{2\pi} \log \frac{\mu}{Q}}, \quad (4.10)$$

where we would have $\tau = \frac{\beta_0}{2\pi} \log \frac{\mu}{Q}$. Stevenson then considers the truncated version of Eq. (4.9)

$$R_N(\tau) \equiv \sum_{n=0}^N (-1)^n n! \sum_{m=0}^n \frac{1}{m!} (-\tau)^m \alpha^{n+1}, \quad (4.11)$$

and uses the so called principle of minimal sensitivity² [76] to obtain an “optimal” value of τ which itself depends on the truncation order N

$$\tau_{\text{optimal}} = \chi'_{\text{Stevenson}} N - \frac{1}{2} \frac{\chi'_{\text{Stevenson}}}{1 + \chi'_{\text{Stevenson}}} \log(N+1) + \mathcal{O}(1), \quad (4.12)$$

where $\chi'_{\text{Stevenson}} \approx 0.278$. Then, it is proved that when one evaluates the series in Eq. (4.11) taking $N \rightarrow \infty$, one obtains

$$\lim_{N \rightarrow \infty} R_N(\tau_{\text{optimal}}) = \int_0^{1/\chi'} dt e^{-t/\alpha_0} \frac{1}{1+t}, \quad (4.13)$$

¹Being accurate, Stevenson actually considered $R = \sum_{n=0}^{\infty} (-1)^n n! \frac{\alpha_0^{n+1}}{\pi^{n+1}}$. We have ignored the π -s to simplify the expressions employed.

²Very briefly, the principle of minimal sensitivity is defined as follows. One considers perturbative expansions of physical quantities $\sum_{n=0}^{\infty} r_n(\mu) \alpha^{n+1}(\mu)$ evaluated at the renormalization scale μ , and then, the truncated version $R_N \equiv \sum_{n=0}^N r_n(\mu) \alpha^{n+1}(\mu)$. Motivated by the fact that physical quantities do not depend on μ , the principle of minimal sensitivity posits that the optimal scale μ_{optimal} on which to evaluate the series is the one for which the dependence on μ of the truncated series is minimal. Thus, one considers $\frac{dR_N}{d\mu} = 0$, or equivalently $\frac{dR_N}{d\tau} = 0$.

which is a finite number. That is, beginning with a divergent expansion, imposing a renormalization scale dictated by the principle of minimal sensitivity, which depends on the truncation order of the series, leads to an expansion that is convergent. Furthermore, noticing that the Borel transform of the series in Eq. (4.7) is

$$\hat{R}(t) = \frac{1}{1+t}, \quad (4.14)$$

we see that the sum of the series in Eq. (4.11), as dictated by the principle of minimal sensitivity, is the Borel sum of the series in Eq. (4.7), where the integral of the Laplace transform is cut-off at a finite value

$$\lim_{N \rightarrow \infty} R_N(\tau_{\text{optimal}}) = \int_0^{1/\chi'} dt e^{-t/\alpha_0} \hat{R}(t). \quad (4.15)$$

This is the key equation we are interested at. Later work generalized this result. In [75], the result in Eq. (4.15) was generalized to a wider class of sign alternating series, and shown to depend on the Borel transform of the formal series in question having a finite radius of convergence.

The consideration of series with fixed sign diverging behavior was done by Chyla et al. in [65, 66]. For sign alternating series, the principle of minimal sensitivity yields a relation between the renormalization scale and the truncation order as given by Eq. (4.12), which is the key in obtaining a finite sum for the infinite series. Applying the principle of minimal sensitivity to fixed sign factorially diverging series does not work, but Chyla et al. observed that we can still consider, analogously to Eq. (4.12), the relation

$$\tau_N = \chi' N, \quad (4.16)$$

provided that $1/\chi' < \rho$, where ρ is the radius of convergence in the t plane of the Borel transform of the formal series. Furthermore, they showed that the linear dependence in N , as given by Eq. (4.16), is the only type of N dependence τ can have to obtain a non-trivial (that is, finite but non-zero) limit for the truncated formal series when $N \rightarrow \infty$. The procedure proposed by Chyla et al. obtains a finite sum for a divergent series, that however, depends on an arbitrary constant χ' , whose only constraint is for its inverse to lie inside the radius of convergence of the Borel transform of the formal series.

The result obtained by Chyla et al. was rederived in [67] by Acoleyen et al. employing a different method that implements the method of steepest descent. Furthermore, the authors were able to obtain the corrections in $1/N$ of Eq. (4.15). The outline of their method is as follows. They considered formal series of physical quantities evaluated at some renormalization scale Q

$$R = \sum_{n=0}^{\infty} r_n(Q) \alpha^{n+1}(Q), \quad (4.17)$$

and they again considered the one loop scale transformation given by Eq. (4.10), and rewrote the series in terms of $\alpha(\mu)$

$$R = \sum_{n=0}^{\infty} r_n(\mu) \alpha^{n+1}(\mu). \quad (4.18)$$

They then truncate the series above

$$R_N(\mu) = \sum_{n=0}^N r_n(\mu) \alpha^{n+1}(\mu), \quad (4.19)$$

and consider a scale change that depends on the truncation order

$$\mu_N = Q e^{N\chi/2}, \quad (4.20)$$

where notice that the equation above is the same as Eq. (4.16) since trivial algebra in the above equation implies

$$\frac{\beta_0}{2\pi} \log \frac{\mu_N}{Q} = \tau = \frac{\beta_0}{4\pi} \chi N, \quad (4.21)$$

and trivially defining³ $\chi' \equiv \frac{\beta_0}{4\pi} \chi$

$$\tau = \chi' N, \quad (4.22)$$

just as in Eq. (4.16). The scale change in Eq. (4.20) is considered at one loop, and then it is proved that for large N

$$\lim_{N \rightarrow \infty} R_N(\mu_N) = \int_0^{1/\chi'} dt e^{\frac{-t}{\alpha(Q)}} \hat{R}(t), \quad (4.23)$$

where above we have the Borel transform of the series in Eq. (4.17)

$$\hat{R}(t) = \sum_{n=0}^{\infty} \frac{r_n(Q)}{n!} t^n. \quad (4.24)$$

Eq. (4.23) is precisely the result that Chyla et al. derived using another method. Also, as we have already mentioned, Acoleyen et al. also gave the leading corrections in inverse powers of N of Eq. (4.23).

We haven't explicitly mentioned it so far, but with Eq. (4.23), we can obtain the PV Borel sum from the truncated series by noticing

$$\int_0^{1/\chi'} dt e^{\frac{-t}{\alpha(Q)}} \hat{R}(t) = \text{PV} \int_0^{\infty} dt e^{\frac{-t}{\alpha(Q)}} \hat{R}(t) - \text{PV} \int_{1/\chi'}^{\infty} dt e^{\frac{-t}{\alpha(Q)}} \hat{R}(t), \quad (4.25)$$

and thus, using Eq. (4.23)

$$\text{PV} \int_0^{\infty} dt e^{\frac{-t}{\alpha(Q)}} \hat{R}(t) = \lim_{N \rightarrow \infty} R_N(\mu_N) + \text{PV} \int_{1/\chi'}^{\infty} dt e^{\frac{-t}{\alpha(Q)}} \hat{R}(t). \quad (4.26)$$

That is, to obtain the PV Borel sum of Eq. (4.17), we need to consider the truncated series of Eq. (4.19) with the relation between truncation order and renormalization scale of Eq. (4.20), take the $N \rightarrow \infty$ limit, and add on top of that

$$\text{PV} \int_{1/\chi'}^{\infty} dt e^{\frac{-t}{\alpha(Q)}} \hat{R}(t). \quad (4.27)$$

Eq. (4.26) has an arbitrary parameter χ' . We have earlier said that $1/\chi'$ has to be smaller than the radius of convergence of the Borel transform ρ , but other than that, we have not imposed further constraints. In [67], it was seen that the value of χ' that made the cut-off Borel sum

$$\int_0^{1/\chi'} dt e^{\frac{-t}{\alpha(Q)}} \hat{R}(t) \quad (4.28)$$

closest to the actual PV Borel sum is such that $1/\chi'$ is slightly less than the first IR renormalon (located at $t_0 \equiv \frac{2\pi d_0}{\beta_0}$) of the Borel transform⁴. Therefore, they chose

$$\frac{1}{\chi'} = \frac{2\pi d_0}{\beta_0} (1 - c' \alpha(Q)), \quad (4.29)$$

³As we have mentioned after Eq. (4.16), $1/\chi'$ has to be smaller than the radius of convergence of the Borel transform in the t plane. χ plays the role that χ' plays in the u plane.

⁴Notice that, in general, there can be UV renormalons closer than the leading IR one. Actually, this is the case that is considered in the paper by Acoleyen et al. in [67], where they talk about the Adler function in the large β_0 approximation, which has an IR renormalon at $u = 2$ and an UV one at $u = -1$.

where $c' > 0$ is a strictly positive number. We will also see that this choice of χ' makes Eq. (4.27) scale like the leading condensate in an OPE⁵. Different terms coming from $\hat{R}(t)$ contribute to Eq. (4.27) differently. The most important one is the one associated to the leading IR renormalon (notice that we pick R with no mass dimensions)

$$\Delta\hat{R}_{\text{IR}}^{(d_0)}(t) \equiv Z_{d_0} \frac{1}{(1-t/t_0)^{1+l}} \sum_{j=0}^{\infty} w_j (1-t/t_0)^j, \quad (4.30)$$

for some Z_{d_0} , w_j and l . For simplicity, for now, we will only consider the $j=0$ term above (in Appendix D it can be seen that further j terms are subleading)

$$\Delta\hat{R}_{\text{IR}}^{(d_0)}|_{j=0}(t) \equiv Z_{d_0} \frac{1}{(1-t/t_0)^{1+l}} = Z_{d_0} \frac{1}{(1-\frac{\beta_0}{2\pi d_0}t)^{1+l}}. \quad (4.31)$$

Thus, from Eq. (4.27), we obtain

$$\text{PV} \int_{1/\chi'}^{\infty} dt e^{\frac{-t}{\alpha(Q)}} \Delta\hat{R}_{\text{IR}}^{(d_0)}|_{j=0}(t) = Z_{d_0} \times \text{PV} \int_{1/\chi'}^{\infty} dt e^{\frac{-t}{\alpha(Q)}} \frac{1}{(1-\frac{\beta_0}{2\pi d_0}t)^{1+l}} \quad (4.32)$$

$$= Z_{d_0} \times \text{PV} \int_{\frac{2\pi d_0}{\beta_0}(1-c'\alpha(Q))}^{\infty} dt e^{\frac{-t}{\alpha(Q)}} \frac{1}{(1-\frac{\beta_0}{2\pi d_0}t)^{1+l}} \quad (4.33)$$

$$= Z_{d_0} \frac{2\pi d_0}{\beta_0} \alpha^{-l}(Q) e^{\frac{-2\pi d_0}{\beta_0 \alpha(Q)}} \times \text{PV} \int_{-c'}^{\infty} dx e^{\frac{-2\pi d_0}{\beta_0}x} \frac{1}{(-x)^{1+l}}, \quad (4.34)$$

where we have substituted the value of χ' of Eq. (4.29), and we have factored out all the $\alpha(Q)$ dependence from inside the integral by performing the variable change

$$x = \frac{1}{\alpha(Q)} \left(-1 + \frac{\beta_0}{2\pi d_0} t \right). \quad (4.35)$$

Defining

$$\Psi \equiv \text{PV} \int_{-c'}^{\infty} dx e^{\frac{-2\pi d_0}{\beta_0}x} \frac{1}{(-x)^{1+l}}, \quad (4.36)$$

we see that Eq. (4.26) basically becomes

$$\text{PV} \int_0^{\infty} dt e^{\frac{-t}{\alpha(Q)}} \hat{R}(t) = \lim_{N \rightarrow \infty} R_N(\mu_N) + Z_{d_0} \frac{2\pi d_0}{\beta_0} \alpha^{-l}(Q) e^{\frac{-2\pi d_0}{\beta_0 \alpha(Q)}} \Psi + \dots, \quad (4.37)$$

and we see that analogously to the method of chapter 3, we obtain the PV Borel sum by adding terms that are exponentially suppressed in negative inverse powers of the strong coupling. As we have already mentioned, by considering terms other than $j=0$ in Eq. (4.30), we obtain subleading corrections to the above equation. In particular, from Eq. (D.4), we know that they amount to

$$\text{PV} \int_0^{\infty} dt e^{\frac{-t}{\alpha(Q)}} \hat{R}(t) = \lim_{N \rightarrow \infty} R_N(\mu_N) + Z_{d_0} \frac{2\pi d_0}{\beta_0} \alpha^{-l}(Q) e^{\frac{-2\pi d_0}{\beta_0 \alpha(Q)}} \sum_{j=0}^{\infty} w_j \alpha^j(Q) \Psi|_{l \rightarrow l-j} + \dots \quad (4.38)$$

The dots in the RHS of the above equation contain the contributions to Eq. (4.27) coming from further singularities in the Borel plane, as well as the analytic part. It can be seen (see Appendix D) that the contributions coming from these terms have the same parametric dependence in $\alpha(Q)$, and thus, all need to be taken into account at the same time. Fleshing out the content hidden in the dots above, we have

$$\text{PV} \int_0^{\infty} dt e^{\frac{-t}{\alpha(Q)}} \hat{R}(t) = \lim_{N \rightarrow \infty} R_N(\mu_N) + Z_{d_0} \frac{2\pi d_0}{\beta_0} e^{\frac{-2\pi d_0}{\beta_0 \alpha(Q)}} \left\{ \alpha^{-l}(Q) \sum_{j=0}^{\infty} w_j \alpha^j(Q) \Psi|_{l \rightarrow l-j} + \mathcal{O}(\alpha(Q)) \right\}, \quad (4.39)$$

⁵The relation between χ' and non-perturbative terms was also appreciated in the papers of chyla et al. [65, 66].

where we are blind to the last $\mathcal{O}(\alpha(Q))$ terms quoted above. Notice that if l and w_j are fixed according to the method of section 2.6 with Eq. (2.94) and so on, we have that

$$l = d_0 b - \gamma, \quad (4.40)$$

where we have defined

$$\gamma \equiv \frac{2\pi\gamma_1}{\beta_0}, \quad (4.41)$$

and therefore, recalling Eq. (2.72), we have that Eq. (4.39) becomes a correction in powers of Λ_{QCD}

$$\text{PV} \int_0^\infty dt e^{\frac{-t}{\alpha(Q)}} \hat{R}(t) = \lim_{N \rightarrow \infty} R_N(\mu_N) + Z_{d_0} \frac{2\pi d_0}{\beta_0} \left(\frac{\beta_0}{4\pi} \right)^{bd_0} \Psi \left(\frac{\Lambda_{\text{QCD}}}{Q} \right)^{d_0} \alpha^\gamma(Q) \{1 + \mathcal{O}(\alpha(Q))\}, \quad (4.42)$$

where we have only explicitly written the leading small $\alpha(Q)$ behavior.

4.1.1 Beyond one loop running in Eq. (4.19)

Let us come back to the relation of Eq. (4.16)

$$\frac{\beta_0}{2\pi} \log \frac{\mu}{Q} = \chi' N. \quad (4.43)$$

This relation between μ and N has been key in obtaining the results outlined in the previous section. Let us write the relation implied by the above equation between $\alpha(\mu)$ and N using the 1 loop relation on Eq. (4.10)

$$N = \frac{2\pi d_0}{\beta_0 \alpha(\mu)} (1 - c' \alpha(Q)) - \frac{2\pi d_0}{\beta_0 \alpha(Q)} (1 - c' \alpha(Q)). \quad (4.44)$$

It can be seen that we need not restrict ourselves to one loop running when writing down Eq. (4.18), as long as we keep the relation between $\alpha(\mu)$ and N as dictated by the equation above. Therefore, considering the running at any loop order will yield the same limit for Eq. (4.19) for $N \rightarrow \infty$, so we might as well stick with 1 loop running for simplicity. Furthermore, it can be seen that dropping the constant term in Eq. (4.44) also yields the same limit. Thus, we will in fact take

$$N_A \equiv \frac{2\pi d_0}{\beta_0 \alpha(\mu)} (1 - c' \alpha(Q)), \quad (4.45)$$

which is the relation we have mentioned in Eq. (4.5), and the one we will use with Method 2.

A few words about c' . As we have seen around Eq. (4.29), c' is a strictly positive number: $c' > 0$. Nonetheless, we should try to keep $c' \alpha(Q)$ close to zero, so as to not deviate much from the optimal truncation formula. Nonetheless, we will see later that we should neither take c' too close to zero, because the leading power correction diverges logarithmically in c' (at least in the large β_0 approximation). Usually, keeping $c' \sim 1$ will be fine. Also, it should be mentioned that in the large β_0 approximation, there is a value of c' that makes the leading power correction vanish, as we will later see.

4.2 The QCD singlet static potential in the large β_0 approximation

We will now test Eq. (4.39) against the exact formula of the PV Borel sum of the QCD singlet static potential in the large β_0 approximation. Adapting Eq. (4.39) to this case by including the leading $d = 1$ renormalon that we have seen in section 2.3, we get

$$V_{\text{large } \beta_0}^{\text{PV}} = V_A - \frac{4C_F}{\beta_0} \tilde{\Lambda} \text{Ei} \left(\frac{2\pi c'}{\beta_0} \right) + \mathcal{O}(\alpha(1/r)), \quad (4.46)$$

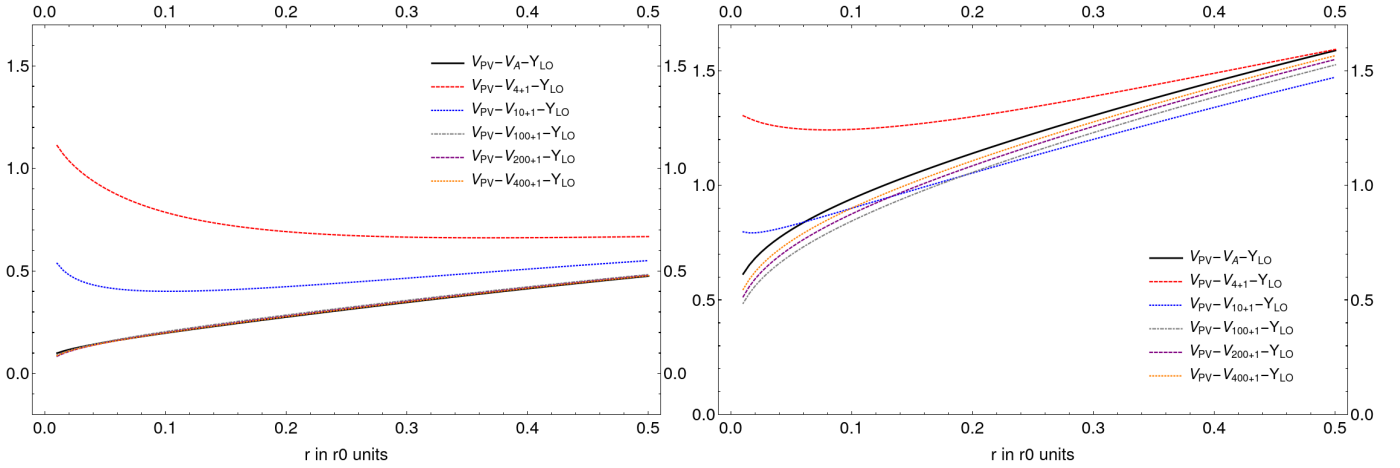


Figure 4.1: **Left panel:** We plot $V_{PV} - V_A - \Upsilon_{LO}$ for $n_f = 0$ in the $\overline{\text{MS}}$ scheme with $c' = 1$ versus the truncated sums $V_{PV} - \sum_{n=0}^{N_A} V_n \alpha^{n+1}(\mu) - \Upsilon_{LO}$, where μ is fixed using N_A defined in Eq. (4.45). **Right panel:** As in the left panel, but in the lattice scheme.

where we have defined⁶

$$V_A \equiv \lim_{N_A \rightarrow \infty} \sum_{n=0}^{N_A} V_n^{\text{large } \beta_0}(\mu(N_A)) \alpha^{n+1}(\mu(N_A)) = \int_0^{\frac{2\pi}{\beta_0}(1-c'\alpha(1/r))} dt e^{-t/\alpha(1/r)} \hat{V}_{\text{large } \beta_0}(t), \quad (4.47)$$

where μ and N_A are correlated as given by Eq. (4.45), we have chosen $Q = 1/r$, and we have defined

$$\tilde{\Lambda} \equiv e^{-c_X/2} \Lambda_{\text{QCD}}, \quad (4.48)$$

where the exponential integral function is

$$\text{Ei}(x) = -\text{PV} \int_{-x}^{\infty} dt \frac{e^{-t}}{t}. \quad (4.49)$$

For future ease, we also define

$$\Upsilon_{LO} \equiv -\frac{4C_F}{\beta_0} \tilde{\Lambda} \text{Ei}\left(\frac{2\pi c'}{\beta_0}\right). \quad (4.50)$$

In Eq. (4.47), we see that V_A is an infinite series. In realistic QCD scenarios, we will not be able to sum the infinite series, nor will we have the full Borel transform to implement the RHS of Eq. (4.47), so it is interesting to consider how high in N_A one needs to go in practice so that we converge to the infinite sum. In Figure 4.1, we can see this for both the $\overline{\text{MS}}$ and lattice schemes. The values of Λ_{QCD} and c_X have been chosen as in section 3.6. We see that we do reach agreement with the limiting value, but that we have to go to rather high values of N_A . This problem can be severe if one tries to apply the method to realistic QCD examples, where at most we will have a handful of exact coefficients. Luckily, we find that the use of the asymptotic expression for the coefficients for $n > N^*$ (~ 3 in the $\overline{\text{MS}}$ and ~ 8 in the lattice scheme) is very efficient, and basically yields the same results as the exact result. Nonetheless, it must not be forgotten that in realistic QCD examples, the asymptotic coefficients will not be known exactly, as in this toy example, and thus, this could jeopardize the whole method. We also mention that numerics suggests that for a given r value, the smaller $\chi - 2$ is, the larger N_A has to be to achieve convergence. Nevertheless, you cannot compare different $\chi - 2$ values for different values of r as also, in general, as r becomes smaller, convergence is reached at higher N_A -s.

⁶Do not confuse this V_A with the V_A of Eq. (G.12) in the context of pNRQCD.

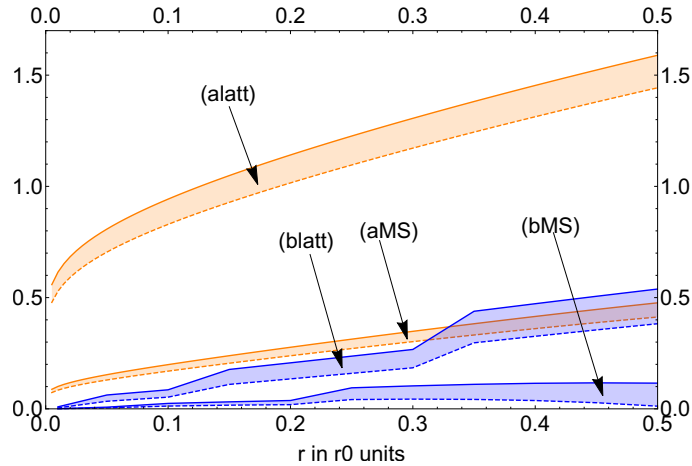


Figure 4.2: We plot (a) $V_{\text{PV}} - V_A - \Upsilon$ for $n_f = 0$ in the lattice and $\overline{\text{MS}}$ scheme. For each case, we generate bands by computing V_A with $c' = 1$ and $c' = c'_{\text{min}} = 0.652$, where c'_{min} is chosen such that $\Upsilon(c'_{\text{min}}) = 0$. We also compare with (b) $V_{\text{PV}} - V_P - \frac{1}{r}\Omega_1$ obtained with method 1 with the bands generated for Fig. 3.5.

Finally, we can compare how well method 2 fares against method 1. We have displayed this in Figure 4.2, where we have included bands taken from Figure 3.5. In both cases, we add a term proportional to Λ_{QCD} on top of a truncated series (although, keep in mind that the parametric dependence in α is not exactly the same, being method 1 the more precise one since $\frac{1}{r}\Omega_1 \sim \Lambda_{\text{QCD}}\alpha^{1/2}$ and $\Upsilon \sim \Lambda_{\text{QCD}}$). We see that method 1 does a better job of approximating the PV Borel sum, for both lattice and $\overline{\text{MS}}$, and that $\overline{\text{MS}}$ works slightly better in both cases.

4.2.1 Alternative method

For the case of the static potential, there is an alternative method to compute the difference between the truncated static potential and the PV Borel sum, by adapting the steps of some papers by Sumino [77, 78, 79, 80]. As a bonus, we will see that this alternative path will allow us to compute subleading $\mathcal{O}(\alpha(1/r))$ terms in Eq. (4.46) that we were unable to obtain before. We will now review these steps. In these papers, Sumino considered the singlet static potential in the large β_0 approximation

$$V_{\text{large } \beta_0} = \sum_{n=0}^{\infty} V_n^{\text{large } \beta_0} \alpha^{n+1}, \quad (4.51)$$

and recall that in Eq. (2.27), we have seen this series to be

$$V_{\text{large } \beta_0} = \frac{-2C_F\alpha(\mu)}{\pi} \sum_{n=0}^{\infty} \int_0^{\infty} dq \frac{\sin(qr)}{qr} \left\{ \frac{\beta_0\alpha(\mu)}{4\pi} \log\left(\frac{\mu^2}{q^2} e^{-cx}\right) \right\}^n. \quad (4.52)$$

He then truncated it at order α^N

$$V_N \equiv \sum_{n=0}^{N-1} V_n(\mu) \alpha^{n+1}(\mu), \quad (4.53)$$

where⁷

$$N = \frac{2\pi d}{\beta_0\alpha(\mu)} \Delta. \quad (4.54)$$

⁷Notice that Eq. (4.54) is slightly different to the convention we have been following in this thesis where we truncate series at α^{N+1} where $N \sim \frac{2\pi d}{\beta_0\alpha}$.

For now, we will leave Δ general, and will come back to it later. Thus, we have

$$V_N \equiv \frac{-2C_F\alpha(\mu)}{\pi} \sum_{n=0}^{N-1} \int_0^\infty dq \frac{\sin(qr)}{qr} \left\{ \frac{\beta_0\alpha(\mu)}{4\pi} \log \left(\frac{\mu^2}{q^2} e^{-cx} \right) \right\}^n \quad (4.55)$$

$$= \frac{-2C_F\alpha(\mu)}{\pi} \int_0^\infty dq \frac{\sin(qr)}{qr} \frac{1-L^N}{1-L}, \quad (4.56)$$

where we have defined

$$L \equiv \frac{\beta_0\alpha(\mu)}{4\pi} \log \left(\frac{\mu^2}{q^2} e^{-cx} \right). \quad (4.57)$$

By virtue of Eq. (4.54), we notice that

$$L = 1 + \frac{d\Delta}{N} \log \frac{\tilde{\Lambda}}{q}, \quad (4.58)$$

where we have defined

$$\tilde{\Lambda} \equiv e^{-cx/2} \Lambda_{\text{QCD}}. \quad (4.59)$$

Substituting Eq. (4.58) in Eq. (4.56)

$$V_N = \frac{4C_F}{\beta_0} \int_0^\infty dq \frac{\sin(qr)}{qr} \frac{1}{\log \frac{\tilde{\Lambda}}{q}} \left\{ 1 - \left[1 + \frac{d\Delta}{N} \log \frac{\tilde{\Lambda}}{q} \right]^N \right\}, \quad (4.60)$$

and we see that we have traded all explicit α dependence in V_N for N dependence. Sumino then makes a variable change

$$k = \frac{q}{\tilde{\Lambda}}, \quad (4.61)$$

and he also redefines⁸ $\rho \equiv \tilde{\Lambda}r$, so that

$$V_N = \frac{4C_F}{\beta_0} \tilde{\Lambda} \int_0^\infty dk \frac{\sin(k\rho)}{k\rho} \frac{1}{-\log k} \left\{ 1 - \left[1 - \frac{d\Delta}{N} \log k \right]^N \right\}. \quad (4.62)$$

Later in the computation, Sumino uses Cauchy's theorem in the complex k plane, so the sine is written as a complex exponential

$$V_N = \frac{4C_F}{\beta_0} \tilde{\Lambda} \text{Im} \int_0^\infty dk \frac{e^{ik\rho}}{k\rho} \frac{1}{-\log k} \left\{ 1 - \left[1 - \frac{d\Delta}{N} \log k \right]^N \right\}. \quad (4.63)$$

He then splits V_N in two terms, such that all N dependence of V_N is put into one term. In order to do that, we split the integrand of Eq. (4.63) in two. Notice that if we do that, we introduce a singularity in the integration path⁹ at $k = 1$, and therefore, we need to regulate the integral before splitting. We do this by introducing a $i\eta$ in the denominator

$$V_N = \frac{4C_F}{\beta_0} \tilde{\Lambda} \text{Im} \lim_{\eta \rightarrow 0} \int_0^\infty dk \frac{e^{ik\rho}}{k\rho} \frac{1}{-\log k - i\eta} \left\{ 1 - \left[1 - \frac{d\Delta}{N} \log k \right]^N \right\} \equiv \frac{4C_F}{\beta_0} \tilde{\Lambda} \left\{ v_1(r\tilde{\Lambda}) + v_2(r\tilde{\Lambda}, d\Delta, N) \right\}, \quad (4.64)$$

where

$$v_1(r\tilde{\Lambda}) \equiv \text{Im} \lim_{\eta \rightarrow 0} \int_0^\infty dk \frac{e^{ik\rho}}{k\rho} \frac{1}{-\log k - i\eta}, \quad (4.65)$$

$$v_2(r\tilde{\Lambda}, d\Delta, N) \equiv - \text{Im} \lim_{\eta \rightarrow 0} \int_0^\infty dk \frac{e^{ik\rho}}{k\rho} \frac{1}{-\log k - i\eta} \left[1 - \frac{d\Delta}{N} \log k \right]^N. \quad (4.66)$$

⁸Do not confuse this ρ with the radius of convergence of the Borel transform that we have seen earlier.

⁹That is, the Landau pole at $q = \tilde{\Lambda}$.

Notice that (by construction), v_1 above is independent of d and Δ , and thus, it doesn't care about how the series is truncated. It was proven in [77] that

$$v_1(r\tilde{\Lambda}) = \frac{1}{r\tilde{\Lambda}} \int_0^\infty dx e^{-x} \arctan \left[\frac{\pi}{2 \log \left(\frac{r\tilde{\Lambda}}{x} \right)} \right], \quad (4.67)$$

where $\arctan(x)$ is defined in the branch $[0, \pi)$. Furthermore, making use of the Sokhotski–Plemelj theorem, we can write from Eq. (4.65)

$$v_1(r\tilde{\Lambda}) = \text{PV} \int_0^\infty dk \frac{\sin(k\rho)}{k\rho} \frac{1}{-\log k} + \frac{\pi}{\rho} \cos \rho, \quad (4.68)$$

which allows us to relate v_1 and the PV static potential

$$V_{\text{large } \beta_0}^{\text{PV}} = \frac{4C_F}{\beta_0} \tilde{\Lambda} \left\{ v_1 - \frac{\pi}{r\tilde{\Lambda}} \cos(r\tilde{\Lambda}) \right\}. \quad (4.69)$$

Let us turn our attention to v_2 , which as opposed to v_1 , depends on how the series is truncated. Sumino in his [77] considers the values $d = 3$ and $\Delta = 1$ in Eq. (4.54), that is, he truncates the series at the optimal point as dictated by the subleading $d = 3$ renormalon. He then considers the large N asymptotics of V_N , and he sees that V_N diverges logarithmically in N . We are more interested in what happens with V_N if one truncates the series as dictated by the leading $d = 1$ renormalon. In this case too, if one considers $d = 1$ and the simplest case with $\Delta = 1$ as given by Eq. (1.86)

$$N_S \equiv \frac{2\pi}{\beta_0 \alpha(\mu)}, \quad (4.70)$$

one again encounters that V_N diverges logarithmically in N_S . In fact, the expression for the large N_S asymptotics of v_2 in this case is (the detailed computation can be found in Appendix E)

$$v_2^{\text{large } N_S}(r\tilde{\Lambda}, 1, N_S) = \frac{-\pi}{\rho} + \int_0^\infty dx \frac{e^{-x} - 1 + x\theta(1-x)}{x^2} \frac{\log \frac{\rho}{x}}{\log^2 \frac{\rho}{x} + \pi^2/4} \quad (4.71)$$

$$+ \frac{1}{2} \log \left(\log^2 \rho + \frac{\pi^2}{4} \right) - \frac{1}{2} (-\gamma_E + \log 2 + \log N_S) + \mathcal{O}(N_S^{-1/2}), \quad (4.72)$$

where θ is a Kronecker delta.

Let us now make contact with the contents of the previous section. We have seen in the previous section that we can get a finite limit for a divergent series, if we correlate truncation point an μ , not as shown in Eq. (4.70), but slightly below the optimal truncation point¹⁰, as seen in Eq. (4.45)

$$N_A = \frac{2\pi}{\beta_0 \alpha(\mu)} (1 - c' \alpha(1/r)). \quad (4.73)$$

Indeed, by taking $N_A \rightarrow \infty$, we obtain a convergent expression for V_N , in compliance with all we have seen in the previous section. The expression for v_2 in this case is (the computation can be found in Appendix E)

$$\lim_{N_A \rightarrow \infty} v_2(r\tilde{\Lambda}, 1 - c' \alpha(1/r), N_A) \equiv v_3 = -\frac{\pi}{\rho} - \rho^{s-2} \int_0^\infty dx \frac{e^{-x} - 1}{x^s} \frac{\frac{\pi}{2} \cos(\frac{\pi}{2}[1-s]) + \ln \frac{\rho}{x} \sin(\frac{\pi}{2}[1-s])}{\ln^2 \frac{\rho}{x} + \frac{\pi^2}{4}}, \quad (4.74)$$

where $s = 2 - c' \alpha(1/r)$. And thus, we have that

$$V_A \equiv \lim_{N_A \rightarrow \infty} V_N = \frac{4C_F}{\beta_0} \tilde{\Lambda} \{v_1 + v_3\}. \quad (4.75)$$

¹⁰Notice that, so far, we have truncated at order α^{N_A+1} , and now we are truncating at α^{N_A} . Nonetheless, both schemes yield the same limit when $N_A \rightarrow \infty$, and therefore, there is no inconsistency by comparing the functions obtained in this section and the previous one.

Of course, this expression is nothing but an alternative version of Eq. (4.47), all we have done is to reimplement what we did earlier in another guise, and we fully expect to have

$$\frac{4C_F}{\beta_0} \tilde{\Lambda} \{v_1 + v_3\} = \int_0^{\frac{2\pi}{\beta_0}(1-c'\alpha(1/r))} dt e^{-t/\alpha(1/r)} \hat{V}_{\text{large } \beta_0}(t). \quad (4.76)$$

Nevertheless, there is one advantage. Notice first that combining Eqs. (4.75) and (4.69), we can relate the truncated series and the PV Borel sum in the following way

$$V_{\text{large } \beta_0}^{\text{PV}} - V_A = \frac{4C_F}{\beta_0} \tilde{\Lambda} \left\{ -\frac{\pi}{r\tilde{\Lambda}} \cos(r\tilde{\Lambda}) - v_3 \right\}. \quad (4.77)$$

We stress again that this is another formulation of Eq. (4.46). Nevertheless, we have seen in the previous section that with the former formulation, we cannot go beyond the leading contribution, which is associated to the closest IR renormalon. Interestingly, with Eq. (4.77), we are able to reproduce the leading term that we have already encountered in Eq. (4.46), and on top of that, to obtain the first correction in $\alpha(1/r)$. The expression found is (the details of the computation can be found in subsection E.2.2)

$$\left(V_{\text{large } \beta_0}^{\text{PV}} - V_A \right)_{r \sim 0} = \frac{4C_F \tilde{\Lambda}}{\beta_0} \left\{ -\text{Ei}\left(\frac{2\pi c'}{\beta_0}\right) + \alpha(1/r) e^{\frac{2\pi c'}{\beta_0}} \frac{\beta_0}{4\pi} (-2 - c_X + 2\gamma_E) + \mathcal{O}(\alpha^2(1/r)) \right\}. \quad (4.78)$$

As we see comparing with Eq. (4.46), the leading term agrees. As a finishing remark, we recall that by taking $c' = 0$ in Eq. (4.45), we essentially obtain Eq. (4.70). It is interesting to see what happens in the $c' \rightarrow 0$ asymptotics of Eq. (4.78)

$$\left(V_{\text{large } \beta_0}^{\text{PV}} - V_A \right)_{r \sim 0} \Big|_{c' \sim 0} = \frac{4C_F \tilde{\Lambda}}{\beta_0} \left\{ -\gamma_E + \log\left(\frac{\beta_0}{2\pi}\right) - \log c' + \alpha \frac{\beta_0}{4\pi} (-2 - c_X + 2\gamma_E) + \mathcal{O}(\alpha^2(1/r)) \right\}, \quad (4.79)$$

and we see that we have a logarithmic divergence in c' .

4.3 The pole mass in the large β_0 approximation

We can revisit the analysis we have done with the static potential for the case of the pole mass in the large β_0 approximation. Moreover, since the normalizations of the leading renormalons of both objects are related by $Z_V = -2Z_m$, we can recycle all the formulas of section 4.2 changing only this factor -2 . Nonetheless, the big difference will be that we do not have as much analytic control over the pole mass, and we are unable to repeat the analysis of subsection 4.2.1. Thus, adapting Eq. (4.39) to this case by including the leading $d = 1$ renormalon that we have seen in section 2.4, we get

$$m_{\text{OS}}^{\text{PV}} - \bar{m} = \tilde{M}_A + \frac{2C_F}{\beta_0} \tilde{\Lambda} \text{Ei}\left(\frac{2\pi c'}{\beta_0}\right) + \mathcal{O}(\alpha(\bar{m})), \quad (4.80)$$

where recall that $\tilde{M} = m_{\text{OS}}^{\text{large } \beta_0} - \bar{m} = \sum_{n=0}^{\infty} r_n \alpha^{n+1}$, as we have seen in Eq. (2.46). We have also defined

$$\tilde{M}_A \equiv \lim_{N_A \rightarrow \infty} \sum_{n=0}^{N_A} r_n(\mu(N_A)) \alpha^{n+1}(\mu(N_A)) = \int_0^{\frac{2\pi}{\beta_0}(1-c'\alpha(\bar{m}))} dt e^{-t/\alpha(\bar{m})} \hat{M}(t), \quad (4.81)$$

where μ and N_A are correlated as given by Eq. (4.45), and we have chosen $Q = \bar{m}$. In this section, Υ takes the form

$$\Upsilon_{\text{LO}} \equiv \frac{2C_F}{\beta_0} \tilde{\Lambda} \text{Ei}\left(\frac{2\pi c'}{\beta_0}\right). \quad (4.82)$$

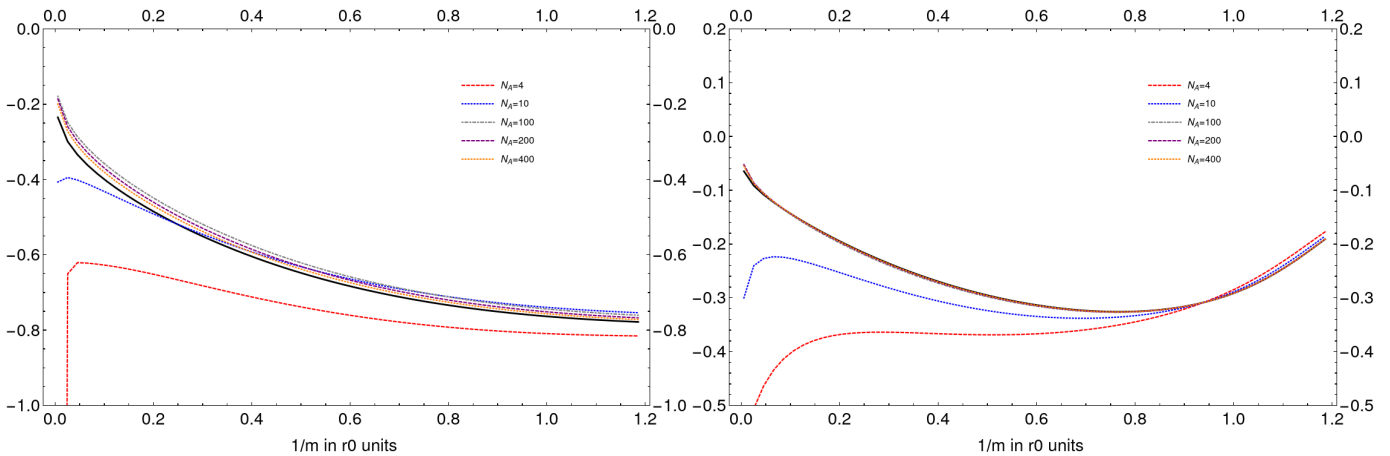


Figure 4.3: **Left panel:** We plot (black line) $m_{\text{OS}}^{\text{PV}} - \bar{m} - \tilde{M}_A - \Upsilon_{\text{LO}}$ for $n_f = 0$ in the lattice scheme with $c = 1$ versus the truncated sums $m_{\text{OS}}^{\text{PV}} - \bar{m} - \sum_{n=0}^{N_A} r_n \alpha^{n+1}(\mu) - \Upsilon_{\text{LO}}$, where μ is fixed using N_A defined in Eq. (4.45), for various values of N_A . **Right panel:** As in the left panel, but in the $\overline{\text{MS}}$ scheme.

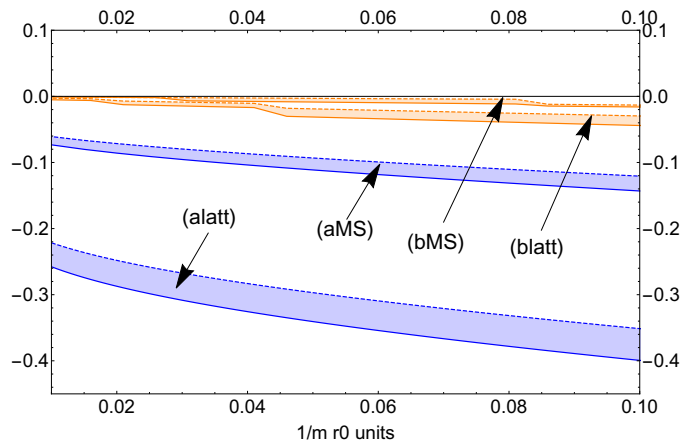


Figure 4.4: We plot (a) $m_{\text{OS}}^{\text{PV}} - \bar{m} - \tilde{M}_A - \Upsilon_{\text{LO}}$ for $n_f = 0$ in the lattice and $\overline{\text{MS}}$ scheme. For each case, we generate bands by computing \tilde{M}_A with $c' = 1$ and $c' = c'_{\text{min}} = 0.652$ and such that $\Upsilon_{\text{LO}}(c'_{\text{min}}) = 0$. We also compare with (b) $m_{\text{OS}}^{\text{PV}} - m_{\text{OS}}^{\text{P}} - \bar{m}\Omega_1$ obtained with method 1 with the bands generated for Fig. 3.10.

Analogously to what we have done in section 4.2, we can check how high we have to go in N_A to reach the limit value. This is displayed in Figure 4.3. The same discussion as in section 4.2 applies. We again find good convergence, albeit again, at relatively high values of N_A .

Finally, we compare method 1 against method 2, analogously to what we did in Figure 4.2. We display this in Figure 4.4. Just like for the case of the static potential, we again find that method 1 does a better job than method 2, and that the $\overline{\text{MS}}$ scheme works slightly better in both cases.

4.4 Qualitative comparison with Method 1

Having reviewed in detail two methods to obtain the PV Borel sum of a formal series from truncated expressions, it is worthwhile to discuss how they compare with each other. Method 2 has the nice feature that μ dependence vanishes from the truncated sum and from the leading power correction in Eq. (4.39), which complies well with the fact that the PV Borel sum is μ independent. This is unlike method 1, where there is always a residual μ dependence, which nevertheless, becomes more and more exponentially suppressed as more terms are included in

the hyperasymptotic expansion. Method 2 also has the nice feature that the leading correction to add on top of the truncated sum has the same scaling as the NP power corrections dictated by the OPE, unlike method 1, due to the $\alpha^{1/2}$ term.

Nonetheless, as we have already mentioned, method 2 has some clear shortcomings. On the one hand, we cannot go beyond Eq. (4.39) and add more and more terms to obtain a better precision, as it is detailed in Appendix D. Method 1 is in principle systematically improvable, as long as we know enough about the Borel plane of the observable in question. Moreover, there are other more practical difficulties. First, in order to apply Eq. (4.23), we need to know the Borel transform exactly, which in general will never be known. If one tries then to use truncated sums for large truncation orders, asymptotic coefficients will need to be used at some (rather early in most cases) point, which will introduce more uncertainties. Furthermore, these asymptotic coefficients will not be known exactly in general, due to uncertainties in the normalizations of the renormalons, which will hinder the method even more.

Due to the fact that it is systematically improvable, and to its cleaner practical implementation, we will favor method 1 in the rest of the thesis.

Chapter 5

Hyperasymptotics of the average plaquette and the gluon condensate

This chapter is based on the article [81]. We will consider the OPE of the average plaquette in gluodynamics¹

$$\langle P \rangle_{\text{MC}} = \sum_{n=0}^{\infty} p_n \alpha^{n+1} + \frac{\pi^2}{36} C_G a^4 \langle G^2 \rangle + \mathcal{O}(a^6 \Lambda_{\text{QCD}}^6), \quad (5.1)$$

and use it to give an estimate of the gluon condensate $\langle G^2 \rangle$,

$$\langle G^2 \rangle = \frac{36}{\pi^2 a^4} C_G^{-1} \left\{ \langle P \rangle_{\text{MC}} - \sum_{n=0}^{\infty} p_n \alpha^{n+1} \right\} + \mathcal{O}(a^2 \Lambda_{\text{QCD}}^6). \quad (5.2)$$

The equation above must be handled with care since, before we are able to use it, we must set a prescription to sum the divergent infinite series $\sum_{n=0}^{\infty} p_n \alpha^{n+1}$. We will consider the PV Borel sum to regulate the perturbative series of the plaquette, and employ the method of chapter 3 to obtain it from truncated versions of the perturbative series. To set the stage, we will very briefly review in the next section gauge theories on the lattice² with the aim of introducing the main character of this chapter: the average plaquette.

5.1 Gauge fields in the lattice, the plaquette and the Wilson action

We consider four dimensional Euclidean space, and we discretize it with a hypercubic lattice [83] of $N = N_1 \times N_2 \times N_3 \times N_4$ lattice sites, where each $N_\mu \in \mathbb{N}$ denotes the total number of lattice sites on the direction μ . We denote the lattice with the symbol Λ_E . The distance between neighboring points, the lattice spacing, will be denoted by a . Points in the lattice will be denoted by $n \equiv (n_1, n_2, n_3, n_4)$, where $n_\mu = 0, 1, \dots, N_\mu - 1$. The position of a given lattice point from the origin is $x = an = (an_1, an_2, an_3, an_4)$. We will denote with $\hat{\mu}$ a step of one lattice spacing unit on the positive direction μ . Thus, if $\phi(n)$ is a field at the lattice point $x = (an_1, an_2, an_3, an_4)$, then $\phi(n + \hat{4})$ is a field located at the point $x' = (an_1, an_2, an_3, a(n_4 + 1))$.

For a lattice formulation of Yang-Mills theory, it proves convenient to use the discretized version of the *gauge transporter*. The continuum version is

$$G(x, y) = \mathcal{P} e^{i \int_{C_{xy}} dx^\mu A_\mu}, \quad (5.3)$$

where C_{xy} is a path that goes from x to y , and \mathcal{P} denotes path ordering. The discretized version³ is

$$U_\mu(n) \equiv e^{iaA_\mu(n)}. \quad (5.4)$$

¹SU(3) Yang-Mills theory without quarks.

²The introductory sections of this chapter are based mainly on the book [82].

³Actually, the discretized version when x and y are infinitesimally close.

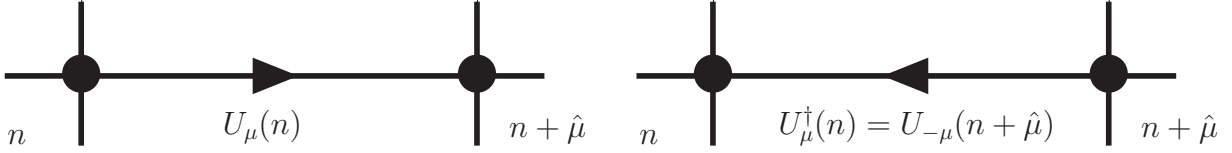


Figure 5.1: **Left image:** Link variable connecting n to $n + \hat{\mu}$. **Right image:** Link variable connecting $n + \hat{\mu}$ to n .

We will call the above object the *link variable*. $A_\mu(n)$ is the discretized version of the gauge connection, and thus, it is a $SU(3)$ Lie algebra valued object. Notice that then $U_\mu(n)$ is a $SU(3)$ matrix. Graphically, this object is meant to be understood as the oriented link going from n towards $n + \hat{\mu}$. Notice that then, $U_{-\mu}(n + \hat{\mu})$ brings us back from $n + \hat{\mu}$ to n , so that $U_\mu(n)U_{-\mu}(n + \hat{\mu}) = \mathbb{1}_{3 \times 3}$. Since we are using unitary matrices $U_\mu(n)U_\mu^\dagger(n) = \mathbb{1}_{3 \times 3}$, and therefore

$$U_\mu^\dagger(n) = U_{-\mu}(n + \hat{\mu}), \quad (5.5)$$

that is, the adjoint matrix $U_\mu^\dagger(n)$ depicts a link going towards n from $n + \hat{\mu}$. This is all portrayed in Figure 5.1. In the lattice, instead of using the field A_μ , it is customary to use the link variable U_μ as the degree of freedom to construct the theory. Gauge transformations of the link variable are implemented via

$$U_\mu(n) \rightarrow U'_\mu(n) = \Xi(n)U_\mu(n)\Xi^\dagger(n + \hat{\mu}), \quad (5.6)$$

where $\Xi(n)$ is also a $SU(3)$ matrix. From Eq. (5.6), one can deduce that the *trace* of the product of link variables in a closed loop is a gauge invariant quantity. The simplest of these products is the *plaquette*, which is a product of link variables starting at the point n , that goes through $n + \hat{\mu}$, $n + \hat{\mu} + \hat{\nu}$, $n + \hat{\nu}$ and back to n . This is illustrated in Figure 5.2. We will denote this object by $U_{\mu\nu}(n)$. Thus, we see that

$$U_{\mu\nu}(n) \equiv U_\mu(n)U_\nu(n + \hat{\mu})U_\mu^\dagger(n + \hat{\nu})U_\nu^\dagger(n). \quad (5.7)$$

Notice that quite trivially, we have that

$$U_{\mu\nu}^\dagger(n) = U_{\nu\mu}(n). \quad (5.8)$$

The lattice action for Yang-Mills fields, the so called Wilson action [83], is a sum over all plaquettes on the lattice, where each plaquette is counted with only one orientation

$$I_{\text{Wilson}}[U] \equiv \frac{2}{g^2} \sum_{n \in \Lambda_E} \sum_{\mu < \nu} \text{Re tr} \{1 - U_{\mu\nu}(n)\}, \quad (5.9)$$

where g is the gauge coupling in the lattice. It can be seen that in a naive small a expansion, this action returns the continuum action for Yang-Mills theory. Noticing that the trace of the transpose of a complex matrix is the same as the trace of the original matrix, one can write also write

$$I_{\text{Wilson}}[U] = \frac{6}{g^2} \sum_{n \in \Lambda_E} \sum_{\mu < \nu} \left(1 - \frac{1}{6} \text{tr} \{U_{\mu\nu}(n) + U_{\mu\nu}^\dagger(n)\}\right), \quad (5.10)$$

or defining as it is customary⁴ $\beta \equiv \frac{6}{g^2} = \frac{3}{2\pi\alpha}$

$$I_{\text{Wilson}}[U] = \beta \sum_{n \in \Lambda_E} \sum_{\mu < \nu} \left(1 - \frac{1}{6} \text{tr} \{U_{\mu\nu}(n) + U_{\mu\nu}^\dagger(n)\}\right). \quad (5.11)$$

⁴Do not confuse this β and the beta function $\mu \frac{d}{d\mu} \alpha(\mu) = \beta$.

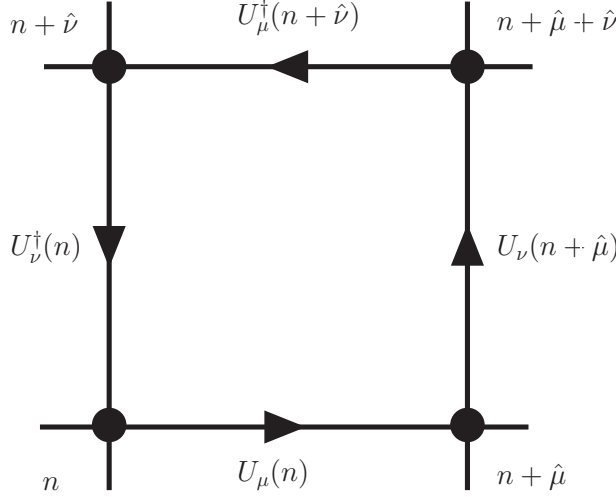


Figure 5.2: The plaquette.

5.2 The average plaquette and the gluon condensate

Let us define

$$P_{n,\mu\nu} \equiv 1 - \frac{1}{6} \text{tr} \{ U_{\mu\nu}(n) + U_{\mu\nu}^\dagger(n) \}, \quad (5.12)$$

where, notice that Eq. (5.8) implies that $P_{n,\mu\nu} = P_{n,\nu\mu}$. We further define

$$P_n \equiv \frac{1}{6} \sum_{\mu < \nu} P_{n,\mu\nu}. \quad (5.13)$$

With these definitions, the Wilson action of Eq. (5.11) can be written in the following way

$$I_{\text{Wilson}}[U] = 6\beta \sum_{n \in \Lambda_E} P_n. \quad (5.14)$$

We now define the *average plaquette* as

$$\langle P \rangle \equiv \frac{1}{N^4} \sum_{n \in \Lambda_E} \langle P_n \rangle, \quad (5.15)$$

where the brackets above denote the following correlation function

$$\langle P_n \rangle = \frac{1}{\mathcal{Z}} \int_{\text{SU}(3)} [dU] e^{-I_{\text{Wilson}}[U]} P_n \quad (5.16)$$

$$= \frac{1}{6\mathcal{Z}} \int_{\text{SU}(3)} [dU] e^{-I_{\text{Wilson}}[U]} \sum_{\mu < \nu} \left(1 - \frac{1}{6} \text{tr} \{ U_{\mu\nu}(n) + U_{\mu\nu}^\dagger(n) \} \right), \quad (5.17)$$

where the integration measure is the Haar measure, and \mathcal{Z} is the partition function

$$\mathcal{Z} \equiv \int_{\text{SU}(3)} [dU] e^{-I_{\text{Wilson}}[U]}. \quad (5.18)$$

$\langle P_n \rangle$ is translation invariant so that $\langle P_n \rangle = \langle P_0 \rangle$

$$\langle P \rangle = \frac{1}{N^4} \sum_{n \in \Lambda_E} \langle P_0 \rangle = \langle P_0 \rangle, \quad (5.19)$$

where of course, we could have taken any other lattice point besides $n = 0$. Let us consider expanding the integrand in Eq. (5.17) in a small $\alpha(1/a)$ expansion, commuting sum and integral, and then performing the path integral

$$\langle P \rangle = \frac{1}{Z} \int_{\text{SU}(3)} [dU] e^{-I_{\text{Wilson}}[U]} P_n \quad (5.20)$$

$$\sim \sum_{n=0}^{\infty} p_n(N) \alpha^{n+1} (1/a) \equiv \langle P \rangle_{\text{pert}}(N). \quad (5.21)$$

The series above is the perturbative expansion of the average plaquette for a lattice with N lattice sites and lattice spacing a . The coefficients of the series above were computed first until $\mathcal{O}(\alpha^3)$ using diagrammatic techniques [84, 85, 86] and with NSPT [87, 88, 89] in [88, 90, 91, 92, 93, 94] at various orders in perturbation theory. We use the data from [94], that was able to obtain the coefficients of the series until $\mathcal{O}(\alpha^{35})$. In this reference, the coefficients $p_n(N)$ were computed for lattices with varying N values, and then, the large volume $N \rightarrow \infty$ expansion of these finite volume coefficients was considered

$$p_n(N) = p_n - \frac{f_n(N)}{N^4} + \mathcal{O}(N^{-6}), \quad (5.22)$$

and the infinite volume coefficients p_n were computed. Coming back to Eq. (5.17), we can perform an OPE of the average plaquette as in Eq. (5.1)

$$\langle P \rangle_{\text{MC}} = \sum_{n=0}^{\infty} p_n \alpha^{n+1} + \frac{\pi^2}{36} C_G a^4 \langle G^2 \rangle + \mathcal{O}(a^6 \Lambda_{\text{QCD}}^6). \quad (5.23)$$

The series in the first term in RHS above is the infinite volume perturbative expansion of the average plaquette, $\langle G^2 \rangle$ is the RG invariant gluon condensate [95]

$$\langle G^2 \rangle \equiv -\frac{2}{\beta_0} \left\langle \Omega \left| \frac{\beta(\alpha)}{\alpha} G_{\mu\nu}^a G_{\mu\nu}^a \right| \Omega \right\rangle = \left\langle \Omega \left| [1 + \mathcal{O}(\alpha)] \frac{\alpha}{\pi} G_{\mu\nu}^a G_{\mu\nu}^a \right| \Omega \right\rangle, \quad (5.24)$$

and the C_G is the Wilson coefficient of the gluon condensate, which is proportional to the inverse of the beta function [96, 97]

$$\begin{aligned} C_G(\alpha) &= 1 + \sum_{k \geq 0} c_k \alpha^{k+1} = -\frac{\beta_0 \alpha^2}{2\pi \beta(\alpha)} \\ &= 1 - \frac{\beta_1}{\beta_0} \frac{\alpha}{4\pi} + \frac{\beta_1^2 - \beta_0 \beta_2}{\beta_0^2} \left(\frac{\alpha}{4\pi} \right)^2 - \frac{\beta_1^3 - 2\beta_0 \beta_1 \beta_2 + \beta_0^2 \beta_3}{\beta_0^3} \left(\frac{\alpha}{4\pi} \right)^3 + \mathcal{O}(\alpha^4). \end{aligned} \quad (5.25)$$

The scheme independent coefficients read

$$\beta_0 = 11, \quad (5.26)$$

$$\beta_1 = 102. \quad (5.27)$$

For $j \leq 3$, the coefficients β_j are scheme dependent. The Wilson action lattice scheme β_2 has been computed diagrammatically [71, 98, 99]

$$\beta_2 = -6299.8999(6). \quad (5.28)$$

The value for β_3 that we use is an update of [100, 101], and was obtained [70] by calculating the normalization of the leading renormalon of the pole mass, and then assuming the corresponding $\overline{\text{MS}}$ -scheme expansion to follow its asymptotic behaviour from orders α^4 onwards

$$\beta_3 = -1.16(3) \times 10^6. \quad (5.29)$$

Similar estimates, $\beta_3 \approx -1.37 \times 10^6$ up to $\beta_3 \approx -1.55 \times 10^6$, were found in [102] using a very different method. For convenience, we also write the expansion coefficients c_k defined in Eq. (5.25)

$$c_0 = -b \frac{\beta_0}{2\pi}, \quad c_1 = s_1 b \left(\frac{\beta_0}{2\pi} \right)^2, \quad c_2 = -2s_2 b^2 \left(\frac{\beta_0}{2\pi} \right)^3, \quad (5.30)$$

where we have employed the constants defined in Eq. (2.73), Eq. (2.74) and Eq. (2.75). As we have already mentioned, Eq. (5.23) can be used to give an estimate of the gluon condensate

$$\langle G^2 \rangle = \frac{36}{\pi^2 a^4} C_G^{-1} \left\{ \langle P \rangle_{\text{MC}} - \sum_{n=0}^{\infty} p_n \alpha^{n+1} \right\} + \mathcal{O}(a^2 \Lambda_{\text{QCD}}^6). \quad (5.31)$$

The series of the plaquette above is divergent, and therefore, in order to obtain the gluon condensate, we need to first choose a method to assign a number to it. Extracting the gluon condensate from the average plaquette was pioneered in [84, 103, 104, 105, 106], and many attempts followed during the next decades, see [85, 88, 107, 90, 108, 109, 91, 110, 111, 93]. Nevertheless, they suffered from insufficiently high perturbative orders and, in some cases, also finite volume effects. The failure to make a controlled contact with the asymptotic regime of the series of the plaquette prevented a reliable lattice determination of $\langle G^2 \rangle$, where one could quantitatively assess the error associated to these determinations. Any reasonable definition consistent with $\langle G^2 \rangle \sim \Lambda^4$ can only be given if the asymptotic behaviour of the perturbative series is under control.

This problem was first solved in [94, 112] where for the first time, the perturbative series of the average plaquette of 4 dimensional SU(3) gluodynamics was computed with superasymptotic accuracy, up until $\mathcal{O}(\alpha^{35})$. The observed asymptotic behaviour was in full compliance with renormalon expectations, with successive contributions starting to diverge for orders around $\alpha^{27} - \alpha^{30}$ within the range of couplings α typically employed in present-day lattice simulations. This made possible a reliable determination of $\langle G^2 \rangle$ that scaled as Λ_{QCD}^4 . In these references, the IR renormalon of the series of the average plaquette was regularized by simply truncating the series superasymptotically

$$\langle G^2 \rangle_{n_0} \equiv \frac{36}{\pi^2 a^4} C_G^{-1} \left\{ \langle P \rangle_{\text{MC}} - \sum_{n=0}^{n_0} p_n \alpha^{n+1} \right\} + \mathcal{O}(a^2 \Lambda_{\text{QCD}}^6), \quad (5.32)$$

where n_0 is chosen such that $|p_{n_0} \alpha^{n_0+1}|$ is numerically smallest. One issue raised was to determine to which extent such a result was independent of the scheme used for the coupling constant. The answer to this question can be given within the framework of hyperasymptotic expansions of renormalizable quantum field theories that we have seen in chapter 3, as developed in [68, 70, 69]. Instead of truncating the perturbative series of the average plaquette, we can use the PV Borel sum to regulate the renormalon, and approximate it from truncated sums using terminants, as we have already seen:

$$\text{PV} \sum_{n=0}^{\infty} p_n \alpha^{n+1} = \sum_{n=0}^N p_n \alpha^{n+1} + T + \dots, \quad (5.33)$$

where T denotes the leading terminant. Since the PV Borel sum is scheme independent, as we have seen in Eq. (3.73), the scheme dependence of using the superasymptotic approximation to the perturbative sum is of $\mathcal{O}(\sqrt{\alpha(1/a)} Z_P \Lambda_{\text{QCD}}^4)$, where Z_P is the normalization of the leading renormalon that we will find in Eq. (5.39). This error then sets the parametric precision of the determination of the gluon condensate using the superasymptotic approximation. Note that the scheme dependence of Z_P and Λ_{QCD}^4 cancels each other. Therefore, the only remaining leading scheme/scale dependence of the error is due to the $\sqrt{\alpha(1/a)}$ prefactor. In this chapter we

revisit the analysis found in [112], and use the PV Borel sum to regulate the perturbative expansion of the average plaquette

$$\langle P \rangle_{\text{MC}} = \text{PV} \sum_{n=0}^{\infty} p_n \alpha^{n+1} + \frac{\pi^2}{36} C_G a^4 \langle G^2 \rangle_{\text{PV}} + \mathcal{O}(a^6 \Lambda_{\text{QCD}}^6), \quad (5.34)$$

$$\langle G^2 \rangle_{\text{PV}} \equiv \frac{36}{\pi^2 a^4} C_G^{-1} \left\{ \langle P \rangle_{\text{MC}} - \text{PV} \sum_{n=0}^{\infty} p_n \alpha^{n+1} \right\} + \mathcal{O}(a^2 \Lambda_{\text{QCD}}^6). \quad (5.35)$$

We will reach better accuracy by incorporating the leading terminant. We will also discuss subleading effects. We confirm that the result we obtain is independent of the scheme/scale used for the renormalization of the coupling constant (up to terms that are higher order than the accuracy reached by the hyperasymptotic approximation).

5.3 The hyperasymptotic expansion of the average plaquette

In order to implement the PV Borel sum of the series of the average plaquette, we will employ Dingle's terminants and the hyperasymptotic expansion of chapter 3. To ease notation, we will denote the PV Borel sum of the average plaquette by S_{PV} . The expansion reads

$$S_{\text{PV}} = \sum_{n=0}^{N_{\text{P}}(4)} p_n \alpha^{n+1} + \Omega_{G^2} + \sum_{n=N_{\text{P}}(4)+1}^{N'} [p_n - p_n^{(\text{as})}] \alpha^{n+1} + \dots. \quad (5.36)$$

The leading IR renormalon of the perturbative series of the plaquette is located at $t = \frac{8\pi}{\beta_0}$ (in compliance with a condensate of dimension four in the OPE), and therefore, in Eq. (5.36) we take

$$N_{\text{P}}(d=4) = \frac{8\pi}{\beta_0 \alpha(1/a)} (1 - c\alpha(1/a)). \quad (5.37)$$

To simplify notation, we also define

$$S_{\text{P}} \equiv \sum_{n=0}^{N_{\text{P}}(4)} p_n \alpha^{n+1}. \quad (5.38)$$

By default (just like in the examples we have seen in the large β_0 approximation), we will take the smallest positive value of c that yields an integer value for N_{P} , but we also explore the dependence of the result on c . In principle, N' would be given by the location of the next singularity in the Borel plane. In practice, we will not have knowledge of enough p_n coefficients to reach the second singularity, and hence, N' will be limited to these known orders. Therefore, we will have an incomplete $\sum_{n=N_{\text{P}}(4)+1}^{N'} [p_n - p_n^{(\text{as})}] \alpha^{n+1}$. We will come back to this later. The large n behavior associated to the $d=4$ renormalon of the coefficients p_n is given by⁵

$$p_n^{(\text{as})} = Z_P \left(\frac{\beta_0}{8\pi} \right)^n \frac{\Gamma(n+1+4b)}{\Gamma(1+4b)} \left\{ 1 + \frac{4b}{n+4b} w_1 + \frac{4b(4b-1)}{(n+4b)(n+4b-1)} w_2 + \mathcal{O}\left(\frac{1}{n^3}\right) \right\}, \quad (5.39)$$

where w_1 and w_2 are those of Eqs. (2.95) and (2.96), adapted to this particular case

$$w_1 = \frac{2\pi c_0}{\beta_0 b} + 4s_1, \quad (5.40)$$

$$w_2 = \frac{4b}{4b-1} \left\{ \frac{4\pi^2 c_1}{\beta_0^2 b^2} + 4s_1 \left(\frac{4s_1}{2} + \frac{2\pi c_0}{\beta_0 b} \right) - 4s_2 \right\}, \quad (5.41)$$

⁵The notation is slightly different in [94, 112, 81], where w_1 is called b_1 and $w_2 = \frac{4b_2 b}{4b-1}$.

where, just as before, s_1 and s_2 are given by Eqs. (2.74) and (2.75), and the small α expansion coefficients of the Wilson coefficient of the gluon condensate are given by Eq. (5.30). Using these values for c_0 and c_1 , we can simplify further

$$w_1 = 4s_1 - 1, \quad (5.42)$$

$$w_2 = \frac{16b}{4b-1} \left\{ s_1 \left(\frac{4s_1}{2} - 1 + \frac{1}{4b} \right) - s_2 \right\}. \quad (5.43)$$

The value of Z_P was determined approximately (for $n_f = 0$) in [94]

$$Z_P = (42 \pm 17) \times 10^4. \quad (5.44)$$

We name Ω_{G^2} the terminant⁶ associated to the $d = 4$ renormalon of the series of the plaquette. It is given by Eq. (3.66)

$$\Omega_{G^2} = \Delta\Omega(4b) + w_1\Delta\Omega(4b-1) + w_2\Delta\Omega(4b-2) + \dots, \quad (5.45)$$

where we take $\Delta\Omega$ from Eq. (3.70). The small $\alpha(1/a)$ expansion of Ω_{G^2} can be written adapting Eqs. (3.72) and (3.73) to this particular case

$$\Omega_{G^2} = K_{\text{IR}}^{(\text{P})} a^4 \Lambda_{\text{QCD}}^4 \alpha^{1/2}(1/a) \left\{ 1 + K_{\text{IR},1}^{(\text{P})} \alpha(1/a) + K_{\text{IR},2}^{(\text{P})} \alpha^2(1/a) + \mathcal{O}(\alpha^3(1/a)) \right\}, \quad (5.46)$$

or

$$\Omega_{G^2} = K_{\text{IR}}^{(\text{P})} \left(\frac{\beta_0 \alpha(1/a)}{4\pi} \right)^{-4b} e^{-\frac{8\pi}{\beta_0 \alpha(1/a)}} \alpha^{1/2}(1/a) \left\{ 1 + \bar{K}_1^{(\text{P})} \alpha(1/a) + \bar{K}_2^{(\text{P})} \alpha^2(1/a) + \mathcal{O}(\alpha^3(1/a)) \right\}, \quad (5.47)$$

where

$$K^{(\text{P})} = \frac{-Z_P}{\Gamma(1+4b)} 2^{2+4b} \pi \beta_0^{-1/2} \left(-\eta_c + \frac{1}{3} \right), \quad (5.48)$$

$$\bar{K}_1^{(\text{P})} = \frac{\beta_0/(4\pi)}{-\eta_c + \frac{1}{3}} \left[-4bw_1 \left(\frac{1}{2}\eta_c + \frac{1}{3} \right) - \frac{1}{12}\eta_c^3 + \frac{1}{24}\eta_c - \frac{1}{1080} \right], \quad (5.49)$$

$$K_1^{(\text{P})} = \bar{K}_1^{(\text{P})} - \frac{2b\beta_0 s_1}{\pi}, \quad (5.50)$$

$$\begin{aligned} \bar{K}_2^{(\text{P})} &= \frac{\beta_0^2/(4\pi)^2}{-\eta_c + \frac{1}{3}} \left[-w_2(4b-1)4b \left(\frac{1}{4}\eta_c + \frac{5}{12} \right) \right. \\ &\quad \left. + w_1 4b \left(-\frac{1}{24}\eta_c^3 - \frac{1}{8}\eta_c^2 - \frac{5}{48}\eta_c - \frac{23}{1080} \right) - \frac{1}{160}\eta_c^5 - \frac{1}{96}\eta_c^4 + \frac{1}{144}\eta_c^3 \right. \\ &\quad \left. + \frac{1}{96}\eta_c^2 - \frac{1}{640}\eta_c - \frac{25}{24192} \right], \end{aligned} \quad (5.51)$$

$$K_2^{(\text{P})} = \frac{1}{8\pi^2} (8\pi^2 \bar{K}_2^{(\text{P})} - 16b\pi s_1 \beta_0 \bar{K}_1^{(\text{P})} + 16b^2 s_1^2 \beta_0^2 + 8b^2 s_2 \beta_0^2), \quad (5.52)$$

and $\eta_c \equiv -4b + \frac{8\pi}{\beta_0} c - 1$. The error on Z_P will give the biggest source of uncertainty in the determination of Ω_{G^2} , of the order of 40%. The other source of error is that, as opposed to the examples in the large β_0 approximation, only approximate expressions are available for Ω_{G^2} (see Eq. (5.45), Eq. (5.46), and Eq. (5.47)), since we do not know the complete set of coefficients w_j . Being that as it may, we can study the convergence pattern of the various expressions we have presented for the terminant. We show the results in Table 5.1 for a representative set of values of α in the interval that we will use later. The first observation is that we observe a very good convergent pattern

⁶Notice that, since the series of the plaquette has no mass dimensions, $\Omega = T$.

β	N_P	$\Omega_{\text{LO}}^{(\Lambda_{\text{QCD}})} \times 10^5$	$\Omega_{\text{LO}}^{(\text{exp})} \times 10^5$	$\Omega_{\text{LO}}^{(\text{exact})} \times 10^5$	$\Omega_{\text{NLO}}^{(\Lambda_{\text{QCD}})} \times 10^5$	$\Omega_{\text{NLO}}^{(\text{exp})} \times 10^5$	$\Omega_{\text{NLO}}^{(\text{exact})} \times 10^5$	$\Omega_{\text{NNLO}}^{(\Lambda_{\text{QCD}})} \times 10^5$	$\Omega_{\text{NNLO}}^{(\text{exp})} \times 10^5$	$\Omega_{\text{NNLO}}^{(\text{exact})} \times 10^5$
5.8	27	-230.14	-16.23	-16.50	-146.41	-23.06	-23.07	-74.79	-24.31	-24.30
6.	28	-50.114	-6.611	-6.723	-32.821	-9.344	-9.349	-18.509	-9.888	-9.886
6.2	29	-14.031	-2.689	-2.735	-9.433	-3.781	-3.783	-5.746	-4.013	-4.011
6.4	30	-4.639	-1.092	-1.111	-3.194	-1.528	-1.529	-2.069	-1.625	-1.624
6.6	31	-1.6640	-0.4426	-0.4505	-1.1705	-0.6165	-0.6170	-0.7974	-0.6571	-0.6561

Table 5.1: A representative set of values of Ω_{G^2} using Eq. (5.46) (Λ_{QCD}), Eq. (5.45) (exact) and Eq. (5.47) (exp). LO, NLO and NNLO with regards to the exact expression mean that in the LO expression, we just take the first term on the RHS of Eq. (5.45). In the NLO, we take also the second term, the one proportional to w_1 , and for NNLO, we take also the one proportional to w_2 . Of course, LO, NLO and NNLO for Eq. (5.47) and Eq. (5.46) mean various orders in the expansion in α inside braces in Eqs. (5.47) and (5.46).

of the weak-coupling expansion of the terminant using Eq. (5.47) or Eq. (5.45): consecutive terms quickly become smaller. The second observation is that the strict weak-coupling expansion used in Eq. (5.47) is quite close to the exact numerical determination of Eq. (5.45) for analogous precision.

On the other hand, if we use Eq. (5.46), the version with Λ_{QCD} , the convergence is not good⁷. As it can be seen in Table 5.1, we have to go to β -values rather larger than 6 to get decent accuracy. What lies behind is the fact that $\Lambda_{\text{QCD}}^{\text{latt}}$ is not well approximated by its weak coupling expansion at low orders. A similar behavior, albeit less severe, will be seen later for the B meson mass in the lattice. The main difference with that case is that now the power of Λ_{QCD} is four instead of one. This makes the relatively bad convergent behavior of the small α expansion of Λ_{QCD} get amplified by a factor of four. Thus, in what follows, we will always use Eq. (5.47) as our approximated expression for Ω_{G^2} , as it produces a nicely convergent series, and the weak coupling expansion is organized in terms of a single parameter α . The error associated to truncating the expansion in Eq. (5.47) is estimated by observing the convergent pattern of the LO, NLO and NNLO results in Table 5.1. From LO to NLO, in the worst cases, the differences are close but below 50%, and from NLO to NNLO the differences are below 10%. One could then expect the NNNLO contribution to be at the level of few percent, which can be neglected altogether in comparison with the $\sim 40\%$ error associated to Z_P .

5.4 Error sources

Let's get back to Eq. (5.35)

$$\langle G^2 \rangle_{\text{PV}} = \frac{36}{\pi^2 a^4} C_G^{-1} \left\{ \langle P \rangle_{\text{MC}} - S_{\text{PV}} \right\} + \mathcal{O}(a^2 \Lambda_{\text{QCD}}^6). \quad (5.53)$$

This equality is expected to hold up to corrections of order $\mathcal{O}(a^2 \Lambda_{\text{QCD}}^6)$. This would be the accuracy we would have in the determination of the gluon condensate, if all the elements of the equation above were known exactly, but unfortunately, this is not the case. Neither S_{PV} nor $\langle P \rangle_{\text{MC}}$ are known exactly. On top of that, we have to account for the fact that C_G^{-1} and the relation between the lattice spacing a and β are also known in an approximated way. We now discuss how we determine them and their associated individual errors.

We take the MC data for $\langle P \rangle_{\text{MC}}$ from [114], and we display it with its associated error in Table 5.2. Similarly to what was done in [112], we restrict ourselves to data for lattices of 32^4 points, and to keep finite volume effects under control to $\beta \leq 6.65$. We also limit ourselves to $\beta \geq 5.8$ to avoid large $\mathcal{O}(a^2)$ corrections. It is noteworthy that at very large β -values there is a strong cancellation between two huge numbers, S_P and $\langle P \rangle_{\text{MC}}$, giving rise to a comparatively much smaller number. We illustrate this cancellation in Fig. 5.4.

⁷We use the value $\Lambda_{\text{QCD}} = e^{-\frac{2\pi d_1}{\beta_0}} \times 0.602 r_0^{-1}$ [113, 74], where $d_1 = 5.88359144663707(1)$ [71, 72, 73].

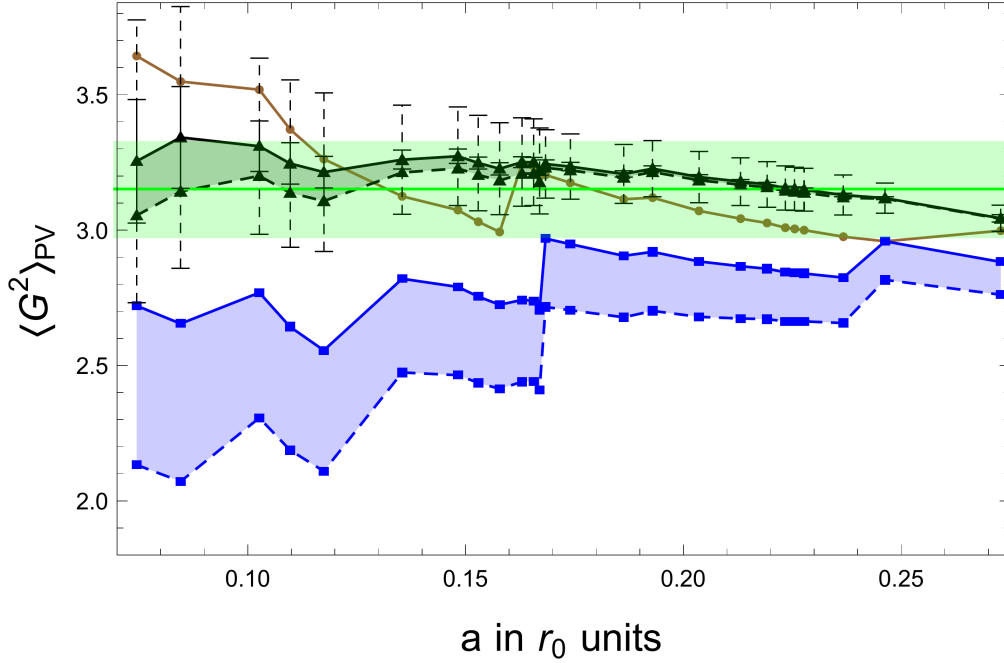


Figure 5.3: Gluon condensate with superasymptotic approximation $(0, N_P)$ (blue lines) and with hyperasymptotic accuracy $(4, 0)$ (black lines). In both cases, for each corresponding β , we show the value obtained for the gluon condensate with the values of N_P using the smallest positive (upper line) and negative (lower line) value of c that yields an integer value of N_P . For the hyperasymptotic approximation with positive c , we also show the statistical errors of the MC determination of the plaquette (inner error), and its combination in quadrature with the statistical error of the partial sum (outer error). We also show the superasymptotic approximation obtained in [112] truncating at the minimal term determined numerically (brown line). The horizontal green band and its central value are our final prediction, and the associated error, for the gluon condensate displayed in Eq. (5.58).

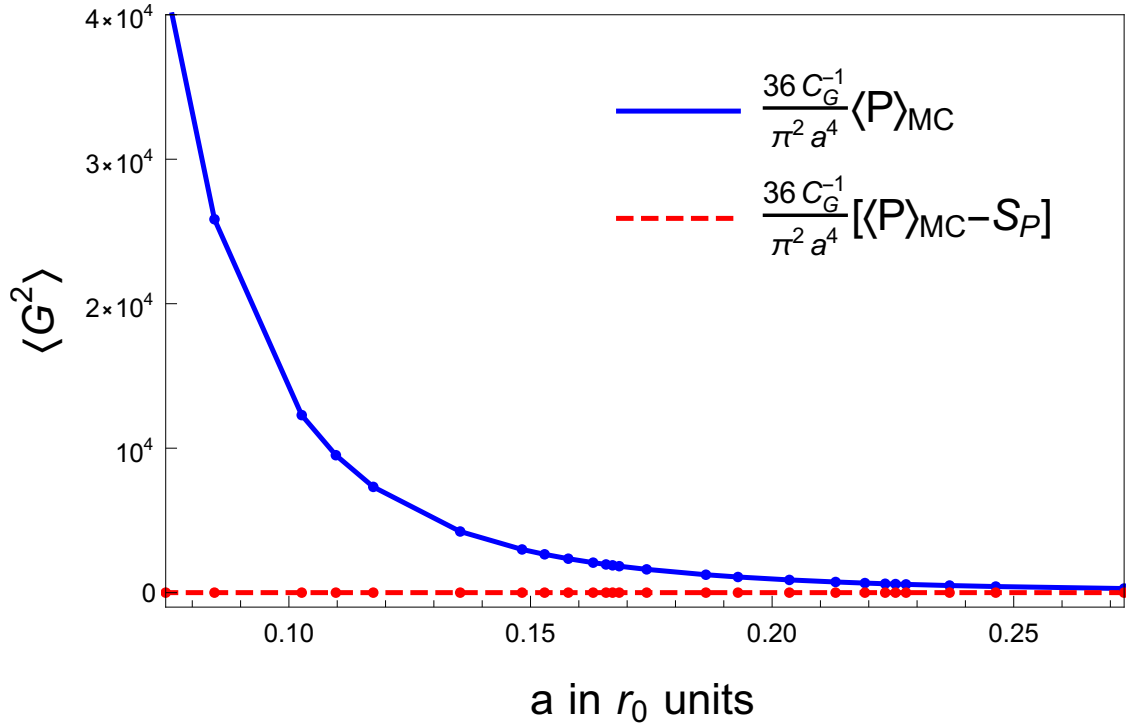


Figure 5.4: $\frac{36 C_G^{-1}}{\pi^2 a^4} \langle P \rangle_{MC}$ (continuous blue line) and $\frac{36 C_G^{-1}}{\pi^2 a^4} [\langle P \rangle_{MC} - S_P]$ (dashed red line). The second line is basically indistinguishable with respect to zero with the scale resolution of this plot. The statistical errors are smaller than the size of the points.

β	a in r_0 units	$1 - \langle P \rangle_{MC}$	$N_P(4)$	c
5.8	0.27285	0.5676510(205)	27	0.3302
5.85	0.24628	0.5751226(54)	27	0.4350
5.87	0.23672	0.5778923(54)	28	0.0392
5.89	0.22771	0.5805461(44)	28	0.0811
5.895	0.22554	0.5811950(46)	28	0.0915
5.9	0.22340	0.5818383(49)	28	0.1020
5.91	0.21921	0.5831025(46)	28	0.1229
5.925	0.21314	0.5849659(46)	28	0.1544
5.95	0.20357	0.5879738(40)	28	0.2067
5.98	0.19293	0.5914373(39)	28	0.2696
6	0.18630	0.5936846(39)	28	0.3114
6.04	0.17404	0.5979958(40)	28	0.3952
6.06	0.16836	0.6000816(34)	28	0.4371
6.065	0.16698	0.6005991(35)	29	0.0099
6.07	0.16563	0.6011049(36)	29	0.0204
6.08	0.16296	0.6021223(38)	29	0.0413
6.1	0.15782	0.6041315(38)	29	0.0832
6.12	0.15292	0.6060953(33)	29	0.1251
6.14	0.14825	0.6080241(35)	29	0.1670
6.2	0.13545	0.6136303(32)	29	0.2926
6.3	0.11746	0.6224187(30)	30	0.0644
6.35	0.10972	0.6265895(30)	30	0.1691
6.4	0.10265	0.6306291(28)	30	0.2738
6.55	0.08460	0.6420618(26)	31	0.1503
6.65	0.07450	0.6491831(19)	31	0.3598

Table 5.2: We depict various quantities associated to the various lattice spacings considered. MC data for the average plaquette extracted from [114] for 32^4 lattices and various values of β . The values of a have been obtained with Eq. (5.54). The $N_P(4)$ -s are the ones associated to the smallest positive values of c , which are listed in the last column.

In the lattice scheme, Eq. (2.72) is not accurate enough to relate the lattice spacing a with β for the β -values used in this paper. Instead, we employ the phenomenological parametrization of [113] ($x = \beta - 6$)

$$a = r_0 \exp(-1.6804 - 1.7331x + 0.7849x^2 - 0.4428x^3), \quad (5.54)$$

obtained by interpolating non-perturbative lattice simulation results. Equation (5.54) was reported to be valid within an accuracy varying from 0.5% up to 1% in the range [113] $5.7 \leq \beta \leq 6.92$, which includes the range $\beta \in [5.8, 6.65]$ we use in this paper. The values of a obtained with Eq. (5.54) for the β -s considered are shown in Table 5.2.

From Eq. (5.25), we get the small α expansion of the inverse Wilson coefficient

$$\begin{aligned} C_G^{-1}(\alpha) &= -\frac{2\pi\beta(\alpha)}{\beta_0\alpha^2} \\ &= 1 + \frac{\beta_1}{\beta_0} \frac{\alpha}{4\pi} + \frac{\beta_2}{\beta_0} \left(\frac{\alpha}{4\pi}\right)^2 + \frac{\beta_3}{\beta_0} \left(\frac{\alpha}{4\pi}\right)^3 + \mathcal{O}(\alpha^4). \end{aligned} \quad (5.55)$$

The corrections to $C_G = 1$ are small. However, the $\mathcal{O}(\alpha^2)$ and $\mathcal{O}(\alpha^3)$ terms are of similar sizes. We will account for this uncertainty in our error budget. For the central value fits, we will use the expansion above including the α^3 term.

We now turn to S_{PV} . As we have mentioned above, we compute it using the hyperasymptotic expansion. This introduces a parametric error according to the order at which we truncate the expansion, as seen in section 3.4. On top of that, we also have uncertainties in the building blocks of the expansion. The coefficients p_n , obtained in Ref. [94], are not known exactly. They carry statistical errors, and successive orders are correlated. Using the covariance matrix, also obtained in Ref. [94], the statistical error of S_{P} can be calculated. In that reference, the coefficients $p_n(N)$ were first computed on finite volumes of N^4 sites, and subsequently extrapolated to their infinite volume limits p_n . This extrapolation is subject to parametric uncertainties that need to be estimated. We follow Ref. [94], and add the differences between determinations using $N \geq \nu$ points for $\nu = 9$ (the central values) and $\nu = 7$ as systematic errors to our statistical errors. This is the same error analysis as the one used in [112].

We emphasize that the order at which we truncate the perturbative series (that is, $\alpha^{N_{\text{P}}+1}$), is different from the one used in [112]⁸. The difference between both determinations gives an estimate of the parametric error of the determination of S_{PV} by using the hyperasymptotic approximation to $(0, N_{\text{P}}(4))$ level. The magnitude of Ω_{G^2} gives an alternative estimate of this error. It is also interesting to see the magnitude of changing N_{P} by one unit by fine tuning c from the smallest positive value that yields an integer value of N_{P} to the smallest (in absolute value) negative value that yields an integer value of N_{P} . Typically, this yields slightly smaller errors. We illustrate this discussion in Fig. 5.3. All these error estimates scale with the parametric uncertainty predicted by theory $\sim \mathcal{O}(e^{-4\frac{2\pi}{\beta_0\alpha(1/a)}}) \sim \mathcal{O}(a^4\Lambda_{\text{QCD}}^4)$ times $\sqrt{\alpha}$, as mentioned in section 3.4.

If we increase the accuracy of the hyperasymptotic expansion by adding the terminant Ω_{G^2} on top of the superasymptotic approximation, the parametric error decreases, and the accuracy reached is $(4,0)$. With this accuracy, the parametric error in the hyperasymptotic expansion is $\sim \mathcal{O}(e^{-4\frac{2\pi}{\beta_0\alpha(1/a)}(1+\log(3/2))}) \sim \mathcal{O}((a\Lambda_{\text{QCD}})^{4(1+\log(3/2))})$. As it has been mentioned before, we only approximately know Ω_{G^2} , and its error will obfuscate the signal of these $\mathcal{O}((a\Lambda_{\text{QCD}})^{4(1+\log(3/2))})$ effects. For Ω_{G^2} , we use the analytic expression in Eq. (5.47) truncated at $\mathcal{O}(\alpha^2)$. The

⁸As we have already mentioned around Eq. (5.32), in this reference the perturbative expansion was truncated at α^{n_0+1} , and in general n_0 is not for all β -s equal to the N_{P} values we use, although the differences are minimal.

error of this expression comes from Z_P , and from the truncation of the weak coupling expansion of the terminant. The largest source of error comes from Z_P , which due to its size, overwhelms the parametric error associated to higher-order terms in the hyperasymptotic expansion. We also emphasize that at $(4, 0)$ level, we add the terminant to S_P , so the statistical error associated to it also needs to be taken into account.

Irrespective of the discussion of the error of the $(4, 0)$ accuracy, it is nice to see that adding the terminant to the superasymptotic expression makes the jumps that we had with the superasymptotic approximation disappear. Adding the terminant also makes the resulting curve flatter. The dependence in N_P (or in other words c) gets much milder too. We illustrate all this in Fig. 5.3.

In principle, we know perturbation theory to high enough orders to include the last term written in Eq. (5.36) and reach $(4, N')$ accuracy. Nevertheless, we find that the errors of p_n for large n hide the signal. We show in Fig. 5.6 how the statistical errors grow as we increase N' . Despite all of this, it is rewarding to see that the dependence in c basically vanishes. We will elaborate more on the $(4, N')$ case later.

5.5 The fits

We now perform the fits for the determination of the gluon condensate, and implement the discussion of the errors of the previous section. Based on Eq. (5.53), we fit

$$\frac{36}{\pi^2} C_G^{-1} \left\{ \langle P \rangle_{\text{MC}} - S_{\text{PV}} \right\} \quad (5.56)$$

to a linear function in a^4 , hereby obtaining the gluon condensate. We perform fits to various orders in the hyperasymptotic expansion of S_{PV} . For our central value fit, the range will be $\beta \in [5.8, 6.65]$, and C_G^{-1} will be truncated at order α^3 , although we will also consider variations to these specifics. The error introduced in the fitting algorithm is the sum in quadrature of the error of the MC determination of $\langle P \rangle_{\text{MC}}$, and the statistical error of S_{PV} coming from uncertainties in the p_n coefficients. As it has already been mentioned, to obtain the latter, we use the covariance matrix and, by error propagation, compute the statistical error of S_{PV} . This is the same method followed in [112], where the series of the plaquette was truncated superasymptotically. We show the size of these two different errors in Fig. 5.3. We now give results for the fits of the gluon condensate for different truncation orders in the hyperasymptotic expansion.

5.5.1 Order $(0, N_P(4))$

We start by considering fits where the perturbative expansion of the plaquette is truncated superasymptotically. We obtain

$$\langle G^2 \rangle_{\text{PV}} = 2.87(2)_{\text{stat.}} (6)_{\text{p}_{\text{ext}}} (4)_{\text{range}} (8)_{C_G} (7)_{r_0} (28)_{\text{hyp}} r_0^{-4} = 2.87(31) r_0^{-4}. \quad (5.57)$$

The first error displayed in Eq. (5.57) is the statistical error of the fit. The following errors are systematic. The second error is the error associated to different infinite volume extrapolations of the coefficients p_n . Up to this point, the discussion runs parallel to the error analysis made in [112]. Nevertheless, unlike in this reference, we do the fit in the range $\beta \in [5.8, 6.65]$. If we do the fit in the range $\beta \in [6, 6.65]$, as it was done in that reference, the result is -0.04 smaller, a small shift. This is indeed the third error in Eq. (5.57). For both ranges the reduced χ^2 are similar: 0.44 and 0.42 for the range $\beta \in [5.8, 6.65]$ and the range $\beta \in [6, 6.65]$, respectively.

The fourth error is the difference of the fits by truncating C_G^{-1} at $\mathcal{O}(\alpha^2)$ or at $\mathcal{O}(\alpha^3)$. The change is significant. This seems to be due to the slow convergence of the weak-coupling expansion in the lattice scheme. We have checked that there is convergence (albeit slow) by including higher-order terms of the beta-function using the estimates obtained in [70].

Following [112], we assign a 2.5% error for the conversion from a to r_0 units. This is the fifth error in Eq. (5.57). The last error is the estimate of the higher-order terms in the hyperasymptotic expansion not included in the superasymptotic approximation. It is taken as the difference between the fits including or not including the leading terminant. This basically gives the same error as considering the difference of doing superasymptotic fits truncating the perturbative sum at the numerical minimal term, or using Eq. (5.37). Other possible ways to estimate the error (like taking c to be negative such that N_P changes by one unit) give smaller errors. This error is by far the major source of uncertainty in Eq. (5.57). In the last equality in Eq. (5.57), we have combined all these errors in quadrature.

For reference's sake, we also state the results of the fits by truncating at the numerically minimal term as it was done in [112]. This yields, $\langle G^2 \rangle = 3.18 r_0^{-4}$ with $\chi_{\text{red}}^2 = 0.69$ for the range $\beta \in [6, 6.65]$, and $\langle G^2 \rangle = 3.05 r_0^{-4}$ with $\chi_{\text{red}}^2 = 1.28$ for the range $\beta \in [5.8, 6.65]$.

5.5.2 Order (4, 0)

We now add the leading terminant to the superasymptotic approximation and obtain

$$\langle G^2 \rangle_{\text{PV}} = 3.15(2)_{\text{stat.}}(5)_{\text{p}^{\text{ext}}}(9)_{\text{range}}(9)_{C_G}(8)_{r_0}(8)_{Z_P} r_0^{-4} = 3.15(18) r_0^{-4}. \quad (5.58)$$

The error analysis follows to a large extent the error analysis of the order $(0, N_P)$. The first error is the statistical error of the fit. We mention that the central value fit yields $\chi_{\text{red}}^2 = 0.43$. The rest of the errors are systematic. The second error is the error associated to different infinite volume extrapolations of the coefficients p_n . We emphasize again, that we do the fits over the whole range $\beta \in [5.8, 6.65]$. If we do the fit in the range $\beta \in [6, 6.65]$, the result is +0.09 larger with a rather small $\chi_{\text{red}}^2 = 0.019$. This is the third error in Eq. (5.57). Having a look to the points in Fig. 5.3, the remaining a dependence is very small but may point to a small negative slope. If anything, this effect is only visible for the largest distances. At short distances, the a dependence is completely hidden by the errors, which reflects in this very small χ_{red}^2 , but even at the largest distances, the errors hide any meaningful signal of these effects. Note that this possible remaining a dependence can be associated to higher-order terms of the hyperasymptotic expansion of S_{PV} , which would then scale as $\mathcal{O}((a\Lambda_{\text{QCD}})^{4(1+\log(3/2))})$ rather than to genuine nonperturbative corrections that would scale as $\mathcal{O}(a^6\Lambda_{\text{QCD}}^6)$. In this respect, and as we will see in the next section, it is worth noting that this small slope somewhat tends to disappear as we work with precision $(4, N')$, albeit with a huge error (see Fig. 5.6).

The fourth error is the difference of the fit truncating to $\mathcal{O}(\alpha^2)$ or to $\mathcal{O}(\alpha^3)$ the perturbative expansion of C_G^{-1} . The fifth error is the one associated to the conversion from a to r_0 units. The last error is the error associated to Z_P , the normalization of the leading renormalon. The error of this quantity is heavily correlated to the knowledge⁹ of the coefficient w_2 . Therefore, to estimate this error, we correlate the change of Z_P to setting $w_2 = 0$, that is, we perform fits taking $Z_P = (42 + 17) \times 10^4$ where w_2 is set to zero everywhere, and then take the difference of

⁹Very briefly, in [94] Z_P was estimated by comparing p_{26} with its asymptotic behavior given by Eq. (5.39), and the error of Z_P comes from including the w_2 term in Eq. (5.39) or not.

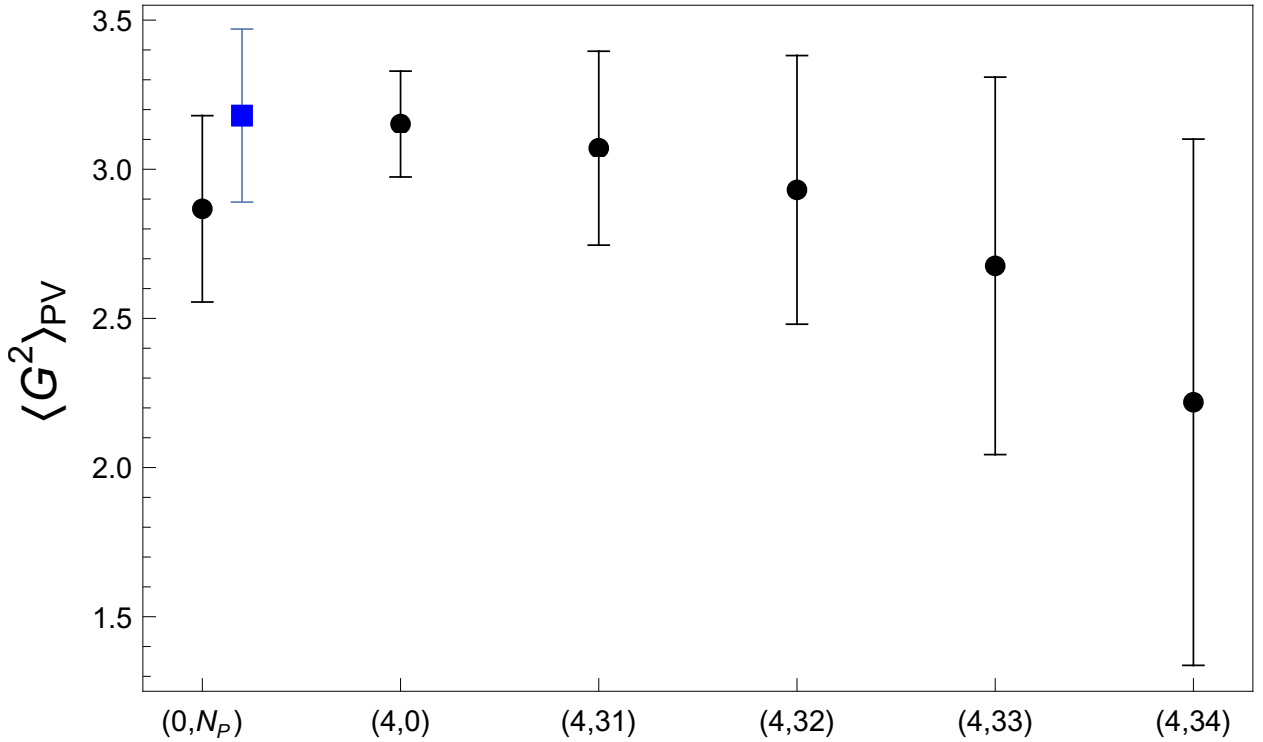


Figure 5.5: Determinations of $\langle G^2 \rangle_{PV}$ with hyperasymptotic approximation $(0, N_P)$, $(4,0)$, $(4,31)$, $(4,32)$, $(4,33)$, $(4,34)$ (black points). We also display the determination obtained in [112] (square blue point). The error displayed is the sum in quadrature of all the errors considered.

the result with the central value fit. As it has been stressed before, the subleading terms of the weak coupling expansion in Eq. (5.47) produce a smaller change and can be neglected.

We now discuss the error associated to the truncation of the hyperasymptotic approximation. As it has been mentioned before, the leading contributions to the hyperasymptotic expansion of S_{PV} that are not included in the $(4,0)$ precision are expected to scale as $\mathcal{O}((a\Lambda_{QCD})^{4(1+\log(3/2))})$, and to be suppressed by a factor $\mathcal{O}((a\Lambda_{QCD})^{4\log(3/2)})$ with respect to the typical size of Ω_{G^2} . Unlike in the case of the superasymptotic approximation, the error committed by truncating the hyperasymptotic approximation of the PV Borel sum at $(4,0)$ level are small compared with other errors. Finally, we combine all the errors in quadrature, producing the last equality in Eq. (5.58). This is our most precise prediction for $\langle G^2 \rangle_{PV}$, which we display in Fig. 5.3.

The central value we obtain does not change much with respect to the central value obtained in [112]. Nevertheless, this is to some extent by accident, as the fit is made over different intervals. On the other hand, the superasymptotic approximation truncated at the numerically minimal term appears to approach better the central value¹⁰. We will see this also for the self-energy of the static quark in a subsequent chapter. Nevertheless, the error is larger because the points are more scattered around, and because of the intrinsic inaccuracy of the superasymptotic approximation. In our case, the total error is basically shrunk by a factor 1/2. Note that the statistical error and the error associated to the infinite volume extrapolation of the coefficients are smaller now. The improvement in the quality of the fit can also be observed by the flatter curve we have now, as seen in Fig. 5.3.

¹⁰In this respect, one could also think of fine tuning the value of c to make N_P coincide with the numerically minimal term n_0 .

5.5.3 Order $(4, N')$

We may try to increase the accuracy reached with the $(4,0)$ hyperasymptotic approximation by adding the last term of Eq. (5.36). Nevertheless, the errors quickly grow and get out of hand. This is mainly due to the error of the coefficients p_n of the perturbative expansion for the last few orders in α . We have repeated the same error analysis as in the previous sections for $N' = 31, 32, 33, 34$. We show the obtained central values and errors in Figure 5.5 (see also Figure 5.6). We see how the errors quickly grow. The most important source to the error comes from the infinite volume extrapolation of the perturbative coefficients p_n .

5.6 Some plots on the asymptotics of the series of the average plaquette

Before finishing the chapter, it is interesting making a parallel with the toy models studied in chapter 3, and reproducing the analogue of Figure 3.6 and Figure 3.11 in a realistic scenario. Figure 5.8 nicely displays, for a four-dimensional gauge theory, the standard behavior expected for a factorially divergent asymptotic series (we take $\beta = 6$ for illustrative purposes). We first discuss the blue points. First, as we add more terms to the perturbative series, we get closer to the MC simulation of the plaquette. We remind the reader that for $\beta = 6$, the $N_P(4)$ for the smallest positive c is 28, as seen in Table 5.2. We see that that past the optimal truncation order, the blue points still keep converging. As it can be seen in Figure 5.7, the fixed order terms $p_n \alpha^{n+1}$ are already growing in absolute value for the last blue points, but they are still not large enough to have the blue points blow up. We can be sensitive to this effect if we also subtract our central value fit result of the gluon condensate Eq. (5.58). We are then in the same situation as for instance the blue points in Figure 3.6 and Figure 3.11, where the nonperturbative contribution is zero by construction. This is what is displayed in the black square points in Figure 5.8. We nicely reach a minimum, and after that the series deteriorates if one continues adding extra perturbative terms.

We can now carry on and subtract the leading terminant. This is what is done for the black squares in Figure 5.9 (we are still in the case $\beta = 6$), and one gets a plateau, which of course corresponds with $\frac{\pi^2}{36} C_G a^4 \langle G^2 \rangle_{PV} \approx 0.001$ for $\beta = 6$. If one also subtracts the gluon condensate, we are in the same situation as the orange points in Figure 3.6. This is what is displayed in the red diamond points in Figure 5.9, whose qualitative behavior is analogous to the one displayed by the aforementioned orange points of the large β_0 case, in the sense that we get a jump after adding the terminant. If more coefficients p_n were known, and if the errors in the currently known ones could be reduced, it would be interesting to carry on with the plot.

5.7 Final remarks

We will now summarize what we have seen in this chapter. We have given the hyperasymptotic expansion of the PV Borel sum of the plaquette, with a precision that includes the terminant associated to the leading $d = 4$ renormalon. Subleading effects have also been considered. This has been used to give a determination of the gluon condensate in SU(3) pure gluodynamics

$$\langle G^2 \rangle_{PV}(n_f = 0) = 3.15(18) r_0^{-4}. \quad (5.59)$$

As we have seen, at present, the limiting factor for improving the determination of the gluon condensate in pure gluodynamics is the error of perturbation theory. All systematic sources of error have its origin in the errors of

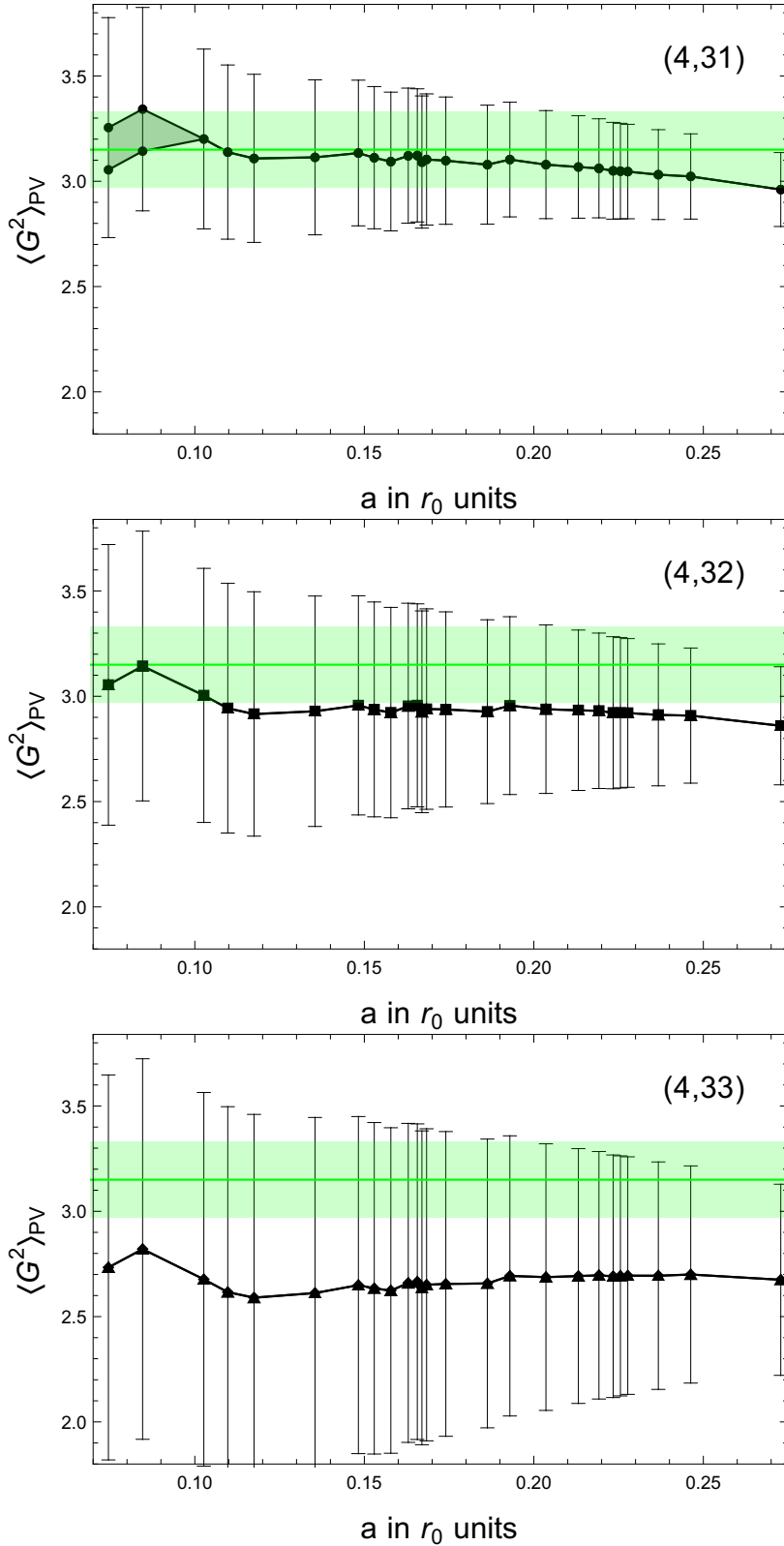


Figure 5.6: Gluon condensate in r_0 units with hyperasymptotic accuracy $(4, N')$ for $N' = 31$ (upper panel), $N' = 32$ (middle panel) and $N' = 33$ (lower panel). In all cases, for each corresponding β , we show the value obtained for the gluon condensate with the values of N_P using the smallest positive (upper line) and negative (lower line) value of c that yields an integer value of N_P . Notice that except in the upper panel, these two lines are on top of each other. In any case, keep in mind that from Table 5.2, we see that for the highest β -s the $N_P(4)$ associated to the positive/negative c is 31/32. Therefore, for some values of a , we cannot add any order at all (specially for the negative c case which has a higher N_P) in the cases $N' = 31$ and $N' = 32$. The error is the statistical error of the MC determination of the plaquette and of the perturbative sum combined in quadrature. The horizontal green band and its central value are our final prediction, and the associated error, for the gluon condensate displayed in Eq. (5.58).

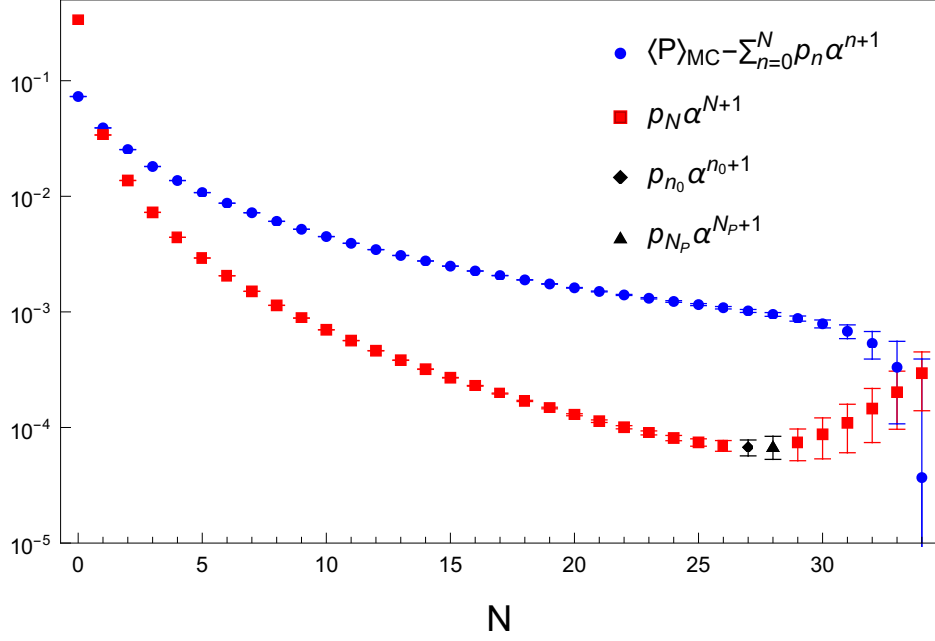


Figure 5.7: We draw $\langle P \rangle_{\text{MC}} - \sum_{n=0}^N p_n \alpha^{n+1}$ (full blue circle points), and $p_N \alpha^{N+1}$ (full red squares points) for different values of N , up to $N = 34$ for $\beta = 6$. The error of the blue points is the statistical error of of the MC simulation and of the sum $\sum_{n=0}^N p_n \alpha^{n+1}$ combined in quadrature (for large N the error of the perturbative sum is dominant). The error displayed here of the perturbative sum does not include the systematic error of the infinite volume extrapolation of the coefficients p_n . The error displayed for the red points is the complete error (statistical plus systematic combined in quadrature) of the p_N coefficients obtained in [94] times α^{N+1} . The black diamond stands for the numerically minimal value of $p_N \alpha^{N+1}$. The black triangle is $p_{N_P} \alpha^{N_P+1}$ using the smallest positive c that makes N_P an integer. Note that the plus/minus error does not display symmetrically in the plot because of the logarithmic scale.

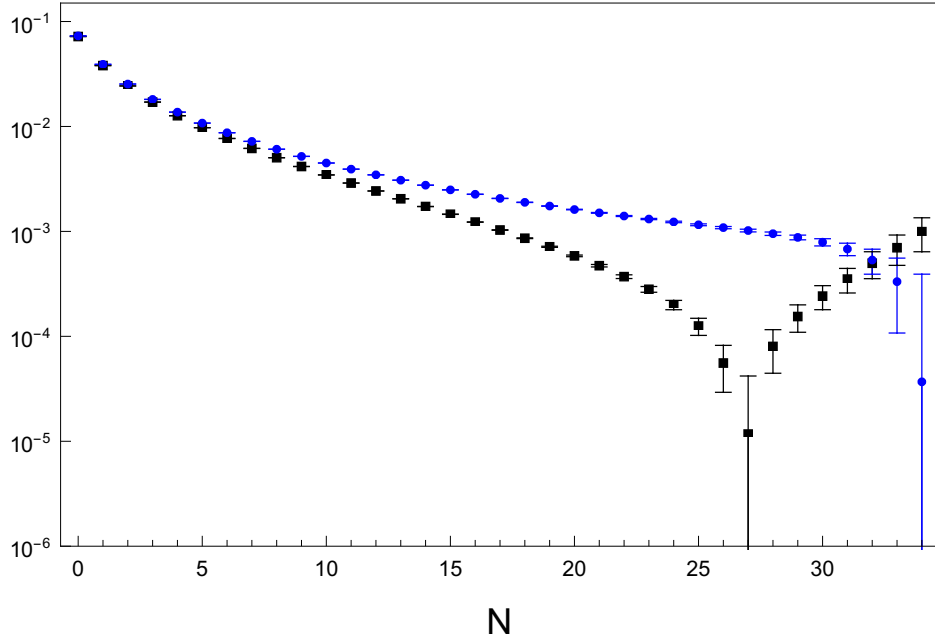


Figure 5.8: We draw $|\langle P \rangle_{\text{MC}} - \sum_{n=0}^N p_n \alpha^{n+1}|$ (blue points) and $|\langle P \rangle_{\text{MC}} - (\sum_{n=0}^N p_n \alpha^{n+1} + \frac{\pi^2}{36} C_G(\alpha) a^4 \langle G^2 \rangle_{\text{PV}})|$ (black squares) for $\beta = 6$ and $N \in [0, 34]$. The error, in all cases, is the statistical error of the sum $\sum_{n=0}^N p_n \alpha^{n+1}$ and of $\langle P \rangle_{\text{MC}}$ combined in quadrature. Note that the plus/minus error does not display symmetrically in the plot because of the logarithmic scale, and also because of the logarithmic scale the error looks different for different points located at the same N .

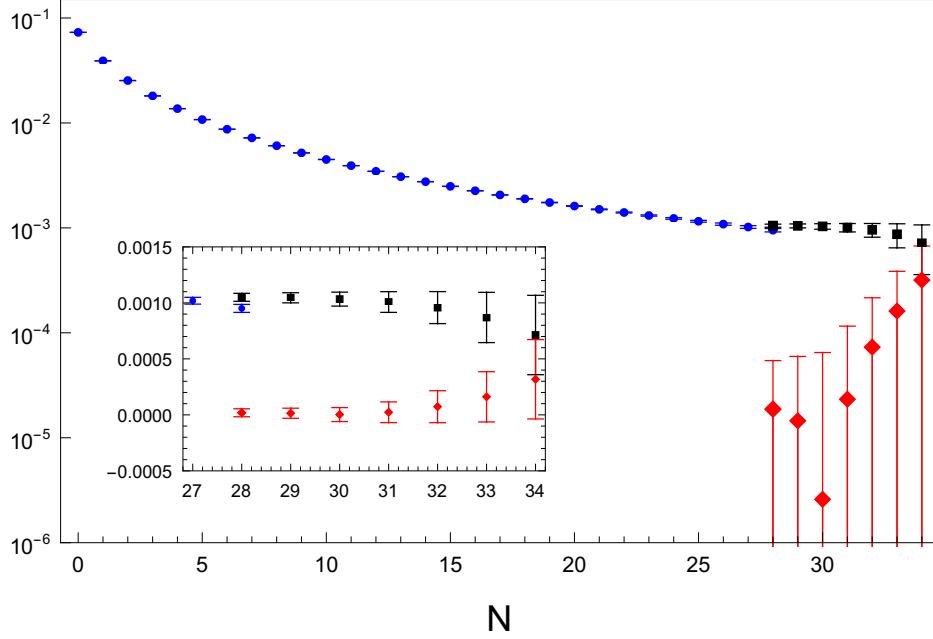


Figure 5.9: For $\beta = 6$, we draw $\langle P \rangle_{\text{MC}} - \sum_{n=0}^N p_n \alpha^{n+1}$ for $N \leq N_P$ (blue points). For $N = N_P$, we draw $\langle P \rangle_{\text{MC}} - \sum_{n=0}^{N_P} p_n \alpha^{n+1} - \Omega_{G^2}$ (black square at $N = 28$). For $N > N_P$, we draw $\langle P \rangle_{\text{MC}} - (\sum_{n=0}^{N_P} p_n \alpha^{n+1} + \Omega_{G^2} + \sum_{n=N_P+1}^N [p_n - p_n^{(\text{as})}] \alpha^{n+1})$ (the remaining black squares). We repeat with red diamonds the points displayed in black squares by subtracting the central value result for the gluon condensate. For $N = N_P$, we draw $\langle P \rangle_{\text{MC}} - (\sum_{n=0}^{N_P} p_n \alpha^{n+1} + \Omega_{G^2} + \frac{\pi^2}{36} C_G(\alpha) a^4 \langle G^2 \rangle_{\text{PV}})$ (red diamond at $N = 28$). For $N > N_P$, we draw $\langle P \rangle_{\text{MC}} - (\sum_{n=0}^{N_P} p_n \alpha^{n+1} + \Omega_{G^2} + \frac{\pi^2}{36} C_G(\alpha) a^4 \langle G^2 \rangle_{\text{PV}} + \sum_{n=N_P+1}^N [p_n - p_n^{(\text{as})}] \alpha^{n+1})$ (red diamonds). The error in all cases is the statistical error of the sum $\sum_{n=0}^N p_n \alpha^{n+1}$ and $\langle P \rangle_{\text{MC}}$ combined in quadrature. Note that the plus/minus error does not display symmetrically in the plot because of the logarithmic scale. Also, because of the logarithmic scale, the error looks different for different points located at the same N . In the small box, a zoom of the points for $N \geq 27$ are shown in non-logarithmic scale.

perturbation theory (even what we call statistical errors of Eq. (5.53) are dominated by the statistical errors of the coefficients p_n). More precise values of these perturbative coefficients, and their knowledge to higher orders, would yield a more precise determination of the normalization of the renormalon Z_P , and would allow working with hyperasymptotic accuracy $(4, N')$.

Nowadays, if we try to reach this accuracy, we find that the error of the coefficients are too large to get accurate results. The situation with active light quarks is in an early stage but starts to be promising. The coefficients of the perturbative coefficients have been computed at finite volume in [115] for QCD with two massless fermions. More data at different volumes, and the infinite volume extrapolation of these coefficients, would then allow us to repeat the analysis we have carried out, and to give a determination of the gluon condensate in QCD with two massless fermions.

Chapter 6

Hyperasymptotics of the heavy quark pole mass and $\bar{\Lambda}$

In this chapter, we will give an estimate of the power correction $\bar{\Lambda}$ of HQET, following the same rationale we have followed in the previous chapter for the gluon condensate. We will consider the $n_f = 3$ and $n_f = 0$ cases. A very important player in this chapter will be the perturbative series relating the pole mass of a quark with its $\overline{\text{MS}}$ mass (for details on the formulas see Appendix F)

$$m_{\text{OS}} = \bar{m} + \sum_{n=0}^{\infty} r_n(\mu/\bar{m})\alpha^{n+1}(\mu). \quad (6.1)$$

This chapter is based on [70].

6.1 $\bar{\Lambda}_{\text{PV}}(n_f = 3)$ from B physics in the $\overline{\text{MS}}$ scheme

B mesons are like the hydrogen atom of QCD, with a heavy b quark playing the role of the proton. In HQET, their mass M_B has the following expansion in inverse powers of the heavy quark

$$M_B = m_{b,\text{OS}} + \bar{\Lambda} + \mathcal{O}\left(m_{b,\text{OS}}^{-1}\right), \quad (6.2)$$

where m_b is the perturbative series relating the $\overline{\text{MS}}$ and the pole mass of the bottom quark, written in terms of the strong coupling of QCD with 3 active massless flavors. The formula used is Eq. (6.1), with $n_f = 3$ and $\bar{m}_b = 4.186$ GeV taken from [116]

$$m_{b,\text{OS}} = \bar{m}_b + \sum_{n=0}^{\infty} r_n(\mu/\bar{m}_b)\alpha^{n+1}(\mu), \quad (6.3)$$

where the coefficients r_n are the ones given in Eq. (F.3). In accordance to what we say in Appendix F, we estimate non-zero charm quark mass effects by adding -2 MeV to the above expression. The series above is understood as a formal series. $\bar{\Lambda} \sim \Lambda_{\text{QCD}}$ is a power correction reminiscent of the power corrections in the OPE. Being bound states of two quarks, B mesons can have either spin 0 or spin 1. The spin 0 version of Eq. (6.2) reads¹

$$M_B = m_{b,\text{OS}} + \bar{\Lambda} - \frac{1}{2m_{b,\text{OS}}}\lambda_1 - \frac{3}{2m_{b,\text{OS}}}\lambda_2 + \mathcal{O}\left(m_{b,\text{OS}}^{-2}\right), \quad (6.4)$$

where $\lambda_1, \lambda_2 \sim \Lambda_{\text{QCD}}^2$ are new power corrections. The spin 1 version of Eq. (6.2) reads

$$M_{B^*} = m_{b,\text{OS}} + \bar{\Lambda} - \frac{1}{2m_{b,\text{OS}}}\lambda_1 + \frac{1}{2m_{b,\text{OS}}}\lambda_2 + \mathcal{O}\left(m_{b,\text{OS}}^{-2}\right). \quad (6.5)$$

¹These formulas can be found for instance in [117].

We see that the expansions are identical up until the term proportional to λ_2 , where we have a spin dependent splitting. In fact, we can work with the so called *spin-averaged* mass by taking

$$\langle M_B \rangle \equiv \frac{1}{4}(M_B + 3M_{B^*}) = m_{b,\text{OS}} + \bar{\Lambda} - \frac{1}{2m_{b,\text{OS}}} \lambda_1 + \mathcal{O}\left(m_{b,\text{OS}}^{-2}\right), \quad (6.6)$$

and get rid of the spin dependent λ_2 term. The above equation is indeed the one we will consider in what is to follow. As we have already mentioned, the expression above is reminiscent to the OPEs we have seen before. It contains a perturbative expansion, the pole mass of the b quark, and on top of that, terms that are exponentially suppressed in α are introduced. The series of the pole mass of the b quark is (expected to be) divergent, so there will be an inherent ambiguity to it. This ambiguity is translated to the power corrections, such that the whole sum, that is, the mass of the B meson, is unambiguous. Analogously to what we did in chapter 5 with the plaquette, we will regulate the formal series $m_{b,\text{OS}}$ using the PV Borel sum, which we will approximate using the method of chapter 3. We will disregard the $m_{b,\text{OS}}^{-1}$ terms, so that

$$\bar{\Lambda}_{\text{PV}} = \langle M_B \rangle - m_{b,\text{OS}}^{\text{PV}} + \mathcal{O}\left(\frac{1}{m_{b,\text{OS}}}\right). \quad (6.7)$$

We will use the above equation to estimate $\bar{\Lambda}_{\text{PV}}$.

The leading renormalon of the series of the pole mass minus its $\overline{\text{MS}}$ mass is located at $u = 1/2$. Defining $\tilde{m} \equiv m_{b,\text{OS}} - \bar{m}_b$, the Borel transform of \tilde{m} around this singularity reads

$$\hat{\tilde{m}}(t(u)) = Z_1 \mu \frac{1}{(1-2u)^{1+b}} \left\{ 1 + w_1(1-2u) + w_2(1-2u)^2 + w_3(1-2u)^3 + \dots \right\}. \quad (6.8)$$

Recall that as always $u = \frac{\beta_0}{4\pi} t$. $Z_1 = 0.56255(260)$ has been extracted from [118, 119]. The coefficients w_i are those of section 2.6, adapted for this specific case. They read

$$w_1 = s_1, \quad (6.9)$$

$$w_2 = \frac{1}{2} \frac{b}{b-1} (s_1^2 - 2s_2), \quad (6.10)$$

$$w_3 = \frac{1}{6} \frac{b^2}{(b-2)(b-1)} (s_1^3 - 6s_1s_2 + 6s_3), \quad (6.11)$$

where b and s_i can also be found in section 2.6. Accordingly, the terminant associated to this renormalon is

$$\Omega_1 = \alpha^{1/2}(\mu) K_{\text{IR}}^{(\text{P})} \frac{\mu}{\bar{m}_b} e^{-\frac{2\pi}{\beta_0 \alpha(\mu)}} \left(\frac{\beta_0 \alpha(\mu)}{4\pi} \right)^{-b} \left\{ 1 + \bar{K}_{\text{IR},1}^{(\text{P})} \alpha(\mu) + \bar{K}_{\text{IR},2}^{(\text{P})} \alpha^2(\mu) + \mathcal{O}(\alpha^3(\mu)) \right\}, \quad (6.12)$$

where

$$K_{\text{IR}}^{(\text{P})} = -\frac{Z_1 2^{1-b}}{\Gamma(1+b)} \beta_0^{-1/2} \left[-\eta_c + \frac{1}{3} \right], \quad (6.13)$$

$$\bar{K}_{\text{IR},1}^{(\text{P})} = \frac{\beta_0/(\pi)}{-\eta_c + \frac{1}{3}} \left[-w_1 b \left(\frac{1}{2} \eta_c + \frac{1}{3} \right) - \frac{1}{12} \eta_c^3 + \frac{1}{24} \eta_c - \frac{1}{1080} \right], \quad (6.14)$$

$$\begin{aligned} \bar{K}_{\text{IR},2}^{(\text{P})} &= \frac{\beta_0^2/\pi^2}{-\eta_c + \frac{1}{3}} \left[-w_2(b-1)b \left(\frac{1}{4} \eta_c + \frac{5}{12} \right) + w_1 b \left(-\frac{1}{24} \eta_c^3 - \frac{1}{8} \eta_c^2 - \frac{5}{48} \eta_c - \frac{23}{1080} \right) \right. \\ &\quad \left. - \frac{1}{160} \eta_c^5 - \frac{1}{96} \eta_c^4 + \frac{1}{144} \eta_c^3 + \frac{1}{96} \eta_c^2 - \frac{1}{640} \eta_c - \frac{25}{24192} \right], \end{aligned} \quad (6.15)$$

where

$$\eta_c = -b + \frac{2\pi c}{\beta_0} - 1. \quad (6.16)$$

With these ingredients, we construct the hyperasymptotic expansion of the PV Borel sum of the pole mass of the bottom quark

$$m_{b,\text{OS}}^{\text{PV}} = m_{b,\text{OS}}^{\text{P}} + \bar{m}_b \Omega_1 + \sum_{n=N_{\text{P}}(1)+1}^{N_{\text{P}}(2)} (r_n - r_n^{(\text{as})}) \alpha^{n+1}(\mu) + \mathcal{O}\left(e^{\frac{-4\pi}{\beta_0 \alpha(\mu)}}\right), \quad (6.17)$$

where

$$m_{b,\text{OS}}^{\text{P}} \equiv \bar{m}_b + \sum_{n=0}^{N_{\text{P}}(1)} r_n(\mu/\bar{m}_b) \alpha^{n+1}(\mu), \quad (6.18)$$

and

$$r_n^{(\text{as})} = Z_1 \mu \left(\frac{\beta_0}{2\pi}\right)^n \frac{\Gamma(n+1+b)}{\Gamma(1+b)} \left\{ 1 + w_1 \frac{b}{n+b} + w_2 \frac{b(b-1)}{(n+b)(n+b-1)} + w_3 \frac{b(b-1)(b-2)}{(n+b)(n+b-1)(n+b-2)} + \dots \right\}. \quad (6.19)$$

In Eq. (6.17), we have assumed the subleading renormalon of the pole mass to be parametrized by $|d| = 2$. Nevertheless, in practice this is not relevant, as we only know until the coefficient r_3 , and we will be limited by this.

Let's now give a value for the superasymptotically truncated pole mass of the bottom quark. For our central value, we consider $\mu = \bar{m}_b$. For such a value of μ , the integer $N_{\text{P}}(1)$ that has the smallest c is $N_{\text{P}}(1) = 3$, with $c = 0.3611$. This yields

$$m_{b,\text{OS}}^{\text{P}} = 5077(\mu)_{-242}^{+134} \text{ MeV}. \quad (6.20)$$

The quoted error comes from varying μ in the range $\mu \in [\bar{m}_b/2, 2\bar{m}_b]$. If instead, we take $N_{\text{P}}(1) = 2$ (with $c = 1.7935$) we get

$$m_{b,\text{OS}}^{\text{P}} = 4922_{-167}^{+107} \text{ MeV}. \quad (6.21)$$

Let's now consider again the $N_{\text{P}} = 3$ case, and include the terminant. This yields the PV Borel sum of the pole mass of the bottom quark to $(D, N) = (1, 0)$ order in the hyperasymptotic expansion

$$m_{b,\text{OS}}^{\text{PV}} = 4836(\mu)_{-17}^{+8} (Z_1)_{+12}^{-11} (\alpha)_{-9}^{+8} \text{ MeV}. \quad (6.22)$$

For the variation of μ , we have taken again the range $\mu \in [\bar{m}_b/2, 2\bar{m}_b]$. We find that the scale dependence of the PV mass is much smaller than for the superasymptotic approximation, in accordance with what we would expect. As we have already mentioned, for the error of Z_1 , we have taken $Z_1(n_f = 3) = 0.5626(260)$. For the uncertainty in α , we take $\Lambda_{\overline{\text{MS}}}^{(n_f=3)} = 332 \pm 17 \text{ MeV}$ from [120].

Notice that with $N_{\text{P}}(1) = 3$, we cannot add more terms in the hyperasymptotic expansion beyond the leading terminant, as we do not know the necessary exact coefficients of the series of the pole mass of the b quark. To roughly estimate the size of subleading terms in the hyperasymptotic expansion, we could compute the PV Borel sum with $N_{\text{P}}(1) = 2$. In the counting of the hyperasymptotic expansion, the precision is then $(1, 3 - N_{\text{P}}(1))$. The difference is below 1 MeV (after including $[r_3 - r_3^{(\text{as})}] \alpha^4$, otherwise, that is, just considering the order $(D, N) = (1, 0)$ with $N_{\text{P}}(1) = 2$, the difference is 7.5 MeV). Even considering $N_{\text{P}}(1) = 1$, which formally allows us to reach the next renormalon located at $2N_{\text{P}}(1) = 2$ (i.e. $(D, N) = (1, N_{\text{P}}(1) = 1)$ precision), the difference is $\sim 7 \text{ MeV}$.

Alternatively, the remaining μ scale dependence of $m_{b,\text{OS}}^{\text{P}}(\bar{m}_b) + \bar{m}_b \Omega_1$ also gives a measure of the uncomputed $\sum_{n=N_{\text{P}}(1)+1}^{N_{\text{P}}(2)} (r_n - r_n^{(\text{as})}) \alpha^{n+1}$ term, as such scale dependence should cancel in the total sum. We will then take it as the associated error. Actually, the error associated to Z_1 is also a measure of the lack of knowledge of higher

order terms in perturbation theory, and therefore, there is some degree of double counting by considering these two errors separately. At last then, we determine $\bar{\Lambda}_{\text{PV}}$ from Eq. (6.7). We obtain

$$\bar{\Lambda}_{\text{PV}} = 477(\mu)_{+17}^{-8}(Z_1)_{-12}^{+11}(\alpha)_{+9}^{-8}(\mathcal{O}(1/m))_{-46}^{+46} \text{ MeV}, \quad (6.23)$$

where we have included an extra error source compared to Eq. (6.22). This extra error is associated to the $\mathcal{O}(1/m)$ corrections in Eq. (6.7). The existence or not of genuine NP $1/m$ corrections may introduce a significant error. In case they exist, if we take the hyperfine energy splitting as a measure of $1/m$ corrections, we find shifts from the central values of order ~ 46 MeV and ~ 140 MeV for B and D mesons respectively. As Eq. (6.23) has been obtained from the B meson spin-averaged mass, we conservatively estimate the error associated to genuine NP $1/m$ corrections to be of order ~ 46 MeV, as it is the most we can do from phenomenology and perturbation theory. Let us recall however, that recent lattice simulations point to much smaller genuine NP $1/m$ corrections for the spin-independent average [121].

6.1.1 Comparison with other works

6.1.1.1 The RS mass

We now compare our analysis with existing threshold masses. We focus on the RS (renormalon subtracted) mass [122], and its relatives². To define the RS mass, one considers the series of the pole mass of Eq. (6.1) evaluated at some $\mu = \nu_f$, and subtracts to it the leading asymptotic behavior associated to the $d = 1$ renormalon of Eq. (6.19)

$$m_{\text{RS}}(\nu_f) = \bar{m} + \sum_{n=0}^{\infty} r_n(\nu_f/\bar{m})\alpha^{n+1}(\nu_f) - \delta m_{\text{RS}}^{(n_0=0)}, \quad (6.24)$$

where

$$\delta m_{\text{RS}}^{(n_0)} \equiv \sum_{n=n_0}^{\infty} Z_1 \nu_f \left(\frac{\beta_0}{2\pi}\right)^n \frac{\Gamma(n+1+b)}{\Gamma(1+b)} \left\{ 1 + w_1 \frac{b}{n+b} + \dots \right\} \alpha^{n+1}(\nu_f), \quad (6.25)$$

and then re-expands the series of Eq. (6.24) for $\alpha(\mu)$

$$m_{\text{RS}}(\nu_f) \equiv \bar{m} + \sum_{n=0}^{\infty} r_n^{\text{RS}}(\mu, \nu_f) \alpha^{n+1}(\mu). \quad (6.26)$$

The series above is a formal series, which in practical applications is typically truncated at $\alpha^{N+1}(\mu)$, where $N = N_{\text{max}} \equiv$ the maximal number of coefficients of the perturbative expansion that are known exactly (we assume that N_{max} is not high enough to make us worry about subleading renormalons). In order to lessen the ν_f scale dependence, the RS¹ scheme was also defined, by taking $n_0 = 1$ in Eq. (6.24) before re-expanding³ in $\alpha(\mu)$. Obviously, one can generalize to RS^(n_0), where the subtraction starts at order α^{n_0+1}

$$m_{\text{RS}^{(n_0)}}(\nu_f) = m_{\text{OS}} - \delta m_{\text{RS}}^{(n_0)} = \bar{m} + \sum_{n=0}^{n_0-1} r_n(\mu/\bar{m})\alpha^{n+1}(\mu) + \sum_{n=n_0}^N r_n^{\text{RS}^{(n_0)}}(\mu, \nu_f)\alpha^{n+1}(\mu). \quad (6.27)$$

To connect with the approach used in this chapter, we take $\nu_f = \mu$. Note that then $r_n^{\text{RS}^{(n_0)}}(\mu, \mu) = r_n(\mu/\bar{m}) - r_n^{\text{as}}(\mu)$. We also fix $n_0 = N = N_{\text{P}}(1)$. This smoothly connects the RS schemes with the schemes where the series

²Conceptually they are equivalent to the kinetic [123] or PS mass [124], as they have an explicit cut-off as well. These other schemes are different at low orders, but they share the same asymptotic behavior.

³Nevertheless, we can not increase n_0 arbitrarily, otherwise the renormalon is not canceled. Moreover, the value of n_0 for which there is no cancellation of the renormalon will depend on μ . Therefore, when including higher orders, one should do it with care once approaching the minimal term.

is truncated at the minimal term. One can then connect the RS masses with the PV Borel sum straightforwardly

$$m_{\text{RS}^{(n_0)}}(\nu_f) = \bar{m} + \sum_{n=0}^{N_{\text{P}}(1)} r_n(\mu/\bar{m})\alpha^{n+1}(\mu) - r_{N_{\text{P}}(1)}^{(\text{as})}(\mu)\alpha^{n+1}(\mu), \quad (6.28)$$

$$m_{\text{RS}^{(n_0)}}(\nu_f) = m_{\text{PV}}^{(0, N_{\text{P}}(1))} - r_{N_{\text{P}}(1)}^{(\text{as})}(\mu)\alpha^{n+1}(\mu), \quad (6.29)$$

where we have used the notation of section 3.4.

6.1.1.2 The BR mass

We now consider the threshold mass named m_{BR} (BR stands for Borel resummation), defined in [125] (see also [126]). The author directly works with the Borel transform, and then regulates the Borel integral using the PV prescription. The Borel transform is approximated by including the exact known coefficients, plus the leading asymptotic behavior. In our notation, the considered expression reads

$$\hat{m}(t)_{N,M} \equiv \sum_{n=0}^N h_n t^n + Z_1 \frac{\mu}{\bar{m}} \frac{1}{\left(1 - \frac{\beta_0 t}{2\pi}\right)^{1+b}} \sum_{j=0}^M w_j \left(1 - \frac{\beta_0 t}{2\pi}\right)^j, \quad (6.30)$$

where $w_0 = 1$. In the above expression, $N = M = 2$ was considered (the known coefficients at that time). Thus

$$m_{\text{BR}} \equiv \bar{m} + \text{PV} \int_0^\infty e^{-t/\alpha(\mu)} \hat{m}(t)_{N,M}. \quad (6.31)$$

The μ dependence of m_{BR} was usually fixed to $\mu = m$, except in [127]. To make a quantitative comparison with our analysis, we make explicit the μ dependence in m_{BR} . Eq. (6.30) contains information of the series truncated at $\alpha^{N+1}(\mu)$, plus the leading divergence, and thus

$$m_{\text{BR}} = \bar{m} + \sum_{n=0}^N r_n(\mu/\bar{m})\alpha^{n+1}(\mu) + T_1(N), \quad (6.32)$$

where $T_1(N)$ is the terminant associated to the tail

$$T_1(N) \sim \sum_{n=N+1}^{\infty} r_n^{(\text{as})}(\mu)\alpha^{n+1}(\mu). \quad (6.33)$$

Since the upper limit of the second sum in the RHS of Eq. (6.30) is M , $T_1(N)$ is computed by including up until w_M in Eq. (3.66). We can relate this terminant to the one we have been considering so far, T_1 , which is associated to a remainder tail that begins at $\alpha^{N_{\text{P}}(1)+2}$. If $N > N_{\text{P}}(1)$, we have

$$T_1 = \sum_{n=N_{\text{P}}(1)+1}^N r_n^{(\text{as})}(\mu)\alpha^{n+1}(\mu) + T_1(N). \quad (6.34)$$

If $N = N_{\text{P}}(1)$, we simply have that $T_1(N) = T_1$, and if $N < N_{\text{P}}(1)$

$$T_1(N) = \sum_{n=N+1}^{N_{\text{P}}(1)} r_n^{(\text{as})}(\mu)\alpha^{n+1}(\mu) + T_1. \quad (6.35)$$

Therefore, if $N < N_{\text{P}}(1)$, from Eq. (6.32), we get

$$m_{\text{BR}} = \bar{m} + \sum_{n=0}^{N_{\text{P}}(1)} r_n(\mu/\bar{m})\alpha^{n+1}(\mu) + T_1 - \sum_{n=N+1}^{N_{\text{P}}(1)} \left(r_n(\mu/\bar{m}) - r_n^{(\text{as})}(\mu)\right)\alpha^{n+1}(\mu), \quad (6.36)$$

$$m_{\text{BR}} = m_{\text{PV}}^{(1,0)} - \sum_{n=N+1}^{N_{\text{P}}(1)} \left(r_n(\mu/\bar{m}) - r_n^{(\text{as})}(\mu) \right) \alpha^{n+1}(\mu), \quad (6.37)$$

where we have used the notation of section 3.4. If $N = N_{\text{P}}(1)$, we simply get

$$m_{\text{BR}} = m_{\text{PV}}^{(1,0)}, \quad (6.38)$$

and if $N > N_{\text{P}}(1)$, from Eq. (6.32), we get

$$m_{\text{BR}} = \bar{m} + \sum_{n=0}^{N_{\text{P}}(1)} r_n(\mu/\bar{m}) \alpha^{n+1}(\mu) + T_1 + \sum_{n=N_{\text{P}}(1)+1}^N \left(r_n(\mu/\bar{m}) - r_n^{(\text{as})}(\mu) \right) \alpha^{n+1}(\mu), \quad (6.39)$$

$$m_{\text{BR}} = m_{\text{PV}}^{(1, N - N_{\text{P}}(1))}. \quad (6.40)$$

6.1.1.3 The MRS mass

We can also connect our results with m_{MRS} (minimal renormalon subtracted), defined in [128]. Let us consider the formal series of the pole mass again

$$m_{\text{OS}} = \bar{m} + \sum_{n=0}^{\infty} r_n(\mu/\bar{m}) \alpha^{n+1}(\mu), \quad (6.41)$$

and let us add and subtract the leading asymptotic behavior

$$m_{\text{OS}} = \bar{m} + \sum_{n=0}^{\infty} \left(r_n(\mu/\bar{m}) - r_n^{(\text{as})}(\mu) \right) \alpha^{n+1}(\mu) + \sum_{n=0}^{\infty} r_n^{(\text{as})}(\mu) \alpha^{n+1}(\mu). \quad (6.42)$$

The borel transform of the last series in the RHS above contains the leading renormalon of the pole mass. As we have seen, one cannot just compute a Borel sum from the Borel transform of this series due to the singularity in the integration path. Nonetheless, one can compute the integral in the Laplace transform until we reach the renormalon

$$\mathcal{J}_{\text{MRS}}(\mu) \equiv \int_0^{\frac{2\pi}{\beta_0}} dt e^{-t/\alpha(\mu)} \sum_{n=0}^{\infty} \frac{r_n^{(\text{as})}(\mu)}{n!} t^n, \quad (6.43)$$

and the part of the full Borel sum where one needs to regulate the integral is

$$\delta m \equiv \int_{\frac{2\pi}{\beta_0}}^{\infty} dt e^{-t/\alpha(\mu)} \sum_{n=0}^{\infty} \frac{r_n^{(\text{as})}(\mu)}{n!} t^n, \quad (6.44)$$

where we emphasize that the above integral needs some prescription to avoid the branch cut singularity. The idea of the MRS mass is just to subtract this ambiguous term δm from the pole mass. That is, heuristically, we can write Eq. (6.42) as

$$m_{\text{OS}} = \bar{m} + \sum_{n=0}^{\infty} \left(r_n(\mu/\bar{m}) - r_n^{(\text{as})}(\mu) \right) \alpha^{n+1}(\mu) + \mathcal{J}_{\text{MRS}} + \delta m, \quad (6.45)$$

where we emphasize that being rigorous, the above equation is meaningless due to the δm term, and is just meant as a heuristics. The idea, as we have said, is then to subtract this δm from the pole mass and to define

$$m_{\text{MRS}} \equiv \bar{m} + \sum_{n=0}^{\infty} \left(r_n(\mu/\bar{m}) - r_n^{(\text{as})}(\mu) \right) \alpha^{n+1}(\mu) + \mathcal{J}_{\text{MRS}}(\mu), \quad (6.46)$$

where notice that the above series is well defined as a formal series. One can relate the MSR mass and the RS mass in the following way

$$m_{\text{RS}}(\nu_f) = m_{\text{MRS}}(\nu_f) - \mathcal{J}_{\text{MRS}}(\nu_f). \quad (6.47)$$

In [128], we can also find the relation between the PV and the MSR mass given by

$$m_{\text{OS}}^{\text{PV}} = m_{\text{MRS}} - \cos(\pi b) \frac{4\pi\Gamma(-b)}{2^{1+b}\beta_0} Z_1^X \Lambda_X. \quad (6.48)$$

6.1.1.4 Determinations of $\bar{\Lambda}$

Earlier direct determinations of $\bar{\Lambda}_{\text{PV}}$ or m_{PV} can be found in [125, 127]. The formulas are equivalent to those used here to one order less (using $N_{\text{P}}(1) = 2$). They also include less terms in the sum in Eq. (6.19). More recently, a determination of $\bar{\Lambda}$ has been obtained in [121] using lattice data. In this case the formulas are equivalent to those used here since we use $N_{\text{P}}(1) = 3$ (see Eq. (57) of Ref. [68]), except for the fact that the scale μ was always fixed equal to the heavy quark mass, and that the mass was obtained in the MRS scheme [128]. As we have seen in Eq. (6.48), the relation between the PV and the MRS mass is also given in this reference. Using it we obtain (where we combine quadratically the error of $Z_1^{\overline{\text{MS}}}$ and $\Lambda_{\overline{\text{MS}}}$)

$$\bar{\Lambda}_{\text{PV}} - \bar{\Lambda}_{\text{MRS}} = \cos(\pi b) \frac{4\pi\Gamma(-b)}{2^{1+b}\beta_0} Z_m^X \Lambda_X \Big|_{n_f=3} = -120(8) \text{ MeV}. \quad (6.49)$$

The prediction of [121] translates then to $\bar{\Lambda}_{\text{PV}} = 435(31)$, where we only include the error quoted in [121]. In particular, we do not include the error in Eq. (6.49). Note that Eq. (6.49) scales like $\mathcal{O}(\Lambda_{\text{QCD}})$, whereas $\bar{m}\Omega_1$ scales like $\mathcal{O}(\sqrt{\alpha}\Lambda_{\text{QCD}})$. There is a 40 MeV difference with the number given in Eq. (6.23). 10 MeV can be understood because the value of \bar{m}_b used in [121] is around 10 MeV bigger. Another 10 MeV can be understood by the inclusion of $1/m$ nonperturbative effects. The remaining 20 MeV difference is more difficult to identify, although they are well inside uncertainties.

Leaving aside the different α 's used, another source of difference is the value of Z_1 . The value used in [121] comes from [129] (where the effect of scale variation was not included in the error analysis). This determination used a sum rule that is free of the leading pole mass renormalon. The possibility of using sum rules to determine the normalization of renormalons was first considered in [130]. For the determination of Z_1 , sum rules were first used in [122]. Later sum rule analyses can be found in [131]. Alternatively, one can use the ratio of the exact and asymptotic expression of the coefficients r_n to determine Z_1 , as in [132, 100, 101, 118, 133]. For an extra discussion on this issue see [134].

Finally, it is worth mentioning that Z_1 can be determined either from the static potential or from the pole mass (and its relatives). The only value of Z_1 that uses the static potential is from [118]. A preference for the determinations of Z_1 from the static potential can be theoretically motivated, as it is less affected by subleading renormalons. There are no UV renormalons, and the next IR renormalon is located at $d = 3$. On the other hand, the pole mass is expected to have renormalons at $|d| = 2$. Only in the event that there is no $d = 2$ renormalon, and the effect of the $d = -2$ renormalon is subleading, both determinations would be on equal footing on theoretical grounds. In any case, irrespective of this discussion, consistent numbers are obtained between different analyses.

6.2 $\bar{\Lambda}_{\text{PV}}(n_f = 0)$ from the lattice scheme

Analogously to what we had in the previous section, in the lattice scheme, we can write

$$E_{\text{MC}} = \delta m + \bar{\Lambda} + \mathcal{O}(a\Lambda_{\text{QCD}}^2), \quad (6.50)$$

where δm is the self energy of a static source in the Wilson action lattice scheme, and E_{MC} is the ground state energy of a static heavy-light meson. Just as in the previous section, we will give an estimate of $\bar{\Lambda}$ by employing the PV Borel sum to regulate the formal series of δm .

6.2.1 The Polyakov loop and δm

Let us look more closely to δm . We will write its perturbative expansion in the following way

$$\delta m = \frac{1}{a} \sum_{n=0}^{\infty} c_n \alpha^{n+1} (1/a), \quad (6.51)$$

where a is the lattice spacing. This object can be computed from the Polyakov loop. Let us consider an asymmetric lattice of $N_S^3 \times N_T$ points (N_S is the spatial extent in a given spatial direction, and N_T the temporal extent), where we apply periodic boundary conditions⁴. The Polyakov loop is then defined by taking the trace of products of the link variable throughout all the (Euclidean) time direction

$$P(n) = \text{tr} \left\{ \prod_{n_4=0}^{N_T-1} U_4(n) \right\}, \quad (6.52)$$

where recall that $n = (n_1, n_2, n_3, n_4)$ denotes a point in the lattice. Notice that due to the periodic boundary conditions we have implemented, we have in the equation above a trace over a closed loop, and therefore, $P(n)$ is gauge invariant. We can define the average value by considering

$$L(N_S, N_T) = \frac{1}{3N_S^3} \sum_{\mathbf{n} \in \Lambda_E} P(n), \quad (6.53)$$

where keep in mind that we denote all the lattice by Λ_E . The above object can be related to the self energy of a static source in the infinite volume limit in the following way [136]

$$\delta m = \lim_{N_S, N_T \rightarrow \infty} \frac{-\log \langle L(N_S, N_T) \rangle}{aN_T}. \quad (6.54)$$

6.2.2 Hyperasymptotics of δm_{PV}

Let us come back to $\bar{\Lambda}$. As we have said, we will estimate it by

$$\bar{\Lambda}_{\text{PV}} = E_{\text{MC}} - \delta m_{\text{PV}} + \mathcal{O}(a\Lambda_{\text{QCD}}^2). \quad (6.55)$$

The coefficients of the series of Eq. (6.51) were computed from Eq. (6.54) using NSPT up until order α^{20} in [101, 100, 132, 135], which are the coefficients that we will use. MC data for E_{MC} can be found in [137, 138, 139]. These points expand over the following energy range: $1/a \sim 2.93 r_0^{-1} \div 9.74 r_0^{-1}$. In order to implement the PV Borel sum of δm , we will employ the method of chapter 3. To be able to do that, it must be mentioned that the large n behavior of the coefficients c_n in Eq. (6.51) needs to be known. As it happens, this large order behavior is closely related to the pole mass of a heavy quark, where it can be seen that the large n asymptotics of the coefficients c_n of Eq. (6.51), and that of r_n/μ in Eq. (6.3) (with $n_f = 0$) is the same, and given by the $u = 1/2$ renormalon we have mentioned many times already (modulo subleading renormalons). Therefore, we can recycle Eq. (6.19)

$$c_n^{(\text{as})} = \frac{1}{\mu} r_n^{(\text{as})}. \quad (6.56)$$

Thus, we write the PV Borel sum of δm in the following way

$$\delta m_{\text{PV}} = \delta m_{\text{P}} + \frac{1}{a} \Omega_1 + \sum_{N_{\text{P}}(1)+1}^{N' \equiv N_{\text{P}}(2)} \frac{1}{a} (c_n - c_n^{(\text{as})}) \alpha^{n+1} + \mathcal{O}(a\Lambda_{\text{QCD}}^2), \quad (6.57)$$

⁴Being accurate, in the sources we use for the coefficients c_n of Eq. (6.51), the authors used periodic boundary conditions in time, and twisted boundary conditions in all spatial directions [101, 100, 132, 135].

β	a in r_0 units	$N_{\text{P}}(1)$	c
5.7	0.34032	6	1.434
5.9	0.22340	7	0.102
6.0	0.18630	7	0.311
6.1	0.15782	7	0.521
6.2	0.13545	7	0.730
6.3	0.11746	7	0.940
6.4	0.10265	7	1.149

Table 6.1: We depict various quantities associated to the various lattice spacings considered. The values of a have been obtained with Eq. (5.54). The $N_{\text{P}}(1)$ -s are the ones associated to the smallest positive values of c , which are listed in the last column.

where we have defined

$$\delta m_{\text{P}} \equiv \sum_{n=0}^{N_{\text{P}}(1)} \frac{1}{a} c_n \alpha^{n+1}, \quad (6.58)$$

and as usual

$$N_{\text{P}}(d) = \frac{2\pi|d|}{\beta_0\alpha} (1 - c\alpha). \quad (6.59)$$

The next renormalon on δm is expected to be at $d = 2$, and thus we truncate the last series in the RHS of Eq. (6.57) at $\alpha^{N_{\text{P}}(2)+1}$. In Table 6.1, we see that $N_{\text{P}}(1) = 6, 7$ for the various lattice spacings considered, and therefore, since we have the c_n coefficients up until c_{19} , we are able to reach order $(D, N) = (1, N_{\text{P}}(1))$ in Eq. (6.57) in the counting of the hyperasymptotic expansion introduced in section 3.4. In principle, we know more coefficients c_n than we make use of in Eq. (6.57), but our ignorance on the normalization of the next renormalon makes it impossible to go further in the hyperasymptotic expansion, since we cannot then compute the subleading terminant.

Due to Eq. (6.56), the expression we use for Ω_1 is Eq. (6.12) with the substitutions $\mu/\bar{m}_b \rightarrow 1$. Keep in mind too that we need to pick the normalization Z_1 , and beta function coefficients appropriate for $n_f = 0$ and the lattice scheme. For the normalization of the renormalon, we employ $Z_1 = 17.9(1.0)$ [101]. The terminant is implemented in exponential form, and truncated at order $\mathcal{O}(\alpha^2)$. The error committed by this truncation is smaller than the error associated to Z_1 , and therefore, we will neglect it in the following.

For the coefficients $c_n^{(\text{as})}$, we use Eq. (6.19) taking into account Eq. (6.56), which we truncate at order $\mathcal{O}(n^{-3})$. This means using the estimates for β_3 and β_4 listed in Table 6.2 (we will see how these are obtained in subsection 6.2.4). Results of the fits truncating the asymptotic coefficient to order n^{-2} and n^{-4} can be found in Table 6.3.

6.2.3 Fits of $\bar{\Lambda}_{\text{PV}}$

We now move onto the fits. We fit $\bar{\Lambda}_{\text{PV}} - Ka$ to the ($\bar{\Lambda}_{\text{PV}}$ and K being the parameters of the fit) RHS of Eq. (6.55), where we take the order $(D, N) = (1, N_{\text{P}}(1))$ in the hyperasymptotic expansion of δm_{PV} . We show our results in Figure 6.1. The figure follows the same logic as Figure 3.3, in the sense that we display various bands corresponding to Eq. (6.55), where δm_{PV} is taken to various orders in the hyperasymptotic expansion. The bands are generated by making the fits with different c values in Eq. (6.59): the smallest (in absolute value) positive and negative values that yield integer values for $N_{\text{P}}(1)$.

We observe that the subtraction of the perturbative expansion accounts for most of the $1/a$ dependence. Still, we have enough precision to be sensitive to $\mathcal{O}(a\Lambda_{\text{QCD}}^2)$ effects. A fit of the RHS of Eq. (6.55) to just $\bar{\Lambda}_{\text{PV}}$ gives a

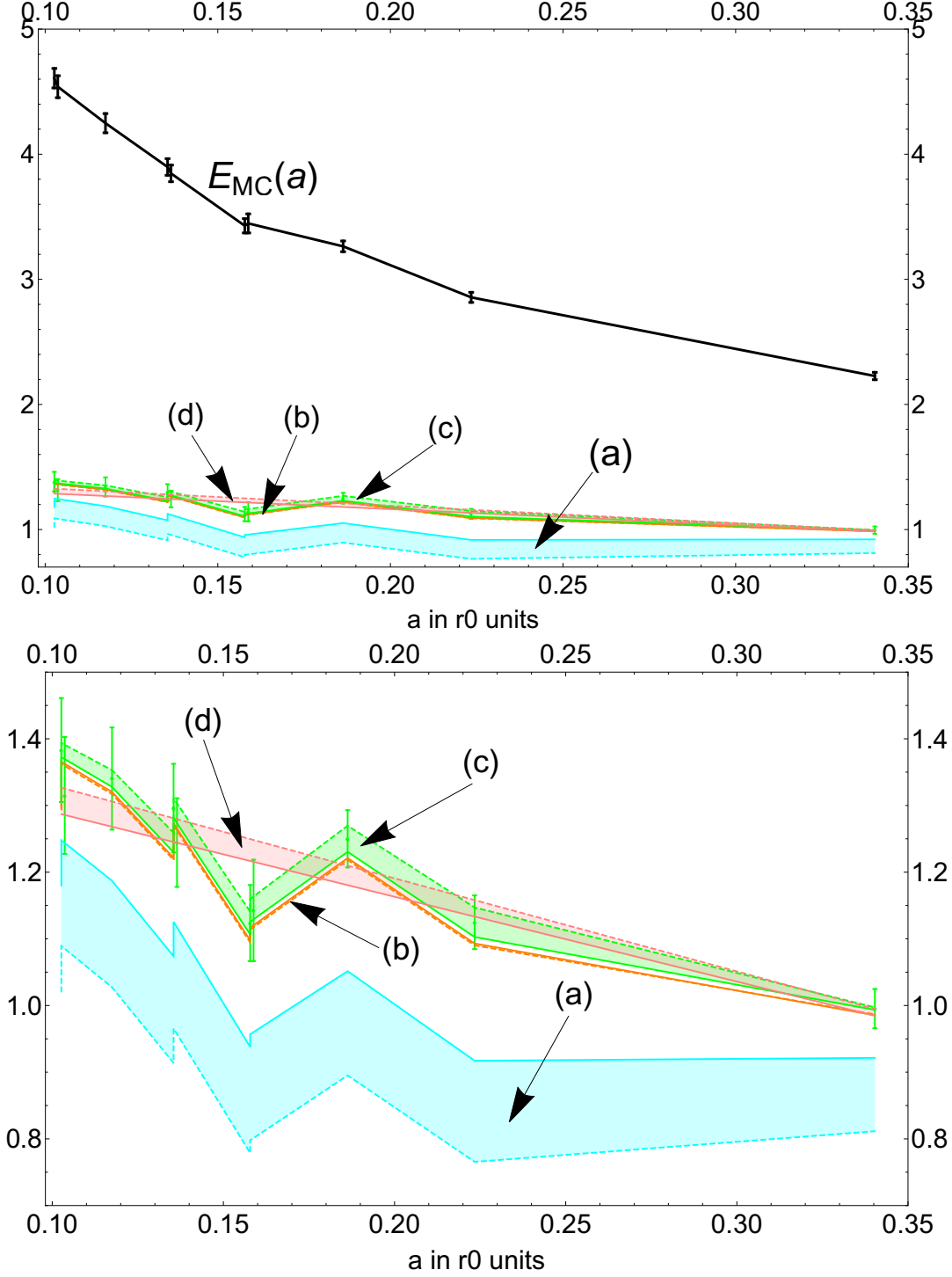


Figure 6.1: **Upper panel:** E_{MC} is the MC lattice data. The continuous lines are drawn to guide the eye. The other lines correspond to Eq. (6.55), where δm_{PV} is truncated at different orders in the hyperasymptotic expansion. (a) $E_{\text{MC}}(a) - \delta m_{\text{P}}(1/a)$, (b) $E_{\text{MC}}(a) - \delta m_{\text{P}}(1/a) - \frac{1}{a}\Omega_1$, (c) $E_{\text{MC}}(a) - \delta m_{\text{P}}(1/a) - \frac{1}{a}\Omega_1 - \sum_{N_{\text{P}}(1)+1}^{N'=N_{\text{P}}(2)} \frac{1}{a}(c_n - c_n^{\text{as}})\alpha^{n+1}$ (in this last case, we also include the error of the MC E_{MC} points in the middle of the band), (d) is the value of $\bar{\Lambda}_{\text{PV}}$ obtained from the fit of the RHS of Eq. (6.55) to $\bar{\Lambda}_{\text{PV}} - Ka$ with the green points. The bands are generated by making the fits with different c values in Eq. (6.59): the smallest (in absolute value) positive and negative values that yield integer values for $N_{\text{P}}(1)$. **Lower panel:** As in the upper panel but with a smaller vertical range. Recall that $r_0^{-1} \approx 400$ MeV.

large $\chi_{\text{red}}^2 \sim 6 - 7$. On the other hand, by fitting the RHS Eq. (6.55) to $\bar{\Lambda}_{\text{PV}} - Ka$, we obtain a fit with a good $\chi_{\text{red}}^2 = 1.17/1.06$ (positive/negative c). Our central value result is

$$\bar{\Lambda}_{\text{PV}} = 1.42 r_0^{-1} (0.04)_{\text{stat}} (0.05)_c (0.16)_{Z_m}. \quad (6.60)$$

This number is not very different from the number obtained in [112], where a superasymptotically truncated δm was used⁵. Let us now discuss the error budget in Eq. (6.60). The first error is the statistical error of the fit. The remaining errors are different ways to estimate the error produced by the approximate knowledge of the hyperasymptotic expansion. One possibility is to take the modulus of the difference with the evaluation using the positive and negative values of c that are smallest in absolute value. This is the second error we quote in Eq. (6.60).

The last error we include is due to the variation of $Z_1(n_f = 0) = 17.9(1.0)$ [101] (correlated with the error of c_n). The error that the uncertainty of Z_1 produces in Ω_1 is small. Comparatively, most of the error associated to Z_1 comes from the differences in $\sum_{n=N_{\text{P}}(1)+1}^{N_{\text{P}}(2)} \frac{1}{a} (c_n - c_n^{(\text{as})}) \alpha^{n+1}$, evaluated for different Z_1 values. Whereas $\sum_{n=N_{\text{P}}(1)+1}^{N_{\text{P}}(2)} \frac{1}{a} (c_n - c_n^{(\text{as})}) \alpha^{n+1}$ is quite small for the central value of Z_1 , it significantly changes after considering the uncertainty in Z_1 . This variation is only partially compensated by the variation of the coefficients c_n , which have smaller errors, producing a significant change in $\sum_{n=N_{\text{P}}(1)+1}^{N_{\text{P}}(2)} \frac{1}{a} (c_n - c_n^{(\text{as})}) \alpha^{n+1}$.

We have also determined the central value in Eq. (6.60), not including the $\mathcal{O}(1/n^3)$ corrections in the asymptotic expressions for $c_n^{(\text{as})}$. The difference we obtain is -0.08. This is significant, showing that $1/n$ corrections in the asymptotic coefficient are sizable in the lattice scheme. Nonetheless, by adding one more term in the asymptotic coefficient instead of subtracting, that is, by including $\mathcal{O}(1/n^4)$ terms, we obtain for the difference with the central value fits -0.03, which is smaller. This suggests a convergent pattern, which we illustrate in Table 6.3.

Overall, the largest source of uncertainty comes from the incomplete knowledge of $\sum_{n=N_{\text{P}}(1)+1}^{N_{\text{P}}(2)} \frac{1}{a} (c_n - c_n^{(\text{as})}) \alpha^{n+1}$, which is closely linked to the incomplete knowledge of Z_1 . In this regard, it is noteworthy that the green band in Figure 6.1 is broader than the orange band, which is one order *less* in the hyperasymptotic expansion. Nevertheless, the difference of the central value result, with the fit to this orange band is -0.008, which is way smaller than the other uncertainties considered.

Finally, we mention that one error that we do not include here is the error associated to the relation between $\alpha(1/a)$ and a . Just as in chapter 5, we have used the phenomenological formula deduced in [113] of Eq. (5.54). The error of this formula is claimed to be around 0.5-1% in the range $\beta \in (5.7, 6.92)$, which contains the range we have used.

6.2.4 Renormalon dominance and the beta function coefficients in the lattice

Taking somewhat of a detour, let us turn our attention to the beta function coefficients in the lattice. β_0 and β_1 are scheme independent and thus, well known. As we saw in Eq. (5.28), β_2 is known numerically, but that's about it. β_3 and onwards are unknown, although estimates exist, and actually, we gave one in Eq. (5.29). In this section, we will see how this estimate was obtained from the coefficients c_n of the series of δm that we have used.

Let us consider the $\overline{\text{MS}}$ and the lattice schemes. Let us consider the strong coupling in the $\overline{\text{MS}}$ scheme $\alpha_{\overline{\text{MS}}}(\mu_i)$, evaluated at some scale μ_i . The idea is to obtain from this the strong coupling at some other scale and in the lattice scheme $\alpha_{\text{latt}}(\mu_f)$. There are two ways to go about doing this, first run the strong coupling in the $\overline{\text{MS}}$ scheme

⁵Their superasymptotic truncation slightly differs from ours, in the sense that they did not truncate at $\alpha^{N_{\text{P}}(1)+1}$, but rather took the order that makes $|c_n \alpha^{n+1}|$ smallest. The difference with what we call δm_{P} is small in any case.

to the scale μ_f , and then convert from $\overline{\text{MS}}$ to lattice, or first convert from $\overline{\text{MS}}$ to lattice at the scale μ_i , and then run the coupling to μ_f . In the the first approach, we obtain $\alpha_{\text{latt}}(\mu_f)$ as a series of $\alpha_{\overline{\text{MS}}}(\mu_i)$, where the coefficients of the series will depend of the beta function coefficients in the $\overline{\text{MS}}$ scheme. In the second approach we obtain $\alpha_{\text{latt}}(\mu_f)$ as a series in $\alpha_{\overline{\text{MS}}}(\mu_i)$, where the coefficients of the series depend on the beta function coefficients in the lattice scheme. Therefore, by comparing the coefficients of both series at various orders in $\alpha_{\overline{\text{MS}}}(\mu_i)$, knowledge of the beta function coefficients in the $\overline{\text{MS}}$ scheme translates to knowledge of the coefficients in the lattice scheme. For instance, comparing the coefficients proportional to $\alpha_{\overline{\text{MS}}}^5(\mu_i)$, in particular the part of the coefficient that is proportional to $\log \frac{\mu_i}{\mu_f}$, we can obtain β_3 . The next order yields β_4 . There is one important caveat to this method though. In order to implement it, we need to know the conversion formula of the strong coupling between both schemes. We have seen this equation already in Eq. (3.99)

$$\alpha_{\overline{\text{MS}}}(\mu) = \alpha_{\text{latt}}(\mu) \left\{ 1 + \sum_{j=1}^{\infty} d_j \alpha_{\text{latt}}^j(\mu) \right\}, \quad (6.61)$$

where [71, 72, 73] $d_1 = 5.88359144663707(1)$, and [71, 98, 99] $d_2 = 43.4073028(2)$. d_3 and onwards are in general unknown, and this is where renormalon dominance comes to help. Let us consider again the series of $a\delta m$

$$a\delta m = \sum_{n=0}^{\infty} c_n \alpha^{n+1}, \quad (6.62)$$

and let us consider the conversion formula of Eq. (6.61). Using this two pieces, we can re-expand the series above in terms of $\alpha_{\overline{\text{MS}}}$

$$a\delta m = \sum_{n=0}^{\infty} c_n^{\overline{\text{MS}}} \alpha_{\overline{\text{MS}}}^{n+1}, \quad (6.63)$$

and obtain the coefficients $c_n^{\overline{\text{MS}}}$ in terms of the coefficients c_n and d_j . In particular, c_3 will only depend on c_n and d_n with $n \leq 3$, of which only d_3 is unknown. Therefore, assuming that in the $\overline{\text{MS}}$ scheme the coefficient $c_3^{\overline{\text{MS}}}$ is already dominated by the renormalon, we can use the asymptotic expression⁶, and in this way obtain d_3 . The obtained value is $d_3 \approx 351.91$, which was obtained in [101, 100]. This approach can be iterated again by considering $c_4^{\overline{\text{MS}}}$ to be dominated by the renormalon, to give an estimate of $d_4 \approx 2996.51$. Nonetheless, we need to keep in mind that this prediction uses the value of d_3 computed before, which is already an estimate. Iterating this procedure a few times, we obtain $d_5 \approx 26299.99$, $d_6 \approx 235183.79$ and $d_7 \approx 2.12 \times 10^6$.

Thus, using this estimate of d_3 , we are now able to estimate $\beta_3 \approx -1.16 \times 10^6$, which was obtained in [101, 100]. Making use of the estimates of d_3 and d_4 , we can obtain $\beta_4 \approx -1.35 \times 10^8$. $\beta_5^{\overline{\text{MS}}}$ is not yet known, and therefore, in principle, we cannot use this approach to estimate β_5 in the lattice. In spite of this, a crude estimate can be given by implementing the method we have already used, despite not knowing $\beta_5^{\overline{\text{MS}}}$. Of course, doing this introduces uncertainties because we are not including $\beta_5^{\overline{\text{MS}}}$ when we do the running in the $\overline{\text{MS}}$ scheme, and therefore, the result is more dubious than for β_3 and β_4 . In any case, we show in Table 6.2 estimates for various beta function coefficients estimated using this approach.

6.2.5 Fits in the $\overline{\text{MS}}$ scheme

It is interesting to consider the scheme dependence of Eq. (6.60). In [112], relative large differences were found for fits to $\bar{\Lambda}$ after (approximated) scheme conversion to the $\overline{\text{MS}}$ scheme. The real problem is not transforming the

⁶The normalization of the renormalon in the $\overline{\text{MS}}$ employed is $Z_1^{\overline{\text{MS}}} = 0.62$ [101].

β_3	β_4	β_5	β_6
$-1.16(3) \times 10^6$	$-1.35(10) \times 10^8$	$-1.44(28) \times 10^{10}$	$-1.41(60) \times 10^{12}$

Table 6.2: Estimates of the coefficients of the beta function for the bare coupling in the lattice scheme using renormalon dominance. The error quoted in the table gives the difference with the values of the beta coefficients obtained if instead of the value of the normalization of the renormalon used here $Z_1^{\overline{\text{MS}}} = 0.62$ [101], one uses $Z_1^{\overline{\text{MS}}} = 0.6$ [118] (which yields more negative values), and it is only meant to illustrate the typical spread of values of the beta coefficients if one uses different values of $Z_1^{\overline{\text{MS}}}$.

latt	$\mathcal{O}(\frac{1}{n^2})$	$\mathcal{O}(\frac{1}{n^3})$	$\mathcal{O}(\frac{1}{n^4})$	$\overline{\text{MS}}$	$N_{\text{tr}} = 7$	$N_{\text{tr}} = 6$	$N_{\text{tr}} = 5$	$N_{\text{tr}} = 4$
$\bar{\Lambda}_{\text{PV}}$	1.33	1.42	1.45	$\bar{\Lambda}_{\text{PV}}$	1.48	1.52	1.59	1.68

Table 6.3: Determinations of $\bar{\Lambda}_{\text{PV}}$ in the lattice and $\overline{\text{MS}}$ schemes from fits of $\bar{\Lambda}_{\text{PV}} - Ka$ to the RHS of Eq. (6.55), where δm_{PV} is given by Eq. (6.57). The first three numbers show the impact in the fit of including the $\mathcal{O}(1/n^m)$ corrections for $m = 2, 3, 4$ in the asymptotic expressions for $c_n^{(\text{as})}$ in the lattice scheme (in the $\overline{\text{MS}}$ this effect is negligible). The other numbers are the fit of $\bar{\Lambda}_{\text{PV}}$ in the $\overline{\text{MS}}$ scheme, using $\alpha_{\overline{\text{MS}}} = \alpha_{\text{latt}} \{1 + \sum_{n=0}^{N_{\text{tr}}} d_n \alpha_{\text{latt}}^n\}$ truncated at $N_{\text{tr}} = 4, 5, 6, 7$.

coefficients c_n from the lattice to the $\overline{\text{MS}}$ scheme, but transforming α_{latt} to $\alpha_{\overline{\text{MS}}}$ with enough precision which needs knowledge of the coefficients d_n of Eq. (6.61) to high orders. Making use of the estimates of the previous subsection makes the determinations of $\bar{\Lambda}_{\text{PV}}$ in the $\overline{\text{MS}}$ and lattice scheme approach each other as we include more terms in the perturbative expansion of the relation between $\alpha_{\overline{\text{MS}}}$ and α_{latt} . We show the comparison in Table 6.3.

6.3 The PV Borel sum of the top quark pole mass

We finish the chapter with a section devoted to obtaining the PV Borel sum of the top quark pole mass. The reason we cannot straightforwardly apply the formalism of terminants that we have applied to the bottom is that the top quark is significantly heavier, with $\bar{m}_t = 163$ GeV, which makes $\alpha(\bar{m}_t)$ smaller, which makes $N_{\text{P}}(1) \sim 7$, which is too high, since we do not know enough coefficients of the series of the pole mass to reach those orders. Therefore, we will try to get around this fact employing different tactics. Before doing that though, we will comment on a few things about the ambiguity of the pole mass.

6.3.1 About the pole mass ambiguity

The top quark mass is one of the key parameters of the standard model. A lot of experimental work has been devoted to its determination (see for instance [140, 141, 142]). Whereas this is a matter of debate, it is typically assumed that the masses obtained from experiment correspond to the pole mass. Thus, there has been an ongoing discussion on the intrinsic uncertainty of these determinations (see for instance [133, 143], and [144] for a more recent discussion). We believe that, without further qualifications, the question is ill posed, or may lead to confusion.

It is well known that the pole mass is well defined (IR finite and gauge independent) at finite (albeit arbitrary) order in perturbation theory [145]. It is also well known that this series is expected to be divergent. Therefore, no numerical value can be assigned to the infinite sum of the perturbative series of the pole mass. Truncated sums are well defined, but depend on the order of truncation, as we have already mentioned many times. These truncated sums can be related with observables, or with intermediate definitions of the heavy quark mass, like the PV mass in a well defined way.

In this context, the shortest answer to the above question is that the ambiguity (of a well defined mass) is *zero*. As a matter of principle, $m_{\text{OS}}^{\text{PV}}$ (or m_{OS}^{P}) can be *defined* with arbitrary accuracy (this also applies to any threshold mass), if one computes high enough orders of the perturbative series, and if \bar{m} is given. One can discuss (actually one can compute) the scheme/scale dependence (if they have) of them.

A different question is to determine the typical difference (not the ambiguity) between (reasonable) different definitions of the pole mass. The short answer to this question is that the differences are (at most) of order Λ_{QCD} for (reasonable) different definitions of the pole mass. We emphasize that one can not be more precise unless stating the specific definition used for the pole mass. For instance, as we have seen, the difference between $m_{\text{OS}}^{\text{PV}}$ and m_{OS}^{P} is of $\mathcal{O}(\sqrt{\alpha}\Lambda_{\text{QCD}})$ with a known prefactor. Truncating the perturbative series at various orders near the ambiguous superasymptotic truncation order is also a legitimate definition of the pole mass, whose typical differences are of order Λ_{QCD} , as we have already seen. One could even use M_B as a definition for the pole mass, whose difference with $m_{b,\text{OS}}^{\text{PV}}$ is of order Λ_{QCD} . If one defines an imaginary mass by doing the Borel integral just above the positive real axis, the difference with $m_{\text{OS}}^{\text{PV}}$ is of $\mathcal{O}(i\Lambda_{\text{QCD}})$. The authors of [133] choose to divide this number by π , and take the modulus as their definition of the ambiguity. These examples illustrate that, even if the ambiguity is of $\mathcal{O}(\Lambda_{\text{QCD}})$, the coefficient multiplying Λ_{QCD} is arbitrary. Overall, it should be clear that not much more can be said, and we are indeed against dwelling too much on this issue. Instead, we strongly advocate to avoid generic discussions about the pole mass, which is not well defined beyond perturbation theory, and restrict the discussion to the precision and errors of specific, well-defined, heavy quark masses which can be related with the perturbative expansion of the pole mass.

Once working with well-defined heavy quark masses like $m_{t,\text{OS}}^{\text{PV}}$ or $m_{t,\text{OS}}^{\text{P}}$, we can address the more relevant question of determining the precision with which \bar{m}_t can be determined if $m_{t,\text{OS}}^{\text{PV}}$ or $m_{t,\text{OS}}^{\text{P}}$ is known (and viceversa) with current knowledge of the perturbative expansion. For reference, we will take the value $\bar{m}_t = 163$ GeV in the following. We will see in the next section that indeed, the precision is quite good, and that the error is significantly smaller than typical numbers assigned for the ambiguity of the pole mass.

6.3.2 Decoupling and running

As we have already mentioned, in order to compute the PV Borel sum of the top quark pole mass, we cannot straightforwardly use the same approach as for the bottom, because we do not have enough terms to reach the asymptotic behavior of the perturbative expansion. Instead, we will exploit the fact that the formal series of the \bar{m} derivative of the top quark pole mass does not have the leading $d = 1$ renormalon found in the series of the pole mass⁷. Then, this function will be used to relate the PV masses of the top quark and a fictitious top quark at a scale low enough, so that we are able to implement terminants. Let us see how this works in practice. We first define⁸

$$\mathcal{F}(\bar{m}, n_f) \equiv \frac{d}{d\bar{m}} \{m_{t,\text{OS}}(\bar{m}) - \bar{m}\}, \quad (6.64)$$

where $m_{t,\text{OS}}(\bar{m})$ is the formal series relating the top quark pole mass with an $\overline{\text{MS}}$ mass given by⁹ \bar{m} . For now, we leave \bar{m} arbitrary. The series of $m_{t,\text{OS}}(\bar{m})$ is computed for $n_f = 5$, and the expansion parameter of the series is the

⁷The idea is similar to what we will do in chapter 7 with the static potential, where we will consider its r derivative to get rid of its $d = 1$ renormalon.

⁸We set $\mu = \bar{m}$ in the series of the pole mass, which simplifies the computation.

⁹Being completely precise, \bar{m} denotes the $\overline{\text{MS}}$ mass evaluated at its own scale in a theory with 6 active quarks, that is $\bar{m} \equiv \bar{m}_{(6)}(\bar{m}_{(6)})$.

strong coupling with 5 active massless flavors. The coefficients r_n are given by Eq. (F.3). That is, we have

$$m_{t,\text{OS}}(\bar{m}) - \bar{m} = \sum_{n=0}^{\infty} r_n^{(n_f)}(\bar{m}) \alpha_{(n_f)}^{n+1}(\bar{m}), \quad (6.65)$$

and the formal series of the \bar{m} derivative of the above series is

$$\mathcal{F}(\bar{m}, n_f) = \frac{d}{d\bar{m}} \{m_{t,\text{OS}}(\bar{m}) - \bar{m}\} \equiv \sum_{j=1}^{\infty} g_j^{(n_f)}(\bar{m}) \left(\frac{\alpha_{(n_f)}(\bar{m})}{\pi} \right)^j \equiv \sum_{n=0}^{\infty} f_n^{(n_f)}(\bar{m}) \alpha_{(n_f)}^{n+1}(\bar{m}). \quad (6.66)$$

Let us consider now the PV Borel sum of the above formal series

$$\text{PV} \frac{d}{d\bar{m}} \{m_{t,\text{OS}}(\bar{m}) - \bar{m}\} \equiv \text{PV} \sum_{n=0}^{\infty} f_n^{(n_f)}(\bar{m}) \alpha_{(n_f)}^{n+1}(\bar{m}), \quad (6.67)$$

and let us also commute

$$\text{PV} \frac{d}{d\bar{m}} \{m_{t,\text{OS}}(\bar{m}) - \bar{m}\} = \frac{d}{d\bar{m}} \text{PV} \{m_{t,\text{OS}}(\bar{m}) - \bar{m}\}, \quad (6.68)$$

so that

$$\frac{d}{d\bar{m}} \text{PV} \{m_{t,\text{OS}}(\bar{m}) - \bar{m}\} \equiv \text{PV} \sum_{n=0}^{\infty} f_n^{(n_f)}(\bar{m}) \alpha_{(n_f)}^{n+1}(\bar{m}). \quad (6.69)$$

As we have said, the above formal series \mathcal{F} is devoid of the $d = 1$ renormalon of the pole mass, and therefore, in order to implement the RHS above, we do not need a leading terminant, and we just write

$$\text{PV} \sum_{n=0}^{\infty} f_n^{(n_f)}(\bar{m}) \alpha_{(n_f)}^{n+1}(\bar{m}) = \sum_{n=0}^{N_{\text{P}}(2)} f_n^{(n_f)}(\bar{m}) \alpha_{(n_f)}^{n+1}(\bar{m}) + \mathcal{O} \left(e^{\frac{-6\pi}{\beta_0 \alpha_{(n_f)}(\bar{m})}} \right), \quad (6.70)$$

where following large β_0 expectations, we assume the leading renormalon of the series of the \bar{m} derivative of the top pole mass is parametrized by $|d| = 2$, and the subleading at $d = 3$. Thus

$$\frac{d}{d\bar{m}} \text{PV} \{m_{t,\text{OS}}(\bar{m}) - \bar{m}\} = \sum_{n=0}^{N_{\text{P}}(2)} f_n^{(n_f)}(\bar{m}) \alpha_{(n_f)}^{n+1}(\bar{m}) + \mathcal{O} \left(e^{\frac{-6\pi}{\beta_0 \alpha_{(n_f)}(\bar{m})}} \right). \quad (6.71)$$

We now integrate the above equation between the actual top quark $\overline{\text{MS}}$ mass and a fictitious top quark mass μ_b

$$\int_{\mu_b}^{\bar{m}_t} d\bar{m} \frac{d}{d\bar{m}} \text{PV} \{m_{t,\text{OS}}(\bar{m}) - \bar{m}\} = \int_{\mu_b}^{\bar{m}_t} d\bar{m} \left\{ \sum_{n=0}^{N_{\text{P}}(2)} f_n^{(n_f)}(\bar{m}) \alpha_{(n_f)}^{n+1}(\bar{m}) + \mathcal{O} \left(e^{\frac{-6\pi}{\beta_0 \alpha_{(n_f)}(\bar{m})}} \right) \right\} \quad (6.72)$$

$$\text{PV} \{m_{t,\text{OS}}(\bar{m}_t) - \bar{m}_t\} - \text{PV} \{m_{t,\text{OS}}(\mu_b) - \mu_b\} = \int_{\mu_b}^{\bar{m}_t} d\bar{m} \left\{ \sum_{n=0}^{N_{\text{P}}(2)} f_n^{(n_f)}(\bar{m}) \alpha_{(n_f)}^{n+1}(\bar{m}) + \mathcal{O} \left(e^{\frac{-6\pi}{\beta_0 \alpha_{(n_f)}(\bar{m})}} \right) \right\}. \quad (6.73)$$

The idea is to pick μ_b low enough, so that we are able to implement Dingle's terminants on it, and consequently, obtain the PV Borel sum of the top quark by the above relation. Nevertheless, there is a caveat to all this that one needs to keep in mind. There are two heavy quarks, the bottom and the charm, with masses much larger than Λ_{QCD} , that generate extra corrections to the pole- $\overline{\text{MS}}$ mass relation of Eq. (6.65) due to the finite mass effects of the bottom and charm quark. Consequently, the corrected version of Eq. (6.65) is

$$m_{t,\text{OS}}(\bar{m}) - \bar{m} = \sum_{n=0}^{\infty} r_n^{(5)}(\bar{m}) \alpha_{(5)}^{n+1}(\bar{m}) + \delta m_b^{(5)}(\bar{m}) + \delta m_c^{(5)}(\bar{m}) + \delta m_{bc}^{(5)}(\bar{m}), \quad (6.74)$$

for $\bar{m} \sim \bar{m}_t$, and we have explicitly written $n_f = 5$. The explicit formulas for non-zero bottom and charm quark mass terms can be found in Appendix F. The $\mathcal{O}(\alpha^2)$ term of $\delta m_Q^{(n_f)}$ was computed in [146], and the $\mathcal{O}(\alpha^3)$ term in [147]. Note as well that at $\mathcal{O}(\alpha^3)$ there is a new contribution including a vacuum polarization of the bottom and

charm at the same time. We name it $\delta m_{bc}^{(n_f)}$, and it has been computed in [143]. Taking into account these terms, Eq. (6.73) becomes

$$\begin{aligned} \text{PV}\{m_{t,\text{OS}}(\bar{m}_t) - \bar{m}_t\} &= \text{PV}\{m_{t,\text{OS}}(\mu_b) - \mu_b\} \\ &+ \int_{\mu_b}^{\bar{m}_t} d\bar{m} \left\{ \sum_{n=0}^{N_{\text{P}}(2)} f_n^{(5)}(\bar{m}) \alpha_{(5)}^{n+1}(\bar{m}) + \frac{d}{d\bar{m}} [\delta m_b^{(5)}(\bar{m}) + \delta m_c^{(5)}(\bar{m}) + \delta m_{bc}^{(5)}(\bar{m})] + \mathcal{O}\left(e^{\frac{-6\pi}{\beta_0 \alpha_{(5)}(\bar{m})}}\right) \right\}. \end{aligned} \quad (6.75)$$

We emphasize that the $f_n^{(n_f)}$ above are the coefficients of the \bar{m} derivative of the series $\sum_{n=0}^{\infty} r_n^{(n_f)} \alpha_{(n_f)}^{n+1}$, where the $r_n^{(n_f)}$ do not contain non-zero charm and bottom effects. The question now becomes how to handle

$$\text{PV}\{m_{t,\text{OS}}(\mu_b) - \mu_b\}. \quad (6.76)$$

We will take μ_b small enough, such that the bottom decouples. As we decrease the value of \bar{m} , the bottom and charm quark will decouple. This decoupling will be absorbed in $\delta m_{b/c/bc}^{(n_f)}$, which are polynomials in powers of $\alpha_{(n_f)}$. In general, this is not just changing n_f in the original expressions from $n_f = 5$ to $n_f = 4$ or 3 . The explicit expressions can be found in the Appendix F. Let us discuss the decoupling in more detail (for the analysis we take $\bar{m}_b = 4.186$ GeV and $\bar{m}_c = 1.223$ GeV [116], but the sensitivity to the specific values we use is very tiny). As already discussed in [31], the natural scale of a n -loop integral is not \bar{m}_t but $\bar{m}_t e^{-n}$. For the case of the bottom versus charm quark, it was observed in [118]¹⁰ that the charm quark effectively decouples at order α^2/α^3 for the case of the charm quark effects in the bottom pole mass- $\overline{\text{MS}}$ mass relation. If we lower the mass of the top, we can also observe at which scales it is more convenient to decouple the bottom and charm quark in the top pole mass- $\overline{\text{MS}}$ mass relation. This is illustrated in Figure 6.2, where we plot the corrections associated to the bottom and charm with and without decoupling, in terms of the fictitious top mass (assuming a single heavy quark). Obviously, for very large top masses it is not convenient to do the decoupling. Nevertheless, as we decrease the mass of the top, it becomes much more effective to decouple, first the bottom, and afterwards the charm quark. Once this is done, the corrections due to the bottom and charm masses are very small. Comparatively to other errors, the uncertainty associated to the $\mathcal{O}(\alpha^4)$ corrections is negligible. Also, the correction associated to the bottom and charm quark masses to Eq. (6.77) (which, as we will shortly see, is the equation we use to obtain the PV pole mass of the top quark) is, comparatively to the total running, very small. From this analysis, and from what we see in Figure 6.2, we will take as central values $\mu_b = 20$ GeV and $\mu_c = 5$ GeV.

Thus, in Eq. (6.76), we implement the top quark pole mass at the scale $\mu_b = 20$ GeV with the bottom quark decoupled, and by integrating its derivative from μ_c to μ_b we are able to write

$$\begin{aligned} m_{t,\text{OS}}^{\text{PV}}(\bar{m}_t) - \bar{m}_t &= m_{t,\text{OS}}^{\text{PV}}(\mu_c) - \mu_c \\ &+ \int_{\mu_c}^{\mu_b} d\bar{m} \left\{ \sum_{n=0}^{N_{\text{P}}(2)} f_n^{(4)}(\bar{m}) \alpha_{(4)}^{n+1}(\bar{m}) + \frac{d}{d\bar{m}} [\delta m_b^{(4)}(\bar{m}) + \delta m_c^{(4)}(\bar{m}) + \delta m_{bc}^{(4)}(\bar{m})] + \mathcal{O}\left(e^{\frac{-6\pi}{\beta_0 \alpha_{(4)}(\bar{m})}}\right) \right\} \\ &+ \int_{\mu_b}^{\bar{m}_t} d\bar{m} \left\{ \sum_{n=0}^{N_{\text{P}}(2)} f_n^{(5)}(\bar{m}) \alpha_{(5)}^{n+1}(\bar{m}) + \frac{d}{d\bar{m}} [\delta m_b^{(5)}(\bar{m}) + \delta m_c^{(5)}(\bar{m}) + \delta m_{bc}^{(5)}(\bar{m})] + \mathcal{O}\left(e^{\frac{-6\pi}{\beta_0 \alpha_{(5)}(\bar{m})}}\right) \right\}. \end{aligned} \quad (6.77)$$

We have taken μ_b small enough so that the bottom decouples, and μ_c small enough so that the bottom and charm decouple, and also such that we reach the asymptotic limit of the pole- $\overline{\text{MS}}$ mass perturbative expansion with the

¹⁰In that reference MeV should read GeV instead from Eq. (8) to Eq. (12).

existing known coefficients. At the fictitious top mass μ_c , we find that $N_P(1) \sim 3$, so that we are able to implement the terminants. Doing just this

$$m_{t,\text{OS}}^{\text{PV}}(\mu_c) = m_{t,\text{OS}}^{\text{P}}(\mu_c) + \mu_c \Omega_1 + \delta m_b^{(3)}(\mu_c) + \delta m_c^{(3)}(\mu_c) + \delta m_{(bc)}^{(3)}(\mu_c) + \mathcal{O}(\mu_c e^{-\frac{2\pi}{\beta_0 \alpha(\mu_c)}(1+\log(2))}), \quad (6.78)$$

where the superasymptotically truncated series $m_{t,\text{OS}}^{\text{P}}(\mu_c)$ is the same as Eq. (6.18) with $\bar{m}_b \rightarrow \mu_c$. The $\mathcal{O}(\mu_c e^{-\frac{2\pi}{\beta_0 \alpha(\mu_c)}(1+\log(2))})$ term stands for subleading corrections in the hyperasymptotic expansions, which are not known. Let us also check the size of the contribution to Eq. (6.77) of the non-zero charm and bottom quark mass terms

$$\begin{aligned} & \int_{\mu_b}^{\bar{m}_t} d\bar{m} \frac{d}{d\bar{m}} (\delta m_b^{(5)}(\bar{m}) + \delta m_c^{(5)}(\bar{m}) + \delta m_{(bc)}^{(5)}(\bar{m})) \\ & + \int_{\mu_c}^{\mu_b} d\bar{m} \frac{d}{d\bar{m}} (\delta m_b^{(4)}(\bar{m}) + \delta m_c^{(4)}(\bar{m}) + \delta m_{(bc)}^{(4)}(\bar{m})) \\ & + \delta m_b^{(3)}(\mu_c) + \delta m_c^{(3)}(\mu_c) + \delta m_{(bc)}^{(3)}(\mu_c) = -2.5|_{\mathcal{O}(\alpha^2)} + 0.8|_{\mathcal{O}(\alpha^3)} = -1.7 \text{ MeV}. \end{aligned} \quad (6.79)$$

The specific value depends on μ_b and μ_c , but the good convergence and smallness of this correction holds true for other values of μ_b and μ_c . We next explore the convergence pattern of \mathcal{F} . We find

$$\int_{\mu_b}^{\bar{m}_t} d\bar{m} \mathcal{F}(\bar{m}, 5) + \int_{\mu_c}^{\mu_b} d\bar{m} \mathcal{F}(\bar{m}, 4) = 8445 + 837 + 53 - 43 = 9291(22) \text{ MeV}. \quad (6.80)$$

We observe a convergent pattern. For the last two terms, the convergence deteriorates. On the other hand, the perturbative expansion becomes sign alternating. This may indicate sensitivity to the $d = -2$ renormalon. We discuss this further in the next section. For sign-alternating asymptotic perturbative expansions, the left-over is $\sim -1/2 \times (\text{the last computed term})$ (see [10])¹¹. Therefore, we take it as the error of the truncation of the perturbative expansion, which is the error we quote in Eq. (6.80).

We also explore the dependence of Eq. (6.77) on μ_b and μ_c . The dependence is very small, as we can see in Figure 6.3. For μ_c the variation is negligible, and for μ_b one gets variations of ~ 5 MeV for a central value of μ_b of around 20 GeV. Therefore, we will neglect these for the total error budget.

Other source of error is associated to the approximate determination of Eq. (6.78) (except for the δm_q terms, which have already been taken into account in Eq. (6.79)). The error analysis is analogous to what we had for the bottom quark in Eq. (6.23), adapted by changing $\bar{m}_b = 4.186 \text{ GeV} \rightarrow \mu_c = 5 \text{ GeV}$ (the error associated to α is only computed for the full Eq. (6.77))

$$(m_{t,\text{OS}}^{\text{P}}(\mu_c) + \mu_c \Omega_1) \Big|_{\mu_c=5 \text{ GeV}} = 5744(\mu)_{-15}^{+7} (Z_1)_{-9}^{+9} \text{ MeV}. \quad (6.81)$$

Finally, we also include the error associated to α . Combining all errors, we obtain

$$m_{t,\text{OS}}^{\text{PV}}(163 \text{ MeV}) = 173033(\text{h.o.})_{-22}^{+22} (\mu)_{-15}^{+7} (Z_1)_{-9}^{+9} (\alpha)_{-123}^{+119} \text{ MeV}. \quad (6.82)$$

By far, the largest uncertainty is associated to α . For the purely theoretical error budget, the error is associated to higher order corrections in perturbation theory. They show up in different ways. One is the approximate knowledge of Z_1 , which shows up in Ω_1 . The other is the error in μ , which is a measure of the $\mathcal{O}(e^{-\frac{2\pi}{\beta_0 \alpha X(\mu)}(1+\log(2))})$ corrections to Eq. (6.78). h.o. stands for the error associated to higher order terms in perturbation theory of Eq. (6.80). All these errors would profit from higher order perturbative computations. We have also explored other sources of

¹¹We emphasize that these arguments do not apply to IR renormalons (and in particular to the $d = 1$ renormalon).

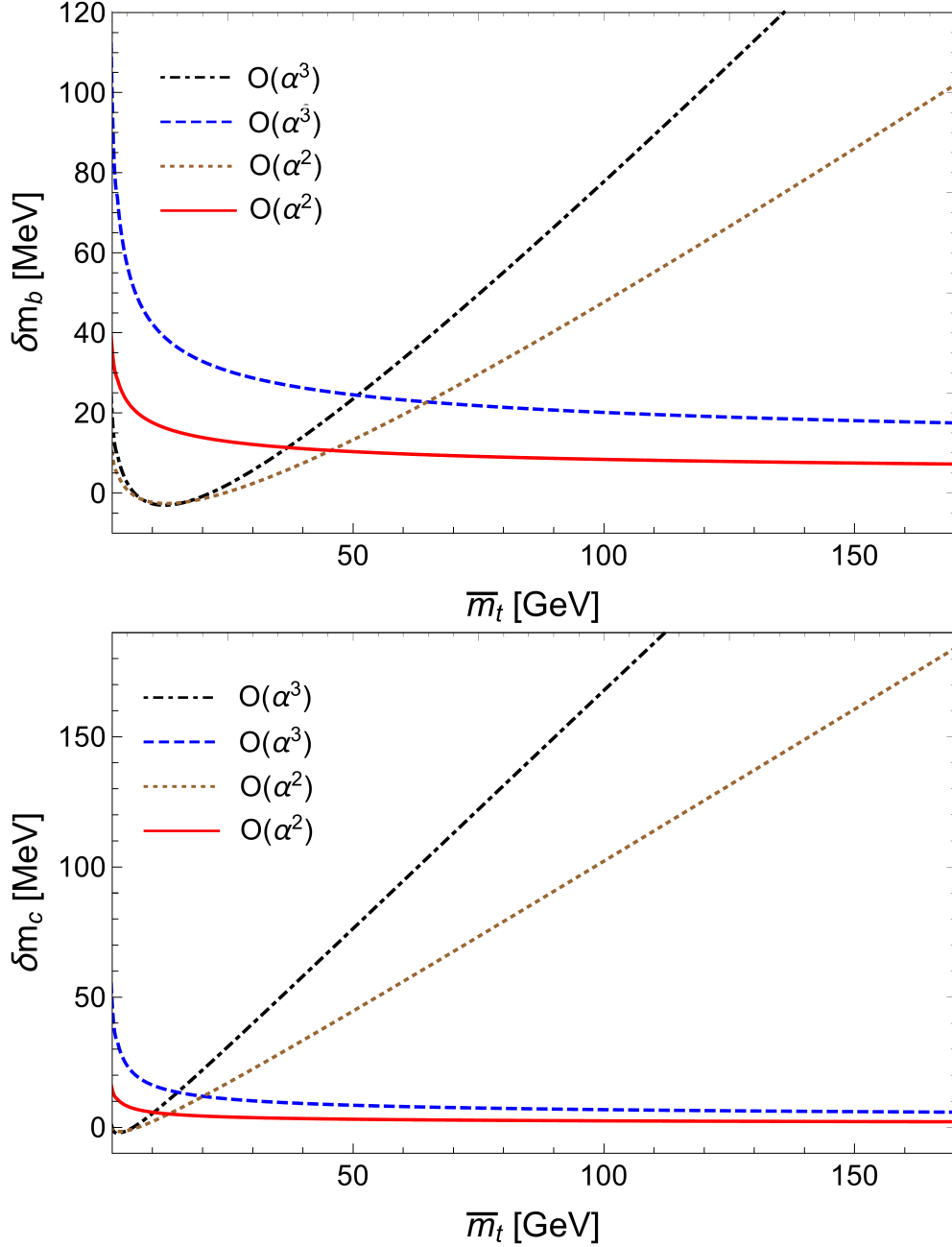


Figure 6.2: **Upper panel:** Plot of the correction to the PV mass of a top mass with varying \bar{m}_t mass due to a heavy quark with $\overline{\text{MS}}$ mass equal to 4.185 GeV (bottom) with and without decoupling (assuming a single heavy quark). The blue dashed line corresponds to the order $\alpha_{(5)}^3$ term of $\delta m_b^{(5)}$. The continuous red line corresponds to the order $\alpha_{(5)}^2$ term of $\delta m_b^{(5)}$. The dashdotted black line corresponds to the order $\alpha_{(4)}^3$ term of $\delta m_b^{(4)}$, and the dotted brown line corresponds to the order $\alpha_{(4)}^2$ term of $\delta m_b^{(4)}$. **Lower panel:** As in the upper panel with a heavy quark with $\overline{\text{MS}}$ equal to 1.223 GeV (charm). The blue dashed line corresponds to the order $\alpha_{(4)}^3$ term of $\delta m_c^{(4)}$. The continuous red line corresponds to the order $\alpha_{(4)}^2$ term of $\delta m_c^{(4)}$. The dashdotted black line corresponds to the order $\alpha_{(3)}^3$ term of $\delta m_c^{(3)}$, and the dotted brown line corresponds to the order $\alpha_{(3)}^2$ term of $\delta m_c^{(3)}$. Explicit formulas for the employed expressions can be found in Appendix F.

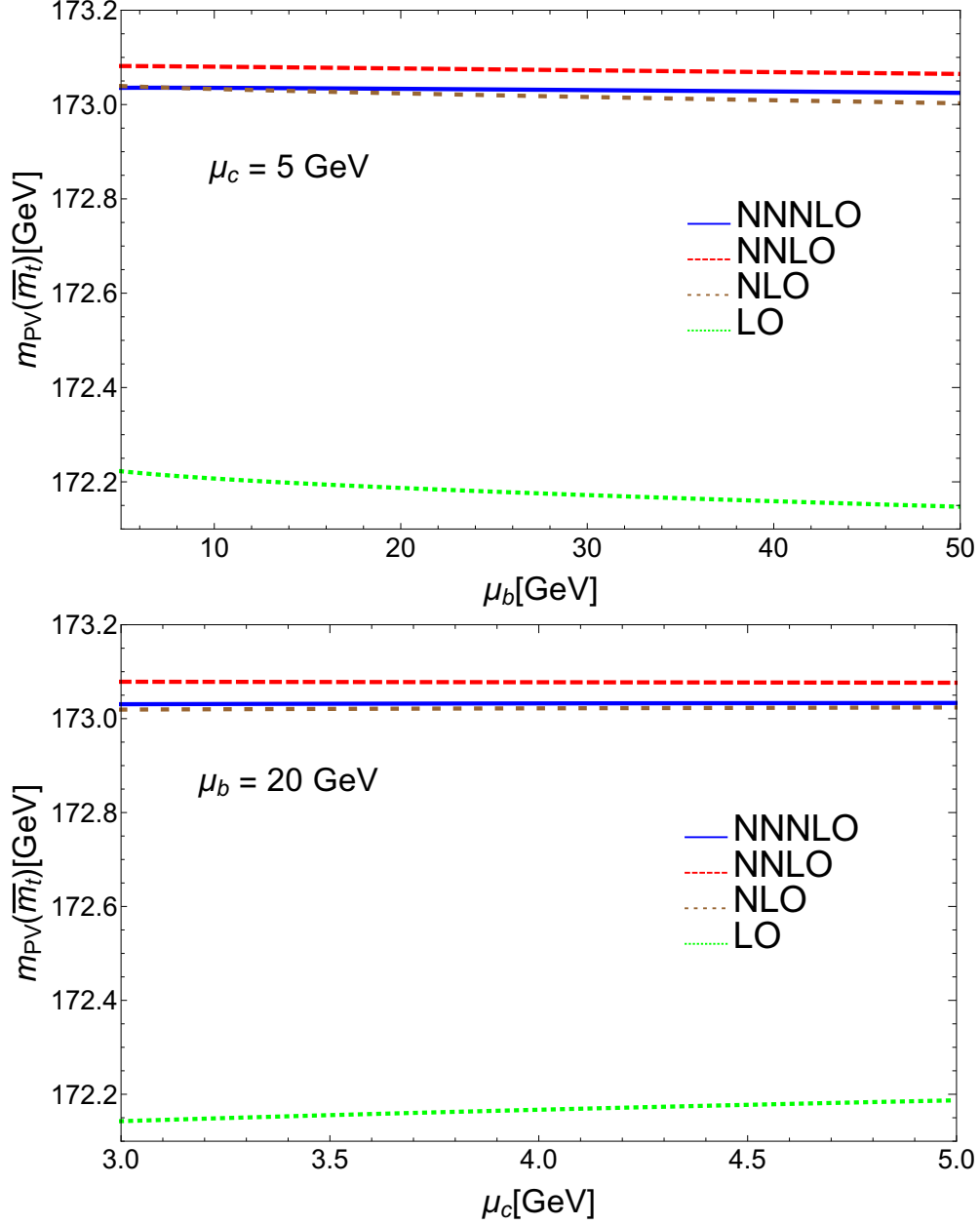


Figure 6.3: Plots of Eq. (6.77) in terms of μ_b (upper panel) and μ_c (lower panel) truncating the perturbative expansion of $\mathcal{F}(\bar{m}, n_f)$ at different orders in α in Eq. (6.80). In the upper figure, we set $\mu_c = 5$ GeV. In the lower figure, we set $\mu_b = 20$ GeV.

$\mathcal{F}(\overline{m}, n_f)$	g_1	g_2	g_3	g_4	g_5
$n_f = 0$	4/3	6.11	25.52	18.46	
$n_f = 3$	4/3	4.32	12.76	-63.37	
$n_f = 6$	4/3	2.53	-0.74	-105.70	
(Large β_0 /exact) $n_f = 10^{20}$	4/3	-5.97×10^{19}	-4.15×10^{38}	-2.54×10^{58}	-5.09×10^{77}
(Large β_0) $n_f = 0$	4/3	9.85	-11.31	114.33	-377.22
(Large β_0) $n_f = 3$	4/3	8.06	-7.57	62.62	-169.04
(Large β_0) $n_f = 6$	4/3	6.27	-4.58	29.46	-61.86

Table 6.4: The coefficients g_n of $\mathcal{F}(\overline{m}, n_f)$. Note that $g_4(n_f = 0)$ has a 9% error from the determination in [149]. The $n_f = 10^{20}$ case is used as a test for comparison with the large β_0 . The last three (four) rows are the coefficients g_n in the large β_0 approximation.

uncertainty, and find them to be comparatively very small: the error (and the effect) associated to the finite mass of the bottom and charm quark is found to be very small, and similarly for variations in the values of μ_b and μ_c .

It is also useful to make the error estimate of the ratio of the pole and $\overline{\text{MS}}$ top mass. We obtain ($\overline{m}_t = 163$ GeV)

$$\left[\frac{m_{t,\text{OS}}^{\text{PV}}}{\overline{m}_t} - 1 \right] \times 10^5 = 6155(\text{h.o.})_{-13}^{+13}(\mu)_{-9}^{+4}(Z_1)_{-6}^{+6}(\alpha)_{-75}^{+73}. \quad (6.83)$$

Note that there is no ambiguity error associated to this number. Except for α , all errors are associated to the lack of knowledge of higher order terms of the perturbative expansion. In comparison with [133], we find that our result is less sensitive to Z_1 and to its associated error.

6.3.3 $|d| = 2$ renormalons?

As we have many times mentioned already, the perturbative expansion of $\mathcal{F}(\overline{m}, n_f)$ is free of the $d = 1$ renormalon. Therefore, it is the ideal object on which to study the subleading renormalons of the pole mass. In principle, these are located at $d = 2$ and $d = -2$. The existence of an IR renormalon at $d = 2$ has been a matter of debate [148]. The existence of an UV renormalon at $d = -2$ can be established in the large β_0 approximation [31, 32], as we have already seen, but not beyond.

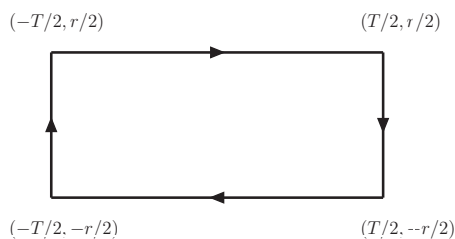
With respect to this discussion, some interesting observations can be drawn out of our analysis. The coefficients g_n show an interesting dependence in n_f (with sign changes of fixed order coefficients for various values of n_f). In Table 6.4, we give the numbers of g_n for different values of n_f and also in the large β_0 approximation. We observe that for $n_f = 3$ the $\mathcal{O}(\alpha^4)$ flips sign. For $n_f = 6$, the $\mathcal{O}(\alpha^3)$ and $\mathcal{O}(\alpha^4)$ flip sign. The situation is somewhat puzzling. Let us first note that the sign of the coefficients would be interchanged compared with the large β_0 predictions (for $n_f = 3$). This could still be understood from a $d = -2$ renormalon, if Z_{-2} flips sign from the large β_0 prediction to real QCD. This would indicate a large dependence of Z_{-2} on n_f compared with what has been seen for Z_1 , where the large β_0 approximation gave the right sign and order of magnitude. For $n_f \rightarrow \infty$, the results agree with QED expectations (β_0 becomes negative, and the perturbative series is non sign-alternating). For $n_f = 6$, we observe that the last two terms are negative. One may then wonder if what we are seeing for $n_f = 6$ (and maybe also for $n_f = 3$) is that the $d = -2$ renormalon's effect is subleading compared to another IR renormalon, which should be subleading, but that for sufficiently low orders could dominate over the UV one. Obviously, we need higher order coefficients g_n to clarify this issue.

It is usual lore that IR renormalons dominate over UV ones (this is somewhat based on large β_0 analyses where UV renormalons are typically suppressed by the factor $\sim e^{d\frac{c_X}{2}}$, whereas IR renormalons are enhanced by it, as we saw in section 3.7). If we take this seriously, and also the numbers we obtain for g_n as an indication of the existence of a $d = -2$ renormalon, this may indicate that the $d = 2$ renormalon is indeed zero. In this respect, it is worth mentioning the analysis of [121], where the NP correction associated to the $d = 2$ renormalon was found to be zero within errors, which is consistent with this discussion.

Chapter 7

Hyperasymptotics of the static quark antiquark energy and $\alpha(M_z)$

7.1 Introduction



Let us consider the Wilson loop depicted on the left

$$W_{\square}[A] = \text{Tr} \left\{ \mathcal{P} e^{ig \oint dx^{\mu} A_{\mu}(x)} \right\}, \quad (7.1)$$

where \mathcal{P} stands for path ordering, and let us consider the following vacuum expectation value

$$\langle W_{\square}[A] \rangle = \int [dA][d\psi][d\bar{\psi}] W_{\square}[A] e^{I_{\text{QCD}}}, \quad (7.2)$$

where I_{QCD} is the Euclidean QCD action¹. The static energy of a quark-antiquark pair separated by a distance r is defined in the following way²

$$E(r) \equiv \lim_{T \rightarrow \infty} \frac{i}{T} \log(\langle W_{\square}[A] \rangle). \quad (7.4)$$

This object has been studied thoroughly due to its relevance in order to understand the dynamics of QCD. A linear growing behavior at long distance is signaled as a proof of confinement. Moreover, it is a necessary ingredient in a Schrödinger-like description of heavy quarkonium dynamics. It will play a very prominent role in this chapter, where we will make use of the static energy computed in the lattice and in the $\overline{\text{MS}}$ scheme in perturbation theory to give a prediction of the strong coupling $\alpha(M_z)$.

The static energy can be determined accurately using MC simulations in the lattice. Throughout the last years, lattice simulations with dynamical fermions have improved their predictions at short distances, see for instance [150, 151, 152, 153, 154, 155, 156, 157, 158]. On the other hand, Eq. (7.4) can also be computed using perturbative techniques in the continuum [159, 160, 161, 162, 163, 164, 165, 166, 167, 168, 169, 170, 171]. The precision reached nowadays is N³LO for fixed order computations, and N³LL order for RG improved computations. Eq. (7.4) computed in the lattice is linearly divergent in $1/a$ (where a is the lattice spacing) by an r -independent constant.

¹Later, we will compare lattice evaluations of Eq. (7.2) with $\overline{\text{MS}}$ calculations. In the lattice case, we will have three massive quarks, but in the continuum case, we will disregard their masses.

²Actually, being completely accurate, the energy of a static quark-antiquark pair in a singlet configuration is

$$E(r) = 2m_{\text{OS}} + \lim_{T \rightarrow \infty} \frac{i}{T} \log(\langle W_{\square}[A] \rangle), \quad (7.3)$$

where m_{OS} is the pole mass, but for reasons that will be mentioned later we can disregard the $2m_{\text{OS}}$.

Therefore, we can compare lattice evaluations of the static energy with theoretical continuum computations by considering the difference

$$E^{\text{latt}}(r) - E^{\text{latt}}(r_{\text{ref}}) = E^{\text{th}}(r) - E^{\text{th}}(r_{\text{ref}}), \quad (7.5)$$

(up to $\mathcal{O}(a)$ lattice artefacts which can be r dependent) that is, we subtract the aforementioned r independent constant by picking an arbitrary reference point r_{ref} ³.

The combination of these two approaches, namely, high-order perturbation theory and lattice data at short distances, potentially allows quantitative comparison between perturbation theory and lattice simulations. Nevertheless, a naive comparison between lattice data and perturbative results may lead to strong disagreement depending on how the perturbative expansion is implemented in practice. This was the state of the art circa 1998, when it was realized that what lies behind the disagreement/agreement, is the large ambiguity associated to the $u = 1/2$ renormalon of the static potential (as we will see in Eq. (7.6), the static energy contains the static potential), which jeopardizes the overall convergence of $E(r)$, clouding the result (see [172] for a discussion on this issue).

As we have already mentioned in this thesis, it was discovered [29] that the $u = 1/2$ renormalon of V cancels with the $u = 1/2$ renormalon of $2m_{\text{OS}}$, where m_{OS} is the pole mass, (keep in mind that schematically $E(r) = V + 2m_{\text{OS}}$), if both series are expanded using the same $\alpha(\mu)$. By taking advantage of this renormalon cancellation, the ambiguities of the series of $E(r)$ are reduced to a point where the series converges better, and meaningful predictions can be obtained. Nonetheless, keep in mind that, as we have said around Eq. (7.5), the lattice can only predict E^{latt} up to an r independent constant. Hence, when considering $E^{\text{th}}(r)$, we will leave out the pole mass. In order to achieve renormalon cancellation, we will work with the r derivative of $E^{\text{th}}(r)$ [172, 173, 174, 172, 126, 167, 175].

Nowadays, more recent unquenched data and knowledge of higher orders in perturbation theory have allowed to obtain competitive determinations of $\Lambda_{\overline{\text{MS}}}^{(n_f=3)}$ (and consequently of $\alpha(M_z)$) from the static energy, see for instance [153, 156, 176, 177, 158]. We revisit⁴ this procedure, by considering N³LL order terms in the $\overline{\text{MS}}$ side, and by handling the renormalons by using the hyperasymptotic expansion of the PV Borel sum that we have seen⁵ in chapter 3. See [178] for the article on which the chapter is based.

We will start the chapter by reviewing what goes inside the continuum $\overline{\text{MS}}$ expressions for the static energy, and later, we will move on to perform the fits to the lattice data to extract $\alpha(M_z)$. On the way to do that, we will see how to use the current perturbative knowledge on the static potential to give an estimate of the normalization of the $u = 3/2$ renormalon of the static potential, which we will need in order to implement the terminants.

7.2 The singlet static energy and the multipole expansion

Taking advantage of the hierarchy of scales⁶ $\Delta V \approx \frac{C_A \alpha(1/r)}{2r} \ll \frac{1}{r}$, the energy $E(r)$ of a static quark-antiquark pair in a colour singlet configuration, separated by a distance r admits an OPE using pNRQCD [179, 180]

$$E(r) = V(r, \nu_{\text{us}}) + \delta E_{\text{us}}(r, \nu_{\text{us}}), \quad (7.6)$$

³In principle, the analysis should not depend on the value of r_{ref} we use in this equation, but in practice, there will be some dependence (we will check this dependence later). By default, we will take the value $r_{\text{ref}} = r_{\text{min}} = 0.353 \text{ GeV}^{-1}$, which will be the the shortest distance we will consider.

⁴For a comparison with other works, see section 7.18.

⁵Actually, and as we will later see, being accurate, we have also made use of taking an r derivative in the static energy to get rid of the $u = 1/2$ renormalon of V .

⁶ ΔV has been defined in Eq. (G.13).

where the singlet static potential $V(r, \nu_{\text{us}})$ encodes physics associated to the scale $1/r$, while $\delta E_{\text{us}}(r, \nu_{\text{us}})$ encodes physics associated to scales smaller than $1/r$. $V(r, \nu_{\text{us}})$ is computed as a formal series in $\alpha(\nu_{\text{s}})$. δE_{us} appears at order $\mathcal{O}(r^2)$ in the multipole expansion

$$\delta E_{\text{us}}(r, \nu_{\text{us}}) = \frac{T_F}{3N_c} r^2 V_A^2 \int_0^\infty dt e^{-t\Delta V} \langle g\mathbf{E}^a(t, \mathbf{0}) \phi_{ab}^{\text{adj}}(t, 0) g\mathbf{E}^b(0, \mathbf{0}) \rangle (\nu_{\text{us}}) + \mathcal{O}(r^3), \quad (7.7)$$

where \mathbf{E}^a is the chromoelectric field, V_A is a Wilson coefficient of pNRQCD (see Appendix G), whose small $\alpha(\nu_{\text{s}})$ expansion reads [166, 169, 167]

$$V_A = 1 + \mathcal{O}(\alpha^2(\nu_{\text{s}})), \quad (7.8)$$

and thus, for all practical purposes, it can taken to be 1. ΔV is the difference between the static octet and the singlet potentials. Its perturbative expansion in $\alpha(\nu_{\text{s}})$ reads

$$\Delta V \equiv V_o - V = \frac{C_A}{2} \frac{\alpha(\nu_{\text{s}})}{r} \left(1 + \frac{\alpha(\nu_{\text{s}})}{4\pi} (a_1 + 2\beta_0 \log(\nu_{\text{s}} e^{\gamma_E} r)) + \mathcal{O}(\alpha^2(\nu_{\text{s}})) \right). \quad (7.9)$$

$\phi_{ab}^{\text{adj}}(t, 0)$ is the Wilson line in the adjoint representation connecting $(t, \mathbf{0})$ and $(0, \mathbf{0})$ by a straight line. Notice that Eq. (7.7) is written in Euclidean time. We will now take a closer look at the two terms in Eq. (7.6).

7.3 The singlet static potential

The perturbative expansion of V is known to N³LO in $\alpha(\nu_{\text{s}})$. We will write it in the following way⁷

$$V = \sum_{n=0}^{\infty} V_n(r, \nu_{\text{s}}, \nu_{\text{us}}) \alpha^{n+1}(\nu_{\text{s}}). \quad (7.10)$$

Of course, the series above is meant to be understood as a formal series. We recall that the perturbative expansion of V is formally ν_{s} independent, that is

$$\frac{d}{d\nu_{\text{s}}} V = 0 \quad (7.11)$$

is satisfied order by order in $\alpha(\nu_{\text{s}})$. The coefficients read

$$V_n(r, \nu_{\text{s}}, \nu_{\text{us}}) = -\frac{C_F}{r} \frac{1}{(4\pi)^n} a_n(r, \nu_{\text{s}}, \nu_{\text{us}}), \quad (7.12)$$

and

$$a_0 = 1, \quad (7.13)$$

$$a_1(r, \nu_{\text{s}}) = a_1 + 2\beta_0 \log(\nu_{\text{s}} e^{\gamma_E} r), \quad (7.14)$$

$$a_2(r, \nu_{\text{s}}) = a_2 + \frac{\pi^2}{3} \beta_0^2 + (4a_1\beta_0 + 2\beta_1) \log(\nu_{\text{s}} e^{\gamma_E} r) + 4\beta_0^2 \log^2(\nu_{\text{s}} e^{\gamma_E} r), \quad (7.15)$$

$$\begin{aligned} a_3(r, \nu_{\text{s}}, \nu_{\text{us}}) = & a_3 + a_1\beta_0^2\pi^2 + \frac{5\pi^2}{6}\beta_0\beta_1 + 16\zeta_3\beta_0^3 \\ & + \left(2\pi^2\beta_0^3 + 6a_2\beta_0 + 4a_1\beta_1 + 2\beta_2 \right) \log(\nu_{\text{s}} e^{\gamma_E} r) + \frac{16}{3}C_A^3\pi^2 \log(\nu_{\text{us}} e^{\gamma_E} r) \\ & + \left(12a_1\beta_0^2 + 10\beta_0\beta_1 \right) \log^2(\nu_{\text{s}} e^{\gamma_E} r) + 8\beta_0^3 \log^3(\nu_{\text{s}} e^{\gamma_E} r), \end{aligned} \quad (7.16)$$

⁷To make the notation more compact, we have written all V_n in Eq. (7.12) as if they all depended on all r, ν_{s} and ν_{us} , but notice that a_0 is just a constant, and that the dependence on ν_{us} does not show up until $a_3(r, \nu_{\text{s}}, \nu_{\text{us}})$.

where $\gamma_E \approx 0.577$ is the Euler-Mascheroni constant and

$$a_1 = \frac{31C_A - 20T_F n_f}{9}, \quad (7.17)$$

$$a_2 = \frac{400n_f^2 T_F^2}{81} - C_F n_f T_F \left(\frac{55}{3} - 16\zeta(3) \right) + C_A^2 \left(\frac{4343}{162} + \frac{16\pi^2 - \pi^4}{4} + \frac{22\zeta(3)}{3} \right) - C_A n_f T_F \left(\frac{1798}{81} + \frac{56\zeta(3)}{3} \right), \quad (7.18)$$

$$a_3 = a_3^{(3)} n_f^3 + a_3^{(2)} n_f^2 + a_3^{(1)} n_f + a_3^{(0)}, \quad (7.19)$$

where

$$a_3^{(3)} = - \left(\frac{20}{9} \right)^3 T_F^3, \quad (7.20)$$

$$a_3^{(2)} = \left(\frac{12541}{243} + \frac{368\zeta(3)}{3} + \frac{64\pi^4}{135} \right) C_A T_F^2 + \left(\frac{14002}{81} - \frac{416\zeta(3)}{3} \right) C_F T_F^2, \quad (7.21)$$

$$a_3^{(1)} = \frac{d_F^{abcd} d_F^{abcd}}{N_A} \left\{ \pi^2 \left(\frac{1264}{9} - \frac{976}{3} \zeta(3) + \log(2)[64 + 672\zeta(3)] \right) + \pi^4 \left(-\frac{184}{3} + \frac{32}{3} \log(2) - 32 \log^2(2) \right) + \frac{10\pi^6}{3} \right\} + T_F \left\{ C_F^2 \left(\frac{286}{9} + \frac{296}{3} \zeta(3) - 160\zeta(5) \right) + C_A C_F \left(-\frac{71281}{162} + 264\zeta(3) + 80\zeta(5) \right) + C_A^2 \left(-\frac{58747}{486} + \pi^2 \left[\frac{17}{27} - 32\theta_4 + \log(2) \left\{ -\frac{4}{3} - 14\zeta(3) \right\} - \frac{19}{3} \zeta(3) \right] - 356\zeta(3) + \pi^4 \left[-\frac{157}{54} - \frac{5}{9} \log(2) + \log^2(2) \right] + \frac{1091}{6} \zeta(5) + \frac{57}{2} \zeta^2(3) + \frac{761}{2520} \pi^6 - 48y_6 \right) \right\}, \quad (7.22)$$

$$a_3^{(0)} = \frac{d_F^{abcd} d_A^{abcd}}{N_A} \left\{ \pi^2 \left(\frac{7432}{9} - 4736\theta_4 + \log(2) \left[\frac{14752}{3} - 3472\zeta(3) \right] - \frac{6616}{3} \zeta(3) \right) + \pi^4 \left(-156 + \frac{560}{3} \log(2) + \frac{496}{3} \log^2(2) \right) + \frac{1511\pi^6}{45} \right\} + C_A^3 \left\{ \frac{385645}{2916} + \pi^2 \left(-\frac{953}{54} + \frac{584}{3} \theta_4 + \frac{175}{2} \zeta(3) + \log(2) \left[-\frac{922}{9} + \frac{217}{3} \zeta(3) \right] \right) + \frac{584}{3} \zeta(3) + \pi^4 \left(\frac{1349}{270} - \frac{20}{9} \log(2) - \frac{40}{9} \log^2(2) \right) - \frac{1927}{6} \zeta(5) - \frac{143}{2} \zeta^2(3) - \frac{4621\pi^6}{3024} + 144y_6 \right\}, \quad (7.23)$$

and⁸

$$\frac{d_F^{abcd} d_F^{abcd}}{N_A} = \frac{18 - 6N_c^2 + N_c^4}{96N_c^2}, \quad (7.24)$$

$$\frac{d_F^{abcd} d_A^{abcd}}{N_A} = \frac{N_c(N_c^2 + 6)}{48}, \quad (7.25)$$

$$\theta_n = \text{Li}_n(1/2) + \frac{(-\log(2))^n}{n!}, \quad (7.26)$$

$$y_6 = \zeta(-5, -1) + \zeta(6), \quad (7.27)$$

where $\zeta(z)$ is the Riemann zeta function, $\zeta(z_1, z_2)$, is the multiple zeta function, and $\text{Li}_n(z)$ is the polylogarithm.

7.3.1 Resumming ultrasoft logarithms in the static potential

Just as it is clear from Eq. (7.16), at N³LO the static potential has a logarithm of the ratio of the soft and ultrasoft scales

$$V_3 \alpha^4(\nu_s) = \frac{-1}{12\pi r} C_A^3 C_F \alpha^4(\nu_s) L + \dots, \quad (7.28)$$

⁸In [171], from where the formulas for $a_3^{(1)}$ and $a_3^{(0)}$ are taken from, what we call θ_n is called α_n , and what we call y_6 is called s_6 . The change of notation is to avoid any ambiguity, as these symbols have already been used in this thesis.

where to ease notation, we have defined $L \equiv \log\left(\frac{\nu_{\text{us}}}{\nu_s}\right)$. This is not just a peculiarity of this order, and further terms will exhibit further such logs. For instance, at order $\alpha^5(\nu_s)$ there is an $\alpha^5(\nu_s)L^2$ and an $\alpha^5(\nu_s)L$ term, at order $\alpha^6(\nu_s)$, we have $\alpha^6(\nu_s)L^3$, $\alpha^6(\nu_s)L^2$ and $\alpha^6(\nu_s)L$, and so it goes from there on. These ultrasoft logarithms in the static potential can be resummed using RG techniques. They have been computed in [166] with N²LL accuracy, and in [167] with N³LL accuracy (see also [168]). Recall that terms that go like $\alpha^n(\nu_s)L^{n-3}$ for $n \geq 4$ are called N²LL, and terms such as $\alpha^n(\nu_s)L^{n-4}$ with $n \geq 5$ are called N³LL. Keep in mind that when one resums these logs, one assumes $\alpha(\nu_s)L \sim 1$, so that in this counting, N²LL logs contribute just as $\mathcal{O}(\alpha^3(\nu_s))$ terms, and N⁴LL logs just as $\mathcal{O}(\alpha^4(\nu_s))$ terms. These ultrasoft logarithms are absorbed in an object called $\delta V_{\text{RG}}(r, \nu_s, \nu_{\text{us}})$

$$V(r, \nu_{\text{us}}) = V(r, \nu_{\text{us}} = \nu_s) + \delta V_{\text{RG}}(r, \nu_s, \nu_{\text{us}}). \quad (7.29)$$

In the equation above, we have just considered the formal series of the static potential, and we have absorbed all the ultrasoft logarithms in the second term on the RHS. With this we mean that if $\delta V_{\text{RG}}(r, \nu_s, \nu_{\text{us}})$ is expanded in $\alpha(\nu_s)$, we recover order by order all the ultrasoft logarithms in $V(r, \nu_{\text{us}})$. Let's take a closer look at δV_{RG} . If we resum only the N²LL logs, it takes the form

$$\delta V_{\text{RG}}^{\text{N}^2\text{LL}}(r, \nu_s, \nu_{\text{us}}) \equiv \frac{1}{8r\beta_0} C_A^3 C_F \alpha^3(\nu_s) \frac{4}{3} \log\left(\frac{\alpha_1(\nu_{\text{us}})}{\alpha(\nu_s)}\right). \quad (7.30)$$

Notice that the strong coupling evaluated at the ultrasoft scale has a subscript. With $\alpha_1(\nu_{\text{us}})$ what is meant is that the running of this object needs to be taken at one loop, that is, when writing $\alpha_1(\nu_{\text{us}})$ as a series in $\alpha(\nu_s)$, we would set $\beta_1 = \beta_2 = \beta_3 = \dots = 0$. If in addition to the N²LL logs, we also resum the N³LL logs in δV_{RG} , we have

$$\begin{aligned} \delta V_{\text{RG}}^{\text{N}^3\text{LL}}(r, \nu_s, \nu_{\text{us}}) \equiv & \frac{1}{8r\beta_0} C_A^3 C_F \alpha^3(\nu_s) \left\{ \frac{4}{3} \log\left(\frac{\alpha_2(\nu_{\text{us}})}{\alpha(\nu_s)}\right) \right. \\ & \left. + 2\pi K (\alpha(\nu_s) - \alpha_1(\nu_{\text{us}})) + \frac{1}{\pi} \alpha(\nu_s) (a_1 + 2\beta_0 \log(\nu_s r e^{\gamma_E})) \log\left(\frac{\alpha_1(\nu_{\text{us}})}{\alpha(\nu_s)}\right) \right\}, \end{aligned} \quad (7.31)$$

where we have defined

$$K \equiv \frac{8}{3} \frac{\beta_1}{\beta_0} \frac{1}{(4\pi)^2} - \frac{1}{27\pi^2} (C_A (47 + 6\pi^2) - 10T_F n_f). \quad (7.32)$$

In some places of Eq. (7.31), the subscript of the strong coupling evaluated at the ultrasoft scale is 2. With this what is meant is that we take the running at two loop level. The need to evaluate $\alpha(\nu_{\text{us}})$ sometimes at one loop and sometimes at two loops is clear once one considers the following small $\alpha(\nu_s)$ expansions

$$\begin{aligned} \alpha(\nu_{\text{us}}) = & \alpha(\nu_s) + \frac{1}{2\pi} \alpha^2(\nu_s) \left\{ -\beta_0 L \right\} + \frac{1}{8\pi^2} \alpha^3(\nu_s) \left\{ 2\beta_0^2 L^2 - \beta_1 L \right\} \\ & + \frac{1}{32\pi^3} \alpha^4(\nu_s) \left\{ -4\beta_0^3 L^3 + 5\beta_0 \beta_1 L^2 - \beta_2 L \right\} + \mathcal{O}(\alpha^5(\nu_s)), \end{aligned} \quad (7.33)$$

and

$$\begin{aligned} \log\left(\frac{\alpha(\nu_{\text{us}})}{\alpha(\nu_s)}\right) = & \frac{1}{2\pi} \alpha(\nu_s) \left\{ -\beta_0 L \right\} + \frac{1}{8\pi^2} \alpha^2(\nu_s) \left\{ \beta_0^2 L^2 - \beta_1 L \right\} \\ & + \frac{1}{96\pi^3} \alpha^3(\nu_s) \left\{ -4\beta_0^3 L^3 + 9\beta_0 \beta_1 L^2 - 3\beta_2 L \right\} + \mathcal{O}(\alpha^4(\nu_s)). \end{aligned} \quad (7.34)$$

We see that by setting the various β_n coefficients to zero, as indicated by the subscripts in Eqs. (7.30) and (7.31), we get only up to N²LL and N³LL terms. Nonetheless, in practice, we will not be so rigorous, and we will not bother with the proper subscripts, and we will just use

$$\delta V_{\text{RG}}^{\text{N}^2\text{LL}}(r, \nu_s, \nu_{\text{us}}) = \frac{1}{8r\beta_0} C_A^3 C_F \alpha^3(\nu_s) \frac{4}{3} \log\left(\frac{\alpha(\nu_{\text{us}})}{\alpha(\nu_s)}\right), \quad (7.35)$$

and

$$\begin{aligned} \delta V_{\text{RG}}^{\text{N}^3\text{LL}}(r, \nu_s, \nu_{\text{us}}) &= \frac{1}{8r\beta_0} C_A^3 C_F \alpha^3(\nu_s) \left\{ \frac{4}{3} \log\left(\frac{\alpha(\nu_{\text{us}})}{\alpha(\nu_s)}\right) \right. \\ &\quad \left. + 2\pi K(\alpha(\nu_s) - \alpha(\nu_{\text{us}})) + \frac{1}{\pi} \alpha(\nu_s) (a_1 + 2\beta_0 \log(\nu_s r e^{\gamma_E})) \log\left(\frac{\alpha(\nu_{\text{us}})}{\alpha(\nu_s)}\right) \right\}, \end{aligned} \quad (7.36)$$

that is, when using the N²LL expression we will keep all N²LL terms and some subleading terms, and when working with the N³LL expression, we will have all N³LL terms and some subleading terms. Finally, and for reference's sake, we write next the first few ultrasoft logarithms of the static potential by expanding $\delta V_{\text{RG}}^{\text{N}^3\text{LL}}$ in $\alpha(\nu_s)$

$$\begin{aligned} \delta V_{\text{RG}}^{\text{N}^3\text{LL}}(r, \nu_s, \nu_{\text{us}}) &= \frac{-1}{12\pi r} C_A^3 C_F \alpha^4(\nu_s) L + \frac{1}{8r\beta_0} C_A^3 C_F \alpha^5(\nu_s) \left\{ L^2 \frac{1}{6\pi^2} \beta_0^2 \right. \\ &\quad \left. + L \left[\frac{-\beta_1}{6\pi^2} + K\beta_0 - \frac{\beta_0}{2\pi^2} (a_1 + 2\beta_0 \log(r\nu_s e^{\gamma_E})) \right] \right\} + \mathcal{O}(\alpha^6(\nu_s)). \end{aligned} \quad (7.37)$$

Thus, summarizing all, we have that the static potential at N²LL order reads

$$V_{\text{N}^2\text{LL}}(r, \nu_s, \nu_{\text{us}}) \equiv \sum_{n=0}^2 V_n(r, \nu_s, \nu_{\text{us}} = \nu_s) \alpha^{n+1}(\nu_s) + \delta V_{\text{RG}}^{\text{N}^2\text{LL}}(r, \nu_s, \nu_{\text{us}}), \quad (7.38)$$

and at N³LL level, we have that

$$V_{\text{N}^3\text{LL}}(r, \nu_s, \nu_{\text{us}}) \equiv \sum_{n=0}^3 V_n(r, \nu_s, \nu_{\text{us}} = \nu_s) \alpha^{n+1}(\nu_s) + \delta V_{\text{RG}}^{\text{N}^3\text{LL}}(r, \nu_s, \nu_{\text{us}}). \quad (7.39)$$

7.4 The ultrasoft energy

Let us come back to Eq. (7.6), and consider now the second term on the RHS. We have seen in Eq. (7.7) that at order r^2 in the multipole expansion $\delta E_{\text{us}}(r, \nu_{\text{us}})$ takes the form

$$\delta E_{\text{us}}(r, \nu_{\text{us}}) = \frac{T_F}{3N_c} r^2 V_A^2 \int_0^\infty dt e^{-t\Delta V} \langle g\mathbf{E}^a(t, \mathbf{0}) \phi_{ab}^{\text{adj}}(t, 0) g\mathbf{E}^b(0, \mathbf{0}) \rangle (\nu_{\text{us}}) + \mathcal{O}(r^3). \quad (7.40)$$

This quantity has a different behavior depending on the relative size between Λ_{QCD} and ΔV . If both scales, Λ_{QCD} and ΔV , are similar in size, δE_{us} is an unknown function of the ratio of these two scales. On the other hand, if $\Lambda_{\text{QCD}} \gg \Delta V$, the above expression can be approximated to

$$\delta E_{\text{us}}(r, \nu_{\text{us}}) = \frac{T_F}{3N_c} r^2 V_A^2 \int_0^\infty dt \langle g\mathbf{E}^a(t, \mathbf{0}) \phi_{ab}^{\text{adj}}(t, 0) g\mathbf{E}^b(0, \mathbf{0}) \rangle \sim r^2 \Lambda_{\text{QCD}}^3. \quad (7.41)$$

Finally, if $\Lambda_{\text{QCD}} \ll \Delta V$, δE_{us} can be computed at weak coupling as an expansion in powers of $\alpha(\nu_{\text{us}})$. This expansion is known to order $r^2(\Delta V)^3 \alpha^2(\nu_{\text{us}}) \sim \frac{1}{r} \alpha^5(\nu_s)$ in the $\overline{\text{MS}}$ scheme⁹. At LO in $\alpha(\nu_{\text{us}})$, we have

$$\delta E_{\text{us}}^{\text{LO in } \alpha(\nu_{\text{us}})} = C_F r^2 (\Delta V)^3 V_A^2 \frac{\alpha(\nu_{\text{us}})}{9\pi} \left(-6 \log \frac{\Delta V}{\nu_{\text{us}}} - 6 \log 2 + 5 \right) + \mathcal{O}(\alpha^2(\nu_{\text{us}})). \quad (7.42)$$

At NLO in $\alpha(\nu_{\text{us}})$ [166]

$$\begin{aligned} \delta E_{\text{us}}^{\text{NLO in } \alpha(\nu_{\text{us}})} &= C_F r^2 (\Delta V)^3 V_A^2 \frac{1}{9\pi} \left\{ \alpha(\nu_{\text{us}}) \left[-6 \log \left(\frac{\Delta V}{\nu_{\text{us}}} \right) - 6 \log 2 + 5 \right] + \frac{\alpha^2(\nu_{\text{us}})}{12\pi} \left[18\beta_0 \log^2 \left(\frac{\Delta V}{\nu_{\text{us}}} \right) \right. \right. \\ &\quad \left. \left. - 6 (C_A(13 + 4\pi^2) - 2\beta_0(-5 + 3 \log 2)) \log \left(\frac{\Delta V}{\nu_{\text{us}}} \right) - 2C_A(-84 + 39 \log 2 + 4\pi^2(-2 + 3 \log 2)) \right. \right. \\ &\quad \left. \left. + 72\zeta(3) + \beta_0(67 + 3\pi^2 - 60 \log 2 + 18 \log^2(2)) \right] \right\} + \mathcal{O}(\alpha^3(\nu_{\text{us}})). \end{aligned} \quad (7.43)$$

⁹Its expression in the large β_0 approximation can be found in [79].

7.4.1 Expanding ΔV and V_A in δE_{us}

So far, we have written δE_{us} as a power series in $\alpha(\nu_{\text{us}})$ with ΔV and V_A taken explicitly. As it has already been said, ΔV and V_A both admit a small $\alpha(\nu_s)$ expansion. Implementing them in Eqs. (7.42) and (7.43), we arrive at

$$\begin{aligned} \delta E_{\text{us}}^{\text{N}^4\text{LL}} = & C_F C_A^3 \frac{1}{72\pi r} \alpha^3(\nu_s) \left\{ \alpha(\nu_{\text{us}}) \left[-6 \log \left(\frac{C_A \alpha(\nu_s)}{2r\nu_{\text{us}}} \right) - 6 \log 2 + 5 + \frac{3}{4\pi} \alpha(\nu_s) (a_1 + 2\beta_0 \log(r\nu_s e^{\gamma_s})) \right] \right. \\ & \times \left(-6 \log \left(\frac{C_A \alpha(\nu_s)}{2r\nu_{\text{us}}} \right) - 6 \log 2 + 3 \right) + \frac{\alpha^2(\nu_{\text{us}})}{12\pi} \left[18\beta_0 \log^2 \left(\frac{C_A \alpha(\nu_s)}{2r\nu_{\text{us}}} \right) \right. \\ & - 6 (C_A(13 + 4\pi^2) - 2\beta_0(-5 + 3 \log 2)) \log \left(\frac{C_A \alpha(\nu_s)}{2r\nu_{\text{us}}} \right) - 2C_A (-84 + 39 \log 2 + 4\pi^2(-2 + 3 \log 2)) \\ & \left. \left. + 72\zeta(3) + \beta_0 (67 + 3\pi^2 - 60 \log 2 + 18 \log^2(2)) \right] + \mathcal{O}(\alpha^3(\nu_{\text{us}})) \right\}, \end{aligned} \quad (7.44)$$

where we have only kept terms that got at most α^5 (regardless of the scale at which it is evaluated). Let us just focus on terms that have at most α^4

$$\delta E_{\text{us}}^{\text{N}^3\text{LL}} = C_F C_A^3 \frac{1}{72\pi r} \alpha^3(\nu_s) \alpha(\nu_{\text{us}}) \left\{ -6 \log \left(\frac{C_A \alpha(\nu_s)}{2r\nu_{\text{us}}} \right) - 6 \log(2) + 5 \right\}. \quad (7.45)$$

Let's think about the ultrasoft logarithms above. We need to keep in mind that we will typically choose $\nu_{\text{us}} \sim \frac{\alpha(\nu_s)}{r}$, so that the logarithm of $\alpha(\nu_s)$ featured in the equation above will be regarded as order 1. Therefore, from Eq. (7.33), we readily see that the equation above contains N^3LL terms¹⁰. Moreover, we easily see that the order $\alpha^2(\nu_{\text{us}})$ terms and the order $\alpha^4(\nu_s)\alpha(\nu_{\text{us}})$ terms in Eq. (7.44) give rise to N^4LL terms. We will not reach this level of precision in this thesis, so we will not consider these terms in what follows. Thus, in our N^3LL expressions for the singlet static energy, we will use Eq. (7.45).

7.5 Cancellation of ν_{us} in $E(r)$

It has been long known [181, 182] that the static potential has IR divergences starting at $\mathcal{O}(\alpha^4(\nu_s))$ when $\nu_{\text{us}} \rightarrow 0$. This divergence parametrized by ν_{us} of the first term on the RHS of Eq. (7.6) gets cancelled with the second term in the RHS, so that $E(r)$ is ν_{us} independent. In order to show this cancellation, we first write the ultrasoft energy as a small $\alpha(\nu_s)$ expansion by expanding $\alpha(\nu_{\text{us}})$ in terms of $\alpha(\nu_s)$ in Eq. (7.44). This yields

$$\begin{aligned} \delta E_{\text{us}}^{\text{N}^4\text{LO in } \alpha(\nu_s)} = & \frac{1}{72\pi r} C_F C_A^3 \left\{ \alpha^4(\nu_s) \left[-6 \log \left(\frac{C_A \alpha(\nu_s)}{2r\nu_{\text{us}}} \right) - 6 \log 2 + 5 \right] + \alpha^5(\nu_s) \left[\frac{3\beta_0}{2\pi} \log^2 \left(\frac{C_A \alpha(\nu_s)}{2r\nu_{\text{us}}} \right) \right. \right. \\ & + \log \left(\frac{C_A \alpha(\nu_s)}{2r\nu_{\text{us}}} \right) \left(\frac{3\beta_0}{\pi} \log \left(\frac{\nu_{\text{us}}}{\nu_s} \right) - \frac{1}{2\pi} (C_A(13 + 4\pi^2) - 2\beta_0(-5 + 3 \log 2)) - \frac{9}{2\pi} (a_1 + 2\beta_0 \log(r\nu_s e^{\gamma_s})) \right) \\ & - \frac{1}{2\pi} \beta_0 \log \left(\frac{\nu_{\text{us}}}{\nu_s} \right) (-6 \log 2 + 5) + \frac{9}{2\pi} (a_1 + 2\beta_0 \log(r\nu_s e^{\gamma_s})) \left(\frac{1}{2} - \log 2 \right) + \frac{1}{12\pi} \left(-2C_A (-84 + 39 \log 2 \right. \\ & \left. \left. + 4\pi^2(-2 + 3 \log 2) + 72\zeta(3) + \beta_0 (67 + 3\pi^2 - 60 \log 2 + 18 \log^2 2) \right) \right] \left. \right\} + \mathcal{O}(\alpha^6(\nu_s)). \end{aligned} \quad (7.47)$$

It is worth mentioning that this object is known one order more in $\alpha(\nu_s)$ than the static potential. Now, from Eq. (7.16), we know that at order $\alpha^4(\nu_s)$ the ν_{us} dependence of V is

$$V = \frac{-1}{12\pi r} C_F C_A^3 \alpha^4(\nu_s) \log \left(\frac{\nu_{\text{us}}}{\nu_s} \right) + \dots \quad (7.48)$$

¹⁰And, analogously to what happened to Eqs. (7.31) and (7.36), we also have more subleading terms. If we wanted to be rigorous, and only keep the N^3LL logs, we would consider

$$\delta E_{\text{us}}^{\text{N}^3\text{LL}} = C_F C_A^3 \frac{1}{72\pi r} \alpha^3(\nu_s) \alpha_1(\nu_{\text{us}}) \left\{ -6 \log \left(\frac{C_A \alpha(\nu_s)}{2r\nu_{\text{us}}} \right) - 6 \log(2) + 5 \right\}. \quad (7.46)$$

From Eq. (7.47), we see that the ν_{us} dependence of the ultrasoft energy at order $\alpha^4(\nu_s)$ is

$$\delta E_{\text{us}} = \frac{-1}{12\pi r} C_F C_A^3 \alpha^4(\nu_s) \log\left(\frac{C_A \alpha(\nu_s)}{2r\nu_{\text{us}}}\right) + \dots \quad (7.49)$$

By summing both

$$E(r) = V + \delta E_{\text{us}} \quad (7.50)$$

$$= \frac{-1}{12\pi r} C_F C_A^3 \alpha^4(\nu_s) \left\{ \log\left(\frac{\nu_{\text{us}}}{\nu_s}\right) + \log\left(\frac{C_A \alpha(\nu_s)}{2r\nu_{\text{us}}}\right) \right\} + \dots \quad (7.51)$$

$$= \frac{-1}{12\pi r} C_F C_A^3 \alpha^4(\nu_s) \log\left(\frac{C_A \alpha(\nu_s)}{2r\nu_s}\right) + \dots, \quad (7.52)$$

and we see that the ν_{us} dependence explicitly cancels, rendering the static energy ν_{us} independent, as it is expected. Similar cancellations will take place at higher orders.

7.6 The singlet static energy revisited

Having fleshed out the terms on the RHS of Eq. (7.6), we now summarize the main formulas to consider for the static energy. If we do not resum ultrasoft logarithms, up until order $\alpha^3(\nu_s)$, we just have the static potential

$$E_{\text{N}^j\text{LO}}(r) = \sum_{n=0}^j V_n \alpha^{n+1}(\nu_s), \quad (7.53)$$

for $j < 3$. For N^3LO order, we will add on top of the series of the static potential the appropriate term from δE_{us} , that is, we will add the order $\alpha^4(\nu_s)$ term in Eq. (7.47)

$$E_{\text{N}^3\text{LO}}(r) = \sum_{n=0}^3 V_n \alpha^{n+1}(\nu_s) + \frac{1}{72\pi r} C_F C_A^3 \alpha^4(\nu_s) \left[-6 \log\left(\frac{C_A \alpha(\nu_s)}{2r\nu_{\text{us}}}\right) - 6 \log 2 + 5 \right]. \quad (7.54)$$

We repeat here that the ν_{us} dependence on the second term of the RHS above disappears with the $\alpha^4(\nu_s)$ term of the static potential. If on the other hand, we do resum ultrasoft logarithms, we have that, at the N^2LL level,

$$E_{\text{N}^2\text{LL}}(r) = V_{\text{N}^2\text{LL}}, \quad (7.55)$$

that is, only the static potential contributes. At the N^3LL level,

$$E_{\text{N}^3\text{LL}}(r) = V_{\text{N}^3\text{LL}} + \delta E_{\text{us}}^{\text{N}^3\text{LL}}. \quad (7.56)$$

7.7 Getting rid of the $u = 1/2$ renormalon

Let's recall Eq. (7.5)

$$E^{\text{latt}}(r) - E^{\text{latt}}(r_{\text{ref}}) = E^{\text{th}}(r) - E^{\text{th}}(r_{\text{ref}}). \quad (7.57)$$

We have reviewed in past sections the theoretical expressions for $E^{\text{th}}(r)$ as given by Eq. (7.6). As it has been mentioned in the introduction to this chapter, the singlet static potential suffers from an r independent $u = 1/2$ renormalon that jeopardizes the overall convergence of $E(r)$. We can completely forget about this renormalon¹¹ by simply taking the r derivative of the static energy, and just working with this object by taking

$$E^{\text{latt}}(r) - E^{\text{latt}}(r_{\text{ref}}) = \int_{r_{\text{ref}}}^r dr' \mathcal{F}(r'), \quad (7.58)$$

¹¹For an analysis without taking the derivative see [178].

where

$$\mathcal{F}(r) \equiv \frac{d}{dr} E(r). \quad (7.59)$$

Eq. (7.58) was originally used in [173] (see also [172]), but its use for competitive determinations of Λ_{QCD} was first made in [153]. We will in the next section take the derivative on the expressions of the static energy we have seen.

7.8 Taking an r derivative in $E(r)$

We now consider the r derivative of the static energy

$$\mathcal{F}(r) = \frac{d}{dr} E(r) = \frac{d}{dr} V(r, \nu_{\text{us}}) + \frac{d}{dr} \delta E_{\text{us}}(r, \nu_{\text{us}}). \quad (7.60)$$

It is customary to define the force as the derivative of the static potential

$$F(r, \nu_{\text{us}}) \equiv \frac{d}{dr} V(r, \nu_{\text{us}}). \quad (7.61)$$

Its perturbative expansion reads

$$F = \sum_{n=0}^{\infty} f_n(r, \nu_s, \nu_{\text{us}}) \alpha^{n+1}(\nu_s), \quad (7.62)$$

where, needless to say, that the series in the RHS is meant to be understood as a formal series. Taking a derivative on the expressions of section 7.3, we obtain

$$\begin{aligned} f_0 &= \frac{C_F}{r^2}, & f_1 &= \frac{C_F}{4\pi r^2} \{a_1(r, \nu_s) - 2\beta_0\}, \\ f_2 &= \frac{C_F}{(4\pi)^2 r^2} \{a_2(r, \nu_s) - 4a_1(r, \nu_s)\beta_0 - 2\beta_1\}, \\ f_3 &= \frac{C_F}{(4\pi)^3 r^2} \left\{ a_3(r, \nu_s, \nu_{\text{us}}) - 6a_2(r, \nu_s)\beta_0 - 4a_1(r, \nu_s)\beta_1 - 2\beta_2 - \frac{16}{3}C_A^3\pi^2 \right\}. \end{aligned} \quad (7.63)$$

Notice that, just as with $V(r, \nu_{\text{us}})$, we have ν_{us} dependence in the coefficient that goes with $\alpha^4(\nu_s)$. Also, just as with $V(r, \nu_{\text{us}})$, we can resum the ultrasoft logarithms of the series of the force. Taking the r derivative in δV_{RG} , we get at N^2LL level

$$\delta F_{\text{RG}}^{\text{N}^2\text{LL}}(r, \nu_s, \nu_{\text{us}}) \equiv \frac{d}{dr} \delta V_{\text{RG}}(r, \nu_s, \nu_{\text{us}}) \Big|_{\text{N}^2\text{LL}} = -\frac{1}{6\beta_0} C_F C_A^3 \frac{1}{r^2} \alpha^3(\nu_s) \log\left(\frac{\alpha_1(\nu_{\text{us}})}{\alpha(\nu_s)}\right), \quad (7.64)$$

and at N^3LL level

$$\begin{aligned} \delta F_{\text{RG}}^{\text{N}^3\text{LL}}(r, \nu_s, \nu_{\text{us}}) &\equiv \frac{d}{dr} \delta V_{\text{RG}}(r, \nu_s, \nu_{\text{us}}) \Big|_{\text{N}^3\text{LL}} = C_F C_A^3 \frac{1}{r^2} \alpha^3(\nu_s) \left\{ -\frac{1}{6\beta_0} \log\left(\frac{\alpha_2(\nu_{\text{us}})}{\alpha(\nu_s)}\right) \right. \\ &\left. + \frac{\pi}{4\beta_0} K \{ \alpha_1(\nu_{\text{us}}) - \alpha(\nu_s) \} + \frac{1}{8\pi} \left(2 - \frac{1}{\beta_0} [a_1 + 2\beta_0 \log(r\nu_s e^{\gamma_E})] \right) \alpha(\nu_s) \log\left(\frac{\alpha_1(\nu_{\text{us}})}{\alpha(\nu_s)}\right) \right\}, \end{aligned} \quad (7.65)$$

where recall that K has been defined in Eq. (7.32). We have bothered to write the proper subscripts for $\alpha(\nu_{\text{us}})$ but, just as with the static energy, in practice, we will not take this detail into account. Thus, the RG improved version of the force at N^2LL reads

$$F_{\text{N}^2\text{LL}}(r, \nu_s, \nu_{\text{us}}) = F(r, \nu_{\text{us}} = \nu_s) \Big|_{\text{N}^2\text{LO}} + \delta F_{\text{RG}}^{\text{N}^2\text{LL}}(r, \nu_s, \nu_{\text{us}}), \quad (7.66)$$

and at N^3LL

$$F_{\text{N}^3\text{LL}}(r, \nu_s, \nu_{\text{us}}) = F(r, \nu_{\text{us}} = \nu_s) \Big|_{\text{N}^3\text{LO}} + \delta F_{\text{RG}}^{\text{N}^3\text{LL}}(r, \nu_s, \nu_{\text{us}}). \quad (7.67)$$

Finally, let's turn our attention to the r derivative of δE_{us} . The analogous of Eq. (7.45) reads

$$\frac{d}{dr} \delta E_{\text{us}}^{\text{N}^3\text{LL}} = C_F C_A^3 \frac{1}{12\pi r^2} \alpha^3(\nu_s) \alpha(\nu_{\text{us}}) \left\{ \log \left(\frac{C_A \alpha(\nu_s)}{2r\nu_{\text{us}}} \right) + \log(2) + 1/6 \right\}. \quad (7.68)$$

Just as with Eq. (7.45), the equation above contains N^3LL logs. Likewise, the order $\alpha^2(\nu_{\text{us}})$ contains N^4LL terms, so we do not consider it in this thesis. Finally, writing δE_{us} as an expansion (modulo logs) in $\alpha(\nu_s)$

$$\begin{aligned} \frac{d}{dr} \delta E_{\text{us}}^{\text{N}^4\text{LO}}(r, \nu_s, \nu_{\text{us}}) &= \frac{1}{72\pi} C_F C_A^3 \frac{1}{r^2} \left\{ \alpha^4(\nu_s) \left[6 \log \left(\frac{C_A \alpha(\nu_s)}{2r\nu_{\text{us}}} \right) + 6 \log 2 + 1 \right] \right. \\ &+ \alpha^5(\nu_s) \left[-\log^2 \left(\frac{C_A \alpha(\nu_s)}{2r\nu_{\text{us}}} \right) \frac{3\beta_0}{2\pi} + \log \left(\frac{C_A \alpha(\nu_s)}{2r\nu_{\text{us}}} \right) \left(-\frac{3\beta_0}{2\pi} \log \left(\frac{\nu_{\text{us}}}{\nu_s} \right) + \frac{9\beta_0}{\pi} \log(r\nu_s e^{\gamma_E}) - \frac{12\beta_0}{\pi} + \frac{9a_1}{2\pi} - K_1 \right) \right. \\ &- \frac{\beta_0}{2\pi} (6 \log 2 + 1) \log \left(\frac{\nu_{\text{us}}}{\nu_s} \right) + \frac{\beta_0}{\pi} (9 \log 2 + \frac{9}{2}) \log(r\nu_s e^{\gamma_E}) + \frac{1}{\pi} a_1 \left(\frac{9}{2} \log 2 + \frac{9}{4} \right) + \frac{\beta_0}{\pi} \left(\frac{9}{2} - 9 \log 2 \right) - K_1 - \frac{1}{12\pi} K_2 \left. \right] \\ &\left. + \mathcal{O}(\alpha^6(\nu_s)) \right\}, \end{aligned} \quad (7.69)$$

where

$$K_1 = -\frac{1}{2\pi} [C_A(13 + 4\pi^2) - 2\beta_0(-5 + 3 \log 2)], \quad (7.70)$$

$$K_2 = -2C_A [-84 + 39 \log 2 + 4\pi^2(-2 + 3 \log 2) + 72\zeta(3)] + \beta_0(67 + 3\pi^2 - 60 \log 2 + 18 \log^2 2). \quad (7.71)$$

We emphasize that the r derivative of $E(r)$ in the above equations has been taken with respect to constant ν_s and ν_{us} . Nevertheless, we will later consider this scales to have the following r dependence

$$\nu_s = \frac{x_s}{r}, \quad (7.72)$$

$$\nu_{\text{us}} = x_{\text{us}} \frac{C_A \alpha(\nu_s)}{2r}, \quad (7.73)$$

for some values of x_s and x_{us} . Therefore, one could at first have some reservations about using the expressions that have been computed above. Fortunately, it can be seen that if we consider this r dependence *before* taking the derivative in $E(r)$, we actually obtain the same formula for $\mathcal{F}(r)$. The individual terms $\frac{d}{dr} V$, $\frac{d}{dr} V_{\text{RG}}$ and $\frac{d}{dr} \delta E_{\text{us}}$ change, but the changes add up to the same $\mathcal{F}(r)$. We show this in Appendix H.

Thus, summarizing all, if we do not resum the ultrasoft logarithms we have for $j < 3$

$$\mathcal{F}_{\text{N}^j\text{LO}} = \sum_{n=0}^j f_n(r, \nu_s, \nu_{\text{us}}) \alpha^{n+1}(\nu_s). \quad (7.74)$$

At N^3LO , we have to add a contribution from the derivative of δE_{us} in Eq. (7.69)

$$\mathcal{F}_{\text{N}^3\text{LO}} = \sum_{n=0}^3 f_n(r, \nu_s, \nu_{\text{us}}) \alpha^{n+1}(\nu_s) + \frac{1}{12\pi} C_F C_A^3 \frac{1}{r^2} \alpha^4(\nu_s) \left\{ \log \left(\frac{C_A \alpha(\nu_s)}{2r\nu_{\text{us}}} \right) + \log 2 + 1/6 \right\}. \quad (7.75)$$

We stress again that the ν_{us} dependence on both terms in the RHS above cancels out. On the other hand, if we resum ultrasoft logarithms, we would have

$$\mathcal{F}_{\text{N}^2\text{LL}} = F_{\text{N}^2\text{LL}}(r, \nu_s, \nu_{\text{us}}), \quad (7.76)$$

$$\mathcal{F}_{\text{N}^3\text{LL}}(r) = F_{\text{N}^3\text{LL}}(r, \nu_s, \nu_{\text{us}}) + C_F C_A^3 \frac{1}{12\pi r^2} \alpha^3(\nu_s) \alpha(\nu_{\text{us}}) \left\{ \log \left(\frac{C_A \alpha(\nu_s)}{2r\nu_{\text{us}}} \right) + \log(2) + 1/6 \right\}. \quad (7.77)$$

7.9 Hyperasymptotics and \mathcal{F}

As we have already mentioned, by construction, F does not have a renormalon at $u = 1/2$. Nonetheless, we expect it to have a renormalon located at $u = 3/2$. As it has been stated in the introduction, the goal of this chapter is to obtain an estimate of $\alpha(M_z)$ by comparing lattice data for the singlet static energy with theoretical expressions for it, where the PV Borel sum is used to assign a sum to the formal series present in the expressions. In our case, we have two such series, that is, recalling

$$E(r) = V(r, \nu_{\text{us}} = \nu_s) + \delta V_{\text{RG}}(r, \nu_s, \nu_{\text{us}}) + \delta E_{\text{us}}(r, \nu_{\text{us}}), \quad (7.78)$$

we have seen V to be a formal series in $\alpha(\nu_s)$, and δE_{us} to be a formal series¹² in $\alpha(\nu_{\text{us}})$. We will employ the terminants of chapter 3 to approximate the PV Borel sum from truncated expressions. V and δE_{us} both have a renormalon at $u = 3/2$. It was shown in [180] that these renormalons cancel out in the total energy $E(r)$, if the series of V and of δE_{us} are evaluated at the same scale, that is $\nu_{\text{us}} = \nu_s$. This cancellation has also been shown to take place in the large β_0 approximation [79]. Therefore, we know that $Z_3^V = -Z_3^{\delta E_{\text{us}}}$, or analogously, $Z_3^F = -Z_3^{\frac{d}{dr}\delta E_{\text{us}}}$. Notice also that since F is the r derivative of V , we have that¹³ $Z_3^F = 2Z_3^V$. Consequently, if we included the $d = 3$ terminants of V and δE_{us} , they would cancel out if we picked $\nu_{\text{us}} = \nu_s$, and if we truncated both series at the same N_{P} . In any case, later in the fits, we will not in general consider $\nu_{\text{us}} = \nu_s$, and the truncation points of the series will not be equal, so the terminants will not cancel each other. Thus, adapting Eq. (3.72), we obtain the $d = 3$ terminant of F :

$$T_3^F = \sqrt{\alpha(\nu_s)} K_{\text{IR}}^{(\text{P})} r \nu_s^3 e^{-\frac{6\pi}{\beta_0 \alpha(\nu_s)}} \left(\frac{\beta_0 \alpha(\nu_s)}{4\pi} \right)^{-3b} \left(1 + \bar{K}_{\text{IR},1}^{(\text{P})} \alpha(\nu_s) + \mathcal{O}(\alpha^2(\nu_s)) \right), \quad (7.79)$$

where $\eta_c = -3b + \frac{6\pi c}{\beta_0} - 1$ and

$$K_{\text{IR}}^{(\text{P})} = -\frac{Z_3^F 2^{1-3b} \pi 3^{3b+1/2}}{\Gamma(1+3b)} \beta_0^{-1/2} \left[-\eta_c + \frac{1}{3} \right], \quad (7.80)$$

$$\bar{K}_{\text{IR},1}^{(\text{P})} = \frac{\beta_0/(3\pi)}{-\eta_c + \frac{1}{3}} \left[-3b_1 b \left(\frac{1}{2} \eta_c + \frac{1}{3} \right) - \frac{1}{12} \eta_c^3 + \frac{1}{24} \eta_c - \frac{1}{1080} \right]. \quad (7.81)$$

The above terminant is to be added on top of F truncated at the scale $\alpha^{N_{\text{P}}(d=3, \nu_s)+1}(\nu_s)$ where

$$N_{\text{P}}(d=3, \nu_s) \equiv \frac{6\pi}{\beta_0 \alpha(\nu_s)} (1 - c\alpha(\nu_s)). \quad (7.82)$$

We will in the fits typically consider $N_{\text{P}}(d=3, \nu_s) = 3$. As we have said, the terminant to add on top of $\frac{d}{dr}\delta E_{\text{us}}$ is the same as in Eq. (7.79) with the changes $Z_3^F \rightarrow Z_3^{\frac{d}{dr}\delta E_{\text{us}}} = -Z_3^F$ and $\nu_s \rightarrow \nu_{\text{us}}$. The truncation point $\alpha^{N_{\text{P}}(d=3, \nu_{\text{us}})+1}(\nu_{\text{us}})$ for $\frac{d}{dr}\delta E_{\text{us}}$ is

$$N_{\text{P}}(d=3, \nu_{\text{us}}) \equiv \frac{6\pi}{\beta_0 \alpha(\nu_{\text{us}})} (1 - c_{\text{us}}\alpha(\nu_{\text{us}})). \quad (7.83)$$

We will in the fits typically consider $N_{\text{P}}(d=3, \nu_{\text{us}}) = 0$.

¹²As shown in Eq. (7.43). Of course, after expanding ΔV and V_A in $\alpha(\nu_s)$, we will also have $\alpha(\nu_s)$ dependence.

¹³Just compare the r dependent part of the Borel transforms around $u = 3/2$ which are $Z_3^F r \nu_s^3$ and $Z_3^V r^2 \nu_s^3$.

7.10 The normalization of the $u = 3/2$ renormalon

In order to implement the formula of the $u = 3/2$ terminant of V or δE_{us} (or of those of their r derivatives), we need to know the normalization of the $u = 3/2$ renormalons of these series. We could in principle try to estimate it by comparing $V_3 - V_3^{(\text{as};d=1)}$ with its large n theoretical expression, but this approach is obfuscated by our approximate knowledge on the normalization of the $u = 1/2$ renormalon Z_1^V , whose inaccuracies would be inherited by Z_3^V if estimated in such a manner. On the other hand, the force is not contaminated by the $u = 1/2$ renormalon, and it is trivial to relate the normalization of the $u = 3/2$ renormalon of the force with that of the static potential (one only needs to realize one is the r -derivative of the other):

$$Z_3^F = 2Z_3^V. \quad (7.84)$$

Therefore, the force is an ideal object to test whether perturbation theory, as we know it at present, is already approaching the asymptotic behavior dictated by the $u = 3/2$ renormalon. From Eq. (1.69), we know this asymptotic behavior of the coefficients of the (dimensionless) force to be¹⁴

$$r^2 f_n^{(\text{as})} = Z_3^F (r\mu)^3 \left(\frac{\beta_0}{6\pi} \right)^n \frac{\Gamma(n+1+3b)}{\Gamma(1+3b)} \left\{ 1 + \frac{3b}{n+3b} w_1 + \mathcal{O}\left(\frac{1}{n^2}\right) \right\}. \quad (7.85)$$

We remark that we can fix $w_1 = 3s_1$ using the procedure of section 2.6, but that our current knowledge on V_A makes us unable to fix w_2 . For reference's sake, we also explicitly write the behavior of the Borel transform of the series of $r^2 F$ associated to this factorial behavior

$$r^2 \Delta \hat{F}(t) = Z_3^F (r\mu)^3 \frac{1}{\left(1 - \frac{\beta_0}{6\pi} t\right)^{1+3b}} \left\{ 1 + w_1 \left(t - \frac{\beta_0}{6\pi} t \right) + \dots \right\}. \quad (7.86)$$

By considering the ratio of the exact coefficients given in Eq. (7.63) and the asymptotic expression above, we can obtain an approximate determination of the normalization of the $u = 3/2$ renormalon. We display the results in Figure 7.1. This figure shows various curves where the ratio has been taken with the exact coefficient to various orders. We also show our central value determinations for the normalizations of the renormalons with the error bands. We determine these central values by considering the N³LO curve at the point x where the derivative of the curve is zero, which are $x \equiv \mu r = 1.30$, and $x = 1.52$ for $n_f = 0$ and 3 respectively. They read

$$Z_3^F \Big|_{n_f=0} = 0.51_{-0.21}^{+0.08}(\Delta x) + 0.05(\text{N}^2\text{LO}) - 0.10(\mathcal{O}(1/n)) + 0.02(\text{us}) = 0.51(24), \quad (7.87)$$

$$Z_3^F \Big|_{n_f=3} = 0.37_{-0.16}^{+0.06}(\Delta x) + 0.02(\text{N}^2\text{LO}) - 0.05(\mathcal{O}(1/n)) + 0.005(\text{us}) = 0.37(17). \quad (7.88)$$

For the error estimates, we explore different possibilities. We vary x by multiplying and dividing the central value by $\sqrt{2}$. This is the first error quoted in Eqs. (7.87) and (7.88), and we see that it is the biggest contribution to the final error. We also consider the difference between the $f_2/f_2^{(\text{as})} Z_3^F$ and $f_3/f_3^{(\text{as})} Z_3^F$ results¹⁵. This is the second error quoted in Eqs. (7.87) and (7.88). We also estimate the importance of subleading $1/n$ corrections by considering the difference of including the $1/n$ term or not in Eq. (7.85), which is the third error quoted in Eqs. (7.87) and (7.88). Finally, we also explore the importance of the ultrasoft associated terms (as they should

¹⁴We will only consider the $d = 3$ renormalon in \mathcal{F} , and therefore, to ease notation, we drop the $d = 3$ label everywhere here, that is, we will not write $f_n^{(\text{as};d=3)}$.

¹⁵Notice that in Figure 7.1, we see that $f_2/f_2^{(\text{as})} Z_3^F$ has no point where the derivative is zero in the range considered, and therefore, we use the value of x used with the N³LO coefficient.

Table 7.1: Normalization constant, Z_3^F , of the leading renormalon of the force for different number of flavours n_f in the $\overline{\text{MS}}$ scheme. We also give predictions of some asymptotic coefficients with $\mu = 1/r$.

n_f	0	1	2	3	4	5	6
Z_3^F	0.51(24)	0.47(22)	0.42(20)	0.37(17)	0.31(14)	0.23(10)	0.15(8)
$r^2 f_4^{(as)}$	8(4)	6(3)	4(2)	3(1)	1.5(7)	0.8(3)	0.3(2)
$r^2 f_5^{(as)}$	31(15)	21(10)	13(6)	8(4)	4(2)	1.8(8)	0.65(33)

not affect, or little, the determination of the normalization of the renormalon). The error associated to ultrasoft effects is estimated by using the coefficient f_3 obtained by eliminating the last term in the second line of a_3 in Eq. (7.16) before taking the r derivative in V . The variation is indeed small, as we show in the last error item in Eqs. (7.87) and (7.88).

The first and second error (and to some extent the third) are somewhat redundant, as they both measure the fact that $n = 3$ is still finite. Nevertheless, we combine them all in quadrature and make the variation symmetric around the central value. This indeed yields a conservative estimate of the error. In the left panels of Figure 7.1, we can see the dependence of Z_3^F , i.e. of $f_n/f_n^{(as)} Z_3^F$, with respect to x for different values of n . Around the scale where the central value has been chosen, they are all inside the error band, even for a coefficient as low as $f_1/f_1^{(as)} Z_3^F$. We also give determinations for other values of n_f using the same error analysis. They can be found in Table 7.1, where we also give estimates of the higher order coefficients of the perturbative series of the force with $\mu = 1/r$.

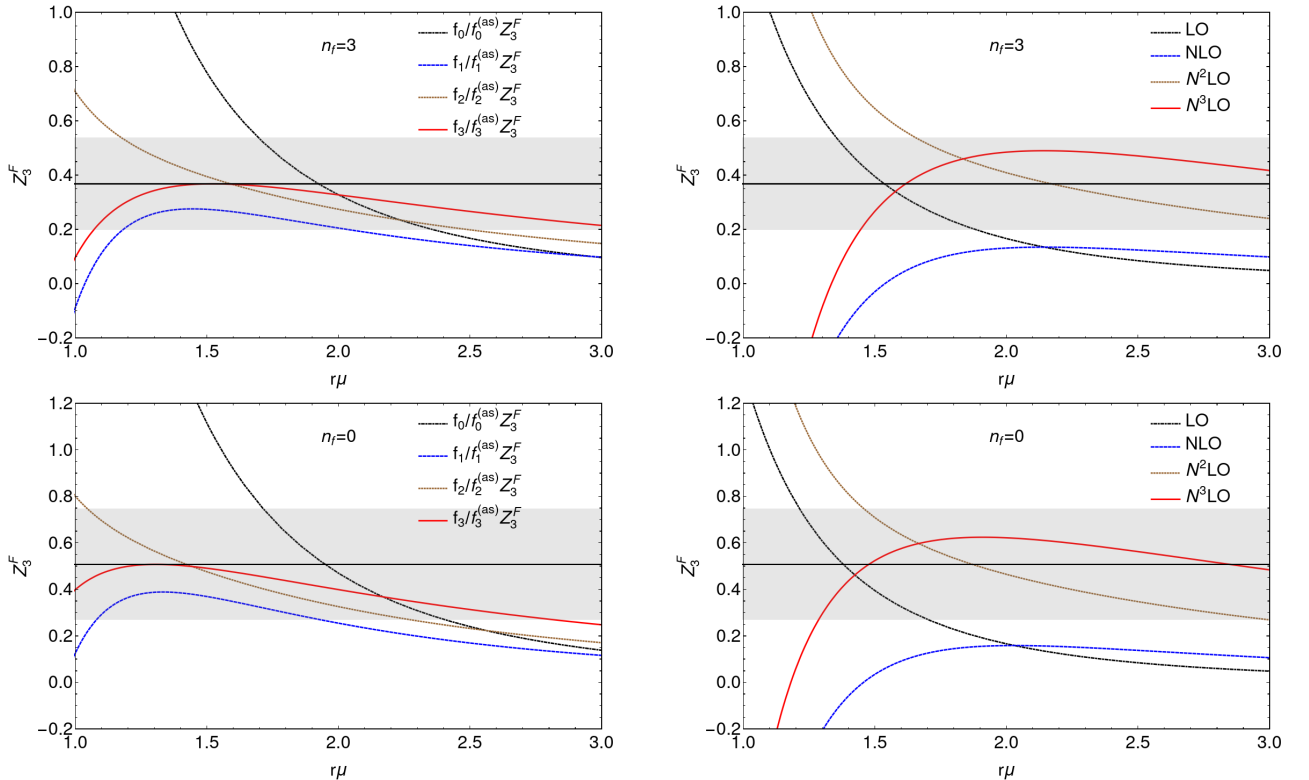


Figure 7.1: **Left figures.** Determination of Z_3^F using $f_n/f_n^{(as)} Z_3^F$ as a function of $r\mu$ and for different values of n in the $\overline{\text{MS}}$ scheme. **Right figures.** Determination of Z_3^F using Eq. (7.92). Upper figures are determinations with $n_f = 3$. Lower figures are determinations with $n_f = 0$.

Our conclusions are different from those in Ref. [183], where it was concluded that it was not possible to

determine the normalization of the $u = 3/2$ renormalon. The authors consider the function

$$\left(1 - \frac{\beta_0}{6\pi}t\right)^{1+3b} r^2 \hat{F}(t), \quad (7.89)$$

which when it is evaluated at $t = \frac{6\pi}{\beta_0}$ clearly yields

$$\left(1 - \frac{\beta_0}{6\pi}t\right)^{1+3b} r^2 \hat{F}(t) \Big|_{t=\frac{6\pi}{\beta_0}} = Z_3^F (r\mu)^3. \quad (7.90)$$

We remark that the expansion around $t = 0$ of Eq. (7.89) has a radius of convergence bigger than $t = \frac{6\pi}{\beta_0}$. Let us write the following Taylor expansion

$$\left(1 - \frac{\beta_0}{6\pi}t\right)^{1+3b} r^2 \hat{F}(t) \equiv \sum_{n=0}^{\infty} v_n t^n. \quad (7.91)$$

Then, by equating the above two equations, we can obtain the normalization of the renormalon as the sum of the following series

$$Z_3^F = \frac{1}{x^3} \sum_{n=0}^{\infty} v_n \left(\frac{6\pi}{\beta_0}\right)^n. \quad (7.92)$$

This method was proposed in [130, 184], and first quantitatively applied to the leading renormalon of the pole mass and the static potential in [122]. The results of the evaluation of Z_3^F using the above series up until N³LO in $\frac{6\pi}{\beta_0}$ is displayed in Figure 7.1, both for $n_f = 0$ and $n_f = 3$. We observe that the convergence is worse than for the determination of Z_3^F using $f_n/f_n^{(\text{as})} Z_3^F$. This was also observed very clearly in [100] for the energy of a static source. In that case, and this case here, we observe convergence but at a slower pace. Actually, the N²LO and N³LO predictions are well inside the error band of our predictions in Eqs. (7.87) and (7.88), although the curves display a bigger dependence on x , and the variation between different orders is bigger than with the previous method. For the method using Eq. (7.92), stability is found for $x \sim 2$. For this method, working with $x = 1$ does not yield a convergent series, which is what was done in [183], which may explain the conclusions reached in that reference.

7.11 The lattice data

For the fits, we will use $n_f = 2 + 1$ lattice data of [158] (supplemented with information given in [155]), which has made an updated error analysis of the data of [154]. Of these data points, we only consider those obtained with $\beta = 8.4$, as they correspond to the shortest distances available $a = 0.025 \text{ fm} = 0.125 \text{ GeV}^{-1}$. The lattice spacing a has been fixed by the scale r_1 which is defined by

$$r^2 \frac{dE(r)}{dr} \Big|_{r=r_1} = 1, \quad (7.93)$$

with $r_1 = 0.3106(17) \text{ fm}$. In this ensemble, the up and down quarks get the masses $m_l = m_s/5$ where m_s , the strange quark mass, has been tuned to its physical value, and the pion mass gets the value 320 MeV in the continuum. This is only statistically significant¹⁶ for $r > 0.4r_1 \sim 0.625 \text{ GeV}^{-1}$ (see [157]). The uncertainty associated with fixing the physical units of the parameter r_1 was seen in [158] to be comparatively small compared with other uncertainties. Therefore, we will neglect it in the following. It was also observed in this reference that the effect of the correlation of the points to the final error was small. Thus, we also neglect this source of error.

¹⁶We thank J.H. Weber for informing us of this.

The discretization errors depend on the size of the parameter r/a . They have been studied in detail in [158], where it was concluded that, for $r/a \leq \sqrt{8}$, tree-level improvement was enough to bring the discretization errors down to the point where they were smaller than the statistical errors and could, in comparison, be neglected. Therefore, we will use tree-level improved data and disregard the lattice data at shortest distances (for $r/a \leq \sqrt{8}$), as well as the special geometry $r/a = \sqrt{12}$. This corresponds to one of the methods followed in [158] to account for discretization effects. This means that the shortest distance we consider is $r_{\min} = 2.827 a$, which in GeV units reads $r_{\min} = 0.353 \text{ GeV}^{-1}$.

To test the sensitivity of the fit to the data, we will consider different ranges of data (similarly to what was done in [153]). We consider the following ranges: Set I: $0.353 \text{ GeV}^{-1} \leq r \leq 0.499 \text{ GeV}^{-1}$, Set II: $0.353 \text{ GeV}^{-1} \leq r \leq 0.612 \text{ GeV}^{-1}$, Set III: $0.353 \text{ GeV}^{-1} \leq r \leq 0.8002 \text{ GeV}^{-1}$ and Set IV: $0.353 \text{ GeV}^{-1} \leq r \leq 1 \text{ GeV}^{-1}$. The number of data points of each set is 8, 17, 31 and 50, respectively.

7.12 The expressions that go on the fits

For the central values of the soft and ultrasoft scales, we take the standard expressions $(\nu_s, \nu_{\text{us}}) = (1/r, C_A \alpha(\nu_s)/(2r))$. Our central value determination of the strong coupling will be done with expressions where logarithms of ratios of the soft and ultrasoft have been resummed, although we will also explore fixed order expressions in section 7.15. We will consider different orders for $\mathcal{F}(r')$ in Eq. (7.58) (we also include fixed order expressions that we will later use)

- LL/LO

$$\mathcal{F}_{\text{LO}}(r) = F(r, \nu_{\text{us}} = \nu_s) \Big|_{\text{LO in } \alpha(\nu_s)}, \quad (7.94)$$

- NLL/NLO

$$\mathcal{F}_{\text{NLO}}(r) = F(r, \nu_{\text{us}} = \nu_s) \Big|_{\text{NLO in } \alpha(\nu_s)}, \quad (7.95)$$

- N²LO

$$\mathcal{F}_{\text{N}^2\text{LO}}(r) = F(r, \nu_{\text{us}} = \nu_s) \Big|_{\text{N}^2\text{LO in } \alpha(\nu_s)}, \quad (7.96)$$

- N²LL

$$\mathcal{F}_{\text{N}^2\text{LL}}(r) = F(r, \nu_{\text{us}} = \nu_s) \Big|_{\text{N}^2\text{LO in } \alpha(\nu_s)} + \frac{d}{dr} \delta V_{\text{RG}}(r, \nu_s, \nu_{\text{us}}) \Big|_{\text{N}^2\text{LL}}, \quad (7.97)$$

- N³LO

$$\mathcal{F}_{\text{N}^3\text{LO}}(r) = F(r, \nu_{\text{us}} = \nu_s) \Big|_{\text{N}^3\text{LO in } \alpha(\nu_s)} + \frac{d}{dr} \delta E_{\text{us}}(r, \nu_{\text{us}} = \nu_s) \Big|_{\text{N}^3\text{LO in } \alpha(\nu_s)}, \quad (7.98)$$

- N³LL

$$\mathcal{F}_{\text{N}^3\text{LL}}(r) = F(r, \nu_{\text{us}} = \nu_s) \Big|_{\text{N}^3\text{LO in } \alpha(\nu_s)} + \frac{d}{dr} \delta V_{\text{RG}}(r, \nu_s, \nu_{\text{us}}) \Big|_{\text{N}^3\text{LL}} + \frac{d}{dr} \delta E_{\text{us}}(r, \nu_{\text{us}}) \Big|_{\text{LO in } \alpha(\nu_{\text{us}})}, \quad (7.99)$$

- N³LO_{hyp}

$$\begin{aligned} \mathcal{F}_{\text{N}^3\text{LO}_{\text{hyp}}}(r) = & F(r, \nu_{\text{us}} = \nu_s) \Big|_{\text{N}^3\text{LO in } \alpha(\nu_s)} + T_3(Z_3^F, N_{\text{P}} = 3, \nu_s) \\ & + \frac{d}{dr} \delta E_{\text{us}}(r, \nu_{\text{us}} = \nu_s) \Big|_{\text{N}^3\text{LO in } \alpha(\nu_s)} + T_3(-Z_3^F, N_{\text{P}} = 0, \nu_{\text{us}} = \nu_s), \end{aligned} \quad (7.100)$$

- N^3LL_{hyp}

$$\begin{aligned} \mathcal{F}_{N^3LL_{\text{hyp}}}(r) = & F(r, \nu_{\text{us}} = \nu_s) \Big|_{N^3LO \text{ in } \alpha(\nu_s)} + T_3(Z_3^F, N_P = 3, \nu_s) + \frac{d}{dr} \delta V_{\text{RG}}(r, \nu_s, \nu_{\text{us}}) \Big|_{N^3LL} \\ & + \frac{d}{dr} \delta E_{\text{us}}(r, \nu_{\text{us}}) \Big|_{LO \text{ in } \alpha(\nu_{\text{us}})} + T_3(-Z_3^F, N_P = 0, \nu_{\text{us}}). \end{aligned} \quad (7.101)$$

Notice that in the last item above, which we name N^3LL_{hyp} , we have introduced the $d = 3$ terminants of the series of F and $\frac{d}{dr} \delta E_{\text{us}}$. We have already mentioned that the renormalons of these two series cancel out if both quantities are expanded in powers of α evaluated at the same scale, and if both perturbative expansions are truncated at the same order. It can be seen in Eq. (7.101) that this is something that we do not do. The natural energy scales in F and $\frac{d}{dr} \delta E_{\text{us}}$ are different, and thus, we evaluate F as a series in $\alpha(\nu_s)$ to order $\alpha(\nu_s)^4$, and $\frac{d}{dr} \delta E_{\text{us}}$ is evaluated as a series in $\alpha(\nu_{\text{us}})$ to just the LO. The terminants are chosen accordingly. We finish by mentioning that we have also performed fits changing the order at which we start including the terminant in the static potential from three to two. We indeed find the variation to be small.

7.13 Central value results

We now state the results of the fits at N^3LL_{hyp} and N^3LL orders with $\nu_s = 1/r$, $\nu_{\text{us}} = \frac{C_A \alpha(\nu_s)}{2r}$ and $r_{\text{ref}} = 0.353 \text{ GeV}^{-1}$ for the various ranges considered. For N^3LL_{hyp} :

- Set I: $\Lambda_{\overline{\text{MS}}}^{(n_f=3)} = 338(2) \text{ MeV}$ with $\chi_{\text{red}}^2 = 0.50$.
- Set II: $\Lambda_{\overline{\text{MS}}}^{(n_f=3)} = 341(1) \text{ MeV}$ with $\chi_{\text{red}}^2 = 0.53$.
- Set III: $\Lambda_{\overline{\text{MS}}}^{(n_f=3)} = 343(1) \text{ MeV}$ with $\chi_{\text{red}}^2 = 0.62$.
- Set IV: $\Lambda_{\overline{\text{MS}}}^{(n_f=3)} = 343(0) \text{ MeV}$ with $\chi_{\text{red}}^2 = 0.67$.

The error shown is the statistical error of the fit. For N^3LL :

- Set I: $\Lambda_{\overline{\text{MS}}}^{(n_f=3)} = 337(2) \text{ MeV}$ with $\chi_{\text{red}}^2 = 0.50$.
- Set II: $\Lambda_{\overline{\text{MS}}}^{(n_f=3)} = 340(1) \text{ MeV}$ with $\chi_{\text{red}}^2 = 0.53$.
- Set III: $\Lambda_{\overline{\text{MS}}}^{(n_f=3)} = 342(1) \text{ MeV}$ with $\chi_{\text{red}}^2 = 0.57$.
- Set IV: $\Lambda_{\overline{\text{MS}}}^{(n_f=3)} = 340(0) \text{ MeV}$ with $\chi_{\text{red}}^2 = 1.22$.

We display these numbers and those of LL, NLL ¹⁷ and N^2LL orders in Figure 7.2. As one would expect, as we increase the number of points in the ranges, the statistical errors get smaller. We observe the dependence of $\Lambda_{\overline{\text{MS}}}$ on the range of the data set to be very small. This small dependence holds irrespective of the order in the approximation for the theoretical expression used. We only see very small differences at N^3LL and N^3LL_{hyp} order between the value obtained from the data Set I and the rest (within one sigma for the statistical error, which is the only one we display in Fig. 7.2), and basically vanishing between the data sets II, III and IV.

To display the reliability of the fits, we also show the reduced χ^2 obtained with each fit in the lower panel of Figure 7.2. For the data sets I and II, the fit yields $\chi_{\text{red}}^2 \sim 0.5$ to all orders in the hyperasymptotic expansion.

¹⁷Of course, LL=LO and $NLL=NLO$.

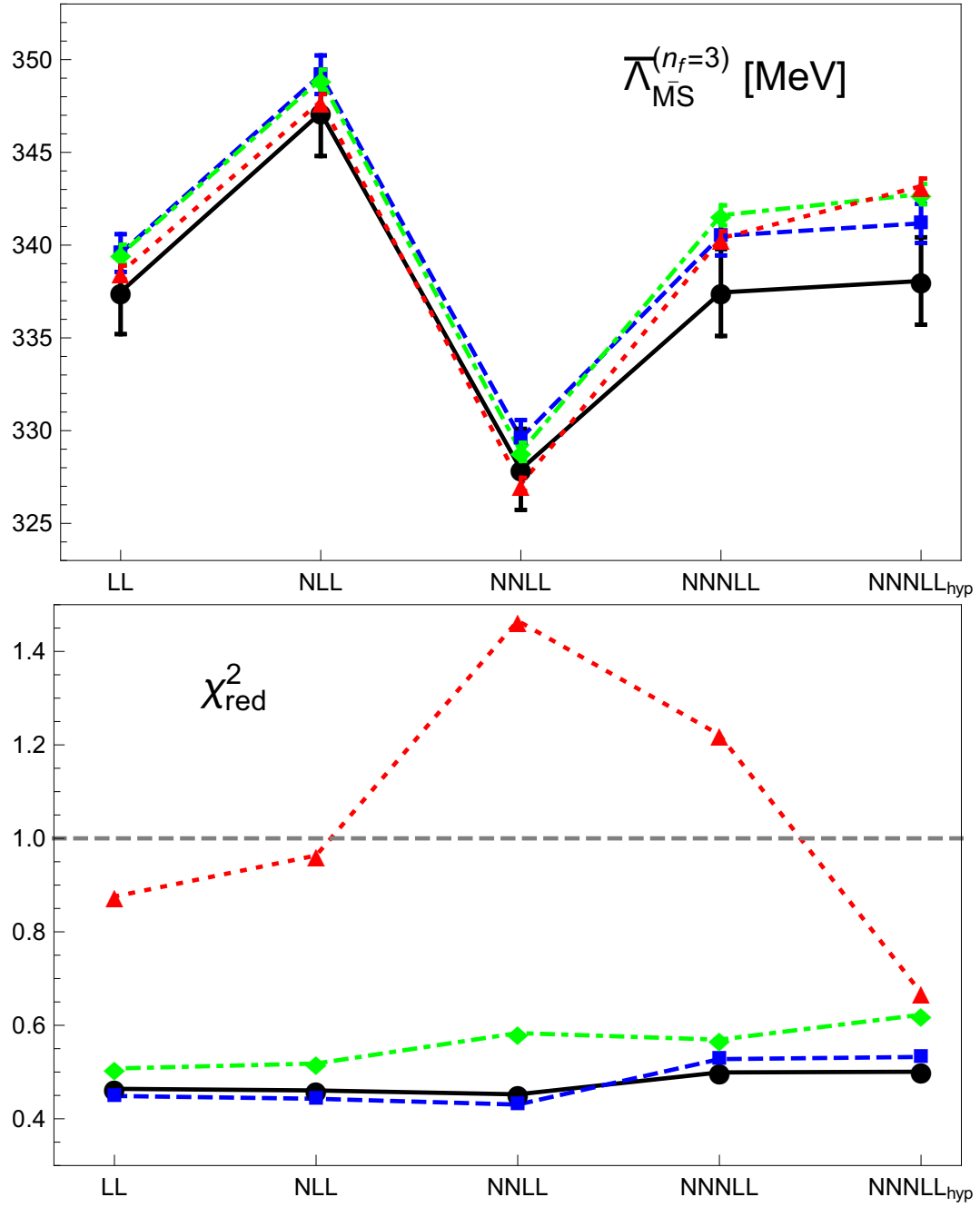


Figure 7.2: **Upper panel** Determination of $\Lambda_{\overline{\text{MS}}}^{(n_f=3)}$ at LL, NLL, N²LL, N³LL and N³LL_{hyp} using the data sets: Set I (continuous black line), Set II (dashed blue line), Set III (dash-dotted green line), and Set IV (dotted red line). The error displayed is only the statistical error of the fits. **Lower panel** χ_{red}^2 for the fit of $\Lambda_{\overline{\text{MS}}}^{(n_f=3)}$ at LL, NLL, N²LL, N³LL and N³LL_{hyp} using the data sets (continuous black line), Set II (dashed blue line), Set III (dash-dotted green line), and Set IV (dotted red line).

Therefore, there is no significant dependence on the number of data points. For the data Set III, there is a mild increase: $\chi_{\text{red}}^2 \sim 0.5 - 0.6$, but still well below 1. It is when we consider data Set IV, which includes points up to $r = 1 \text{ GeV}^{-1}$, that we see a significant increase in the χ_{red}^2 . The magnitude of this increase, however, depends on the order, and even in the worst case is not much bigger than 1. The LL and NLL fits yield χ_{red}^2 slightly below 1, with a slight increase when going from LL to NLL. The χ_{red}^2 reaches the maximum, 1.46, at N²LL. Order N³LL shows a decrease of the reduced χ^2 , albeit still above 1, and at order N³LL_{hyp} the χ_{red}^2 significantly drops getting close to the $\chi_{\text{red}}^2 \sim 0.6$ value we have for other data sets.

Set IV is the more sensitive to the IR, as it goes up to $r \sim 1 \text{ GeV}^{-1}$. This may reflect in a larger sensitivity to ultrasoft associated physics, which will then need to be described more accurately. This matches with what we see for the χ_{red}^2 with set IV: LL, NLL, N²LL and N³LL show a bigger χ_{red}^2 (we emphasize, nevertheless, that they are still of order 1), which then goes down to a value similar to the one obtained with the other data sets after the inclusion of the terminants. It is non-trivial that the larger sensitivity to the IR we expect for data Set IV to be well described by our weak-coupling analysis. Indeed, it is surprising that the ultrasoft effects do not blow up in any of the fits since $\alpha(\nu_{\text{us}})$ is evaluated at a rather low scale. For illustration, we show the values $\alpha(\nu_{\text{us}})$ takes for the various ranges considered¹⁸: for Set I $\alpha(\nu_{\text{us}}) \in (0.46, 0.57)$, for Set II $\alpha(\nu_{\text{us}}) \in (0.46, 0.65)$, for Set III $\alpha(\nu_{\text{us}}) \in (0.46, 0.75)$, and for Set IV $\alpha(\nu_{\text{us}}) \in (0.46, 0.78)$. For this last data set, the very last points, those with larger r -s, reach a regime where ν_{us} grows as r increases, that is, as ν_s decreases ν_{us} starts to increase. Therefore, their inclusion in the fits should be taken with caution.

Overall, by only looking at the χ_{red}^2 , we do not have a clear signal of which data set to use and, indeed, the fits yield similar numbers and χ_{red}^2 at N³LL_{hyp}. Therefore, we will use set I as it is less sensitive, in principle, to long distances, although, as we said, the χ_{red}^2 of the fits does not give a clear signal of a deterioration of the quality of the fit (something that one would expect if our perturbative approximations were not a good approximation to the data).

Another motivation to use the data Set I is that the $\beta = 8.4$ ensemble suffers from frozen topological charge in the MC evolution. It has been shown (see [157]) that the effects of frozen topology in different sectors are statistically irrelevant for $r < 0.4r_1 \sim 0.62 \text{ GeV}^{-1}$. Therefore, by using the data Set I this problem is completely avoided. On top of that, as mentioned above, the effects due to finite light-quark masses are not statistically significant for this energy range.

In order to see the quality of our fit, we also compare our theoretical expression using the values of $\Lambda_{\overline{\text{MS}}}^{(n_f=3)}$ obtained from the fit with the lattice data. It is customary to compare directly with the potential (this can be done after fixing a normalization constant K that we fix below). The comparison is very good in the whole range we compare (up to 1 GeV), as we can see in the upper panel of Fig. 7.3. Nevertheless, such comparisons do not allow us to see the fine details due to the dependence in powers of r of the potential. For such comparison, it is better to define

$$\alpha_V(r) \equiv -\frac{r}{C_F} \left(\int_{r_{\text{ref}}}^r dr' \mathcal{F}^{\text{RG}}(r') + K \right), \quad (7.102)$$

and we adjust K , such that most of the r dependence vanishes. We show the comparison in the lower panel of Fig. 7.3. It is remarkable that pure perturbation theory predicts very well the data down to 1 GeV. The error band

¹⁸To produce these numbers, we take $\Lambda_{\overline{\text{MS}}}^{(n_f=3)} = 330 \text{ MeV}$.

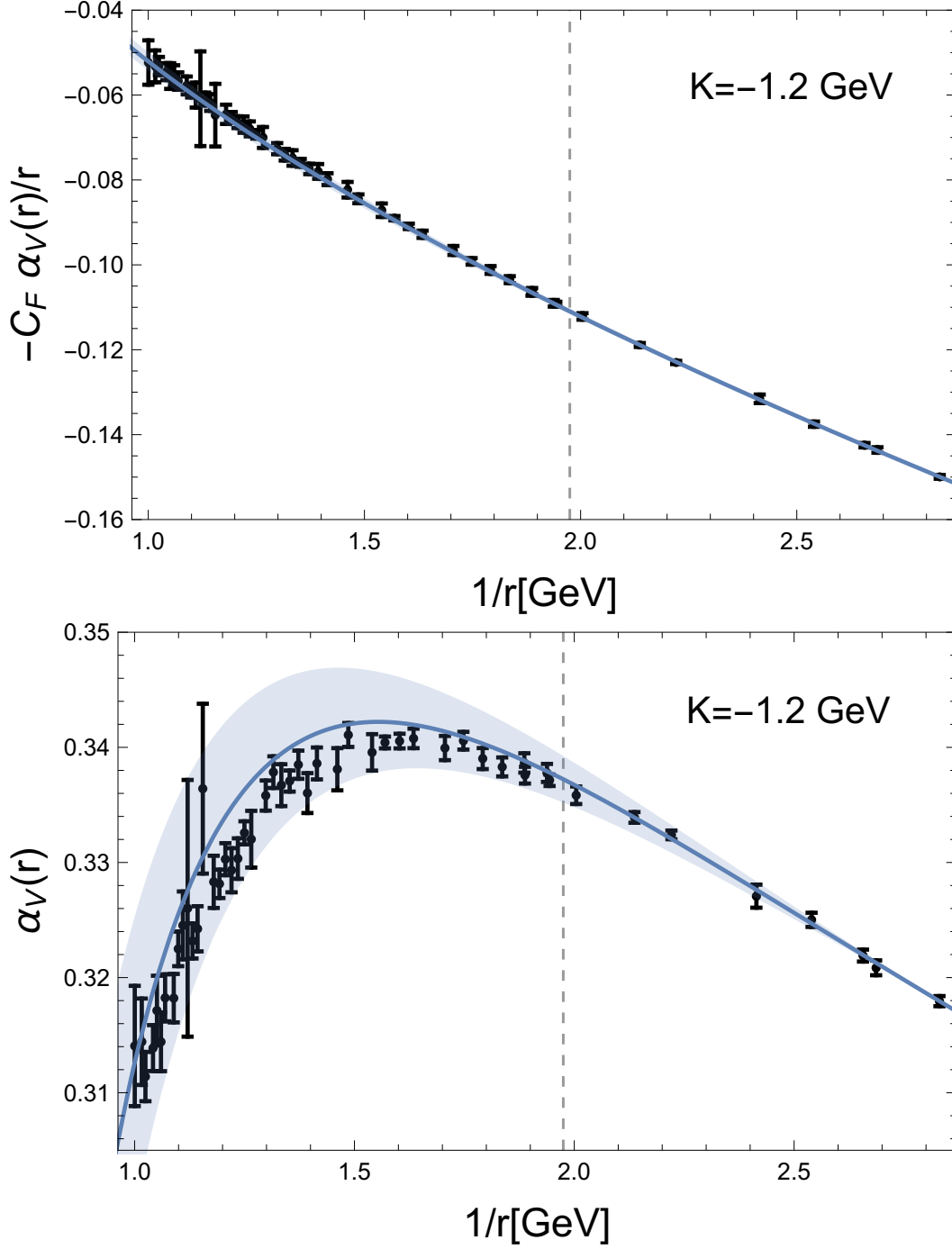


Figure 7.3: **Upper panel:** $-C_F \frac{\alpha_V(r)}{r} \equiv \int_{r_{\text{ref}}}^r dr' \mathcal{F}^{\text{RG}}(r') + K$ at $\text{N}^3\text{LL}_{\text{hyp}}$ with $\Lambda_{\overline{\text{MS}}}^{(n_f=3)} = 338(12)$ MeV and $K = -1.2$ GeV (solid blue line and blue band) versus the lattice points $E^{\text{latt}}(r) - E^{\text{latt}}(r_{\text{ref}}) + K$. Only points to the right of the vertical dashed line are included in the fit. **Lower panel:** $\alpha_V(r)$ at $\text{N}^3\text{LL}_{\text{hyp}}$ with $\Lambda_{\overline{\text{MS}}}^{(n_f=3)} = 338(12)$ MeV and $K = -1.2$ GeV (solid blue line and blue band) versus the lattice points $-\frac{r}{C_F} (E^{\text{latt}}(r) - E^{\text{latt}}(r_{\text{ref}}) + K)$. Only points to the right of the vertical dashed line are included in the fit.

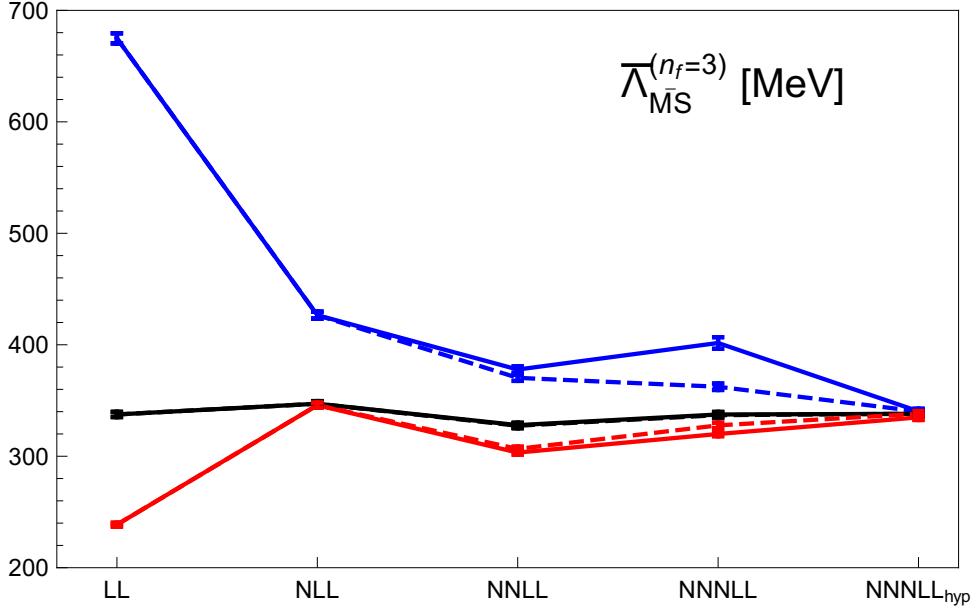


Figure 7.4: Determination of $\Lambda_{\overline{\text{MS}}}^{(n_f=3)}$ at LL, NLL, N²LL, N³LL and N³LL_{hyp} using data Set I with $\nu_{\text{us}} = C_A\alpha(\nu_s)/(2r)$ and $\nu_s = 2/r$ (continuous blue line), $\nu_s = 1/r$ (continuous black line) and $\nu_s = 1/(\sqrt{2}r)$ (continuous red line). We also plot the determination of $\Lambda_{\overline{\text{MS}}}^{(n_f=3)}$ at LL, NLL, N²LL, N³LL and N³LL_{hyp} using data Set I with $\nu_{\text{us}} = 1$ GeV and $\nu_s = 2/r$ (dashed blue line), $\nu_s = 1/r$ (dashed black line) and $\nu_s = 1/(\sqrt{2}r)$ (dashed red line). With the resolution set by the figure, the continuous and dashed black lines are hardly distinguishable. This also happens to a large extent with the continuous and dashed red lines. The error displayed is only the statistical error of the fits.

perfectly encodes all the data. This means, in particular, that with the precision of our computation, we do not see any trace of nonperturbative effects down to scales $1/r \sim 1$ GeV.

7.13.1 Dependence on ν_s

We now test the sensitivity of the fits on ν_s . We will mainly work with data Set I with which we can do variations of the parameters without entering in a regime where perturbation theory breaks down. We consider variations of ν_s with $\nu_s = x_s/r$ within the range $x_s \in [1/\sqrt{2}, 2]$. The lower limit of ν_s is chosen so as to avoid reaching scales too low for our weak coupling analysis to break down. Had we chosen $x_s = 1/2$ as lower bound, for data Set I, we would have obtained¹⁹ for the largest distances values of $\alpha(\nu_s) \sim 0.5$. If we stick to $x_s = 1/2^{1/2}$, we stay around $\alpha(\nu_s) \sim 0.3$ which is safer. It is important to keep in mind that for our central value of the ultrasoft scale $\nu_{\text{us}} = C_A\alpha(\nu_s)/(2r)$, variations on ν_s imply variations on ν_{us} . Due to this, and since for data Set I the central value of ν_{us} yields values of the ultrasoft scale around $\nu_{\text{us}} = 1$ GeV, we will also consider variations of ν_s fixing $\nu_{\text{us}} = 1$ GeV.

We display the results of the fits for data Set I in Figure 7.4. For $\nu_s = 1/r$ both fits, with $\nu_{\text{us}} = C_A\alpha(\nu_s)/(2r)$ and with $\nu_{\text{us}} = 1$ GeV, yield very similar results. Indeed, in the figure, the fits with $(\nu_s, \nu_{\text{us}}) = (1/r, C_A\alpha(\nu_s)/(2r))$ (continuous black line) and with $(\nu_s, \nu_{\text{us}}) = (1/r, 1 \text{ GeV})$ (dashed black line) are hardly distinguishable with the resolution set by the figure. The fits with $\nu_s = 2/r$ exhibit a different behavior compared to the $\nu_s = 1/r$ fits. On the one hand, working with $\nu_s = 1/r$ gives a result that changes very little as we add more terms in the expansion. On the other hand, when working with $\nu_s = 2/r$, the LL result is quite off the expected result, but then, adding

¹⁹We use $\Lambda_{\overline{\text{MS}}}^{(n_f=3)} = 330$ MeV to get this number.

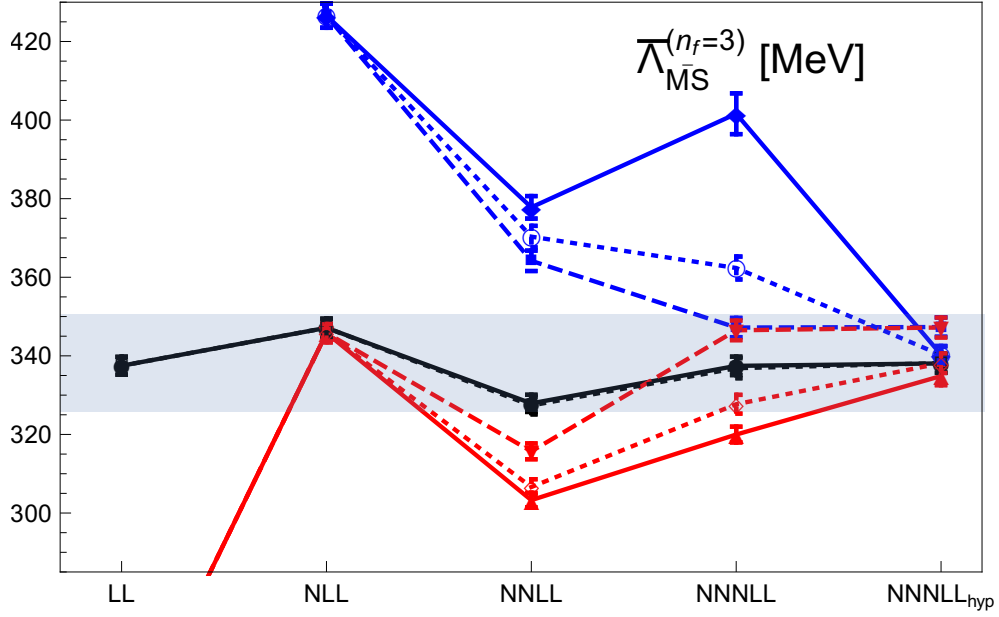


Figure 7.5: Determination of $\Lambda_{\overline{\text{MS}}}^{(n_f=3)}$ at LL, NLL, N²LL, N³LL and N³LL_{hyp} using data Set I with different options for the (soft, ultrasoft) scale: **A**) with $(\nu_s, \nu_{\text{us}}) = (1/r, C_A \alpha(\nu_s)/(2r))$ (continuous black line with filled black points), with $(\nu_s, \nu_{\text{us}}) = (2/r, C_A \alpha(\nu_s)/(2r))$ (continuous blue line with filled blue diamonds), and with $(\nu_s, \nu_{\text{us}}) = (1/(\sqrt{2}r), C_A \alpha(\nu_s)/(2r))$ (continuous red line with filled red triangles); **B**) with $(\nu_s, \nu_{\text{us}}) = (2/r, 2C_A \alpha(\nu_s)/(2r))$ (dashed blue line with filled blue squares), and with $(\nu_s, \nu_{\text{us}}) = (1/(\sqrt{2}r), C_A \alpha(\nu_s)/(2\sqrt{2}r))$ (dashed red line with filled red inverted triangles); and **C**) with $(\nu_s, \nu_{\text{us}}) = (1/r, 1 \text{ GeV})$ (dotted black line with empty black points), with $(\nu_s, \nu_{\text{us}}) = (2/r, 1 \text{ GeV})$ (dotted blue line with empty blue points), and with $(\nu_s, \nu_{\text{us}}) = (1/(\sqrt{2}r), 1 \text{ GeV})$ (dotted red line with empty red diamonds). The error displayed is only the statistical error of the fits. We also show the error band generated by our prediction Eq. (7.105). Note that the resolution in this figure has been increased with respect to the one in Figure 7.4.

higher order terms makes the prediction converge to the same result as with $\nu_s = 1/r$. The convergence is perfect within statistical errors, and also irrespective of which of the two values of the ultrasoft scale $\nu_{\text{us}} = C_A\alpha(\nu_s)/(2r)$ or $\nu_{\text{us}} = 1 \text{ GeV}$ we decide to pick. Nonetheless, as opposed to what we had for $\nu_s = 1/r$, these two cases (the two blue lines in Figure 7.4) do not agree until we reach $\text{N}^3\text{LL}_{\text{hyp}}$, with the N^3LL order values differing quite significantly from each other. Nevertheless, this difference is nicely eliminated after the inclusion of the terminants associated to the $u = 3/2$ renormalons. Furthermore, the inclusion of these terminants is fundamental to get agreement between these fits and the fits with $\nu_s = 1/r$.

A similar discussion holds for the case with $\nu_s = 1/(\sqrt{2}r)$, even though the overall behavior is better. The LL result is closer to the value obtained with $\nu_s = 1/r$, and the difference between the determinations with $(\nu_s, \nu_{\text{us}}) = (1/(\sqrt{2}r), C_A\alpha(\nu_s)/(2r))$ or with $(\nu_s, \nu_{\text{us}}) = (1/(\sqrt{2}r), 1 \text{ GeV})$ at N^3LL is small.

In the whole parameter range we have studied, the χ_{red}^2 is reasonable. Therefore, all fits are equally good in this respect. The only exception is the N^3LL prediction for $(\nu_s, \nu_{\text{us}}) = (2/r, C_A\alpha(\nu_s)/(2r))$, which has a $\chi_{\text{red}}^2 \simeq 1.9$. We find then significant that, as seen in Figure 7.4, this point moves away from the convergent pattern that is observed in the other fits. It is also then significant that the inclusion of the terminants brings agreement with the other fits, and lowers the χ_{red}^2 down to $\chi_{\text{red}}^2 = 0.42$, much below 1.

We state now the data plotted in Figure 7.4 for the $\text{N}^3\text{LL}_{\text{hyp}}$ case, and draw our error estimate:

- For $(\nu_s, \nu_{\text{us}}) = (1/2^{1/2}r, 1 \text{ GeV})$, we get $\Lambda_{\overline{\text{MS}}}^{(n_f=3)} = 338(2) \text{ MeV}$ with $\chi_{\text{red}}^2 = 0.47$.
- For $(\nu_s, \nu_{\text{us}}) = (1/2^{1/2}r, C_A\alpha(\nu_s)/2r)$, we get $\Lambda_{\overline{\text{MS}}}^{(n_f=3)} = 335(2) \text{ MeV}$ with $\chi_{\text{red}}^2 = 0.50$.
- For $(\nu_s, \nu_{\text{us}}) = (2/r, 1 \text{ GeV})$, we get $\Lambda_{\overline{\text{MS}}}^{(n_f=3)} = 340(2) \text{ MeV}$ with $\chi_{\text{red}}^2 = 0.47$.
- For $(\nu_s, \nu_{\text{us}}) = (2/r, C_A\alpha(\nu_s)/2r)$, we get $\Lambda_{\overline{\text{MS}}}^{(n_f=3)} = 340(2) \text{ MeV}$ with $\chi_{\text{red}}^2 = 0.42$.

The quoted errors are the statistical errors of the fits. Comparing with the central value result (which we remind is $\Lambda_{\overline{\text{MS}}}^{(n_f=3)} = 338 \text{ MeV}$), we conclude that in the range $\nu_s \in [1/(\sqrt{2}r), 2/r]$ the result is stable at the 2 MeV level if we fix $\nu_{\text{us}} = 1 \text{ GeV}$, and at around the 3 MeV level if we instead set $\nu_{\text{us}} = C_A\alpha(\nu_s)/(2r)$. Thus, we conclude that with the present level of precision reached by theoretical expression, the dependence on ν_s of the fit to be of order $\sim 2 \text{ MeV}$, which can be neglected compared with other uncertainties.

7.13.2 Dependence on ν_{us}

We now test the sensitivity of the fits on ν_{us} . Just as in the previous section, we only explore data Set I. In order to keep the hierarchy of scales between the soft and the ultrasoft scale, we have varied them in a correlated way as a function of a single parameter x

$$(\nu_s, \nu_{\text{us}}) = \left(x \frac{1}{r}, x \frac{C_A\alpha(x/r)}{2r} \right). \quad (7.103)$$

The range we take for x is $x \in [1/\sqrt{2}, 2]$, similarly to what we did in the previous section. We note that if we take $x = 1/2$, the $\text{N}^3\text{LL}_{\text{hyp}}$ fit is quite bad with a $\chi_{\text{red}}^2 = 3.97$ and $\Lambda_{\overline{\text{MS}}}^{(n_f=3)} \simeq 411(7) \text{ MeV}$, with the situation improving noticeably by taking $x = 1/\sqrt{2}$ with $\Lambda_{\overline{\text{MS}}}^{(n_f=3)} = 347(3) \text{ MeV}$ with $\chi_{\text{red}}^2 = 0.56$. The other edge of the range we have considered, that is, $x = 2$ yields $\Lambda_{\overline{\text{MS}}}^{(n_f=3)} = 347(2) \text{ MeV}$ with $\chi_{\text{red}}^2 = 0.53$. Notice that the difference between the $x = 1$ and the $x = 1/\sqrt{2}$ results, and the $x = 1$ and the $x = 2$ results is 9 MeV. Therefore, the fit with $x = 1$ can be considered to be close to a minimum in the family of fits with the correlation of Eq. (7.103).

The results of the fits are displayed in Fig. 7.5. In this figure, we also plot the lines featured in Fig. 7.4. The new fits are the family of fits named **B** (the dashed lines) in the caption of 7.5, whereas the fits presented in the previous section are **A** (the continuous lines) and **C** (the dotted lines).

It is noteworthy that the new family of fits **B** already find good agreement at the N³LL level. Both the $x = 2$ and $x = 1/2^{1/2}$ yield $\Lambda_{\overline{\text{MS}}}^{(n_f=3)} = 347$ MeV, whilst the $x = 1$ fit yields $\Lambda_{\overline{\text{MS}}}^{(n_f=3)} = 337$ MeV, that is, the difference is merely 10 MeV. Notice that as Fig. 7.5 clearly shows, this is not so when we consider the fits **A** that feature $\nu_{\text{us}} = C_A \alpha(x/r)/(2r)$, or the fits **B** with $\nu_{\text{us}} = 1$ GeV, where there are big differences at the N³LL level.

Nonetheless, when we add the terminants and go to N³LL_{hyp} level, all lines in Fig. 7.5 find good agreement. This reflects that terminants play a crucial role to diminish the dependence in ν_{us} , and to get convergence to the same value, irrespective of how we correlate the soft scale with the ultrasoft scale. These are the results of the fits at the N³LL_{hyp} level that we use to draw our error estimates

- For $(\nu_s, \nu_{\text{us}}) = \left(\frac{1}{2^{1/2}r}, \frac{1}{2^{1/2}} \frac{C_A \alpha(\nu_s)}{2r}\right)$, we get $\Lambda_{\overline{\text{MS}}}^{(n_f=3)} = 347$ MeV with $\chi_{\text{red}}^2 = 0.56$.
- For $(\nu_s, \nu_{\text{us}}) = \left(\frac{2}{r}, 2 \frac{C_A \alpha(\nu_s)}{2r}\right)$, we get $\Lambda_{\overline{\text{MS}}}^{(n_f=3)} = 347$ MeV with $\chi_{\text{red}}^2 = 0.53$.

Comparing with the central value $\Lambda_{\overline{\text{MS}}}^{(n_f=3)} = 338$ MeV, we obtain a difference of 9 MeV (with the same sign) with both values above. In this respect, the fit with $x = 1$ can be considered a (close to the) minimum within the families of fits with $(\nu_s, \nu_{\text{us}}) = \left(x \frac{1}{r}, x \frac{C_A \alpha(x/r)}{2r}\right)$.

7.13.3 Dependence on Z_3^F

We have also studied the dependence of our central value on Z_3^F . We find it to be very small compared with other uncertainties, since the contribution associated to Ω_3^F is small for our central value determinations. The variation does not change the last digit. Therefore, we will omit it for the final error budget. It is worth mentioning, though, that for other values of ν_s and ν_{us} , the terminant is a crucial element to get agreement with our central value. For completeness, we state the result of the fits considering the errors in Z_3^F

- For $Z_3^F = 0.37 + 0.17$, we get $\Lambda_{\overline{\text{MS}}}^{(n_f=3)} = 338(2)$ MeV with $\chi_{\text{red}}^2 = 0.50$.
- For $Z_3^F = 0.37 - 0.17$, we get $\Lambda_{\overline{\text{MS}}}^{(n_f=3)} = 338(2)$ MeV with $\chi_{\text{red}}^2 = 0.50$.

7.13.4 Other estimates of higher order contributions

For the error analysis, we need to determine the error associated to our lack of knowledge of the complete perturbative series of the static energy. We have several ways to estimate this error. We have studied the error produced by the variation of ν_s , and found it to be very small, of the order of 2 MeV. We have also studied the error produced by the variation of ν_{us} , and found it to be of around 9 MeV for data Set I. As an alternative way to estimate the error, we considered the difference between the N³LL and N³LL_{hyp}, i.e. adding or subtracting the terminants. This produces a very small shift. Alternatively, we have also performed fits changing the order at which we start including the terminant in the force from $N_{\text{P}}(d=3) = 3$ to $N_{\text{P}}(d=3) = 2$. We indeed find the variation to be small: ~ 6 MeV. The fits, so far, have been performed using the running of α with 4 loop accuracy [185]. We have also made fits implementing the running of α with 5 loop accuracy [186], and found a 3 MeV difference with our central value. To consider more conservative estimates of the error, we have also looked at the difference between

N^2LL and N^3LL fits. For data Set I, we obtain similar numbers, marginally larger than from the variation in ν_{us} : ~ 10 MeV. We take the largest of all these possibilities. We believe this yields a conservative error estimate for higher order contributions.

7.13.5 Dependence on r_{ref}

The fit should be independent of r_{ref} used in Eq. (7.58). In practice, however, the result may depend on the value of r_{ref} use. We state below the N^3LL_{hyp} fits where all the values of r found in data Set I are used as r_{ref} (except, of course, for $r_{\text{ref}} = 0.353 \text{ GeV}^{-1}$ which is our central value, and has already been used)

- For $r_{\text{ref}} = 0.372 \text{ GeV}^{-1}$, we get $\Lambda_{\overline{\text{MS}}}^{(n_f=3)} = 332(3) \text{ MeV}$ with $\chi_{\text{red}}^2 = 0.99$.
- For $r_{\text{ref}} = 0.376 \text{ GeV}^{-1}$, we get $\Lambda_{\overline{\text{MS}}}^{(n_f=3)} = 337(3) \text{ MeV}$ with $\chi_{\text{red}}^2 = 0.51$.
- For $r_{\text{ref}} = 0.394 \text{ GeV}^{-1}$, we get $\Lambda_{\overline{\text{MS}}}^{(n_f=3)} = 342(4) \text{ MeV}$ with $\chi_{\text{red}}^2 = 0.86$.
- For $r_{\text{ref}} = 0.414 \text{ GeV}^{-1}$, we get $\Lambda_{\overline{\text{MS}}}^{(n_f=3)} = 336(4) \text{ MeV}$ with $\chi_{\text{red}}^2 = 1.95$.
- For $r_{\text{ref}} = 0.450 \text{ GeV}^{-1}$, we get $\Lambda_{\overline{\text{MS}}}^{(n_f=3)} = 335(4) \text{ MeV}$ with $\chi_{\text{red}}^2 = 0.87$.
- For $r_{\text{ref}} = 0.468 \text{ GeV}^{-1}$, we get $\Lambda_{\overline{\text{MS}}}^{(n_f=3)} = 338(3) \text{ MeV}$ with $\chi_{\text{red}}^2 = 0.5$.
- For $r_{\text{ref}} = 0.499 \text{ GeV}^{-1}$, we get $\Lambda_{\overline{\text{MS}}}^{(n_f=3)} = 346(3) \text{ MeV}$ with $\chi_{\text{red}}^2 = 1.21$.

Comparing with the central value $\Lambda_{\overline{\text{MS}}}^{(n_f=3)} = 338$, we find the largest difference to be of 8 MeV. For other data sets, the spread is slightly smaller, except for data Set IV, where it is slightly larger ~ 9 MeV. This one is obtained with the largest distance $r_{\text{ref}} = 1 \text{ GeV}^{-1}$ we have in our data set²⁰, which, on the other hand, produces a rather large $\chi_{\text{red}}^2 \simeq 4.8$.

7.14 Final numbers

Out of this analysis, we proceed to give our prediction, for which we use data Set I. It reads

$$\Lambda_{\overline{\text{MS}}}^{(n_f=3)} = 338(2)_{\text{stat}}(10)_{\text{h.o.}}(8)_{r_{\text{ref}}} \text{ MeV} . \quad (7.104)$$

The central value is taken from the fit of the N^3LL_{hyp} expression with $(\nu_s, \nu_{us}) = (1/r, C_A \alpha(\nu_s)/(2r))$ to data Set I. The first error is the statistical error of the fit. The second one is the error associated to higher order corrections. We estimate it by taking the biggest number among the different estimates for higher order corrections we have discussed above, which corresponds to the difference between the N^3LL and N^2LL number. The final error comes from variations on r_{ref} . This error is a mixture of two sources: on the one hand, it is partially related to our lack of knowledge of higher order logarithms, and, on the other, on the error of the lattice data point. Still, we will treat it as an additional source of error. We then combine all errors in quadrature, and obtain

$$\Lambda_{\overline{\text{MS}}}^{(n_f=3)} = 338(12) \text{ MeV} . \quad (7.105)$$

²⁰This fit yields $\Lambda_{\overline{\text{MS}}}^{(n_f=3)} = 334 \text{ MeV}$ with $\chi_{\text{red}}^2 = 4.8$. Notice that the 9 MeV difference comes from comparing with the central value fit in data Set IV which yields $\Lambda_{\overline{\text{MS}}}^{(n_f=3)} = 343 \text{ MeV}$.

Note that the determinations of $\Lambda_{\overline{\text{MS}}}^{(n_f=3)}$ obtained at LL, NLL, N²LL and N³LL are all perfectly inside the one sigma error bar quoted in Eq. (7.105), as you can see in Fig. 7.5. We also give the strong coupling constant at the scale of M_τ

$$\alpha^{(n_f=3)}(M_\tau) = 0.3151(65). \quad (7.106)$$

This number can be compared with other determinations of the strong coupling at around these low energies. One can, for instance, compare with determinations using the heavy quarkonium spectrum [187, 116]. Those also have as a fundamental input the static potential but, at present, they suffer from larger errors than those presented here. In this respect, applying hyperasymptotic expansions to these analyses may improve the accuracy of such determinations.

Out of these numbers, we can also determine $\alpha^{(n_f=5)}(M_z)$. We follow the preferred method advocated in [188], which has built in the error from decoupling and truncation when going from the scales we have made the fit, up to the M_z mass. We obtain

$$\alpha^{(n_f=5)}(M_z) = 0.1181(8)_{\Lambda_{\overline{\text{MS}}}(4)_{M_\tau \rightarrow M_z}} = 0.1181(9). \quad (7.107)$$

The first error is the error associated to the error of our determination of $\Lambda_{\overline{\text{MS}}}^{(n_f=3)}$, and the second to the transformation of this number to $\alpha^{(n_f=5)}(M_z)$ as described in [188]. In the last equality, we have combined the errors in quadrature. Our number is perfectly consistent with the world average number [120], or with the lattice final FLAG average value [189], and with a very competitive error.

As we have mentioned above, our prediction has been obtained using data Set I, which is the one less sensitive to long distances. Nevertheless, we have performed similar error analyses for the other data sets. We find

$$\text{Set II} \quad \Lambda_{\overline{\text{MS}}}^{(n_f=3)} = 341(1)_{\text{stat}}(11)_{\text{h.o.}}(6)_{\text{r.ref}} \text{ MeV} = 341(14) \text{ MeV}, \quad (7.108)$$

$$\text{Set III} \quad \Lambda_{\overline{\text{MS}}}^{(n_f=3)} = 343(1)_{\text{stat}}(13)_{\text{h.o.}}(7)_{\text{r.ref}} \text{ MeV} = 343(14) \text{ MeV}, \quad (7.109)$$

$$\text{Set IV} \quad \Lambda_{\overline{\text{MS}}}^{(n_f=3)} = 343(0)_{\text{stat}}(13)_{\text{h.o.}}(9)_{\text{r.ref}} \text{ MeV} = 343(16) \text{ MeV}. \quad (7.110)$$

Notice that all the central values obtained with the different data sets are within one sigma of our preferred value. The data sets II, III, IV have smaller statistical errors, but larger errors associated to higher orders in perturbation theory effects, as they suffer from a larger difference between the N²LL and N³LL result.

7.15 Comparison with fixed order computations

Fixed order computations can be obtained from the RG improved ones by setting $\nu_s = \nu_{\text{us}}$ and therefore, this approximation does not incorporate the resummation of large ultrasoft logarithms. This effect can be important. We show the results of the fixed order computation and the comparison with the RG improved result in Fig. 7.6. Let us first remind that the first two orders are equal, i.e.: LL=LO and NLO=NLL, as there are no ultrasoft logarithms to resum. The difference shows up at higher orders. For the same value of ν_s , and for order NLO and N³LO versus N²LL and N³LL, the fits at fixed order give significantly lower values than those that perform the resummation of logarithms. On top of that, the incorporation of the $u = 3/2$ terminants does not improve the convergence of the determination, unlike when resumming the large ultrasoft logarithms, where we see a very nice convergence pattern.

This shows that the resummation of large logarithms appears to be compulsory to find convergence, and to cancel the scale dependence that we have in the terminants. The magnitude of the incorporation of the terminants is larger for larger ν_s . This may say that using $N_P(d=3) = 0$ for the ultrasoft contribution for a scale as large as $\nu_{us} = 2/r$ could be a bad approximation. In this respect, notice that as we lower ν_{us} (see the fits with $\nu_{us} = 1/r$, and, particularly, with $\nu_{us} = 1/(\sqrt{2}r)$ in Fig. 7.6), the convergence of the fixed order computation significantly improves.

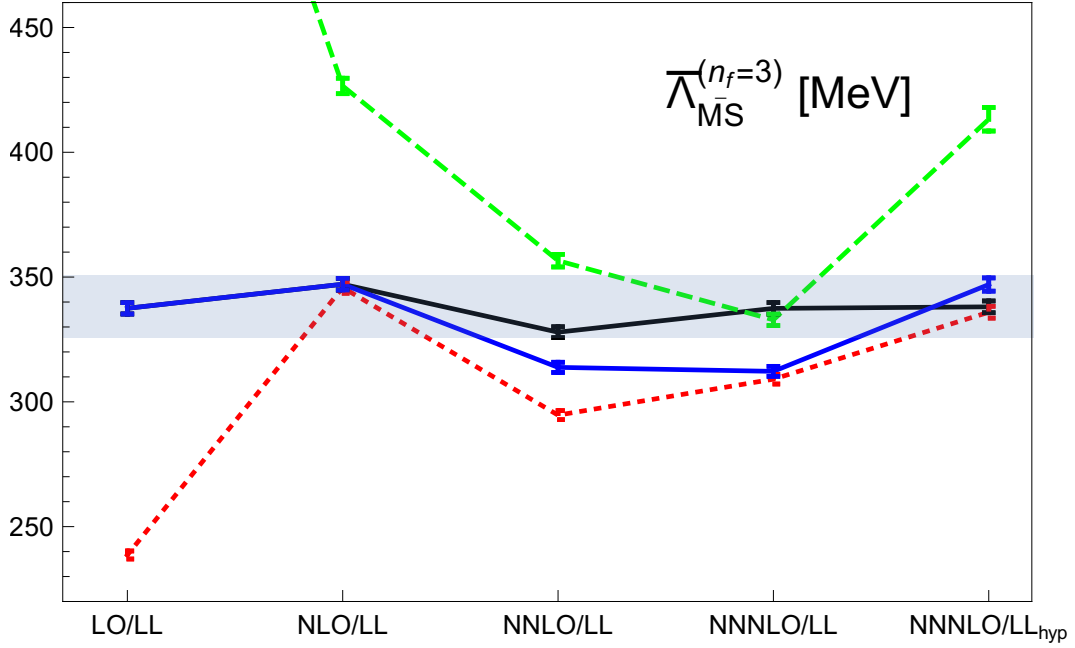


Figure 7.6: Determination of $\Lambda_{\overline{\text{MS}}}^{(n_f=3)}$ at LL, NLL, N²LL, N³LL and N³LL_{hyp} using the data Set I with $(\nu_s, \nu_{us}) = (1/r, C_A \alpha(\nu_s)/(2r))$ (continuous black line). We also give the determination of $\Lambda_{\overline{\text{MS}}}^{(n_f=3)}$ at LO(LL), NLO(NLL), N²LO, N³LO and N³LO_{hyp} using the data Set I with $\nu_s = \nu_{us} = 2/r$ (dashed green line), $\nu_s = \nu_{us} = 1/r$ (continuous blue line) and $\nu_s = \nu_{us} = 1/(\sqrt{2}r)$ (dotted red line). The error displayed is only the statistical error of the fits. We also show the error band generated by our prediction Eq. (7.105).

7.16 What if $\nu_s = \text{constant}$?

In principle, the optimal way to resum the large logarithms is to scale ν_s with $1/r$ and ν_{us} with $\alpha(\nu_s)/r$. In practice, the range of scales we have is not that large. We then consider fits with fixed ν_s and ν_{us} . We choose $(\nu_s, \nu_{us}) = (1/r_{\text{ref}}, 1 \text{ GeV})$. For the data sets I, II, III and IV, the N³LL_{hyp} fits yield $\Lambda_{\overline{\text{MS}}}^{(n_f=3)} = (339, 342, 344, 346)$ MeV respectively. Note that, for the data sets I and II, the result is identical (difference is indeed below 1 MeV and only gets to 1 MeV after rounding) to the central values obtained before and displayed in Eq. (7.104) and Eq. (7.108) respectively. For the data Set III, the difference is 1 MeV, and for the data Set IV, the difference is slightly more significant: 3 MeV. This agreement is very rewarding, since fits at low orders in the hyperasymptotic approximation show large differences with the analogous fits using the default scales: $(\nu_s, \nu_{us}) = (1/r, C_A \alpha(\nu_s)/(2r))$.

For the data Set I, we show the values of $\Lambda_{\overline{\text{MS}}}^{(n_f=3)}$ obtained with $(\nu_s, \nu_{us}) = (1/r_{\text{ref}}, 1 \text{ GeV})$ (i.e. the RG improved results) and with $\nu_s = \nu_{us} = 1/r_{\text{ref}}$ (i.e. the fixed order results) in Fig. F.2. For the RG improved results, we observe how the LL, NLL are outside the error band (actually the LL fit have a large $\chi_{\text{red}}^2 \simeq 3.9$, which then goes below 1 as we increase the accuracy), but then steadily converge to the central value, such that, as we said, the

difference for the $N^3\text{LL}_{\text{hyp}}$ prediction is below 1 MeV. The fixed order fits, which are also displayed in Fig. F.2, show the same kind of behavior to the one discussed in the previous section.

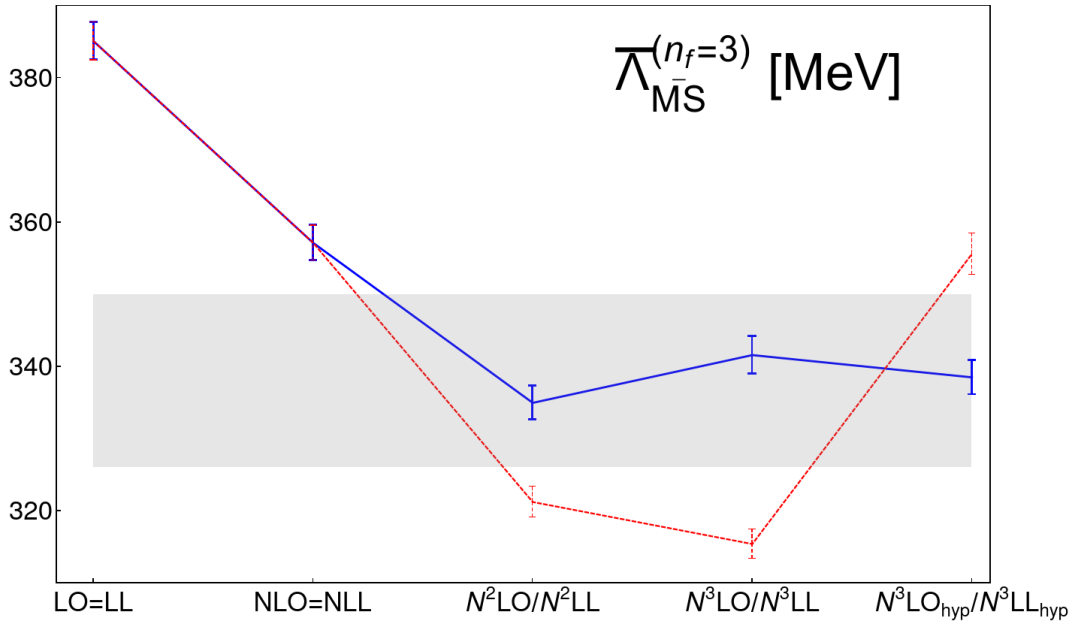


Figure 7.7: Determination of $\Lambda_{\overline{\text{MS}}}^{(n_f=3)}$ at LO=LL, NLO=NLL, $N^2\text{LL}/\text{O}$, $N^3\text{LL}/\text{O}$, and $N^3\text{LL}/\text{O}_{\text{hyp}}$ using data set I with $(\nu_s, \nu_{\text{us}}) = (1/r_{\text{ref}}, 1 \text{ GeV})$ (blue continuous line) and with $(\nu_s, \nu_{\text{us}}) = (1/r_{\text{ref}}, 1/r_{\text{ref}})$ (red dashed line). The error displayed is only the statistical error of the fits. We also show the error band generated by our prediction in Eq. (7.105).

7.17 A nonperturbative $\frac{d}{dr}\delta E_{\text{us}}$

In all the determinations so far, we have assumed that the ultrasoft scale is in the perturbative regime, and consequently, we have used a small $\alpha(\nu_{\text{us}})$ expansion for $\frac{d}{dr}\delta E_{\text{us}}$. In this situation, nonperturbative effects are parametrically suppressed compared with the precision obtained with our hyperasymptotic approximation. This assumption is safer if we take the points at shortest distances. For the points of the data Set I, ν_{us} moves in the range $\nu_{\text{us}} = \frac{C_A\alpha(\nu_s)}{2r} \in (1.06, 0.86) \text{ GeV}$, for which we consider safe to use perturbation theory at the ultrasoft scale.

If the ultrasoft scale is in the nonperturbative regime, we can say little from first principles about $\frac{d}{dr}\delta E_{\text{us}}$. To make an estimate, we consider the data Set IV after subtracting the points of the data Set I (that is, we take the set with largest distances, and subtract the points at smallest distances that we used in the previous section for the central value determination of $\Lambda_{\overline{\text{MS}}}$ in the purely perturbative regime). As a test, we assume that for this set of data the ultrasoft scale is in the nonperturbative regime.

To simplify the parametrization of these nonperturbative effects, we assume that we are in the regime where $1/r \gg \Lambda_{\text{QCD}} \gg \alpha(1/r)/r$. In this situation, $\delta E_{\text{us}} = k\Lambda_{\overline{\text{MS}}}^3 r^2$ (where k is a nonperturbative dimensionless constant), instead of Eq. (7.42), and of course, $\frac{d}{dr}\delta E_{\text{us}} = 2k\Lambda_{\overline{\text{MS}}}^3 r$. Moreover, the terminant of $\frac{d}{dr}\delta E_{\text{us}}$ is not included on the fits, as it makes no sense to talk about terminants if we have no perturbative series in the first place. We want to see how sensitive the determination of $\Lambda_{\overline{\text{MS}}}$ is to considering the ultrasoft scale to be in the nonperturbative regime, which implies that we also have to fit the parameter k in δE_{us} . The soft scale is the same, $\nu_s = 1/r$, and we have fixed $\nu_{\text{us}} = 1 \text{ GeV}$ in $\frac{d}{dr}\delta V_{\text{RG}}$. The fit yields $\Lambda_{\overline{\text{MS}}} = 356(3) \text{ MeV}$ (the error is only the statistical error of

the fit) with a $\chi_{\text{red}}^2 = 0.55$. Notice that this number for $\Lambda_{\overline{\text{MS}}}$ is consistent with the value obtained from the pure perturbative fit (only a little bit more than one sigma away of Eq. (7.105)). For the value of k we obtain

$$k = -0.82(7). \quad (7.111)$$

In principle, we did not care much about k . Nevertheless, its value rings a bell. In the perturbative regime, we have that

$$\delta E_{\text{us}}^{\text{PV}} = \sum_{n=0}^{N_{\text{P}}(d=3)} c_n \alpha^{n+1}(\nu_{\text{us}}) - \frac{1}{r} \Omega_3^V(\nu_{\text{us}}), \quad (7.112)$$

where we set $N_{\text{P}}(d=3) = 0$. At low scales, this expression is dominated by the terminant, which, we remind, has the following form

$$-\frac{1}{r} \Omega_3^V(\nu_{\text{us}}) = k' \sqrt{\alpha(\nu_{\text{us}})} \Lambda_{\overline{\text{MS}}}^3 r^2 (1 + k'_1 \alpha(\nu_{\text{us}}) + \mathcal{O}(\alpha^2(\nu_{\text{us}}))). \quad (7.113)$$

The dependence on ν_{us} is mild and, effectively, the terminant scales as

$$-\frac{1}{r} \Omega_3^V(\nu_{\text{us}}) \sim k_{\text{terminant}} \Lambda_{\overline{\text{MS}}}^3 r^2, \quad (7.114)$$

and for $\nu_{\text{us}} = 1$ GeV, we get

$$k_{\text{terminant}} \simeq -1.25(58), \quad k_{\text{terminant}} \simeq -1.04(48), \quad (7.115)$$

where in the first number, we have used $\Lambda_{\overline{\text{MS}}}^{(n_f=3)} = 338$ MeV, the outcome of the perturbative fit, and in the second $\Lambda_{\overline{\text{MS}}}^{(n_f=3)} = 356$ MeV, the outcome of the nonperturbative fit. In these numbers, we have put the central value and the error of the normalization Z_3^V obtained in Eq. (7.88). Therefore, what the nonperturbative fit seems to be doing is to effectively fit the terminant assuming that the $\mathcal{O}(\alpha(\nu_{\text{us}}))$ term of $\delta E_{\text{us}}^{\text{PV}}$ is subdominant. Notice that Eq. (7.111) is, within one statistical standard deviation, the value predicted by perturbation theory, Eq. (7.115). We take this as a very strong confirmation that our weak coupling analysis is safe, and that, indeed, one can apply perturbation theory to scales as small as $1/r \sim 1$ GeV.

Finally, to confirm this picture, we do the fit over the complete data Set IV assuming $\delta E_{\text{us}} = k \Lambda_{\overline{\text{MS}}}^3 r^2$. The results barely change: we obtain $\Lambda_{\overline{\text{MS}}} = 355(3)$ with also $\chi_{\text{red}}^2 = 0.55$ and $k = -0.8$. Overall, we can even take this analysis as a strong indication that the data has enough precision to be sensitive (and, to some extent fit, albeit with large errors) the value of Z_3^V . This discussion could also explain why the nonperturbative fit also has a small χ_{red}^2 , as it loosely corresponds to the perturbative expression, but letting the normalization of the terminant to be a free parameter of the fit.

7.18 Comparison with earlier work

Determinations of $\Lambda_{\overline{\text{MS}}}^{(n_f=3)}$ using lattice data of the static energy have been obtained in the past. Some recent determinations are those of [176, 177]. They compare with a different data set including lattice data at longer distances. They work directly with the potential. The precision of the theoretical expression is N³LO in our counting. No resummation of ultrasoft logarithms, nor the incorporation of the terminants is considered, but they use an alternative method for dealing with the renormalons. In the large β_0 , it is possible to see what is the precision that corresponds to in the hyperasymptotic approximation, but not beyond the large β_0 . The ultrasoft scale is assumed to be in the nonperturbative situation. Therefore, the comparison should better be done with the

number we have just obtained in the previous section. If we set $\delta E_{\text{us}} = k\Lambda_{\overline{\text{MS}}}^3 r^2$, fix $\nu_s = \nu_{\text{us}} = 1/r$, and we work with N³LO precision in F plus the $u = 3/2$ terminant of F , we obtain $\Lambda_{\overline{\text{MS}}}^{(n_f=3)} = 305(2)$ MeV, where we only put the statistical error. This number is smaller than the number obtained in [176, 177].

Closer to our analysis are [153, 158]. In particular from the last reference, we borrow the lattice data. In these references, they use the force as the starting point, and later integrate it to recover the static energy, as we have done above. Their central values are obtained by fitting to the N³LO result after adding the N²LL ultrasoft contributions. Therefore, they mix different orders according to our counting, and do not include the complete N³LL result. The number they obtain is smaller than ours. In this respect, note that our numbers with analogous N³LO precision are also smaller.

7.19 Final remarks

Summarizing it all, making use of lattice data and theoretical expressions for the singlet static energy, using its r derivative as a starting point, using the hyperasymptotic expansion to handle the $u = 3/2$ renormalons, and implementing N³LL resummation of ultrasoft logs, we have obtained a precise determinations of $\Lambda_{\overline{\text{MS}}}$ and $\alpha^{(n_f=5)}(M_z)$

$$\Lambda_{\overline{\text{MS}}}^{(n_f=3)} = 338(12) \text{ MeV}, \quad \alpha(M_\tau) = 0.3151(65), \quad \alpha(M_z) = 0.1181(9). \quad (7.116)$$

The resummation of logarithms and the introduction of the terminants associated to the $u = 3/2$ renormalon are essential to get a very well convergent series. This, together with precise data at short distances, allows us to get accurate values for $\Lambda_{\overline{\text{MS}}}$. The lack of any of these novel elements significantly deteriorates the convergence, and consequently, the accuracy of the prediction.

The largest source of error comes from unknown higher order corrections in perturbation theory. The statistical errors of the fit are small, although the dependence on r_{ref} , which is a mixture of lattice and theory error, is large. Increasing the number of points of the data set gives a very mild tendency to increase the value till stabilizing at 343 MeV, very well inside the error we give.

Conclusions

In an OPE of an observable, we have a tower of contributions of various condensates together with their Wilson coefficients. These Wilson coefficients are thought to be well approximated by power series expansions in the strong coupling α , which in general are expected to be divergent and asymptotic. Therefore, the way these divergent series are regularized will see itself reflected on the various condensates of the expansion, so as to keep the whole thing independent of these choices.

In particular, in this thesis, we have explored Borel summation with the PV prescription as a means to regulate divergent series in QCD. In chapter 3 and chapter 4, two methods to compute PV Borel sums from truncated versions of the series have been highlighted by exploiting the singularity structure in the Borel plane. Special emphasis has been put in the method of chapter 3, which shows more promise. In this method, the computation of the PV Borel sum is organized in a hyperasymptotic expansion, where we have a hierarchy of exponential suppression in the terms of the expansion. These terms can be systematically computed if one knows enough exact coefficients of the perturbative expansion, and if one knows the structure of the various singularities in the Borel plane.

The method has then been applied to the OPE of the average plaquette, which has been used to give an estimate of the gluon condensate in chapter 5. In chapter 6, an analogous procedure has been carried out to give an estimate of $\bar{\Lambda}$, both from the lattice and B physics.

Finally, in chapter 7, an estimate of the QCD strong coupling has been obtained from lattice data of the singlet static quark antiquark energy. Resummation of N³LL logarithms and the use of terminants is essential to obtain a stable result.

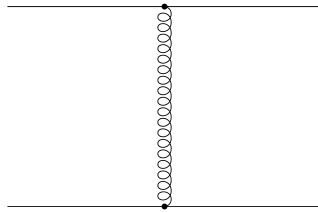
Appendix A

The large β_0 approximation

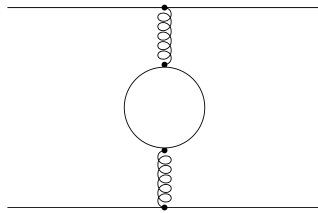
The large β_0 approximation [190, 32, 191] will be frequently used in this thesis, so we will briefly review it in this appendix. Let us consider a dimensionless observable R computed in QCD perturbation theory

$$R = \sum_{n=0}^{\infty} r_n \alpha^{n+1}. \quad (\text{A.1})$$

We will consider observables whose LO (order α^1) features a one gluon exchange diagram. One such example would be the QCD static potential, where the LO diagram is:



Notice that at NLO, the coefficient r_1 will have a contribution that will be the LO diagram with a quark loop insertion in the gluon line. For the static potential we would have



We stress here that quark loop insertions in gluon lines are proportional to the number of quark flavors n_f , and actually, the only source of n_f dependence. Each of these quark loops gives a factor

$$\Psi(q^2) \equiv -\frac{n_f}{6\pi} \alpha(\mu) \log \left(\frac{\mu^2}{q^2} e^{-c_X} \right), \quad (\text{A.2})$$

where q is the total Euclidean momenta going through the gluon line, μ is the renormalization scale, and c_X is a scheme dependent constant. For instance, for the $\overline{\text{MS}}$ scheme, we have that $c_{\overline{\text{MS}}} = -5/3$. Therefore, we can write the NLO coefficient as an order one polynomial in n_f

$$r_1 = r_{11} n_f + r_{10}, \quad (\text{A.3})$$

for some r_{11} and r_{10} . At order α^3 , we will have the LO diagram with two quark loop insertions, as well as contributions coming from diagrams featuring only one quark loop. Therefore, this time the polynomial in n_f will

be order two

$$r_2 = r_{22}n_f^2 + r_{21}n_f + r_{20}, \quad (\text{A.4})$$

for some r_{22} , r_{21} and r_{20} . We see that in general, the coefficient r_n will be an order n polynomial in n_f

$$r_n = r_{nn}n_f^n + r_{n(n-1)}n_f^{n-1} + \dots + r_{n1}n_f + r_{n0}. \quad (\text{A.5})$$

Now, let's recall the one loop coefficient of the beta function

$$\beta_0 = 11 - \frac{2}{3}n_f \rightarrow n_f = -\frac{3}{2}\beta_0 + \frac{33}{2}. \quad (\text{A.6})$$

Therefore, the n_f polynomial of Eq. (A.5) can also be written as an order n polynomial in β_0

$$r_n = r'_{nn}\beta_0^n + r'_{n(n-1)}\beta_0^{n-1} + \dots + r'_{n1}\beta_0 + r'_{n0}. \quad (\text{A.7})$$

Obviously

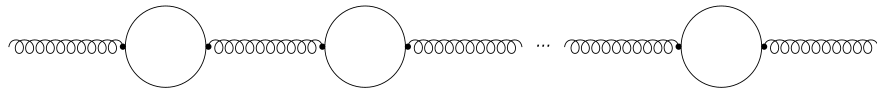
$$r'_{nn} = (-3/2)^n r_{nn}. \quad (\text{A.8})$$

The large β_0 approximation consists basically of just taking the term with highest power of β_0 in Eq. (A.7)

$$r_n^{\text{large } \beta_0} = r'_{nn}\beta_0^n. \quad (\text{A.9})$$

The reason to consider this idea is that in some cases it was appreciated that just keeping the highest power in β_0 approximated fairly well the exact results [191]. Regardless of this, the reason the large β_0 will be of importance to us is that it will allow us to work with formal series that are known at all orders in α , and we will be able to obtain closed expressions for Borel transforms.

From Eq. (A.8), we see that in order to obtain the perturbative series of R in the large β_0 approximation, we only need to compute diagrams that feature the LO diagram with n quark loop insertions in the gluon line (because this diagrams will yield the highest power of n_f at each order of α). The computation of such a diagram with n quark loop insertions (for $n \geq 1$) is simplified once one notices [190]



$$= -i\delta_{ab} \frac{1}{k^2 + i\eta} \left(\eta_{\mu\nu} - \frac{k_\mu k_\nu}{k^2 + i\eta} \right) \Psi^n(q^2 = -k^2), \quad (\text{A.10})$$

where a, b are SU(3) adjoint representation color indices, and k is the (Minkowski) momentum going through the gluon chain (that is $k^2 = -q^2$). We see above, that a gluon propagator with n quark loop insertions is equivalent to a gluon propagator in the Landau gauge times the factor Ψ^n . Therefore, if we write the LO term in the following way

$$r_0\alpha(\mu) \equiv \alpha(\mu) \int_0^\infty dq F(q), \quad (\text{A.11})$$

we see that the n -th order coefficient with the highest power of n_f will be given by

$$r_{nn}n_f^n \alpha^{n+1}(\mu) = \alpha(\mu) \int_0^\infty dq F(q) \Psi^n(q^2) \quad (\text{A.12})$$

$$= \alpha(\mu) \int_0^\infty dq F(q) \left\{ -\frac{n_f \alpha(\mu)}{6\pi} \log \left(\frac{\mu^2}{q^2} e^{-cx} \right) \right\}^n, \quad (\text{A.13})$$

because the diagram leading to Eq. (A.12) is basically the diagram leading to Eq. (A.11) with an extra Ψ^n factor. Thus, from Eqs. (A.8) and (A.9), we see that in the large β_0 approximation we have

$$R_{\text{large } \beta_0} = \sum_{n=0}^{\infty} r_n^{\text{large } \beta_0} \alpha^{n+1}(\mu) \quad (\text{A.14})$$

$$= \alpha(\mu) \sum_{n=0}^{\infty} \int_0^{\infty} dq F(q) \left\{ \frac{\beta_0 \alpha(\mu)}{4\pi} \log \left(\frac{\mu^2}{q^2} e^{-c_x} \right) \right\}^n. \quad (\text{A.15})$$

We finish mentioning that it is customary to consider only one loop running in the strong coupling while working in the large β_0 approximation.

Appendix B

Renormalization scale and scheme invariance of the PV Borel sum of an observable

B.1 On the renormalization scale dependence of perturbative expansions of observables

Let us consider a QCD observable, that we will call R_{obs} . Let us also consider the perturbative expansion of this observable, which we will call R

$$R = \sum_{n=0}^{\infty} r_n(\mu) \alpha^{n+1}(\mu), \quad (\text{B.1})$$

where in the above series, we have made explicit the dependence on the renormalization scale μ . As we have already mentioned, we assume the above series to be asymptotic to R_{obs} as $\alpha \rightarrow 0$. From Eq. (1.10), we know that this implies that¹

$$R_{\text{obs}} - \sum_{n=0}^{N-1} r_n(\mu) \alpha^{n+1}(\mu) = \mathcal{O}(\alpha^{N+1}(\mu)), \quad (\text{B.2})$$

for any integer value N . Let us now consider the series defined at another renormalization scale μ' . Again, we will have

$$R_{\text{obs}} - \sum_{n=0}^{N-1} r_n(\mu') \alpha^{n+1}(\mu') = \mathcal{O}(\alpha^{N+1}(\mu')). \quad (\text{B.3})$$

The relation between both couplings can be written solving the beta function equation

$$\alpha(\mu') = \alpha(\mu) \{1 + \mathcal{O}(\alpha(\mu))\}. \quad (\text{B.4})$$

All of this implies that, we have

$$R_{\text{obs}} - \sum_{n=0}^{N-1} r_n(\mu) \alpha^{n+1}(\mu) = \mathcal{O}(\alpha^{N+1}(\mu)), \quad (\text{B.5})$$

$$R_{\text{obs}} - \sum_{n=0}^{N-1} r_n(\mu') \alpha^{n+1}(\mu') = \mathcal{O}(\alpha^{N+1}(\mu')), \quad (\text{B.6})$$

or in other words, the two series above only differ by a term that for small $\alpha(\mu)$ behaves like $\alpha^{N+1}(\mu)$. Taking infinitesimal variations of μ , we can write

$$\frac{d}{d\mu} \sum_{n=0}^{N-1} r_n(\mu) \alpha^{n+1}(\mu) = \mathcal{O}(\alpha^{N+1}(\mu)). \quad (\text{B.7})$$

¹Following the notation of Eq. (1.10), we redefine $r_n \equiv a_{n+1}$, and assume our series not to have a constant value, that is, $r_{-1} = 0$.

Thus, the LHS above when expanded in $\alpha(\mu)$ cannot have terms smaller than order $\alpha^{N+1}(\mu)$. Moreover, since N in principle can be made to be arbitrarily large, we actually have that *all* the coefficients of the $\alpha(\mu)$ expansion of the LHS above actually vanish. This is what is meant when one says that R is formally μ independent, and we denote this by

$$\frac{d}{d\mu}R = 0. \quad (\text{B.8})$$

We emphasize again that what we are not taking a derivative of R (since R in general is divergent), but rather, that the formal series obtained by introducing the derivative inside

$$\frac{d}{d\mu}R \equiv \sum_{n=0}^{\infty} \frac{d}{d\mu} \left\{ r_n(\mu) \alpha^{n+1}(\mu) \right\}, \quad (\text{B.9})$$

is zero to all orders in $\alpha(\mu)$.

B.2 Renormalization scale invariance of the PV Borel sum

Let us continue with the formal series in powers of the QCD gauge coupling of an observable

$$R = \sum_{n=0}^{\infty} r_n(\mu) \alpha^{n+1}(\mu), \quad (\text{B.10})$$

where we again explicitly denote the renormalization scale μ . As we have just seen, if R is a perturbative expansion that is (assumed to be) asymptotic to an observable, then it satisfies formally (that is at every order in $\alpha(\mu)$)

$$\mu \frac{d}{d\mu} R = 0. \quad (\text{B.11})$$

We define $\tau \equiv \log \frac{\mu}{\Lambda_{\text{QCD}}}$. Notice that $\frac{d}{d\tau} = \mu \frac{d}{d\mu}$. Slightly abusing notation, we will name $\alpha(\tau) \equiv \alpha(\mu(\tau))$, and $r_n(\tau) \equiv r_n(\mu(\tau))$, so that

$$R = \sum_{n=0}^{\infty} r_n(\tau) \alpha^{n+1}(\tau). \quad (\text{B.12})$$

The Borel transform of R is

$$\hat{R}(t, \tau) = \sum_{n=0}^{\infty} \frac{r_n(\tau)}{n!} t^n, \quad (\text{B.13})$$

where we make explicit the RG scale dependence. We now consider $\hat{R}_{\text{an}}(t, \tau)$, the analytic continuation in the complex t plane of the function above. $\hat{R}_{\text{an}}(t, \tau)$ is assumed to have some singularities in the complex plane, in particular, in the positive real line. With this object, we consider a lateral Borel sum either just above or just below the real line, as in Eq. (1.35). We do assume that we can define these lateral Borel sums without encountering any singularity on the way.

We want to prove the RG scale invariance of the PV Borel sum. From Eq. (1.41), we clearly see that this object is the averaged sum of two lateral Borel sums, so τ invariance of both lateral sums implies τ invariance of the PV Borel sum. This is what we will look at. Thus, we are interested at

$$I_{\pm} \equiv \frac{d}{d\tau} \int_{C_{\pm}} dt e^{-t/\alpha(\tau)} \hat{R}_{\text{an}}(t, \tau). \quad (\text{B.14})$$

Inserting the τ derivative inside the integral

$$I_{\pm} = \int_{C_{\pm}} dt \frac{\partial}{\partial \tau} \left\{ e^{-t/\alpha(\tau)} \hat{R}_{\text{an}}(t, \tau) \right\}, \quad (\text{B.15})$$

defining

$$\frac{d}{dt}G_\tau(t) \equiv \frac{\partial}{\partial\tau}\{e^{-t/\alpha(\tau)}\hat{R}_{\text{an}}(t, \tau)\}, \quad (\text{B.16})$$

so that

$$I_\pm = \int_0^{\infty e^{\pm i\eta}} dt \frac{\partial}{\partial\tau}\{e^{-t/\alpha(\tau)}\hat{R}_{\text{an}}(t, \tau)\} \quad (\text{B.17})$$

$$= G_\tau(\infty e^{\pm i\eta}) - G_\tau(0). \quad (\text{B.18})$$

We will next get $G_\tau(t)$ for t inside ρ , the radius of convergence of the Borel transform. In order to do that, let's come back to Eq. (B.16)

$$\frac{d}{dt}G_\tau(t) = \frac{\partial}{\partial\tau}\{e^{-t/\alpha(\tau)}\hat{R}_{\text{an}}(t, \tau)\} \quad (\text{B.19})$$

$$= e^{-t/\alpha(\tau)}\left\{\frac{t}{\alpha^2}\frac{d\alpha}{d\tau}\hat{R}_{\text{an}}(t, \tau) + \frac{\partial}{\partial\tau}\hat{R}_{\text{an}}(t, \tau)\right\}. \quad (\text{B.20})$$

For $0 \leq |t| < \rho$ the Borel transform is just the series in Eq. (B.13), so we can substitute

$$\frac{d}{dt}G_\tau(t) = e^{-t/\alpha(\tau)}\left\{\frac{t}{\alpha^2}\frac{d\alpha}{d\tau}\sum_{n=0}^{\infty}\frac{r_n(\tau)}{n!}t^n + \frac{\partial}{\partial\tau}\sum_{n=0}^{\infty}\frac{r_n(\tau)}{n!}t^n\right\}. \quad (\text{B.21})$$

Introducing the τ derivative inside the infinite sum

$$\frac{d}{dt}G_\tau(t) = e^{-t/\alpha(\tau)}\left\{\frac{t}{\alpha^2}\frac{d\alpha}{d\tau}\sum_{n=0}^{\infty}\frac{r_n(\tau)}{n!}t^n + \sum_{n=0}^{\infty}\frac{d}{d\tau}r_n(\tau)\frac{1}{n!}t^n\right\}. \quad (\text{B.22})$$

We will now show that the RG equation of α allows us to write the equation above as a derivative in t of a function, thus obtaining $G_\tau(t)$. First, let's recall that

$$\frac{d}{d\tau}\alpha(\tau) = -2\alpha(\tau)\sum_{j=0}^{\infty}\beta_j\left(\frac{\alpha(\tau)}{4\pi}\right)^{j+1} \quad (\text{B.23})$$

$$\equiv -\sum_{j=0}^{\infty}b_j\alpha^{j+2}(\tau). \quad (\text{B.24})$$

Now, we turn our attention to the τ dependence of $r_n(\tau)$. As saw in Eq. (B.11)

$$\frac{d}{d\tau}R = 0, \quad (\text{B.25})$$

which is satisfied at every order in α . Therefore, we obtain

$$\sum_{n=0}^{\infty}\frac{d}{d\tau}r_n(\tau)\alpha^{n+1} - \sum_{n=0}^{\infty}\sum_{j=0}^{\infty}b_j(n+1)r_n(\tau)\alpha^{n+j+2}(\tau) = 0, \quad (\text{B.26})$$

where in the first term on the LHS above, the τ derivative is understood to act only on r_n . This readily implies that

$$\frac{d}{d\tau}r_n(\tau) = \sum_{j=0}^{n-1}b_j(n-j)r_{n-j-1}(\tau), \quad (\text{B.27})$$

where to arrive here, we have defined $r_n \equiv 0$ for negative n . Now, we can come back to Eq. (B.22), and plug in Eqs. (B.24) and (B.27), which yields

$$\frac{d}{dt}G_\tau(t) = e^{-t/\alpha(\tau)}\left\{-\sum_{j=0}^{\infty}\sum_{n=0}^{\infty}b_j\alpha^j(\tau)\frac{r_n(\tau)}{n!}t^{n+1} + \sum_{l=0}^{\infty}\sum_{m=0}^{\infty}b_l r_m(\tau)\frac{m+1}{(m+l+1)!}t^{m+l+1}\right\}. \quad (\text{B.28})$$

Noticing that the $j = 0$ term above cancels the $l = 0$ term², we can write

$$\frac{d}{dt}G_\tau(t) = e^{-t/\alpha(\tau)} \left\{ - \sum_{j=1}^{\infty} \sum_{n=0}^{\infty} b_j \alpha^j(\tau) \frac{r_n(\tau)}{n!} t^{n+1} + \sum_{l=1}^{\infty} \sum_{m=0}^{\infty} b_l r_m(\tau) \frac{m+1}{(m+l+1)!} t^{m+l+1} \right\}. \quad (\text{B.29})$$

We will have no more cancellations between $j = l = 1$ terms, nor for any other $j = l$ terms. What instead happens is that the sum of the $j = l$ terms gives rise to a total derivative on t , which allows us to extract $G_\tau(t)$. In order to see this, let's first simplify matters, and pretend that we only considered two loop running in equation Eq. (B.24). If so, all $b_i = 0$ for $i > 1$, which implies that Eq. (B.29) is just

$$\frac{d}{dt}G_\tau(t) = e^{-t/\alpha(\tau)} \left\{ - \sum_{n=0}^{\infty} b_1 \alpha(\tau) \frac{r_n(\tau)}{n!} t^{n+1} + \sum_{m=0}^{\infty} b_1 r_m(\tau) \frac{m+1}{(m+2)!} t^{m+2} \right\}. \quad (\text{B.30})$$

Using the product rule for derivatives, it is simple enough to realize that

$$e^{-t/\alpha(\tau)} t^{m+2} = (2+m)\alpha(\tau) e^{-t/\alpha(\tau)} t^{m+1} - \alpha \frac{d}{dt} \{ e^{-t/\alpha(\tau)} t^{m+2} \}. \quad (\text{B.31})$$

Introducing the RHS above in the second term in braces in Eq. (B.30), one sees a cancellation that leaves us with

$$\frac{d}{dt}G_\tau(t) = - \sum_{m=0}^{\infty} b_1 r_m(\tau) \frac{m+1}{(m+2)!} \alpha(\tau) \frac{d}{dt} \{ e^{-t/\alpha(\tau)} t^{m+2} \} \quad (\text{B.32})$$

$$= - \alpha(\tau) b_1 \frac{d}{dt} \sum_{m=0}^{\infty} r_m(\tau) \frac{m+1}{(m+2)!} e^{-t/\alpha(\tau)} t^{m+2}. \quad (\text{B.33})$$

Likewise, the $j = l = 2$ terms in Eq. (B.29) give rise to another total derivative in t . In this case, one needs to use instead of Eq. (B.31)

$$e^{-t/\alpha(\tau)} t^{m+3} = (3+m)(2+m)\alpha^2(\tau) e^{-t/\alpha(\tau)} t^{m+1} - \alpha(\tau) \frac{d}{dt} \{ e^{-t/\alpha(\tau)} t^{m+3} \} - (3+m)\alpha^2(\tau) \frac{d}{dt} \{ e^{-t/\alpha(\tau)} t^{m+2} \}. \quad (\text{B.34})$$

For a general value of l , one needs to use

$$e^{-t/\alpha(\tau)} t^{m+l+1} = \left(\prod_{s=2}^{l+1} (s+m) \right) \alpha^l e^{-t/\alpha(\tau)} t^{m+1} - \sum_{p=1}^l \left(\prod_{s=l-p+3}^{l+1} (m+s) \right) \alpha^p(\tau) \frac{d}{dt} \{ e^{-t/\alpha(\tau)} t^{m+l-p+2} \}, \quad (\text{B.35})$$

where we emphasize that $\prod_a^b(\dots) = 1$ if $b < a$. Thus, substituting Eq. (B.35) in Eq. (B.29), we obtain

$$\begin{aligned} \frac{d}{dt}G_\tau(t) &= - e^{-t/\alpha(\tau)} \sum_{j=1}^{\infty} \sum_{n=0}^{\infty} b_j \alpha^j(\tau) \frac{r_n(\tau)}{n!} t^{n+1} + e^{-t/\alpha(\tau)} \sum_{l=1}^{\infty} \sum_{m=0}^{\infty} b_l \alpha^l(\tau) r_m(\tau) \frac{m+1}{(m+l+1)!} \left(\prod_{s=2}^{l+1} (s+m) \right) t^{m+1} \\ &\quad - \sum_{l=1}^{\infty} \sum_{m=0}^{\infty} b_l r_m(\tau) \frac{m+1}{(m+l+1)!} \sum_{p=1}^l \left(\prod_{s=l-p+3}^{l+1} (s+m) \right) \alpha^p(\tau) \frac{d}{dt} \{ e^{-t/\alpha(\tau)} t^{m+l-p+2} \}. \end{aligned} \quad (\text{B.36})$$

Upon noticing

$$\frac{m+1}{(m+l+1)!} \left(\prod_{s=2}^{l+1} (s+m) \right) = \frac{1}{m!}, \quad (\text{B.37})$$

the first line in Eq. (B.36) cancels out, leaving us with

$$\frac{d}{dt}G_\tau(t) = - \sum_{l=1}^{\infty} \sum_{m=0}^{\infty} b_l r_m(\tau) \frac{m+1}{(m+l+1)!} \sum_{p=1}^l \left(\prod_{s=l-p+3}^{l+1} (s+m) \right) \alpha^p(\tau) \frac{d}{dt} \{ e^{-t/\alpha(\tau)} t^{m+l-p+2} \}. \quad (\text{B.38})$$

²Notice that this means that had we only included one loop running in Eq. (B.24), we would have $\frac{d}{dt}G_\tau(t) = 0$, and thus $G_\tau = C$ for some complex constant C , which implies that $I = 0$ in Eq. (B.18).

We can further simplify this expression by noticing

$$\frac{m+1}{(m+l+1)!} \left(\prod_{s=l-p+3}^{l+1} (s+m) \right) = \frac{m+1}{(m+l-p+2)!}, \quad (\text{B.39})$$

so that

$$\frac{d}{dt} G_\tau(t) = - \sum_{l=1}^{\infty} \sum_{m=0}^{\infty} \sum_{p=1}^l b_l r_m(\tau) \frac{m+1}{(m+l-p+2)!} \alpha^p(\tau) \frac{d}{dt} \left\{ e^{-t/\alpha(\tau)} t^{m+l-p+2} \right\} \quad (\text{B.40})$$

$$\equiv - \frac{d}{dt} \left\{ e^{-t/\alpha(\tau)} \sum_{l=1}^{\infty} \sum_{m=0}^{\infty} \sum_{p=1}^l b_l r_m(\tau) a(l, m, p) \alpha^p(\tau) t^{m+l-p+2} \right\}, \quad (\text{B.41})$$

where

$$a(l, m, p) \equiv \frac{m+1}{(m+l-p+2)!}. \quad (\text{B.42})$$

Thus (modulo an irrelevant additive constant)

$$G_\tau(t) = -e^{-t/\alpha(\tau)} \sum_{l=1}^{\infty} \sum_{m=0}^{\infty} \sum_{p=1}^l b_l r_m(\tau) a(l, m, p) \alpha^p(\tau) t^{m+l-p+2}. \quad (\text{B.43})$$

Having obtained this expression, let's come back to Eq. (B.18)

$$I_{\pm} = G_\tau(\infty e^{\pm i\eta}) - G_\tau(0). \quad (\text{B.44})$$

Recall that we have derived the expression in Eq. (B.43) for $|t| < \rho$, that is, for values of t inside the radius of convergence of the Borel transform. Therefore, we can readily say that at $t = 0$, we have that $G_\tau(0) = 0$. Assuming that upon performing the l, m, p sums in Eq. (B.43), we get a function in t that after being analytically extended in the t plane, does not overpower the exponential suppression of the $e^{-t/\alpha(\tau)}$ term, we would have that $G_\tau(\infty e^{\pm i\eta}) = 0$. We will assume this is indeed the case. This leaves us with

$$I_{\pm} = 0, \quad (\text{B.45})$$

and thus, the lateral Borel sums are renormalization scale invariant, and therefore, so is the PV Borel sum of R . The computation given here first appeared in [68] for finite amount of l terms in the first sum of Eq. (B.43), and it was confirmed in [192], where the infinite sum in l in Eq. (B.43) was also considered.

B.3 Renormalization scheme invariance of the PV Borel sum

Let's now worry about the renormalization scheme dependence of the PV Borel sum. Being more specific, let us consider again the series in Eq. (B.10)

$$R = \sum_{n=0}^{\infty} r_n \alpha^{n+1}, \quad (\text{B.46})$$

and let's consider the following renormalization scheme change for the strong coupling

$$\alpha' = \alpha + \sum_{j=1}^{\infty} d_j \alpha^{j+1}. \quad (\text{B.47})$$

We can invert Eq. (B.47), and write

$$\alpha = \alpha' + \sum_{j=1}^{\infty} \omega_j \alpha'^{j+1}, \quad (\text{B.48})$$

where the coefficients ω_j depend on d_j . In particular, it is simple to find that

$$\omega_1 = -d_1, \quad (\text{B.49})$$

$$\omega_2 = 2d_1^2 - d_2, \quad (\text{B.50})$$

where we could write similar relations for all ω_j . We can use Eq. (B.48) to re-expand R in α'

$$R = \sum_{n=0}^{\infty} r'_n \alpha'^{n+1}. \quad (\text{B.51})$$

The scheme change is parametrized by the arbitrary coefficients d_j . Just as with scale dependence, formally, we have

$$\frac{\partial}{\partial d_i} R = \frac{\partial}{\partial d_i} \sum_{n=0}^{\infty} r'_n \alpha'^{n+1} = 0, \quad (\text{B.52})$$

$$\sum_{n=0}^{\infty} \left[\frac{\partial}{\partial d_i} r'_n \alpha'^{n+1} + r'_n (n+1) \alpha'^n \frac{\partial}{\partial d_i} \alpha' \right] = 0, \quad (\text{B.53})$$

where in the first term in the LHS above, the partial derivative is understood to only act in r'_n . Consider now

$$\frac{\partial}{\partial d_i} \alpha' = \alpha'^{i+1}, \quad (\text{B.54})$$

where we have used Eq. (B.47). Using Eq. (B.48), we can write the RHS above as a formal series in α'

$$\frac{\partial}{\partial d_i} \alpha' \equiv \sum_{j=0}^{\infty} \#_j^{(i)} \alpha'^{j+2}, \quad (\text{B.55})$$

where notice that $\#_j^{(i)} = 0$ for $j < i - 1$. Introducing this equation in Eq. (B.53)

$$\sum_{n=0}^{\infty} \frac{\partial}{\partial d_i} r'_n \alpha'^{n+1} + \sum_{n=0}^{\infty} \sum_{j=0}^{\infty} \#_j^{(i)} (n+1) r'_n \alpha'^{n+j+2} = 0, \quad (\text{B.56})$$

which readily implies

$$\frac{\partial}{\partial d_i} r'_n = \sum_{j=0}^{n-1} -\#_j^{(i)} (n-j) r'_{n-j-1}, \quad (\text{B.57})$$

where we have used in the middle steps $r'_n \equiv 0$ for negative n . As the reader may have noticed, there is a clear similitude between both equations above, and Eqs. (B.26) and (B.27). The idea of the proof for the renormalization scheme dependence is the same we have employed for the scale dependence in section B.2. We consider the Borel transform of Eq. (B.51), that is, of the series of R written in terms of α'

$$\hat{R}(t, d_j) = \sum_{n=0}^{\infty} \frac{r'_n}{n!} t^n, \quad (\text{B.58})$$

where with d_j , we make explicit the dependence on all d_j coefficients. Just as in section B.2, we consider the analytic continuation in the t plane of the function above, and with it construct lateral Borel sums. The PV Borel sum will be the averaged sum of two lateral Borel sums. Thus, d_i independence of both lateral sums imply d_i independence of the PV Borel sum, and thus, renormalization scheme independence. Thus, analogously to what we saw in Eq. (B.14), we are interested in

$$I_{i,\pm} \equiv \frac{\partial}{\partial d_i} \int_{C_{\pm}} dt e^{-t/\alpha'} \hat{R}_{\text{an}}(t, d_j). \quad (\text{B.59})$$

The algebra is the same we had in the previous section, and therefore, following analogous steps, we arrive to an equation that is analogous to Eq. (B.22)

$$\frac{d}{dt}G_{d_i}(t) = e^{-t/\alpha'} \left\{ \frac{t}{\alpha'^2} \frac{\partial \alpha'}{\partial d_i} \sum_{n=0}^{\infty} \frac{r'_n}{n!} t^n + \sum_{n=0}^{\infty} \frac{\partial}{\partial d_i} r'_n \frac{1}{n!} t^n \right\}, \quad (\text{B.60})$$

where analogously to Eq. (B.16), we have defined

$$\frac{d}{dt}G_{d_i}(t) \equiv \frac{\partial}{\partial d_i} \left\{ e^{-t/\alpha'} \hat{R}_{\text{an}}(t, d_j) \right\}. \quad (\text{B.61})$$

Introducing Eqs. (B.55) and (B.57) in Eq. (B.60), we arrive at

$$\frac{d}{dt}G_{d_i}(t) = e^{-t/\alpha'} \left\{ \sum_{j=1}^{\infty} \sum_{n=0}^{\infty} \#_j^{(i)} \alpha'^j \frac{r'_n}{n!} t^{n+1} - \sum_{l=1}^{\infty} \sum_{m=0}^{\infty} \#_l^{(i)} r'_m \frac{m+1}{(m+l+1)!} t^{m+l+1} \right\}. \quad (\text{B.62})$$

Notice the similarity with Eq. (B.29). Both equations are the *same* equation with the correspondences

$$G_{d_i} \leftrightarrow G_{\tau}, \quad (\text{B.63})$$

$$\alpha' \leftrightarrow \alpha(\tau), \quad (\text{B.64})$$

$$r'_n \leftrightarrow r_n(\tau), \quad (\text{B.65})$$

$$b_j \leftrightarrow -\#_j^{(i)}. \quad (\text{B.66})$$

Therefore, everything that is done in the previous section after Eq. (B.29) can be recycled here using the dictionary displayed above. Thus, just as we had τ independence, we will also have d_i independence of the PV Borel sum of R , or in other words, independence in the renormalization scheme chosen for the strong gauge coupling.

Appendix C

The computation of $\Delta\Omega$

In this appendix, we will compute Eqs. (3.71) and (3.82). We start off with the IR case.

C.1 The IR case

The starting point in order to compute Eq. (3.71) is Eq. (3.70)

$$\Delta\Omega_{\text{IR}}(l) = Z_d \frac{\mu^d}{Q^d} \frac{1}{\Gamma(1+db-\gamma)} \left(\frac{\beta_0}{2\pi d} \right)^{N_{\text{P}}(d)+1} \alpha^{N_{\text{P}}(d)+2}(\mu) \text{PV} \int_0^\infty dx \frac{x^{db-\gamma+N_{\text{P}}(d)+1} e^{-x}}{1-x \frac{\beta_0 \alpha(\mu)}{2\pi d}}. \quad (\text{C.1})$$

We will review two methods. The first will use some relations found in Dingle's book [10], and in the second, we will expand around the singularity of the integrand of the equation above. Let us consider first the first method. Let us consider just the integral in the equation above and define

$$H \equiv \text{PV} \int_0^\infty dx \frac{x^{db-\gamma+N_{\text{P}}(d)+1} e^{-x}}{1-x \frac{\beta_0 \alpha(\mu)}{2\pi d}}. \quad (\text{C.2})$$

It can be seen that

$$H = \Gamma(db - \gamma + N_{\text{P}}(d) + 2) \bar{\Lambda}_{db-\gamma+N_{\text{P}}(d)+1}(-x), \quad (\text{C.3})$$

where

$$x \equiv \frac{2\pi d}{\beta_0 \alpha(\mu)}, \quad (\text{C.4})$$

and $\bar{\Lambda}_s(-x)$ is a formula found in page 407 on Dingle's book [10]. It reads

$$\bar{\Lambda}_s(-x) \equiv \frac{1}{\Gamma(s+1)} \text{PV} \int_0^\infty d\epsilon e^{-\epsilon} \frac{\epsilon^s}{1-\epsilon/x}. \quad (\text{C.5})$$

We will be interested in the case

$$s = db - \gamma + N_{\text{P}}(d) + 1. \quad (\text{C.6})$$

The procedure is the following, we will first obtain the small $\alpha(\mu)$ expansion of H , and then, we will use this to obtain the small $\alpha(\mu)$ expansion of $\Delta\Omega_{\text{IR}}(l)$. As we see in Eq. (C.3), H has two parts: a gamma function and the function of Eq. (C.5). Making use of the Stirling series of Eq. (1.1), we can write

$$\begin{aligned} \Gamma(db - \gamma + N_{\text{P}}(d) + 2) &\sim (2\pi)^{1/2} e^{-\frac{2\pi d}{\beta_0 \alpha(\mu)}} \left(\frac{2\pi d}{\beta_0 \alpha(\mu)} \right)^{1/2+1-\eta_c} \left(\frac{\beta_0 \alpha(\mu)}{2\pi d} \left[-\eta_c + \frac{2\pi d}{\beta_0 \alpha(\mu)} \right] \right)^{1/2-\eta_c} \\ &\times \exp \left(\frac{2\pi d}{\beta_0 \alpha(\mu)} \sum_{n=2}^{\infty} (-1)^{n+1} \frac{1}{n} \left\{ -\frac{\beta_0}{2\pi d} \eta_c \alpha(\mu) \right\}^n \right) \times \left\{ 1 + \frac{1}{12s} + \frac{1}{288s^2} + \mathcal{O}(s^{-3}) \right\}, \end{aligned} \quad (\text{C.7})$$

where we have defined $\eta_c \equiv -db + \gamma - 1 + \frac{2\pi dc}{\beta_0}$, and we again stress that $s \equiv db - \gamma + N_P(d) + 1$. In the expression above, we see that all the non analytic behavior in $\alpha(\mu)$ is in the first line, and the rest is ready to be expanded in $\alpha(\mu)$. Notice that the last braces in the above equation follow the same pattern as in Eq. (1.1). The term found in Eq. (C.5) will be worked out using some expressions found in [10]. We consider $\bar{\Lambda}_s(-x)$, and expand it around $x = s$

$$\bar{\Lambda}_s(-x) = \bar{\Lambda}_s(-s) + \frac{d}{dx} \bar{\Lambda}_s(-x) \Big|_{x=s} (x-s) + \frac{1}{2} \frac{d^2}{dx^2} \bar{\Lambda}_s(-x) \Big|_{x=s} (x-s)^2 + \dots, \quad (\text{C.8})$$

where notice that from Eqs. (C.6) and (C.4), we have that

$$x - s = -db + \gamma - 1 + \frac{2\pi dc}{\beta_0} = \eta_c \quad (\text{C.9})$$

is just a constant. In order to obtain $\bar{\Lambda}_s(-s)$, we employ equation (60) from page 419 of [10] that reads

$$\bar{\Lambda}_s(-s) = -\frac{1}{3} + \frac{4}{135s} + \frac{8}{2835s^2} - \frac{16}{8505s^3} - \frac{8992}{12629925s^4} + \frac{334144}{492567075s^5} + \frac{698752}{1477701225s^6} + \dots, \quad (\text{C.10})$$

which can be easily expanded in $\alpha(\mu)$. To obtain the derivatives in Eq. (C.8), we use the recursive relations found in equation (47) on page 416 in [10]

$$x\bar{\Lambda}_s^{(1)}(-x) = (s-x+1)\bar{\Lambda}_s(-x) + x, \quad (\text{C.11})$$

$$2x\bar{\Lambda}_s^{(2)}(-x) = (s-x)\bar{\Lambda}_s^{(1)}(-x) - \bar{\Lambda}_s(-x) + 1, \quad (\text{C.12})$$

$$nx\bar{\Lambda}_s^{(n)}(-x) = (s-x+2-n)\bar{\Lambda}_s^{(n-1)}(-x) - \bar{\Lambda}_s^{(n-2)}(-x) \quad \text{for } n > 2, \quad (\text{C.13})$$

where we have defined

$$\bar{\Lambda}_s^{(n)}(-x) \equiv \frac{1}{n!} \frac{d^n}{dx^n} \bar{\Lambda}_s(-x). \quad (\text{C.14})$$

with these pieces, it is easy to obtain the various derivatives of $\bar{\Lambda}_s(-x)$ at $x = s$, and hence, to construct the small $\alpha(\mu)$ expansion of $\bar{\Lambda}_s(-x)$. The first few orders read

$$\bar{\Lambda}_s(-x) = \eta_c - \frac{1}{3} + \alpha(\mu) \frac{\beta_0}{d\pi} \left\{ \frac{2}{135} - \frac{1}{6}\eta_c + \frac{1}{3}\eta_c^2 - \frac{1}{6}\eta_c^3 \right\} + \mathcal{O}(\alpha^2(\mu)). \quad (\text{C.15})$$

Combining Eqs. (C.7) and (C.15) in Eq. (C.3), we obtain

$$H = - \left(\frac{2\pi d}{\beta_0 \alpha(\mu)} \right)^{1-\eta_c + \frac{2\pi d}{\beta_0 \alpha(\mu)}} e^{\frac{-2\pi d}{\beta_0 \alpha(\mu)}} \alpha^{1/2}(\mu) \left\{ \frac{\beta_0^{1/2}}{d^{1/2}} \left[-\eta_c + \frac{1}{3} \right] + \alpha(\mu) \frac{\beta_0^{3/2}}{\pi d^{3/2}} \left[-\frac{1}{12}\eta_c^3 + \frac{1}{24}\eta_c - \frac{1}{1080} \right] \right. \\ \left. + \alpha^2(\mu) \frac{\beta_0^{5/2}}{\pi^2 d^{5/2}} \left[-\frac{1}{160}\eta_c^5 - \frac{1}{96}\eta_c^4 + \frac{1}{144}\eta_c^3 + \frac{1}{96}\eta_c^2 - \frac{1}{640}\eta_c - \frac{25}{24192} \right] + \mathcal{O}(\alpha^3(\mu)) \right\}. \quad (\text{C.16})$$

Plugging this in Eq. (C.1), we readily obtain

$$\Delta\Omega_{\text{IR}}(l) = -Z_d \frac{\mu^d}{Q^d} \frac{1}{\Gamma(1+db-\gamma)} \left(\frac{2\pi d}{\beta_0} \right)^{db-\gamma+1} e^{\frac{-2\pi d}{\beta_0 \alpha(\mu)}} \alpha^{1/2-db+\gamma}(\mu) \left\{ \frac{\beta_0^{1/2}}{d^{1/2}} \left[-\eta_c + \frac{1}{3} \right] \right. \\ \left. + \alpha(\mu) \frac{\beta_0^{3/2}}{\pi d^{3/2}} \left[-\frac{1}{12}\eta_c^3 + \frac{1}{24}\eta_c - \frac{1}{1080} \right] + \alpha^2(\mu) \frac{\beta_0^{5/2}}{\pi^2 d^{5/2}} \left[-\frac{1}{160}\eta_c^5 - \frac{1}{96}\eta_c^4 + \frac{1}{144}\eta_c^3 \right. \right. \\ \left. \left. + \frac{1}{96}\eta_c^2 - \frac{1}{640}\eta_c - \frac{25}{24192} \right] + \mathcal{O}(\alpha^3(\mu)) \right\}. \quad (\text{C.17})$$

C.1.1 An alternative method

There is one alternative method to compute this expansion, which we will now highlight. Let us come back to Eq. (C.2)

$$H = \text{PV} \int_0^\infty dx \frac{x^{db-\gamma+N_{\text{P}}(d)+1} e^{-x}}{1 - x \frac{\beta_0 \alpha(\mu)}{2\pi d}}. \quad (\text{C.18})$$

We will basically expand around a Gaussian term around the singularity in $x = \frac{2\pi d}{\beta_0 \alpha(\mu)}$. We first perform the variable change

$$y = -1 + \frac{\beta_0 \alpha(\mu)}{2\pi d} x, \quad (\text{C.19})$$

$$H = - \left(\frac{2\pi d}{\beta_0 \alpha(\mu)} \right)^{1-\eta_c + \frac{2\pi d}{\beta_0 \alpha(\mu)}} e^{\frac{-2\pi d}{\beta_0 \alpha(\mu)}} \text{PV} \int_{-1}^\infty dy \frac{1}{y} e^{\frac{-2\pi d}{\beta_0 \alpha(\mu)} y + (-\eta_c + \frac{2\pi d}{\beta_0 \alpha(\mu)}) \log(1+y)}. \quad (\text{C.20})$$

We assume the above integral to be dominated by its behavior around $y = 0$, and thus, expand the logarithm around $y = 0$

$$H \approx - \left(\frac{2\pi d}{\beta_0 \alpha(\mu)} \right)^{1-\eta_c + \frac{2\pi d}{\beta_0 \alpha(\mu)}} e^{\frac{-2\pi d}{\beta_0 \alpha(\mu)}} \text{PV} \int_{-1}^\infty dy \frac{1}{y} e^{\frac{-2\pi d}{\beta_0 \alpha(\mu)} y - (-\eta_c + \frac{2\pi d}{\beta_0 \alpha(\mu)}) \sum_{k=1}^\infty \frac{(-1)^k}{k} y^k}, \quad (\text{C.21})$$

where we employ the \approx symbol as the Taylor expansion we have employed only holds for $|y| < 1$. We now normalize everything with respect to the order y^2 term in the exponent above by changing variables

$$\zeta = y \left\{ \frac{1}{2} \left(-\eta_c + \frac{2\pi d}{\beta_0 \alpha(\mu)} \right) \right\}^{1/2}, \quad (\text{C.22})$$

so that

$$H \approx - \left(\frac{2\pi d}{\beta_0 \alpha(\mu)} \right)^{1-\eta_c + \frac{2\pi d}{\beta_0 \alpha(\mu)}} e^{\frac{-2\pi d}{\beta_0 \alpha(\mu)}} \times \text{PV} \int_{-\left\{ \frac{1}{2} \left(-\eta_c + \frac{2\pi d}{\beta_0 \alpha(\mu)} \right) \right\}^{1/2}}^\infty d\zeta \frac{1}{\zeta} e^{-\zeta^2} \\ \times \exp \left\{ \frac{-2^{1/2} \eta_c \alpha^{1/2}(\mu)}{\left(\frac{2\pi d}{\beta_0} - \alpha(\mu) \eta_c \right)^{1/2}} \zeta + \frac{2^{3/2} / 3 \alpha^{1/2}(\mu)}{\left(\frac{2\pi d}{\beta_0} - \alpha(\mu) \eta_c \right)^{1/2}} \zeta^3 + \frac{\alpha(\mu)}{\left(-\frac{2\pi d}{\beta_0} + \alpha(\mu) \eta_c \right)^{1/2}} \zeta^4 + \mathcal{O} \left(\alpha^{3/2}(\mu) \zeta^5 \right) \right\}. \quad (\text{C.23})$$

We can now expand the second exponential in the integrand above in powers of α and ζ . Extending the inferior limit of the integral to $-\infty$, we can integrate to obtain precisely the expansion in Eq. (C.16). We have no rigorous proof, but it seems unlikely that the series in Eq. (C.16) is anything but an asymptotic expansion. Notice that in order to derive it above, we have approximated $\log(1+y)$ with its small y behavior, and then commuted sum and integral, which typically yields asymptotic expansions. Notice also that in Eq. (C.3), we write H as a product of a gamma function and $\bar{\Lambda}_s$, where the gamma function is expanded using the asymptotic Stirling series.

C.2 The UV case

The computation of Eq. (3.82) runs parallel to what we have seen in the previous section. The starting point is Eq. (3.81)

$$\Delta\Omega_{\text{UV}}(l') = (-1)^{N_{\text{P}}(d)+1} Z_d \frac{Q^{|d|}}{\mu^{|d|}} \frac{1}{\Gamma(l'+1)} \left(\frac{\beta_0}{2\pi|d|} \right)^{N_{\text{P}}(d)+1} \alpha^{N_{\text{P}}(d)+2}(\mu) \int_0^\infty dx \frac{e^{-x} x^{N_{\text{P}}(d)+1+l'}}{1 + \frac{x\beta_0\alpha(\mu)}{2\pi|d|}}. \quad (\text{C.24})$$

Analogously to what we have done earlier, we define

$$J \equiv \int_0^\infty dx \frac{e^{-x} x^{N_{\text{P}}(d)+1+l'}}{1 + \frac{x\beta_0\alpha(\mu)}{2\pi|d|}}, \quad (\text{C.25})$$

for which we can write

$$J = \Gamma(l' + N_{\text{P}}(d) + 2)\Lambda_{l'+N_{\text{P}}(d)+1}(x), \quad (\text{C.26})$$

where x is given again by Eq. (C.4), and $\Lambda_s(x)$ is defined in equation (22) on page 407 of [10]

$$\Lambda_s(x) = \frac{1}{\Gamma(s+1)} \int_0^\infty d\epsilon e^{-\epsilon} \frac{\epsilon^s}{1+\epsilon/x}. \quad (\text{C.27})$$

We are interested in the case

$$s = l' + N_{\text{P}}(d) + 1. \quad (\text{C.28})$$

We use Eq. (C.7) for the gamma function again with the substitution $db - \gamma \rightarrow l'$. $\Lambda_s(x)$ is dealt with just as $\bar{\Lambda}_s(-x)$. We expand it around $x = s$

$$\Lambda_s(x) = \Lambda_s(s) + \frac{d}{dx}\Lambda(x)\Big|_{x=s} (x-s) + \frac{1}{2} \frac{d^2}{dx^2}\Lambda(x)\Big|_{x=s} (x-s)^2 + \dots, \quad (\text{C.29})$$

where now

$$x - s = -l' - 1 + \frac{2\pi|d|c}{\beta_0} \equiv \eta_c. \quad (\text{C.30})$$

$\Lambda_s(s)$ is obtained via equation (59) on page 419 of [10]

$$\Lambda_s(s) = \frac{1}{2} - \frac{1}{8s} + \frac{1}{32s^2} + \frac{1}{128s^3} - \frac{13}{512s^4} + \frac{47}{2048s^5} + \frac{73}{8192s^6} - \frac{2447}{32768s^7} + \dots \quad (\text{C.31})$$

We will again use the recursive relations of equation (46) on page 415 of [10] to obtain the various derivatives of $\Lambda_s(x)$

$$x\Lambda_s^{(1)}(x) = (s+x+1)\Lambda_s(x) - x, \quad (\text{C.32})$$

$$2x\Lambda_s^{(2)}(x) = (s+x)\Lambda_s^{(1)}(x) + \Lambda_s(x) - 1, \quad (\text{C.33})$$

$$nx\Lambda_s^{(n)}(x) = (s+x+2-n)\Lambda_s^{(n-1)}(x) + \Lambda_s^{(n-2)}(x) \quad \text{for } n > 2, \quad (\text{C.34})$$

where we have defined

$$\Lambda_s^{(n)}(x) \equiv \frac{1}{n!} \frac{d^n}{dx^n} \Lambda_s(x). \quad (\text{C.35})$$

With these expressions, it is simple to obtain the small $\alpha(\mu)$ expansion of $\Lambda_s(x)$. The first few orders read

$$\Lambda_s(x) = \frac{1}{2} + \frac{\beta_0}{16d\pi} \alpha(\mu)(-1 + 2\eta_c) + \frac{\beta_0^2}{128|d|^2\pi^2} \alpha^2(\mu)(1 - 6\eta_c + 4\eta_c^2) + \mathcal{O}(\alpha^3(\mu)). \quad (\text{C.36})$$

Therefore, combining Eqs. (C.36) and (C.7) in Eq. (C.26), we can write

$$J = e^{-\frac{2\pi|d|}{\beta_0\alpha(\mu)}} \left(\frac{2\pi|d|}{\beta_0\alpha(\mu)} \right)^{1-\eta_c + \frac{2\pi|d|}{\beta_0\alpha(\mu)}} \alpha^{1/2}(\mu) \left\{ \frac{\beta_0^{1/2}}{2|d|^{1/2}} + \frac{\beta_0^{3/2}}{24\pi|d|^{3/2}} \alpha(\mu) \left[-1 + 3\eta_c^2 \right] \right. \\ \left. + \frac{\beta_0^{5/2}}{2304\pi^2|d|^{5/2}} \alpha^2(\mu) \left[13 - 48\eta_c - 60\eta_c^2 + 48\eta_c^3 + 36\eta_c^4 \right] + \mathcal{O}(\alpha^3(\mu)) \right\}. \quad (\text{C.37})$$

Plugging this in Eq. (C.24), we obtain Eq. (3.82)

$$\Delta\Omega_{\text{UV}}(l') = (-1)^{N_{\text{P}}(d)+1} Z_d \frac{Q^{|d|}}{\mu^{|d|}} \frac{\pi^{1+l'} 2^{l'}}{\Gamma(l'+1)} \left(\frac{\beta_0}{|d|} \right)^{-l'-1/2} \alpha(\mu)^{1/2-l'} e^{-\frac{2\pi|d|}{\beta_0\alpha(\mu)}} \left\{ 1 + \frac{\alpha(\mu)}{\pi} \frac{\beta_0}{12|d|} \left[-1 + 3\eta_c^2 \right] \right. \\ \left. + \frac{\alpha^2(\mu)}{\pi^2} \frac{\beta_0^2}{1152|d|^2} \left[13 - 48\eta_c - 60\eta_c^2 + 48\eta_c^3 + 36\eta_c^4 \right] + \mathcal{O}(\alpha^3(\mu)) \right\}. \quad (\text{C.38})$$

Appendix D

Further contributions from the Borel plane in Method 2

In this chapter, we will prove Eq. (4.39)¹, which shows why Method 2 is not systematically improvable beyond the leading IR renormalon. In Eq. (4.39), we have seen how to relate the PV Borel sum of a formal series with the truncated series (when $N \rightarrow \infty$) through the leading IR renormalon. In doing so, we have considered the leading renormalon in Eq. (4.27). We will explore other terms in this section, and unfortunately, we will see that we cannot systematically improve on Eq. (4.39) by including them. We also assume that we only have singularities in the Borel plane located in the real line. The starting point is Eq. (4.26).

$$\text{PV} \int_0^\infty dt e^{\frac{-t}{\alpha(Q)}} \hat{R}(t) = \lim_{N \rightarrow \infty} R_N(\mu_N) + \text{PV} \int_{1/\chi'}^\infty dt e^{\frac{-t}{\alpha(Q)}} \hat{R}(t), \quad (\text{D.1})$$

where we need to explore the last term in the RHS above

$$\text{PV} \int_{1/\chi'}^\infty dt e^{\frac{-t}{\alpha(Q)}} \hat{R}(t). \quad (\text{D.2})$$

We will start by considering the subleading terms on the leading IR renormalon that we have neglected so far.

D.1 Subleading contributions from the leading IR renormalon

Let us come back to Eq. (4.30). So far, we have only considered the leading $j = 0$ term there, and we will now consider the full term associated to the leading IR renormalon. In this particular case, we will obtain systematic improvement. Thus, we consider

$$\text{PV} \int_{1/\chi'}^\infty dt e^{\frac{-t}{\alpha(Q)}} \Delta \hat{R}_{\text{IR}}^{(d_0)}(t) = Z_{d_0} \times \text{PV} \int_{\frac{2\pi d_0}{\beta_0} (1-c'\alpha(Q))}^\infty dt e^{\frac{-t}{\alpha(Q)}} \frac{1}{(1 - \frac{\beta_0}{2\pi d_0} t)^{1+l}} \sum_{j=0}^\infty w_j \left(1 - \frac{\beta_0}{2\pi d_0} t\right)^j. \quad (\text{D.3})$$

Notice that any $j \neq 0$ term is basically the $j = 0$ with the changes $Z_{d_0} \rightarrow Z_{d_0} w_j$ and $l \rightarrow l - j$. Therefore, we can recycle Eq. (4.34) with these changes, and obtain

$$\text{PV} \int_{1/\chi'}^\infty dt e^{\frac{-t}{\alpha(Q)}} \Delta \hat{R}_{\text{IR}}^{(d_0)}(t) = Z_{d_0} \frac{2\pi d_0}{\beta_0} \alpha^{-l}(Q) e^{\frac{-2\pi d_0}{\beta_0 \alpha(Q)}} \sum_{j=0}^\infty w_j \alpha^j(Q) \Psi|_{l \rightarrow l-j}, \quad (\text{D.4})$$

and we see that each further term in the series in j is subleading in $\alpha(Q)$.

¹This is equation (36) in Acoleten et al.'s paper [67], where it appeared first.

D.2 The analytic part of $\hat{R}(t)$

We now consider the analytic part of the Borel transform in Eq. (D.2)

$$\text{PV} \int_{\frac{2\pi d_0}{\beta_0}(1-c'\alpha(Q))}^{\infty} dt e^{\frac{-t}{\alpha(Q)}} \Delta \hat{R}_{\text{analytic}}(t), \quad (\text{D.5})$$

where notice that the PV above is superfluous, since we have no singularities in the integration path. In order to flesh out the $\alpha(Q)$ dependence of the above integral, we will expand the Borel transform around the leading IR renormalon (the function is analytic by construction so we can expand it anywhere we want)

$$\Delta \hat{R}_{\text{analytic}}(t) = \sum_{n=0}^{\infty} b_n \left(t - \frac{2\pi d_0}{\beta_0}\right)^n. \quad (\text{D.6})$$

and we perform the variable change

$$x = \frac{1}{\alpha(Q)} \left(t - \frac{2\pi d_0}{\beta_0}\right), \quad (\text{D.7})$$

which leads to

$$\text{PV} \int_{\frac{2\pi d_0}{\beta_0}(1-c'\alpha(Q))}^{\infty} dt e^{\frac{-t}{\alpha(Q)}} \Delta \hat{R}_{\text{analytic}}(t) = e^{\frac{-2\pi d_0}{\beta_0 \alpha(Q)}} \sum_{n=0}^{\infty} b_n \alpha^{n+1}(Q) \Gamma(n+1, \frac{-2\pi d_0}{\beta_0} c'). \quad (\text{D.8})$$

D.3 UV renormalons

We now consider UV renormalons in the Borel transform

$$\text{PV} \int_{\frac{2\pi d_0}{\beta_0}(1-c'\alpha(Q))}^{\infty} dt e^{\frac{-t}{\alpha(Q)}} \Delta \hat{R}_{\text{UV}}^{(d)}(t) = Z_d \int_{\frac{2\pi d_0}{\beta_0}(1-c'\alpha(Q))}^{\infty} dt e^{\frac{-t}{\alpha(Q)}} \frac{1}{(1 - \frac{\beta_0}{2\pi d} t)^{1+l_d}} \sum_{j=0}^{\infty} w_j^{(d)} \left(1 - \frac{\beta_0}{2\pi d} t\right)^j, \quad (\text{D.9})$$

where $d < 0$, and again, the PV is not needed, so we can forget about it. Due to the exponential suppression of the integrand, we can expect the integral to be dominated by its behavior around its lower end. Motivated by this, we expand around $t = \frac{2\pi d_0}{\beta_0}$

$$\frac{1}{(1 - \frac{\beta_0}{2\pi d} t)^{1+l_d-j}} = \sum_{n=0}^{\infty} \frac{1}{n!} \left(\frac{\beta_0}{2\pi d}\right)^n \frac{\Gamma(n+1+l_d-j)}{\Gamma(1+l_d-j)} \frac{1}{(1 - \frac{d_0}{d})^{n+l_d-j+1}} \left(t - \frac{2\pi d_0}{\beta_0}\right)^n, \quad (\text{D.10})$$

and thus, employing this expansion above in Eq. (D.9), and performing the variable change of Eq. (D.7), we obtain

$$\int_{\frac{2\pi d_0}{\beta_0}(1-c'\alpha(Q))}^{\infty} dt e^{\frac{-t}{\alpha(Q)}} \Delta \hat{R}_{\text{UV}}(t) = Z_d \sum_{n=0}^{\infty} \frac{1}{n!} \left(\frac{\beta_0}{2\pi d}\right)^n \Gamma(n+1, \frac{-2\pi d_0}{\beta_0} c') \alpha^{n+1}(Q) e^{\frac{-2\pi d_0}{\beta_0 \alpha(Q)}} \sum_{j=0}^{\infty} w_j^{(d)} \frac{\Gamma(n+1+l_d-j)}{\Gamma(1+l_d-j)} \frac{1}{(1 - \frac{d_0}{d})^{n+l_d-j+1}}. \quad (\text{D.11})$$

Looking at the above formula, we note first that any UV renormalon, regardless of the value of d , has the same parametric dependence in $\alpha(Q)$, and thus, we have no hierarchy in the contributions. We also note that the parametric dependence in $\alpha(Q)$ is the same as in Eq. (D.8), and therefore, all UV renormalons and the analytic part of the Borel transform have to be taken into account together, which is unfeasible in realistic cases.

D.4 Subleading IR renormalons

We will now explore the contribution to Eq. (D.2) of subleading IR renormalons, that is, those with $d > d_0$

$$\text{PV} \int_{\frac{2\pi d_0}{\beta_0}(1-c'\alpha(Q))}^{\infty} dt e^{\frac{-t}{\alpha(Q)}} \Delta \hat{R}_{\text{IR}}^{(d)}(t) = Z_d \times \text{PV} \int_{\frac{2\pi d_0}{\beta_0}(1-c'\alpha(Q))}^{\infty} dt e^{\frac{-t}{\alpha(Q)}} \frac{1}{(1 - \frac{\beta_0}{2\pi d}t)^{1+l_d}} \sum_{j=0}^{\infty} w_j^{(d)} \left(1 - \frac{\beta_0}{2\pi d}t\right)^j, \quad (\text{D.12})$$

where now $d > 0$. We again expect that the integral above to be dominated by its behavior around the lower edge, due to the exponential suppression of the integrand. Nevertheless, since now d is positive, we have a singularity present at $t = \frac{2\pi d}{\beta_0}$, and therefore, we will also take into account this region. Thus, we divide the integration path in two parts: between the leading IR renormalon and the one we are considering, and the rest

$$\begin{aligned} \text{PV} \int_{\frac{2\pi d_0}{\beta_0}(1-c'\alpha(Q))}^{\infty} dt e^{\frac{-t}{\alpha(Q)}} \Delta \hat{R}_{\text{IR}}^{(d)}(t) = & Z_d \left\{ \int_{\frac{2\pi d_0}{\beta_0}(1-c'\alpha(Q))}^{\frac{2\pi d}{\beta_0}(1-c'\alpha(Q))} dt e^{\frac{-t}{\alpha(Q)}} \frac{1}{(1 - \frac{\beta_0}{2\pi d}t)^{1+l_d}} \sum_{j=0}^{\infty} w_j^{(d)} \left(1 - \frac{\beta_0}{2\pi d}t\right)^j \right. \\ & \left. + \text{PV} \int_{\frac{2\pi d}{\beta_0}(1-c'\alpha(Q))}^{\infty} dt e^{\frac{-t}{\alpha(Q)}} \frac{1}{(1 - \frac{\beta_0}{2\pi d}t)^{1+l_d}} \sum_{j=0}^{\infty} w_j^{(d)} \left(1 - \frac{\beta_0}{2\pi d}t\right)^j \right\}. \quad (\text{D.13}) \end{aligned}$$

As we have said, the first integral in the RHS above will be dominated by its behavior around the lower edge. Thus, we expand as in Eq. (D.10), and extending the upper integration limit to infinity, we obtain

$$\begin{aligned} Z_d \int_{\frac{2\pi d_0}{\beta_0}(1-c'\alpha(Q))}^{\frac{2\pi d}{\beta_0}(1-c'\alpha(Q))} dt e^{\frac{-t}{\alpha(Q)}} \frac{1}{(1 - \frac{\beta_0}{2\pi d}t)^{1+l_d}} \sum_{j=0}^{\infty} w_j^{(d)} \left(1 - \frac{\beta_0}{2\pi d}t\right)^j = \\ Z_d \sum_{n=0}^{\infty} \frac{1}{n!} \left(\frac{\beta_0}{2\pi d}\right)^n \Gamma(n+1, \frac{-2\pi d_0}{\beta_0}c'\alpha^{n+1}(Q)) e^{\frac{-2\pi d_0}{\beta_0\alpha(Q)}} \sum_{j=0}^{\infty} w_j^{(d)} \frac{\Gamma(n+1+l_d-j)}{\Gamma(1+l_d-j)} \frac{1}{(1 - \frac{d_0}{d})^{n+l_d-j+1}}, \quad (\text{D.14}) \end{aligned}$$

where we find the same parametric dependence in $\alpha(Q)$ as for UV renormalons and the analytic part. The second integral in the RHS in Eq. (D.13) is the same expression as in Eq. (D.3), with the substitution $d_0 \rightarrow d$. Therefore, we can recycle Eq. (D.4), and perform $d_0 \rightarrow d$.

$$\begin{aligned} Z_d \times \text{PV} \int_{\frac{2\pi d_0}{\beta_0}(1-c'\alpha(Q))}^{\infty} dt e^{\frac{-t}{\alpha(Q)}} \frac{1}{(1 - \frac{\beta_0}{2\pi d}t)^{1+l_d}} \sum_{j=0}^{\infty} w_j^{(d)} \left(1 - \frac{\beta_0}{2\pi d}t\right)^j \\ = Z_d \frac{2\pi d}{\beta_0} \alpha^{-l_d}(Q) e^{\frac{-2\pi d}{\beta_0\alpha(Q)}} \sum_{j=0}^{\infty} w_j^{(d)} \alpha^j(Q) \Psi|_{l \rightarrow l_d - j, d_0 \rightarrow d}, \quad (\text{D.15}) \end{aligned}$$

and we see that the parametric dependence in $\alpha(Q)$ is even smaller than what we have seen so far with the rest of the terms. Nevertheless, due to Eq. (D.14), we still find that subleading renormalons contribute parametrically in $\alpha(Q)$ just as UV renormalons and the analytic term.

Appendix E

The computation of v_2

In this appendix, we will explicitly show the computation of Eqs. (4.72) and (4.74). We will basically adapt the steps of Sumino's papers [77, 78, 79, 80] to our particular cases. For context on the various expressions presented here, one should look subsection 4.2.1. We start with Eq. (4.72).

E.1 The $d = 1$, $\Delta = 1$ and $N = N_S$ case

The starting point is Eq. (4.66)

$$v_2(r\tilde{\Lambda}, d\Delta, N) = -\text{Im} \lim_{\eta \rightarrow 0} \int_0^\infty dk \frac{e^{ik\rho}}{k\rho} \frac{1}{-\log k - i\eta} \left[1 - \frac{d\Delta}{N} \log k \right]^N. \quad (\text{E.1})$$

We remind that $\rho = \tilde{\Lambda}r$. Using the Sokhotski-Plemelj theorem, we can trade the $i\eta$ for a PV, and write

$$v_2(r\tilde{\Lambda}, d\Delta, N) = -\frac{\pi}{\rho} \cos \rho - \text{PV} \int_0^\infty dk \frac{\sin(k\rho)}{k\rho} \frac{1}{-\log k} \left[1 - \frac{d\Delta}{N} \log k \right]^N. \quad (\text{E.2})$$

We will pick $d = \Delta = 1$ and $N = N_S$, as given by Eq. (4.70).

$$v_2(r\tilde{\Lambda}, 1, N_S) = -\frac{\pi}{\rho} \cos \rho - \text{PV} \int_0^\infty dk \frac{\sin(k\rho)}{k\rho} \frac{1}{-\log k} \left[1 - \frac{1}{N_S} \log k \right]^{N_S}. \quad (\text{E.3})$$

Let us ignore everything but the integral

$$I \equiv -\text{PV} \int_0^\infty dk \frac{\sin(k\rho)}{k\rho} \frac{1}{-\log k} \left[1 - \frac{1}{N_S} \log k \right]^{N_S}, \quad (\text{E.4})$$

which we will write as a complex exponential

$$I = -\lim_{\epsilon \rightarrow 0} \lim_{\delta \rightarrow 0} \text{Im} \int_{(\delta, 1-\epsilon) \cup (1+\epsilon, \infty)} dk \frac{e^{ik\rho}}{k\rho} \frac{1}{-\log k} \left[1 - \frac{1}{N_S} \log k \right]^{N_S}, \quad (\text{E.5})$$

where, for later convenience, we have explicitly shown various limits. Let us now recall that

$$\lim_{N_S \rightarrow \infty} \left[1 - \frac{1}{N_S} \log k \right]^{N_S} = \frac{1}{k}, \quad (\text{E.6})$$

and, therefore, by naively taking the $N_S \rightarrow \infty$ limit, we would write

$$\lim_{N_S \rightarrow \infty} I = -\lim_{\epsilon \rightarrow 0} \lim_{\delta \rightarrow 0} \text{Im} \int_{(\delta, 1-\epsilon) \cup (1+\epsilon, \infty)} dk \frac{e^{ik\rho}}{k^2\rho} \frac{1}{-\log k}. \quad (\text{E.7})$$

The order k^1 stemming (the order k^0 is real, and does not survive after taking the imaginary part) from the exponential above yields and integral that is divergent as $\delta \rightarrow 0$

$$-\lim_{\delta \rightarrow 0} \int_{(\delta, 1-\epsilon)} dk \frac{1}{k} \frac{1}{-\log k} = -\infty. \quad (\text{E.8})$$

The rest of contributions $\sim k^2, k^3$ and so on, are well behaved. This term is thus, the source of the divergence in v_2 as $N_S \rightarrow \infty$, and consequently, it will prove useful to explicitly subtract it

$$I = - \lim_{\epsilon \rightarrow 0} \lim_{\delta \rightarrow 0} \text{Im} \left\{ \int_{\delta}^{1-\epsilon} dk \frac{e^{ik\rho} - ik\rho}{k\rho} \frac{1}{-\log k} \left[1 - \frac{1}{N_S} \log k \right]^{N_S} \right. \\ \left. + \int_{\delta}^{1-\epsilon} dk \frac{i}{-\log k} \left[1 - \frac{1}{N_S} \log k \right]^{N_S} + \int_{1+\epsilon}^{\infty} dk \frac{e^{ik\rho}}{k\rho} \frac{1}{-\log k} \left[1 - \frac{1}{N_S} \log k \right]^{N_S} \right\}. \quad (\text{E.9})$$

We emphasize that in the way we have written the integral above, it is extremely important to take the imaginary part before taking the $\delta \rightarrow 0$ limit on the first integral because, otherwise, we get a divergent contribution in the IR stemming from the $\mathcal{O}(k^0)$ term coming from the exponential in the first integral. We can make things more flexible amputating this purely real divergence too without changing anything

$$I = - \lim_{\epsilon \rightarrow 0} \lim_{\delta \rightarrow 0} \text{Im} \left\{ \int_{\delta}^{1-\epsilon} dk \frac{e^{ik\rho} - 1 - ik\rho}{k\rho} \frac{1}{-\log k} \left[1 - \frac{1}{N_S} \log k \right]^{N_S} \right. \\ \left. + \int_{\delta}^{1-\epsilon} dk \frac{i}{-\log k} \left[1 - \frac{1}{N_S} \log k \right]^{N_S} + \int_{1+\epsilon}^{\infty} dk \frac{e^{ik\rho} - 1}{k\rho} \frac{1}{-\log k} \left[1 - \frac{1}{N_S} \log k \right]^{N_S} \right\}. \quad (\text{E.10})$$

We have also included the -1 in the $(1+\epsilon, \infty)$ integral because it changes nothing, since it will not survive taking the imaginary part, and because it will be convenient later. Now that the pathological term when $N_S \rightarrow \infty$ has been subtracted, we take the $N_S \rightarrow \infty$ limit whenever it is safe

$$I_{\text{large } N_S} = - \lim_{\epsilon \rightarrow 0} \lim_{\delta \rightarrow 0} \text{Im} \left\{ \int_{\delta}^{1-\epsilon} dk \frac{e^{ik\rho} - 1 - ik\rho}{k^2\rho} \frac{1}{-\log k} \right. \\ \left. + \int_{\delta}^{1-\epsilon} dk \frac{i}{-\log k} \left[1 - \frac{1}{N_S} \log k \right]^{N_S} + \int_{1+\epsilon}^{\infty} dk \frac{e^{ik\rho} - 1}{k^2\rho} \frac{1}{-\log k} \right\}. \quad (\text{E.11})$$

E.1.1 The $\log N_S$ term

At this point, we will deal with the second term in braces. Recall that, as we have said, in this term lies the divergence as $N_S \rightarrow \infty$

$$I_1 \equiv \int_{\delta}^{1-\epsilon} dk \frac{i}{-\log k} \left[1 - \frac{1}{N_S} \log k \right]^{N_S}. \quad (\text{E.12})$$

The above integral is pathological when $\epsilon \rightarrow 0$. Of course, this pathological behavior in ϵ will cancel out when the rest of the terms in Eq. (E.23) are taken into account, but for now, it is useful to flesh it out. This can be done by

$$I_1 = \int_{\delta}^{1-\epsilon} dk \frac{i}{-\log k} \left(\left[1 - \frac{1}{N_S} \log k \right]^{N_S} - 1 \right) + \int_{\delta}^{1-\epsilon} dk \frac{i}{-\log k}. \quad (\text{E.13})$$

The seeming singularity at $k = 1$ in the integrand in the first integral in the RHS above is just spurious, and thus, we can just take $\epsilon = 0$ there

$$I_1 = \int_{\delta}^1 dk \frac{i}{-\log k} \left(\left[1 - \frac{1}{N_S} \log k \right]^{N_S} - 1 \right) + \int_{\delta}^{1-\epsilon} dk \frac{i}{-\log k}. \quad (\text{E.14})$$

The last integral in the RHS above can be done analytically

$$\int_{\delta}^{1-\epsilon} dk \frac{i}{-\log k} = -i \text{LogIntegral}(1-\epsilon) + i \text{LogIntegral}(\delta), \quad (\text{E.15})$$

where we have used the Log integral function. It is known that $\text{LogIntegral}(0) = 0$, and therefore, we can forget about the last term in the RHS above. Expanding the remaining term around $\epsilon = 0$

$$\int_{\delta}^{1-\epsilon} dk \frac{i}{-\log k} = -i \log \epsilon - i\gamma_E + \mathcal{O}(\epsilon), \quad (\text{E.16})$$

where γ_E is the Euler-Mascheroni constant $\gamma_E \approx 0.5777$. Let's now deal with the first term in the RHS of Eq. (E.14). We have seen this integral to be pathological for $\delta \rightarrow 0$, when $N_S \rightarrow \infty$ has been taken. We will not take the $N_S \rightarrow \infty$ limit, but rather, we will extract the asymptotic behavior for large N_S . Thus, we can safely take $\delta = 0$, and proceed in the following way

$$I_2 \equiv -i \int_0^1 dk \frac{1}{\log k} \left(\left[1 - \frac{1}{N_S} \log k \right]^{N_S} - 1 \right). \quad (\text{E.17})$$

We change the integration variable

$$x = \log k \quad (\text{E.18})$$

$$I_2 = -i \int_{-\infty}^0 dx e^x \frac{1}{x} \left(\left[1 - \frac{x}{N_S} \right]^{N_S} - 1 \right) \quad (\text{E.19})$$

$$= -i \int_{-\infty}^0 dx e^x \frac{1}{x} \left(e^{N_S \log \left(1 - \frac{x}{N_S} \right)} - 1 \right) \quad (\text{E.20})$$

$$= -i \int_{-\infty}^0 dx e^x \frac{1}{x} \left(e^{-x - x^2/(2N_S) + \mathcal{O}(N_S^{-2})} - 1 \right) \quad (\text{E.21})$$

$$= -i \int_{-\infty}^0 dx \frac{1}{x} \left[e^{-x^2/2N_S + \mathcal{O}(N_S^{-2})} - e^x \right] = \frac{i}{2} (\gamma_E + \log(2N_S)) + \mathcal{O}(N_S^{-1/2}), \quad (\text{E.22})$$

and we see that we have succeeded in obtaining the logarithmic divergence in N_S . Gathering all the pieces, we so far have

$$I_{\text{large } N_S} = - \lim_{\epsilon \rightarrow 0} \lim_{\delta \rightarrow 0} \text{Im} \left\{ \int_{\delta}^{1-\epsilon} dk \frac{-i}{k - \log k} + \int_{(\delta, 1-\epsilon) \cup (1+\epsilon, \infty)} dk \frac{e^{ik\rho} - 1}{k^2 \rho} \frac{1}{-\log k} \right. \\ \left. - i \log \epsilon + \mathcal{O}(\epsilon) + \frac{i}{2} (-\gamma_E + \log(2N_S)) + \mathcal{O}(N_S^{-1/2}) \right\}. \quad (\text{E.23})$$

We will smoke out the ϵ behavior of the first line above by performing a Wick rotation to the imaginary k line on both integrals. Let us first define

$$\Xi \equiv \int_{(\delta, 1-\epsilon) \cup (1+\epsilon, \infty)} dk \frac{e^{ik\rho} - 1}{k^2 \rho} \frac{1}{-\log k}, \quad (\text{E.24})$$

$$\Phi \equiv \int_{\delta}^{1-\epsilon} dk \frac{i}{k \log k}, \quad (\text{E.25})$$

and, of course

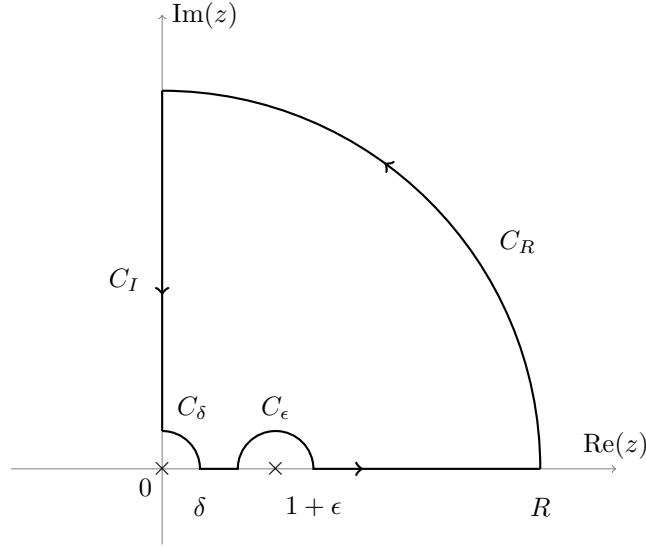
$$I_{\text{large } N_S} = - \lim_{\epsilon \rightarrow 0} \lim_{\delta \rightarrow 0} \text{Im} \left\{ \Phi + \Xi + \frac{i}{2} (-\gamma_E + \log(2N_S)) - i \log \epsilon + \mathcal{O}(\epsilon) \right\}. \quad (\text{E.26})$$

E.1.2 Wick rotating Ξ

Let's focus first on Ξ . We consider the following function

$$f(z) = \frac{e^{iz\rho} - 1}{z^2 \rho} \frac{1}{-\log z}, \quad (\text{E.27})$$

and we will Wick rotate it to the imaginary axis following this contour



Cauchy's theorem tells us

$$\Xi + \int_{C_I} dz f(z) + \int_{C_\epsilon} dz f(z) + \int_{C_\delta} dz f(z) + \int_{C_R} dz f(z) = 0. \quad (\text{E.28})$$

E.1.2.1 The path C_ϵ

$z = 1$ is a simple pole, and therefore, a well known theorem tells us that

$$\lim_{\epsilon \rightarrow 0} \int_{C_\epsilon} dz f(z) = -i\pi \text{Res}_{z=1}(f(z)) = i\pi \frac{e^{i\rho} - 1}{\rho}. \quad (\text{E.29})$$

E.1.2.2 The path C_δ

$$\int_{C_\delta} f(z) dz = \int_{C_\delta} dz \frac{e^{iz\rho} - 1}{z^2 \rho} \frac{1}{-\log z} \quad (\text{E.30})$$

$$= \sum_{n=1}^{\infty} \frac{1}{n!} \rho^{n-1} i^n \int_{C_\delta} dz z^{n-2} \frac{1}{-\log z} \quad (\text{E.31})$$

$$= \sum_{n=1}^{\infty} \frac{1}{n!} \rho^{n-1} i^{n+1} \delta^{n-1} \int_{\pi/2}^0 d\varphi e^{(n-1)i\varphi} \frac{1}{-\log(\delta e^{i\varphi})}. \quad (\text{E.32})$$

All the integrals above vanish except the one for $n = 1$, which leaves us with

$$\int_{C_\delta} f(z) dz = \pi + i \log(\log(i\delta)) - i \log(-\log \delta). \quad (\text{E.33})$$

E.1.2.3 The path C_R

An application of Jordan's lemma shows us that

$$\lim_{R \rightarrow \infty} \int_{C_R} dz f(z) = 0. \quad (\text{E.34})$$

E.1.2.4 The path C_I

We choose the parametrization $z(x) = \frac{ix}{\rho}$

$$\int_{C_I} dz f(z) = \int_{\delta\rho}^{\infty\rho} dx \frac{e^{-x} - 1}{x^2} \frac{-i}{\log\left(\frac{ix}{\rho}\right)}. \quad (\text{E.35})$$

E.1.2.5 Final result for Ξ

Summing up all the pieces, Cauchy's theorem yields

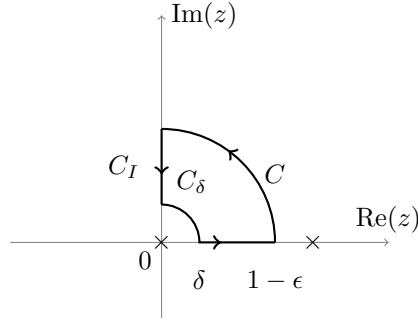
$$\Xi = -i\pi \frac{1}{\rho} (e^{i\rho} - 1) + \int_{\delta\rho}^{\infty\rho} dx \frac{e^{-x} - 1}{x^2} \frac{i}{\log \frac{ix}{\rho}} - \pi - i \log(\log(i\delta)) + i \log(-\log \delta). \quad (\text{E.36})$$

E.1.3 Wick rotating Φ

Let's Wick rotate Φ now. To this end, we consider

$$g(z) = \frac{i}{z \log z}, \quad (\text{E.37})$$

and the contour



Cauchy's theorem tells us

$$\Phi + \int_{C_I} dz g(z) + \int_{C_\delta} dz g(z) + \int_C dz g(z) = 0. \quad (\text{E.38})$$

E.1.3.1 The path C_I

We follow the path $z(x) = \frac{ix}{\rho}$. Thus

$$\int_{C_I} dz g(z) = \int_{\rho\delta}^{\rho(1-\epsilon)} dx \frac{-i}{x} \frac{1}{\log \left(\frac{ix}{\rho} \right)}. \quad (\text{E.39})$$

E.1.3.2 The path C

We follow the path $z(\varphi) = (1-\epsilon)e^{i\varphi}$

$$\int_C dz g(z) = \int_0^{\pi/2} d\varphi \frac{-1}{\log([1-\epsilon]e^{i\varphi})} = \pi - i \log(-\log(1-\epsilon)) + i \log(\log(i-i\epsilon)) = \frac{\pi}{2} + i \log \frac{\pi}{2} - i \log \epsilon + \mathcal{O}(\epsilon), \quad (\text{E.40})$$

and we see that the $-i \log \epsilon$ term will cancel the one in Eq. (E.26).

E.1.3.3 The path C_δ

We choose the parametrization $z(\varphi) = \delta e^{i\varphi}$

$$\int_{C_\delta} dz g(z) = \int_{\pi/2}^0 d\varphi \frac{-1}{\log(\delta e^{i\varphi})} = -\pi - i \log(\log(i\delta)) + i \log(-\log \delta), \quad (\text{E.41})$$

and we see that this term will cancel the singular behavior in δ in Eq. (E.36).

E.1.3.4 Final result for Φ

Summing up all the pieces, we get

$$\Phi = \int_{\delta\rho}^{(1-\epsilon)\rho} dx \frac{i}{x} \frac{1}{\log\left(\frac{ix}{\rho}\right)} - \frac{\pi}{2} - i \log \frac{\pi}{2} + i \log \epsilon + \mathcal{O}(\epsilon) + \pi + i \log(\log(i\delta)) - i \log(-\log \delta). \quad (\text{E.42})$$

We see that the part with logs of δ will cancel out with the analogous term in Ξ .

E.1.4 Final result

Gathering all the pieces, taking the imaginary part, and taking the $\epsilon \rightarrow 0$ limit in Eq. (E.26)

$$I_{\text{large } N_S} = \lim_{\delta \rightarrow 0} \left\{ \int_{\rho\delta}^{\infty} dx \frac{e^{-x} - 1}{x^2} \frac{\log \frac{\rho}{x}}{\log^2 \frac{\rho}{x} + \pi^2/4} + \int_{\rho\delta}^{\rho} dx \frac{x}{x^2} \frac{\log \frac{\rho}{x}}{\log^2 \frac{\rho}{x} + \frac{\pi^2}{4}} \right\} \quad (\text{E.43})$$

$$+ \frac{\pi}{\rho} (\cos \rho - 1) + \log \frac{\pi}{2} - \frac{1}{2} (-\gamma_E + \log 2 + \log N_S) + \mathcal{O}(N_S^{-1/2}). \quad (\text{E.44})$$

We have not taken the $\delta \rightarrow 0$ limit yet because each integral above is singular around $x = 0$ on its own. Of course, the singular behavior disappears when both terms are taken inside the same integral. Before doing that though, we will kick the awkward ρ in the second integral on the RHS of the first line above by noticing the immediate integral

$$\int dx \frac{1}{x} \frac{\log \frac{\rho}{x}}{\log^2 \frac{\rho}{x} + \frac{\pi^2}{4}} = -\frac{1}{2} \log \left(\pi^2 + 4 \log^2 \left(\frac{\rho}{x} \right) \right), \quad (\text{E.45})$$

which implies

$$\int_{\rho\delta}^{\rho} dx \frac{1}{x} \frac{\log \frac{\rho}{x}}{\log^2 \frac{\rho}{x} + \frac{\pi^2}{4}} = \int_{\rho\delta}^1 dx \frac{1}{x} \frac{\log \frac{\rho}{x}}{\log^2 \frac{\rho}{x} + \frac{\pi^2}{4}} - \log \frac{\pi}{2} + \frac{1}{2} \log \left(\log^2 \rho + \frac{\pi^2}{4} \right). \quad (\text{E.46})$$

Plugging now the above equation in Eq. (E.44), summing up both integrals, taking the $\delta \rightarrow 0$ limit, and plugging everything in Eq. (E.3), we obtain

$$v_2^{\text{large } N_S}(r\tilde{\Lambda}, 1, N_S) = \frac{-\pi}{\rho} + \int_0^{\infty} dx \frac{e^{-x} - 1 + x\theta(1-x)}{x^2} \frac{\log \frac{\rho}{x}}{\log^2 \frac{\rho}{x} + \pi^2/4} \quad (\text{E.47})$$

$$+ \frac{1}{2} \log \left(\log^2 \rho + \frac{\pi^2}{4} \right) - \frac{1}{2} (-\gamma_E + \log 2 + \log N_S) + \mathcal{O}(N_S^{-1/2}). \quad (\text{E.48})$$

where we have used a Kronecker delta to make the expression more compact. This equation is precisely Eq. (4.72).

E.2 The $d = 1$, $\Delta = 1 - c'\alpha(1/r)$ and $N = N_A$ case

Let us come back to Eq. (E.2), but this time, we pick $d = 1$, $\Delta = 1 - c'\alpha(1/r)$ and $N = N_A$. We emphasize again that we can take $N = N_A$ and be consistent with what is done in section 4.2, even though, in that case we have truncated at the order $\alpha^{N_A+1}(\mu(N_A))$, and in this one at $\alpha^{N_A}(\mu(N_A))$, because after taking the $N_A \rightarrow \infty$ limit, we get the same (finite) result. Therefore, Eq. (E.2) becomes in this case

$$v_2(r\tilde{\Lambda}, 1 - c'\alpha(1/r), N_A) = \frac{-\pi}{\rho} \cos \rho - \text{PV} \int_0^{\infty} dk \frac{\sin(k\rho)}{k\rho} \frac{1}{\log \frac{1}{k}} \left[1 + \frac{\Delta}{N_A} \log \frac{1}{k} \right]^{N_A}. \quad (\text{E.49})$$

Just like in the previous section, we are interested in the large order asymptotics of the expression above. We again notice that

$$\lim_{N_A \rightarrow \infty} \left[1 + \frac{\Delta}{N_A} \log \frac{1}{k} \right]^{N_A} = \frac{1}{k^\Delta}, \quad (\text{E.50})$$

where $\Delta < 1$. Taking this limit in the equation above

$$\lim_{N_A \rightarrow \infty} v_2(r\tilde{\Lambda}, 1 - c'\alpha(1/r), N_A) = \frac{-\pi}{\rho} \cos \rho - \text{PV} \int_0^\infty dk \frac{\sin(k\rho)}{k^{1+\Delta} \rho \log \frac{1}{k}}. \quad (\text{E.51})$$

In this case, and unlike in Eq. (E.7), there is no trouble in the integral above, nor around the origin, at infinity, or around the singularity at $k = 1$. This is due to Δ being smaller than one. If $\Delta = 1$, we have problems in the IR, as we have already seen. Thus, the large N_A asymptotics in this case is just given by the above equation

$$\lim_{N_A \rightarrow \infty} v_2(r\tilde{\Lambda}, 1 - c'\alpha(1/r), N_A) = \frac{-\pi}{\rho} \cos \rho - \text{PV} \int_0^\infty dk \frac{\sin(k\rho)}{k^{2-c'\alpha(1/r)} \rho \log \frac{1}{k}}. \quad (\text{E.52})$$

Nevertheless, we will again perform a Wick rotation to the imaginary k line, and by doing so, we will get rid of the PV in the integral. Before performing the Wick rotation, we will first write the sine above as a complex exponential. There is one problem, though, if one straightforwardly does that. If we write

$$\lim_{N_A \rightarrow \infty} v_2(r\tilde{\Lambda}, 1 - c'\alpha(1/r), N_A) = \frac{-\pi}{\rho} \cos \rho - \lim_{\epsilon \rightarrow 0} \lim_{\delta \rightarrow 0} \text{Im} \int_{(\delta, 1-\epsilon) \cup (1+\epsilon, \infty)} dk \frac{e^{ik\rho}}{k^{2-c'\alpha(1/r)} \rho \log \frac{1}{k}}, \quad (\text{E.53})$$

we are unable to commute the δ limit and the Im operation (and we are gonna want to do this) because the exponential has a $\sim k^0$ term that is absent in the sine, that makes the integral divergent in the IR. Consequently, we introduce a -1 that will kill this divergence, and that is irrelevant as it will not survive since it is real, but that allows us to commute operations

$$\lim_{N_A \rightarrow \infty} v_2(r\tilde{\Lambda}, 1 - c'\alpha(1/r), N_A) = \frac{-\pi}{\rho} \cos \rho - \lim_{\epsilon \rightarrow 0} \lim_{\delta \rightarrow 0} \text{Im} \int_{(\delta, 1-\epsilon) \cup (1+\epsilon, \infty)} dk \frac{e^{ik\rho} - 1}{k^{2-c'\alpha(1/r)} \rho \log \frac{1}{k}}, \quad (\text{E.54})$$

$$\lim_{N_A \rightarrow \infty} v_2(r\tilde{\Lambda}, 1 - c'\alpha(1/r), N_A) = \frac{-\pi}{\rho} \cos \rho - \text{Im} \lim_{\epsilon \rightarrow 0} \lim_{\delta \rightarrow 0} \int_{(\delta, 1-\epsilon) \cup (1+\epsilon, \infty)} dk \frac{e^{ik\rho} - 1}{k^{2-c'\alpha(1/r)} \rho \log \frac{1}{k}}. \quad (\text{E.55})$$

E.2.1 Wick rotation

Let us define

$$\Upsilon \equiv \int_{(\delta, 1-\epsilon) \cup (1+\epsilon, \infty)} dk \frac{e^{ik\rho} - 1}{k^{2-c'\alpha(1/r)} \rho \log \frac{1}{k}}, \quad (\text{E.56})$$

and of course, we have that

$$\lim_{N_A \rightarrow \infty} v_2(r\tilde{\Lambda}, 1 - c'\alpha(1/r), N_A) = \frac{-\pi}{\rho} \cos \rho - \text{Im} \lim_{\epsilon \rightarrow 0} \lim_{\delta \rightarrow 0} \Upsilon. \quad (\text{E.57})$$

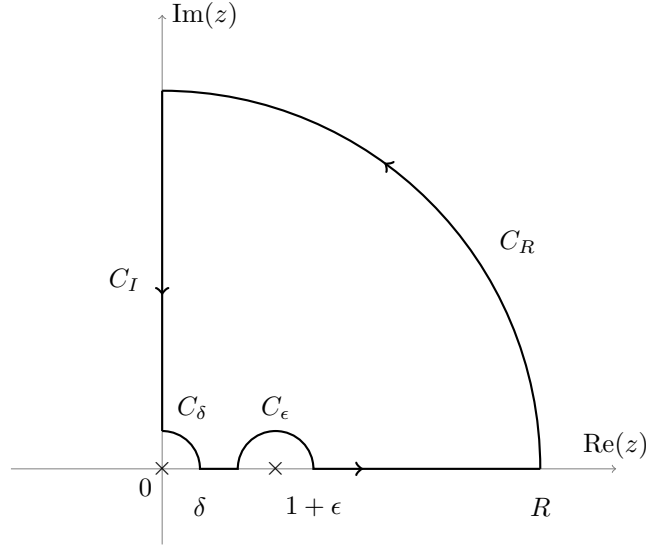
It is Υ what we will Wick rotate. In order to do that, we consider the complex function

$$F(z) = \frac{e^{iz\rho} - 1}{z^s \rho \log \frac{1}{z}}, \quad (\text{E.58})$$

where we have defined $s \equiv 2 - c'\alpha(1/r)$. By Cauchy's theorem

$$\Upsilon + \int_{C_\delta} dz F(z) + \int_{C_\epsilon} dz F(z) + \int_{C_R} dz F(z) + \int_{C_I} dz F(z), \quad (\text{E.59})$$

where we have considered the same contour as in Eq. (E.28)



E.2.1.1 The path C_ϵ

It is easy to verify that the singularity at $z = 1$ is a simple pole. Then, a well known theorem tells us that

$$\lim_{\epsilon \rightarrow 0} \int_{C_\epsilon} dz F(z) = -i\pi \text{Res}_{z=1} F(z) = -i\pi \frac{1}{\rho} (1 - e^{i\rho}). \quad (\text{E.60})$$

E.2.1.2 The path C_R

An application of Jordan's lemma tells us that

$$\lim_{R \rightarrow \infty} \int_{C_R} dz F(z) = 0. \quad (\text{E.61})$$

E.2.1.3 The path C_δ

$$\lim_{\delta \rightarrow 0} \int_{C_\delta} dz F(z) \quad (\text{E.62})$$

$$= \lim_{\delta \rightarrow 0} \int_{C_\delta} dz \frac{e^{iz\rho} - 1}{z^s \rho} \frac{1}{\log \frac{1}{z}} \quad (\text{E.63})$$

$$= \lim_{\delta \rightarrow 0} \int_{C_\delta} dz \frac{\sum_{n=1}^{\infty} \frac{1}{n!} (iz\rho)^n}{z^s \rho} \frac{1}{\log \frac{1}{z}} \quad (\text{E.64})$$

$$= \lim_{\delta \rightarrow 0} \sum_{n=1}^{\infty} \frac{1}{n!} \rho^{n-1} i^n \int_{C_\delta} dz z^{n-s} \frac{1}{\log \frac{1}{z}}, \quad (\text{E.65})$$

we pick the parametrization $z = \delta e^{i\theta}$

$$\lim_{\delta \rightarrow 0} \int_{C_\delta} dz F(z) = \lim_{\delta \rightarrow 0} \sum_{n=1}^{\infty} \frac{1}{n!} \rho^{n-1} i^{n+1} \delta^{n-s+1} \int_{\pi/2}^0 d\theta e^{i\theta(n-s+1)} \frac{1}{\log(\frac{1}{\delta} e^{-i\theta})} \quad (\text{E.66})$$

$$= \sum_{n=1}^{\infty} \frac{1}{n!} \rho^{n-1} i^{n+1} \lim_{\delta \rightarrow 0} \left(\delta^{n-s+1} \int_{\pi/2}^0 d\theta e^{i\theta(n-s+1)} \frac{1}{\log(\frac{1}{\delta} e^{-i\theta})} \right). \quad (\text{E.67})$$

It can be seen that

$$\lim_{\delta \rightarrow 0} \left\{ \delta^{n-s+1} \int_{\pi/2}^0 d\theta e^{i\theta(n-s+1)} \frac{1}{\log(\frac{1}{\delta} e^{-i\theta})} \right\} = 0, \quad (\text{E.68})$$

which leaves us with

$$\lim_{\delta \rightarrow 0} \int_{C_\delta} dz F(z) = 0. \quad (\text{E.69})$$

E.2.1.4 The path C_I

Let us deal with imaginary line. We pick the parametrization $z = \frac{ix}{\rho}$

$$\int_{C_I} dz F(z) \quad (\text{E.70})$$

$$= -i^{1-s} \rho^{s-2} \int_{\rho\delta}^{\rho\infty} dx \frac{e^{-x} - 1}{x^s} \frac{1}{\log\left(\frac{\rho}{xi}\right)}. \quad (\text{E.71})$$

E.2.1.5 Final result for Υ

Gathering all the pieces

$$\Upsilon = i\pi \frac{1}{\rho} (1 - e^{i\rho}) + i^{1-s} \rho^{s-2} \int_0^\infty dx \frac{e^{-x} - 1}{x^s} \frac{1}{\log\left(\frac{\rho}{xi}\right)}, \quad (\text{E.72})$$

where we have taken all the due limits since there is no issue in doing so. Thus, finishing up all the remaining algebra in Eq. (E.57), we finally arrive at

$$v_3 = \lim_{N_A \rightarrow \infty} v_2(r\tilde{\Lambda}, 1 - c'\alpha(1/r), N_A) = -\frac{\pi}{\rho} - \rho^{s-2} \int_0^\infty dx \frac{e^{-x} - 1}{x^s} \frac{\frac{\pi}{2} \cos\left(\frac{\pi}{2}[1-s]\right) + \log\frac{\rho}{x} \sin\left(\frac{\pi}{2}[1-s]\right)}{\log^2\frac{\rho}{x} + \frac{\pi^2}{4}}, \quad (\text{E.73})$$

which is precisely Eq. (4.74).

E.2.2 The $r \sim 0$ asymptotics

The goal of this section will be to show the computation of Eq. (4.78). In order to do that, we begin by recalling Eq. (4.77)

$$V_{\text{large } \beta_0}^{\text{PV}} - V_A = \frac{4C_F \tilde{\Lambda}}{\beta_0} \left\{ \frac{\pi}{r\tilde{\Lambda}} [1 - \cos(r\tilde{\Lambda})] + (\tilde{\Lambda}r)^{s-2} L \right\}, \quad (\text{E.74})$$

where

$$L \equiv \int_0^\infty dx \frac{e^{-x} - 1}{x^s} \frac{\frac{\pi}{2} \cos\left(\frac{\pi}{2}[1-s]\right) + \log\frac{\rho}{x} \sin\left(\frac{\pi}{2}[1-s]\right)}{\log^2\frac{\rho}{x} + \frac{\pi^2}{4}}. \quad (\text{E.75})$$

The idea is to obtain the $r \sim 0$ asymptotics of Eq. (E.74), which will get us an expansion in $\alpha(1/r)$. The first term in braces in Eq. (E.74) is trivial to handle

$$\frac{\pi}{r\tilde{\Lambda}} [1 - \cos(\tilde{\Lambda}r)] = \frac{\pi}{2} r\tilde{\Lambda} - \frac{\pi}{4!} r^3 \tilde{\Lambda}^3 + \frac{\pi}{6!} r^5 \tilde{\Lambda}^5 + \dots, \quad (\text{E.76})$$

and, therefore, for $r \sim 0$, we can neglect these power terms. We will now turn our attention to

$$(\tilde{\Lambda}r)^{s-2} L, \quad (\text{E.77})$$

and, in particular, to

$$(\tilde{\Lambda}r)^{s-2} = \left(e^{-c_X/2} e^{\frac{-2\pi}{\beta_0 \alpha}} \right)^{-c' \alpha}, \quad (\text{E.78})$$

$$= e^{\frac{2\pi c'}{\beta_0}} \left\{ 1 + \frac{1}{2} c' c_X \alpha + \frac{1}{8} c'^2 c_X^2 \alpha^2 + \mathcal{O}(\alpha^3) \right\}, \quad (\text{E.79})$$

where from now on, we will write α instead of $\alpha(1/r)$ to ease notation. We see that we have a power series expansion in α . Thus, all that remains to be done is to consider L . Notice now that

$$\frac{\frac{\pi}{2} \cos\left(\frac{\pi}{2}[1-s]\right) + \log\frac{\rho}{x} \sin\left(\frac{\pi}{2}[1-s]\right)}{\log^2\frac{\rho}{x} + \frac{\pi^2}{4}} = \text{Im} \left(e^{i\frac{\pi}{2}(1-s)} \frac{1}{\log\frac{\rho}{x} - \frac{i\pi}{2}} \right), \quad (\text{E.80})$$

which simplifies L to

$$L = \text{Im} \left(e^{i\frac{\pi}{2}(1-s)} \int_0^\infty dx \frac{e^{-x} - 1}{x^s} \frac{1}{\log \frac{\rho}{x} - \frac{i\pi}{2}} \right). \quad (\text{E.81})$$

Notice that

$$e^{i\frac{\pi}{2}(1-s)} = e^{i\frac{\pi}{2}(-1+c'\alpha)} = -ie^{i\frac{\pi}{2}c'\alpha} \quad (\text{E.82})$$

$$= -i + \frac{\pi}{2}c\alpha + \mathcal{O}(\alpha^2), \quad (\text{E.83})$$

which is another analytic function in α , so that we can ignore it for now, and just consider

$$J \equiv \int_0^\infty dx \frac{e^{-x} - 1}{x^s} \frac{1}{\log \frac{\rho}{x} - \frac{i\pi}{2}}. \quad (\text{E.84})$$

Making all the α dependence explicit

$$J = \int_0^\infty dx \frac{e^{-x} - 1}{x^{2-c'\alpha}} \frac{1}{-\frac{c_X}{2} - \frac{2\pi}{\beta_0\alpha} - \log x - \frac{i\pi}{2}}. \quad (\text{E.85})$$

It will prove convenient to split the integral in two

$$J = \int_0^1 dx \frac{e^{-x} - 1}{x^{2-c'\alpha}} \frac{1}{-\frac{c_X}{2} - \frac{2\pi}{\beta_0\alpha} - \log x - \frac{i\pi}{2}} + \int_1^\infty dx \frac{e^{-x} - 1}{x^{2-c'\alpha}} \frac{1}{-\frac{c_X}{2} - \frac{2\pi}{\beta_0\alpha} - \log x - \frac{i\pi}{2}}. \quad (\text{E.86})$$

We will name the first integral above J_1 , and the second J_2 , so that $J = J_1 + J_2$. We will further write

$$J_1 = \int_0^1 dx \frac{e^{-x} - 1}{x^{2-c'\alpha}} \frac{1}{-\frac{c_X}{2} - \frac{2\pi}{\beta_0\alpha} - \log x - \frac{i\pi}{2}} \quad (\text{E.87})$$

$$= \int_0^1 dx \frac{e^{-x} - 1 + x - x}{x^{2-c'\alpha}} \frac{1}{-\frac{c_X}{2} - \frac{2\pi}{\beta_0\alpha} - \log x - \frac{i\pi}{2}} \quad (\text{E.88})$$

$$= \int_0^1 dx \frac{e^{-x} - 1 + x}{x^{2-c'\alpha}} \frac{1}{-\frac{c_X}{2} - \frac{2\pi}{\beta_0\alpha} - \log x - \frac{i\pi}{2}} - \int_0^1 dx x^{-1+c'\alpha} \frac{1}{-\frac{c_X}{2} - \frac{2\pi}{\beta_0\alpha} - \log x - \frac{i\pi}{2}}. \quad (\text{E.89})$$

Focus on

$$- \int_0^1 dx x^{-1+c'\alpha} \frac{1}{-\frac{c_X}{2} - \frac{2\pi}{\beta_0\alpha} - \log x - \frac{i\pi}{2}} \quad (\text{E.90})$$

$$= \frac{1}{2} e^{\frac{-2\pi c'}{\beta_0}} e^{\frac{-1}{2}c'(c_X+i\pi)\alpha} \left\{ 2\text{Ei} \left(\frac{1}{2}c'(c_X+i\pi)\alpha + \frac{2c'\pi}{\beta_0} \right) + 2\log(c'\alpha) - \log \left(c'c_X\alpha + i\pi c'\alpha + \frac{4\pi c'}{\beta_0} \right) \right. \\ \left. - 2\log \left(\frac{-2\beta_0\alpha}{4\pi + (c_X+i\pi)\beta_0\alpha} \right) + \log \left(\frac{4\beta_0}{4\pi c' + c'(c_X+i\pi)\beta_0\alpha} \right) \right\}, \quad (\text{E.91})$$

where the integral has been carried out using Wolfram Mathematica. If one notices

$$2\log(c'\alpha) - 2\log \left(\frac{-2\beta_0\alpha}{4\pi + (c_X+i\pi)\beta_0\alpha} \right) = 2\log \left(\frac{2\pi c'}{\beta_0} \right) - 2\pi i + \frac{1}{2\pi}(c_X+i\pi)\beta_0\alpha + \mathcal{O}(\alpha^2), \quad (\text{E.92})$$

then, it is easy to expand Eq. (E.91) in α to obtain

$$- \int_0^1 dx x^{-1+c'\alpha} \frac{1}{-\frac{c_X}{2} - \frac{2\pi}{\beta_0\alpha} - \log x - \frac{i\pi}{2}} \quad (\text{E.93})$$

$$= -e^{\frac{-2\pi c'}{\beta_0}} \left[\pi i - \text{Ei} \left(\frac{2\pi c'}{\beta_0} \right) \right] - \frac{\alpha}{4}(c_X+i\pi) \left\{ \frac{-\beta_0}{\pi} + c' e^{\frac{-2\pi c'}{\beta_0}} \left[-2\pi i + 2\text{Ei} \left(\frac{2\pi c'}{\beta_0} \right) \right] \right\} + \mathcal{O}(\alpha^2). \quad (\text{E.94})$$

Let's now deal with the other part in equation Eq. (E.89)

$$\int_0^1 dx \frac{e^{-x} - 1 + x}{x^{2-c'\alpha}} \frac{1}{-\frac{c_X}{2} - \frac{2\pi}{\beta_0\alpha} - \log x - \frac{i\pi}{2}}. \quad (\text{E.95})$$

We will expand the integrand in α , and then, integrate term by term

$$\int_0^1 dx \frac{e^{-x} - 1 + x}{x^{2-c'\alpha}} \frac{1}{\frac{-c_X}{2} - \frac{2\pi}{\beta_0\alpha} - \log x - \frac{i\pi}{2}} \quad (\text{E.96})$$

$$= \alpha \frac{\beta_0}{2\pi} \left(\frac{1}{e} - \gamma_E + \text{Ei}(-1) \right) + \mathcal{O}(\alpha^2). \quad (\text{E.97})$$

This wraps up J_1 , which up til order α is

$$J_1 = -e^{-\frac{2\pi c'}{\beta_0}} \left[\pi i - \text{Ei}\left(\frac{2\pi c'}{\beta_0}\right) \right] + \alpha \left[\frac{\beta_0}{2\pi} \left(\frac{1}{e} - \gamma_E + \text{Ei}(-1) \right) - \frac{1}{4}(c_X + i\pi) \left\{ \frac{-\beta_0}{\pi} + c' e^{-\frac{2\pi c'}{\beta_0}} \left[-2\pi i + 2\text{Ei}\left(\frac{2\pi c'}{\beta_0}\right) \right] \right\} \right] + \mathcal{O}(\alpha^2). \quad (\text{E.98})$$

Let us turn our attention to J_2 now

$$J_2 = \int_1^\infty dx \frac{e^{-x} - 1}{x^{2-c'\alpha}} \frac{1}{\frac{-c_X}{2} - \frac{2\pi}{\beta_0\alpha} - \log x - \frac{i\pi}{2}}. \quad (\text{E.99})$$

We will again expand the integrand in α , and then, integrate term by term

$$J_2 = \alpha \frac{\beta_0}{2\pi} \left(\frac{-1}{e} + 1 - \text{Ei}(-1) \right) + \mathcal{O}(\alpha^2). \quad (\text{E.100})$$

Combining Eqs. (E.98) and (E.100), we obtain J

$$J = -e^{-\frac{2\pi c'}{\beta_0}} \left[\pi i - \text{Ei}\left(\frac{2\pi c'}{\beta_0}\right) \right] + \alpha \left[\frac{\beta_0}{2\pi} (1 - \gamma_E) - \frac{1}{4}(c_X + i\pi) \left\{ \frac{-\beta_0}{\pi} + c' e^{-\frac{2\pi c'}{\beta_0}} \left[-2\pi i + 2\text{Ei}\left(\frac{2\pi c'}{\beta_0}\right) \right] \right\} \right] + \mathcal{O}(\alpha^2). \quad (\text{E.101})$$

and, thus, from Eq. (E.81)

$$L = \text{Im} \left\{ \left(-i + \frac{\pi}{2} c' \alpha + \mathcal{O}(\alpha^2) \right) J \right\} \quad (\text{E.102})$$

$$= -e^{-\frac{2\pi c'}{\beta_0}} \text{Ei}\left(\frac{2\pi c'}{\beta_0}\right) + \alpha \left\{ \frac{-\beta_0}{2\pi} (1 - \gamma_E) - \frac{c_X \beta_0}{4\pi} + \frac{1}{2} c_X c' e^{-\frac{2\pi c'}{\beta_0}} \text{Ei}\left(\frac{2\pi c'}{\beta_0}\right) \right\} + \mathcal{O}(\alpha^2). \quad (\text{E.103})$$

Coming back to Eq. (E.77)

$$(\tilde{\Lambda} r)^{s-2} L \quad (\text{E.104})$$

$$= -\text{Ei}\left(\frac{2\pi c'}{\beta_0}\right) + \alpha e^{\frac{2\pi c'}{\beta_0}} \frac{\beta_0}{4\pi} (-2 - c_X + 2\gamma_E) + \mathcal{O}(\alpha^2), \quad (\text{E.105})$$

and finally, we can write

$$\left(V_{\text{large } \beta_0}^{\text{PV}} - V_A \right)_{r \sim 0} = \frac{4C_F \tilde{\Lambda}}{\beta_0} \left\{ -\text{Ei}\left(\frac{2\pi c'}{\beta_0}\right) + \alpha e^{\frac{2\pi c'}{\beta_0}} \frac{\beta_0}{4\pi} (-2 - c_X + 2\gamma_E) + \mathcal{O}(\alpha^2) \right\}, \quad (\text{E.106})$$

which is precisely Eq. (4.78).

Appendix F

The pole mass of a quark

The pole mass of a quark will be an important object in this thesis, so we will very briefly review some facts in this appendix. The pole mass of a quark is defined as a pole in the quark propagator. It is well known that it is IR finite and gauge independent in perturbation theory [145]. Let's first consider the case of QCD with one massive and n_l massless quarks, that is, $n_f = n_l + 1$. Obviously, the massive quark is the one whose pole mass we are considering. Let m_{OS} denote the pole mass, and let \bar{m} be the $\overline{\text{MS}}$ mass of the heavy quark whose pole mass we are considering (evaluated at its own scale $\bar{m}(\bar{m})$). Let us write the perturbative expansion of the relation between the pole and $\overline{\text{MS}}$ masses in the following way

$$m_{\text{OS}} = \bar{m} + \sum_{n=0}^{\infty} r_n \alpha^{n+1}(\bar{m}). \quad (\text{F.1})$$

Notice that we have evaluated the renormalization scale at $\mu = \bar{m}$. The coefficients $r_{0,1,2}$ are known analytically from [193], [146], [194], [195], [196], [197]. r_3 was computed in [149] and [198]. Displaying them

$$m_{\text{OS}} = \bar{m} + \bar{m} \left\{ \frac{\alpha(\bar{m})}{\pi} \frac{4}{3} + \left(\frac{\alpha(\bar{m})}{\pi} \right)^2 [-1.0414n_l + 13.4434] + \left(\frac{\alpha(\bar{m})}{\pi} \right)^3 [0.6527n_l^2 - 26.655n_l + 190.595] \right. \\ \left. + \left(\frac{\alpha(\bar{m})}{\pi} \right)^4 [-0.678141n_l^3 + 43.3963n_l^2 - (745.721 \pm 0.040)n_l + 3567.60 \pm 1.64] + \mathcal{O}(\alpha^5(\bar{m})) \right\}. \quad (\text{F.2})$$

We emphasize again, that the coefficients r_n above are written in the case $\mu = \bar{m}$, and can be written for arbitrary μ by re-expanding the series in $\alpha(\mu)$. We can also write the series above, where the expansion parameter is the strong coupling of QCD with n_l massless active quarks, by decoupling the heavy quark. This yields

$$m_{\text{OS}} = \bar{m} + \bar{m} \left\{ \frac{\alpha_{n_l}(\bar{m})}{\pi} \frac{4}{3} + \left(\frac{\alpha_{n_l}(\bar{m})}{\pi} \right)^2 \left[6.248 \frac{\beta_0(n_l)}{4} - 3.739 \right] \right. \\ \left. + \left(\frac{\alpha_{n_l}(\bar{m})}{\pi} \right)^3 \left[23.497 \frac{\beta_0^2(n_l)}{4^2} + 6.248 \frac{\beta_1(n_l)}{4^2} + 1.019 \frac{\beta_0(n_l)}{4} - 29.94 \right] \right. \\ \left. + \left(\frac{\alpha_{n_l}(\bar{m})}{\pi} \right)^4 \left[-0.678141n_l^3 + 43.3963n_l^2 - (745.721 \pm 0.040)n_l + 3567.60 \pm 1.64 \right. \right. \\ \left. \left. + n_l \left(\frac{11\pi^2}{648} + \frac{12295}{46656} \right) + \frac{83099\zeta(3)}{20736} - \frac{11\pi^2}{108} - \frac{209567}{23328} - \frac{11\pi^2 \log 2}{324} \right] + \mathcal{O}(\alpha_{n_l}^5(\bar{m})) \right\}, \quad (\text{F.3})$$

where α_{n_l} is the coupling of QCD with n_l active massless quarks.

F.1 The bottom quark pole mass

Let us consider now the particular case of the bottom quark. If we compute the pole mass using QCD with $n_f = 5 = 4 + 1$ active flavors, that is, with $n_l = 4$ massless and one massive quark (the bottom itself), the result

is of course Eq. (F.2). This formal series can be re-expanded in α_4 , that is, the coupling of QCD with 4 active massless quarks, and the result would be given by Eq. (F.3). We can improve on Eq. (F.3) by considering also massive charm quark effects δm_c on the pole mass of the bottom quark

$$m_{b,\text{OS}} = \bar{m}_b + \sum_{n=0}^{\infty} r_n^{(4)} \alpha_{(4)}^{n+1} + \delta m_c, \quad (\text{F.4})$$

where $r_n^{(4)}$ denotes the coefficients of Eq. (F.3) for the case $n_l = 4$. In [118], it was seen that the δm_c above yields a badly convergent series, but that the massive charm contributions can be rendered small by simply re-expanding the above series in terms of the strong coupling of QCD with three massless quarks $\alpha_{(3)}$

$$m_{b,\text{OS}} = \bar{m}_b + \sum_{n=0}^{\infty} r_n^{(3)} \alpha_{(3)}^{n+1} + \delta m_c. \quad (\text{F.5})$$

It was seen in the aforementioned reference, that the effects due to the massive charm in the above equation are ~ 2 MeV. When we work with the bottom quark in chapter 6, we will use the above equation.

F.2 Massive bottom and charm effects in the top quark pole mass

Just like for the bottom quark, the top quark pole mass also has corrections due to non-zero charm and bottom quark mass effects. Thus, we write

$$m_{t,\text{OS}} = \bar{m}_t + \sum_{n=0}^{\infty} r_n^{(5)} \alpha_{(5)}^{n+1} + \delta m_b^{(5)}(\bar{m}_t) + \delta m_c^{(5)}(\bar{m}_t) + \delta m_{bc}^{(5)}(\bar{m}_t). \quad (\text{F.6})$$

The $\mathcal{O}(\alpha^2)$ term of $\delta m_Q^{(n_f)}$ was computed in [146], and the $\mathcal{O}(\alpha^3)$ term in [147]. Note as well, that at $\mathcal{O}(\alpha^3)$ there is a new contribution including a vacuum polarization of the bottom and charm at the same time. We name it $\delta m_{bc}^{(5)}$, and it has been computed in [143]. They read¹

$$\delta m_{b/c}^{(5)} = \delta m_{b/c}^{(1)} \frac{\alpha_{(5)}^2(\bar{m})}{\pi^2} + \delta m_{b/c}^{(2,5/4)} \frac{\alpha_{(5)}^3(\bar{m})}{\pi^3}, \quad (\text{F.7})$$

$$\delta m_{bc}^{(5)} = \delta m_{bc}^{(2)} \frac{\alpha_{(5)}^3(\bar{m})}{\pi^3}, \quad (\text{F.8})$$

where the order $\alpha_{(5)}^2$ term reads

$$\begin{aligned} \delta m_q^{(1)} \equiv & \frac{\bar{m}}{3} \left\{ \left(1 - \frac{\bar{m}_q}{\bar{m}}\right) \left(1 - \frac{\bar{m}_q^3}{\bar{m}^3}\right) \left[\text{Li}_2\left(\frac{\bar{m}_q}{\bar{m}}\right) - \frac{1}{2} \log^2\left(\frac{\bar{m}_q}{\bar{m}}\right) + \log\left(1 - \frac{\bar{m}_q}{\bar{m}}\right) \log\left(\frac{\bar{m}_q}{\bar{m}}\right) - \frac{\pi^2}{3} \right] \right. \\ & + \left(1 + \frac{\bar{m}_q}{\bar{m}}\right) \left(1 + \frac{\bar{m}_q^3}{\bar{m}^3}\right) \left[\text{Li}_2\left(-\frac{\bar{m}_q}{\bar{m}}\right) - \frac{1}{2} \log^2\left(\frac{\bar{m}_q}{\bar{m}}\right) + \log\left(1 + \frac{\bar{m}_q}{\bar{m}}\right) \log\left(\frac{\bar{m}_q}{\bar{m}}\right) + \frac{\pi^2}{6} \right] \\ & \left. - \frac{\bar{m}_q^2}{\bar{m}^2} \left(\log\left(\frac{\bar{m}_q}{\bar{m}}\right) + \frac{3}{2} \right) + \log^2\left(\frac{\bar{m}_q}{\bar{m}}\right) + \frac{\pi^2}{6} \right\}, \end{aligned} \quad (\text{F.9})$$

where $\text{Li}_2(z)$ is the dilogarithm function. Notice that this term above is n_f -independent. The order $\alpha_{(5)}^3$ corrections are

$$\delta m_q^{(2,n_f)} = \frac{\bar{m}}{64} \left\{ h\left(\frac{\bar{m}_q}{\bar{m}}\right) + w\left(1, \frac{\bar{m}_q}{\bar{m}}\right) + n_{fp} \left(\frac{\bar{m}_q}{\bar{m}}\right) \right\}, \quad (\text{F.10})$$

$$\delta m_{bc}^{(2)} = \frac{\bar{m}}{64} w\left(\frac{\bar{m}_b}{\bar{m}}, \frac{\bar{m}_c}{\bar{m}}\right), \quad (\text{F.11})$$

¹Expressions for $\delta m_b^{(6)}$, $\delta m_c^{(6)}$ and $\delta m_{bc}^{(6)}$ can be found in [143].

where $n_f = 5$ for $q = b$, and $n_f = 4$ for $q = c$, and we use the representation for the functions $h(x)$, $w(x, y)$ and $p(x)$ given in [143]. They read

$$h(1) = 1870.7877, \quad (\text{F.12})$$

$$\begin{aligned} h(r) &= r(1486.55 - 1158.03 \log r) \\ &+ r^2(-884.044 - 683.967 \log r) + r^3(906.021 - 1126.84 \log r) \\ &+ r^4(225.158 + 11.4991 \log r - 80.3086 \log^2 r + 21.3333 \log^3 r) \\ &+ r^5(126.996 - 182.478 \log r) + r^6(-22.8899 + 38.3536 \log r - 54.5284 \log^2 r) \\ &+ r^7(15.3830 - 34.8914 \log r) + r^8(2.52528 - 3.82270 \log r - 20.4593 \log^2 r) + \mathcal{O}(r^9), \end{aligned} \quad (\text{F.13})$$

$$p(1) = -82.1208, \quad (\text{F.14})$$

$$p(r) = \frac{32}{27} \int_0^\infty dz \left\{ \frac{z}{2} + \left(1 - \frac{z}{2}\right) \left(1 + \frac{4}{z}\right)^{1/2} \right\} \text{P}\left(\frac{r^2}{z}\right) \left(\log z - \frac{5}{3}\right) \quad (\text{F.15})$$

$$\begin{aligned} &= r(-66.4668 + 70.1839 \log r) + r^2 14.2222 + r^3(14.4143 + 70.1839 \log r) \\ &+ r^4(-23.1242 + 18.0613 \log r + 15.4074 \log^2 r - 4.74074 \log^3 r) - r^5 31.5827 \\ &+ r^6(11.9886 - 1.70667 \log r) - 4.17761 r^7 + r^8(2.40987 - 0.161088 \log r) + \mathcal{O}(r^9), \end{aligned} \quad (\text{F.16})$$

$$w(1, 1) = 6.77871, \quad (\text{F.17})$$

$$\begin{aligned} w(1, r) &= r^2 14.2222 - r^3 18.7157 + r^4(7.36885 - 11.1477 \log r) \\ &+ r^6(3.92059 - 3.60296 \log r + 1.89630 \log^2 r) \\ &+ r^8(0.0837382 - 0.0772789 \log r + 0.457144 \log^2 r) + \mathcal{O}(r^9), \end{aligned} \quad (\text{F.18})$$

$$w(r_1, r_2) = p(r_2) + \frac{32}{27} \int_0^\infty dz \left\{ \frac{z}{2} + \left(1 - \frac{z}{2}\right) \left(1 + \frac{4}{z}\right)^{1/2} \right\} \text{P}\left(\frac{r_1^2}{z}\right) \text{P}\left(\frac{r_2^2}{z}\right), \quad (\text{F.19})$$

where

$$\text{P}(x) = \Pi(x) + \log x + \frac{5}{3}, \quad (\text{F.20})$$

$$\Pi(x) = \frac{1}{3} - (1 - 2x) \left\{ 2 - (1 + 4x)^{1/2} \log \left(\frac{(1 + 4x)^{1/2} + 1}{(1 + 4x)^{1/2} - 1} \right) \right\}. \quad (\text{F.21})$$

We can also write this non-zero charm and bottom quark mass corrections after decoupling the bottom and the charm quark. The expressions read

$$\delta m_b^{(4)} = \left[\delta m_b^{(1)} + \delta m_{b,\text{dec}}^{(1)} \right] \frac{\alpha_{(4)}^2(\overline{m})}{\pi^2} + \left[\delta m_b^{(2,5)} + \delta m_{b,\text{dec}}^{(2)} \right] \frac{\alpha_{(4)}^3(\overline{m})}{\pi^3}, \quad (\text{F.22})$$

$$\delta m_c^{(4)} = \delta m_c^{(1)} \frac{\alpha_{(4)}^2(\overline{m})}{\pi^2} + \delta m_c^{(2,4)} \frac{\alpha_{(4)}^3(\overline{m})}{\pi^3}, \quad (\text{F.23})$$

$$\delta m_{bc}^{(4)} = \left[\delta m_{bc}^{(2)} + \delta m_{bc,\text{dec}}^{(2)} \right] \frac{\alpha_{(4)}^3(\overline{m})}{\pi^3}, \quad (\text{F.24})$$

$$\delta m_b^{(3)} = \left[\delta m_b^{(1)} + \delta m_{b,\text{dec}}^{(1)} \right] \frac{\alpha_{(3)}^2(\overline{m})}{\pi^2} + \left[\delta m_b^{(2,5)} + \delta m_{b,\text{dec}}^{(2)} \right] \frac{\alpha_{(3)}^3(\overline{m})}{\pi^3}, \quad (\text{F.25})$$

$$\delta m_c^{(3)} = \left[\delta m_c^{(1)} + \delta m_{c,\text{dec}}^{(1)} \right] \frac{\alpha_{(3)}^2(\overline{m})}{\pi^2} + \left[\delta m_c^{(2,4)} + \delta m_{c,\text{dec}}^{(2)} \right] \frac{\alpha_{(3)}^3(\overline{m})}{\pi^3}, \quad (\text{F.26})$$

$$\delta m_{bc}^{(3)} = \left[\delta m_{bc}^{(2)} + \delta m_{bc,\text{dec}}^{(2)} + \delta m_{cb,\text{dec}}^{(2)} \right] \frac{\alpha_{(3)}^3(\overline{m})}{\pi^3}, \quad (\text{F.27})$$

where $\delta m_{(q,\text{dec})}^{(i)}$ are generated by the decoupling and read

$$\delta m_{(q,\text{dec})}^{(1)} = -\frac{2}{9}\bar{m} \left(\frac{71}{32} + \log \left(\frac{\bar{m}_q^2}{\bar{m}^2} \right) + \frac{\pi^2}{4} \right), \quad (\text{F.28})$$

$$\begin{aligned} \delta m_{(q,\text{dec})}^{(2,n_f)} &= \bar{m} \left\{ \left[\frac{2353}{11664} + \frac{7}{27}\zeta(3) + \frac{13\pi^2}{162} - \left(\frac{\pi^2}{54} + \frac{71}{432} \right) \log \left(\frac{\bar{m}^2}{\bar{m}_q^2} \right) \right] n_f + \frac{8\text{Li}_4\left(\frac{1}{2}\right)}{27} \right. \\ &\quad - \frac{751}{216}\zeta(3) + \frac{61\pi^4}{1944} - \frac{113\pi^2}{72} - \frac{29869}{2916} + \frac{\log^4(2)}{81} + \frac{2}{81}\pi^2 \log^2(2) - \frac{11}{81}\pi^2 \log(2) \\ &\quad \left. + \left(\frac{1225}{288} - \frac{1}{18}\zeta(3) + \frac{\pi^2}{9} + \frac{1}{27}\pi^2 \log(2) \right) \log \left(\frac{\bar{m}^2}{\bar{m}_q^2} \right) + \frac{1}{27} \log^2 \left(\frac{\bar{m}^2}{\bar{m}_q^2} \right) \right\} \\ &\quad + \frac{1}{3} \log \left(\frac{\bar{m}^2}{\bar{m}_q^2} \right) \delta m_q^{(1)}. \end{aligned} \quad (\text{F.29})$$

Note that $\delta m_{(b,\text{dec})}^{(2)} = \delta m_{(b,\text{dec})}^{(2,5)}$, and $\delta m_{(c,\text{dec})}^{(2)} = \delta m_{(b,\text{dec})}^{(2,4)}$. This last expression indeed corresponds to Eq. (17) of [118] changing \bar{m}_b by \bar{m} . Finally, we also have

$$\delta m_{bc,\text{dec}}^{(2)} = \frac{1}{3} \log \left(\frac{\bar{m}^2}{\bar{m}_b^2} \right) \delta m_c^{(1)}, \quad (\text{F.30})$$

$$\delta m_{cb,\text{dec}}^{(2)} = \frac{1}{3} \log \left(\frac{\bar{m}^2}{\bar{m}_c^2} \right) [\delta m_b^{(1)} + \delta m_{b,\text{dec}}^{(1)}]. \quad (\text{F.31})$$

Appendix G

pNRQCD

To provide some context on the expressions used throughout chapter 7, we provide here a very brief appendix devoted to the effective theory of QCD called pNRQCD [179, 180]. This appendix is not meant to be comprehensive, and we refer the reader to the original articles¹ for a more thorough treatment.

Bound states of a heavy quark and a heavy antiquark are known as *heavy quarkonium*. Examples include the J/ψ and the Υ mesons, which are bound states of charm-anticharm and bottom-antibottom quarks respectively. These heavy quarkonium systems are characterized by three widely separated scales: the hard scale given by m , the mass of the heavy quarks, the soft scale given by the typical relative momentum of the quark and the antiquark $|\mathbf{p}| \sim mv$, where $v \ll 1$, and the ultrasoft (US) scale, which is given by the typical kinetic energy $E \sim mv^2$ of the heavy quark and antiquark. Also, since quarks are heavy $m \gg \Lambda_{\text{QCD}}$. The hierarchy is $m \gg |\mathbf{p}| \gg E$ and $m \gg \Lambda_{\text{QCD}}$. This hierarchy of scales is fully exploited to construct pNRQCD, an EFT of QCD designed with heavy quarkonium systems in mind.

In order to construct it, one begins with QCD, and sets up a cut-off $\nu_{\text{NR}} = (\nu_{\text{p}}, \nu_{\text{s}})$, where ν_{p} is the cut-off of the relative three momentum of the heavy quark and antiquark, and ν_{s} is the cut-off of the energy of the heavy quark and antiquark. These cut-offs satisfy $E, |\mathbf{p}|, \Lambda_{\text{QCD}} \ll \nu_{\text{p/s}} \ll m$, so that the hard scales are integrated out. We are then left with NRQCD [201]. To go from NRQCD to pNRQCD, one also integrates out the soft scale by imposing the cut-off $\nu_{\text{pNR}} = (\nu_{\text{p}}, \nu_{\text{us}})$, where ν_{p} is again the cut-off of the relative three momentum of the heavy quarks, and ν_{us} is the cut-off of the energy of the heavy quark-antiquark pair. They satisfy the inequalities $|\mathbf{p}| \ll \nu_{\text{p}} \ll m$ and $\mathbf{p}^2/m \ll \nu_{\text{us}} \ll |\mathbf{p}|$. One distinguishes two cases depending on the relative size of $|\mathbf{p}|$ and Λ_{QCD} . The $|\mathbf{p}| \gg E \gtrsim \Lambda_{\text{QCD}}$ will be called weakly coupled pNRQCD, whereas the case $|\mathbf{p}| \sim \Lambda_{\text{QCD}}$ is called strongly coupled pNRQCD. We focus here on the weakly coupled version.

In the weak-coupling regime, the degrees of freedom of pNRQCD are heavy quark-antiquark pairs, gluons and light quarks with cut-off ν_{pNR} . These degrees of freedom can be represented with the same fields of NRQCD, namely Pauli spinors for the heavy quark and the heavy antiquark, Yang-mills gauge fields for gluons, and Dirac spinors for light quarks. Additionally, we can also use singlet $S(\mathbf{r}, \mathbf{R}, t)$ and octet $O(\mathbf{r}, \mathbf{R}, t)$ fields for the heavy quark-antiquark pair, where

$$\mathbf{R} = \frac{1}{m_1 + m_2} (m_1 \mathbf{x}_1 + m_2 \mathbf{x}_2), \quad (\text{G.1})$$

is the center of mass position, and the relative position is

$$\mathbf{r} = \mathbf{x}_1 - \mathbf{x}_2, \quad (\text{G.2})$$

¹This appendix draws mainly from the reviews [199, 200].

where $\mathbf{x}_1, \mathbf{x}_2$ and m_1, m_2 are the position and the masses of the quark and the antiquark. The most general action that can be written using singlet and octet fields, ultrasoft gluons and light quarks compatible with the symmetries of QCD to NLO in the multiple expansion is

$$\begin{aligned} \mathbb{I}_{\text{PNRQCD}}[\mathbf{S}, \mathbf{O}, A, \bar{q}, q] = & \int dt \int d^3R \left\{ \int d^3r \left(\text{Tr} \left[\mathbf{S}^\dagger (i\partial_0 - h_s(\mathbf{r}, \mathbf{p}, \mathbf{P}_R, \mathbf{S}_1, \mathbf{S}_2)) \mathbf{S} + \mathbf{O}^\dagger (iD_0 - h_o(\mathbf{r}, \mathbf{p}, \mathbf{P}_R, \mathbf{S}_1, \mathbf{S}_2)) \mathbf{O} \right] \right. \right. \\ & \left. \left. + gV_A(r) \text{Tr} \left[\mathbf{O}^\dagger \mathbf{r} \cdot \mathbf{E} \mathbf{S} + \mathbf{S}^\dagger \mathbf{r} \cdot \mathbf{E} \mathbf{O} \right] + g\frac{1}{2}V_B(r) \text{Tr} \left[\mathbf{O}^\dagger \mathbf{r} \cdot \mathbf{E} \mathbf{O} + \mathbf{O}^\dagger \mathbf{O} \mathbf{r} \cdot \mathbf{E} \right] \right) - \frac{1}{4}(G^a)_{\mu\nu}(G^a)^{\mu\nu} + \sum_{i=1}^{n_f} \bar{q}_i i\not{D} q_i \right\}. \end{aligned} \quad (\text{G.3})$$

There is a lot of information packed in the above expression, so we will now flesh it all out. Gluon and light quark fields are evaluated at the center of mass coordinate: $A_\mu(t, \mathbf{R}), q(t, \mathbf{R})$. For the singlet and octet fields, we choose the color normalizations

$$\mathbf{S} = \frac{\mathbb{1}_c}{N_c^{1/2}} S \quad \mathbf{O} = \frac{T^a}{T_F^{1/2}} O^a. \quad (\text{G.4})$$

For h_s and h_o , we have

$$h_s(\mathbf{r}, \mathbf{p}, \mathbf{P}_R, \mathbf{S}_1, \mathbf{S}_2) = \frac{\mathbf{p}^2}{2m_r} + \frac{\mathbf{P}_R^2}{2m_t} + V_s(\mathbf{r}, \mathbf{p}, \mathbf{P}_R, \mathbf{S}_1, \mathbf{S}_2), \quad (\text{G.5})$$

$$h_o(\mathbf{r}, \mathbf{p}, \mathbf{P}_R, \mathbf{S}_1, \mathbf{S}_2) = \frac{\mathbf{p}^2}{2m_r} + \frac{\mathbf{P}_R^2}{2m_t} + V_o(\mathbf{r}, \mathbf{p}, \mathbf{P}_R, \mathbf{S}_1, \mathbf{S}_2), \quad (\text{G.6})$$

where

$$m_r \equiv \frac{m_1 m_2}{m_1 + m_2}, \quad (\text{G.7})$$

$$m_t \equiv m_1 + m_2. \quad (\text{G.8})$$

Furthermore, $\mathbf{p} = -i\nabla_{\mathbf{r}}, \mathbf{P}_R = -i\nabla_{\mathbf{R}}$ when it acts on singlet fields, and $\mathbf{P}_R = -i\mathbf{D}_R$ when it acts on octet fields. We also have that

$$iD_0 \mathbf{O} = i\partial_0 \mathbf{O} - g[A_0(\mathbf{R}, t), \mathbf{O}]. \quad (\text{G.9})$$

Also, $\mathbf{S}_1 = \sigma_1/2$ and $\mathbf{S}_2 = \sigma_2/2$, where the sigmas are Pauli matrices. It is worth noticing the similarity between $h_{s/o}$ in Eqs. (G.5) and (G.6) and the Hamiltonian of a two body system in ordinary quantum mechanics. V_s and V_o are the singlet and octet potentials respectively. They can be expanded in an expansion in inverse powers of the heavy quark masses

$$V_s = V_s^{(0)} + \frac{V_s^{(1,0)}}{m_1} + \frac{V_s^{(0,1)}}{m_2} + \frac{V_s^{(2,0)}}{m_1^2} + \frac{V_s^{(0,2)}}{m_2^2} + \frac{V_s^{(1,1)}}{m_1 m_2} + \dots, \quad (\text{G.10})$$

$$V_o = V_o^{(0)} + \frac{V_o^{(1,0)}}{m_1} + \frac{V_o^{(0,1)}}{m_2} + \frac{V_o^{(2,0)}}{m_1^2} + \frac{V_o^{(0,2)}}{m_2^2} + \frac{V_o^{(1,1)}}{m_1 m_2} + \dots. \quad (\text{G.11})$$

In this thesis, we will only be concerned about the singlet static potential $V_s^{(0)}$. Therefore, to ease notation, we will often drop the subscript and the superscript, and simply call it V . We have seen in section 7.3 its explicit form. For V_A , it can be seen that [166, 167]

$$V_A = 1 + \mathcal{O}(\alpha^2), \quad (\text{G.12})$$

and therefore, for all practical purposes, we can set $V_A = 1$ in this thesis. V_B will not enter our expressions, so we will not bother about it. The octet static potential $V_o^{(0)}$ will only enter our expressions via

$$\Delta V \equiv V_o^{(0)} - V_s^{(0)} = \frac{C_A}{2} \frac{\alpha(\nu_s)}{r} \left\{ 1 + \frac{\alpha(\nu_s)}{4\pi} (a_1 + 2\beta_0 \log(\nu_s e^{\gamma_E} r)) + \mathcal{O}(\alpha^2(\nu_s)) \right\}, \quad (\text{G.13})$$

where $\gamma_E \approx 0.577$ is the Euler-Mascheroni constant, and a_1 is given in Eq. (7.17).

Appendix H

The r derivative of the singlet static energy with $\nu_S = \frac{x_S}{r}$ and $\nu_{US} = x_{US} \frac{C_A \alpha(\nu_S)}{2r}$

In chapter 7, we have performed many fits using the r derivative of the singlet static energy. This derivative has been taken assuming *constant* values of ν_S and ν_{US} . Nevertheless, we have typically set

$$\nu_S(r) = x_S/r, \quad (\text{H.1})$$

$$\nu_{US}(r) = x_{US} \frac{C_A \alpha(\nu_S(r))}{2r}, \quad (\text{H.2})$$

for some constant value of x_S and x_{US} . These expressions have r dependence, and therefore, one may wonder what happens if we set the r dependence given in Eqs. (H.1) and (H.2) *before* taking the r derivative. In this appendix, we show the expressions one obtains if this is done. The end result is that, whilst the building blocks of the derivative of the static energy do change, when adding them all up, the changes cancel out, leaving us with the same expressions. We will show this for the N³LL case.

Thus, we consider now the the singlet static energy with N³LL precision, with the soft and ultrasoft scales given by Eqs. (H.1) and (H.2). We then take an r derivative, and from the resulting expression only keep terms up to N³LL order

$$\mathcal{F}_{\text{N}^3\text{LL}}^{\text{new}} = \frac{d}{dr} V(r, \nu_S(r), \nu_S(r)) \Big|_{\text{N}^3\text{LO}} + \frac{d}{dr} \delta V_{\text{RG}}(r, \nu_S(r), \nu_{US}(r)) \Big|_{\text{N}^3\text{LL}} + \frac{d}{dr} \delta E_{\text{US}}^{\text{N}^3\text{LL}}(r, \nu_S(r), \nu_{US}(r)) \Big|_{\text{N}^3\text{LL}}. \quad (\text{H.3})$$

We have added the superscript *new* to distinguish it from the old expressions, where the r derivatives have been considered for constant ν_S and ν_{US} , and the r dependence given by Eqs. (H.1) and (H.2) has been considered after taking the r derivative. Defining for the first term on the RHS above

$$\frac{d}{dr} V(r, \nu_S(r), \nu_S(r)) \equiv \sum_{n=0}^{\infty} f_n^{\text{new}} \alpha^{n+1}(\nu_S(r)), \quad (\text{H.4})$$

we have

$$\begin{aligned} f_0^{\text{new}} &= \frac{C_F}{r^2}, & f_1^{\text{new}} &= \frac{C_F}{4\pi r^2} (a_1(r, \nu_S(r)) - 2\beta_0), \\ f_2^{\text{new}} &= \frac{C_F}{(4\pi)^2 r^2} (a_2(r, \nu_S(r)) - 4a_1(r, \nu_S(r))\beta_0 - 2\beta_1), \\ f_3^{\text{new}} &= \frac{C_F}{(4\pi)^3 r^2} (a_3(r, \nu_S(r), \nu_S(r)) - 6a_2(r, \nu_S(r))\beta_0 - 4a_1(r, \nu_S(r))\beta_1 - 2\beta_2). \end{aligned} \quad (\text{H.5})$$

From Eq. (7.63) we can deduce that the relation between the new force and the old is

$$\left. \frac{d}{dr} V(r, \nu_s(r), \nu_s(r)) \right|_{\text{N}^3\text{LO}} = \left. \frac{d}{dr} V(r, \nu_s, \nu_s) \right|_{\nu_s=\nu_s(r)} \Big|_{\text{N}^3\text{LO}} + C_F C_A^3 \frac{1}{12\pi r^2} \alpha^4(\nu_s(r)). \quad (\text{H.6})$$

For the second term in the RHS of Eq. (H.3)

$$\begin{aligned} \left. \frac{d}{dr} \delta V_{\text{RG}}(r, \nu_s(r), \nu_{\text{us}}(r)) \right|_{\text{N}^3\text{LL}} &= C_F C_A^3 \frac{1}{r^2} \alpha^3(\nu_s(r)) \left\{ -\frac{1}{6\beta_0} \log\left(\frac{\alpha(\nu_{\text{us}}(r))}{\alpha(\nu_s(r))}\right) \right. \\ &\quad \left. + \left(\frac{\pi}{4\beta_0} K + \frac{1}{12\pi}\right) \{\alpha(\nu_{\text{us}}(r)) - \alpha(\nu_s(r))\} + \frac{1}{8\pi} \left(2 - \frac{1}{\beta_0} [a_1 + 2\beta_0 \log(r\nu_s(r)e^{\gamma_E})]\right) \alpha(\nu_s(r)) \log\left(\frac{\alpha(\nu_{\text{us}}(r))}{\alpha(\nu_s(r))}\right) \right\}. \end{aligned} \quad (\text{H.7})$$

Recall that K has been defined in Eq. (7.32). Comparing with its analogous version Eq. (7.65), we find

$$\left. \frac{d}{dr} \delta V_{\text{RG}}(r, \nu_s(r), \nu_{\text{us}}(r)) \right|_{\text{N}^3\text{LL}} = \left. \frac{d}{dr} \delta V_{\text{RG}}(r, \nu_s, \nu_{\text{us}}) \right|_{\nu_s=\nu_s(r), \nu_{\text{us}}=\nu_{\text{us}}(r)} \Big|_{\text{N}^3\text{LL}} + C_F C_A^3 \frac{1}{12\pi r^2} \alpha^3(\nu_s(r)) \{\alpha(\nu_{\text{us}}(r)) - \alpha(\nu_s(r))\}. \quad (\text{H.8})$$

Considering now the last term on the RHS of Eq. (H.3)

$$\left. \frac{d}{dr} \delta E_{\text{us}}^{\text{N}^3\text{LL}}(r, \nu_s(r), \nu_{\text{us}}(r)) \right|_{\text{N}^3\text{LL}} = C_F C_A^3 \frac{1}{12\pi r^2} \alpha(\nu_{\text{us}}) \alpha^3(\nu_s) \left\{ -\log(x_{\text{us}}) + \log 2 - \frac{5}{6} \right\}. \quad (\text{H.9})$$

Comparing with its analogous version Eq. (7.68)

$$\left. \frac{d}{dr} \delta E_{\text{us}}^{\text{N}^3\text{LL}}(r, \nu_s(r), \nu_{\text{us}}(r)) \right|_{\text{N}^3\text{LL}} = \left. \frac{d}{dr} \delta E_{\text{us}}^{\text{N}^3\text{LL}}(r, \nu_s, \nu_{\text{us}}) \right|_{\nu_s=\nu_s(r), \nu_{\text{us}}=\nu_{\text{us}}(r)} \Big|_{\text{N}^3\text{LL}} - C_F C_A^3 \frac{1}{12\pi r^2} \alpha(\nu_{\text{us}}) \alpha^3(\nu_s). \quad (\text{H.10})$$

We see that adding up Eq. (H.6), Eq. (H.8) and Eq. (H.10) that the extra terms cancel out, and therefore, considering the r dependence before or after taking the r derivative leads to the same function.

Bibliography

- [1] F. J. Dyson, Phys. Rev. **85**, 631 (1952).
- [2] P. D. Miller, *Applied Asymptotic Analysis* (American Mathematical Society, 2006).
- [3] D. Sauzin, Introduction to 1-summability and resurgence, 2014, 1405.0356.
- [4] G. H. Hardy, *Divergent Series* (Oxford Clarendon Press, 1949).
- [5] E. Borel, Annales scientifiques de l'École Normale Supérieure **3e série**, **16**, 9 (1899).
- [6] M. Mariño, *Instantons and Large N: An Introduction to Non-Perturbative Methods in Quantum Field Theory* (Cambridge University Press, 2015).
- [7] G. 't Hooft, Subnucl. Ser. **15**, 943 (1979).
- [8] U. Aglietti and Z. Ligeti, Phys. Lett. **B364**, 75 (1995), hep-ph/9503209.
- [9] G. Darboux, Journal de Mathématiques Pures et Appliquées (1878).
- [10] R. B. Dingle, *Asymptotic Expansions: Their Derivation and Interpretation* (Academic Press, London, 1973).
- [11] F. W. J. Olver, *Asymptotics and Special Functions* (A. K. Peters, Wellesley, MA, 1997), pp. xviii+572, Reprint, with corrections, of original Academic Press edition, 1974.
- [12] M. V. Berry and C. J. Howls, Proc. R. Soc. **A 430**, 653 (1990).
- [13] M. Berry, *Asymptotics, Superasymptotics, Hyperasymptotics...* (Springer US, Boston, MA, 1991), pp. 1–14.
- [14] J. P. Boyd, Acta Appl. Math. **56**, 1 (1999).
- [15] J. Fischer, Int. J. Mod. Phys. A **12**, 3625 (1997), hep-ph/9704351.
- [16] J. Fischer, Acta Phys. Polon. B **27**, 2549 (1996), hep-ph/9512269.
- [17] C. M. Bender and T. T. WU, Phys. Rev. Lett. **27**, 461 (1971).
- [18] C. M. Bender and T. Wu, Phys. Rev. D **7**, 1620 (1973).
- [19] E. Brezin, J. Le Guillou, and J. Zinn-Justin, Phys. Rev. D **15**, 1544 (1977).
- [20] D. J. Gross and V. Periwal, Phys. Rev. Lett. **60**, 2105 (1988).
- [21] C. M. Bender and T. T. Wu, Phys. Rev. Lett. **37**, 117 (1976).

- [22] M. Mariño and T. Reis, *JHEP* **07**, 216 (2020), 1912.06228.
- [23] C. Pazarbaşı and D. Van Den Bleeken, *JHEP* **08**, 096 (2019), 1906.07198.
- [24] A. A. Penin and A. A. Pivovarov, *Phys. Lett. B* **401**, 294 (1997), hep-ph/9612204.
- [25] C. Lam, *Nuovo Cim. A* **55**, 258 (1968).
- [26] L. Lipatov, *Sov. Phys. JETP* **45**, 216 (1977).
- [27] G. Parisi, *Phys. Lett. B* **66**, 167 (1977).
- [28] Y. Sumino, *Understanding Interquark Force and Quark Masses in Perturbative QCD*, 2014, 1411.7853.
- [29] A. Pineda, *Heavy quarkonium and nonrelativistic effective field theories*, PhD thesis, 1998.
- [30] M. Beneke and V. M. Braun, *Nucl. Phys. B* **426**, 301 (1994), hep-ph/9402364.
- [31] P. Ball, M. Beneke, and V. M. Braun, *Nucl. Phys. B* **452**, 563 (1995), hep-ph/9502300.
- [32] M. Neubert, *Phys. Rev. D* **51**, 5924 (1995), hep-ph/9412265.
- [33] K. G. Wilson, *Phys. Rev.* **179**, 1499 (1969).
- [34] K. Wilson and W. Zimmermann, *Commun. Math. Phys.* **24**, 87 (1972).
- [35] W. Zimmermann, *Annals Phys.* **77**, 570 (1973).
- [36] M. A. Shifman, A. Vainshtein, and V. I. Zakharov, *Nucl. Phys. B* **147**, 385 (1979).
- [37] M. A. Shifman, A. Vainshtein, and V. I. Zakharov, *Nucl. Phys. B* **147**, 448 (1979).
- [38] M. A. Shifman, A. Vainshtein, and V. I. Zakharov, *Nucl. Phys. B* **147**, 519 (1979).
- [39] V. Novikov, M. A. Shifman, A. Vainshtein, and V. I. Zakharov, *Nucl. Phys. B* **174**, 378 (1980).
- [40] R. Tarrach, *Nucl. Phys. B* **196**, 45 (1982).
- [41] J. C. Collins, A. Duncan, and S. D. Joglekar, *Phys. Rev. D* **16**, 438 (1977).
- [42] S. Narison and R. Tarrach, *Phys. Lett. B* **125**, 217 (1983).
- [43] G. Parisi, *Phys. Lett. B* **76**, 65 (1978).
- [44] A. H. Mueller, *Nucl. Phys. B* **250**, 327 (1985).
- [45] G. Grunberg, *Phys. Lett. B* **325**, 441 (1994).
- [46] M. Beneke and V. M. Braun, p. 1719 (2000), hep-ph/0010208.
- [47] M. Beneke, *Phys. Rept.* **317**, 1 (1999), hep-ph/9807443.
- [48] M. Beneke and M. Jamin, *JHEP* **09**, 044 (2008), 0806.3156.

- [49] J. Écalle, *Les fonctions résurgentes. Tome I* (Université de Paris-Sud Département de Mathématique, Orsay, 1981).
- [50] J. Écalle, *Les fonctions résurgentes. Tome II* (Université de Paris-Sud Département de Mathématique, Orsay, 1981).
- [51] J. Écalle, *Les fonctions résurgentes. Tome III* (Université de Paris-Sud Département de Mathématique, Orsay, 1985).
- [52] G. A. Edgar, *Transseries for beginners*, 2009, 0801.4877.
- [53] J. Zinn-Justin, *Phys. Rept.* **70**, 109 (1981).
- [54] A. Voros, *Annales de l'I.H.P. Physique théorique* **39**, 211 (1983).
- [55] A. Voros, *Annales de l'institut Fourier* **43**, 1509 (1993).
- [56] E. Delabaere and F. Pham, *Annales de l'I.H.P. Physique théorique* **71**, 1 (1999).
- [57] U. D. Jentschura and J. Zinn-Justin, *Phys. Lett. B* **596**, 138 (2004), hep-ph/0405279.
- [58] G. V. Dunne and M. Unsal, *JHEP* **11**, 170 (2012), 1210.2423.
- [59] G. V. Dunne and M. Ünsal, *Phys. Rev. D* **87**, 025015 (2013), 1210.3646.
- [60] P. Argyres and M. Unsal, *Phys. Rev. Lett.* **109**, 121601 (2012), 1204.1661.
- [61] P. C. Argyres and M. Unsal, *JHEP* **08**, 063 (2012), 1206.1890.
- [62] M. Shifman, *J. Exp. Theor. Phys.* **120**, 386 (2015), 1411.4004.
- [63] G. V. Dunne, M. Shifman, and M. Unsal, *Phys. Rev. Lett.* **114**, 191601 (2015), 1502.06680.
- [64] P. M. Stevenson, *Nucl. Phys. B* **231**, 65 (1984).
- [65] J. Chyla and C. Burdik, *Czech. J. Phys.* **40**, 367 (1990).
- [66] J. Chyla, *Czech. J. Phys.* **42**, 263 (1992).
- [67] K. Van Acoleyen and H. Verschelde, *Phys. Rev. D* **69**, 125006 (2004), hep-ph/0307070.
- [68] C. Ayala, X. Lobregat, and A. Pineda, *Phys. Rev.* **D99**, 074019 (2019), 1902.07736.
- [69] C. Ayala, X. Lobregat, and A. Pineda, *Hyperasymptotic approximation to the operator product expansion, in 22nd High-Energy Physics International Conference in Quantum Chromodynamics (QCD 19) Montpellier, Languedoc, France, July 2-5, 2019*, 2019, 1910.04090.
- [70] C. Ayala, X. Lobregat, and A. Pineda, *Phys. Rev. D* **101**, 034002 (2020), 1909.01370.
- [71] M. Luscher and P. Weisz, *Nucl. Phys. B* **452**, 234 (1995), hep-lat/9505011.
- [72] A. Hasenfratz and P. Hasenfratz, p. 241 (1980).

- [73] P. Weisz, Phys. Lett. B **100**, 331 (1981).
- [74] S. Capitani, M. Lüscher, R. Sommer, and H. Wittig, Nucl. Phys. B **544**, 669 (1999), hep-lat/9810063, [Erratum: Nucl.Phys.B 582, 762–762 (2000)].
- [75] C. Maxwell, Phys. Rev. D **28**, 2037 (1983).
- [76] P. M. Stevenson, Phys. Rev. D **23**, 2916 (1981).
- [77] Y. Sumino, Phys. Lett. B **571**, 173 (2003), hep-ph/0303120.
- [78] Y. Sumino, Renormalon cancellation and perturbative QCD potential as a Coulomb plus linear potential, in *International Conference on Color Confinement and Hadrons in Quantum Chromodynamics - Confinement 2003*, 2003, hep-ph/0310093.
- [79] Y. Sumino, Phys. Lett. B **595**, 387 (2004), hep-ph/0403242.
- [80] Y. Sumino, Phys. Rev. D **76**, 114009 (2007), hep-ph/0505034.
- [81] C. Ayala, X. Lobregat, and A. Pineda, JHEP **12**, 093 (2020), 2009.01285.
- [82] Gattringer, Christof and Lang, Christian B. *Quantum chromodynamics on the lattice* Vol. 788 (Springer, Berlin, 2010).
- [83] K. G. Wilson, Phys. Rev. D **10**, 45 (1974).
- [84] A. Di Giacomo and G. Rossi, Phys. Lett. B **100**, 481 (1981).
- [85] B. Alles, M. Campostrini, A. Feo, and H. Panagopoulos, Phys. Lett. B **324**, 433 (1994), hep-lat/9306001.
- [86] B. Alles, A. Feo, and H. Panagopoulos, Phys. Lett. B **426**, 361 (1998), hep-lat/9801003, [Erratum: Phys.Lett.B 553, 337–338 (2003)].
- [87] F. Di Renzo, G. Marchesini, P. Marenzoni, and E. Onofri, Nucl. Phys. B Proc. Suppl. **34**, 795 (1994).
- [88] F. Di Renzo, E. Onofri, G. Marchesini, and P. Marenzoni, Nucl. Phys. B **426**, 675 (1994), hep-lat/9405019.
- [89] F. Di Renzo and L. Scorzato, JHEP **10**, 073 (2004), hep-lat/0410010.
- [90] F. Di Renzo, E. Onofri, and G. Marchesini, Nucl. Phys. B **457**, 202 (1995), hep-th/9502095.
- [91] P. E. Rakow, PoS **LAT2005**, 284 (2006), hep-lat/0510046.
- [92] E.-M. Ilgenfritz *et al.*, PoS **LAT2009**, 236 (2009), 0910.2795.
- [93] R. Horsley *et al.*, Phys. Rev. D **86**, 054502 (2012), 1205.1659.
- [94] G. S. Bali, C. Bauer, and A. Pineda, Phys. Rev. **D89**, 054505 (2014), 1401.7999.
- [95] A. Vainshtein, V. I. Zakharov, and M. A. Shifman, JETP Lett. **27**, 55 (1978).
- [96] A. Di Giacomo, H. Panagopoulos, and E. Vicari, Phys. Lett. B **240**, 423 (1990).

- [97] A. Di Giacomo, H. Panagopoulos, and E. Vicari, Nucl. Phys. B **338**, 294 (1990).
- [98] C. Christou, A. Feo, H. Panagopoulos, and E. Vicari, Nucl. Phys. B **525**, 387 (1998), hep-lat/9801007, [Erratum: Nucl.Phys.B 608, 479–480 (2001)].
- [99] A. Bode and H. Panagopoulos, Nucl. Phys. B **625**, 198 (2002), hep-lat/0110211.
- [100] G. S. Bali, C. Bauer, A. Pineda, and C. Torrero, Phys. Rev. D **87**, 094517 (2013), 1303.3279.
- [101] G. S. Bali, C. Bauer, and A. Pineda, PoS **LATTICE2013**, 371 (2014), 1311.0114.
- [102] M. Guagnelli, R. Petronzio, and N. Tantalo, Phys. Lett. B **548**, 58 (2002), hep-lat/0209112.
- [103] J. Kripfganz, Phys. Lett. B **101**, 169 (1981).
- [104] T. Banks, R. Horsley, H. Rubinstein, and U. Wolff, Nucl. Phys. B **190**, 692 (1981).
- [105] A. Di Giacomo and G. Paffuti, Phys. Lett. B **108**, 327 (1982).
- [106] E.-M. Ilgenfritz and M. Muller-Preussker, Phys. Lett. B **119**, 395 (1982).
- [107] X.-D. Ji, (1995), hep-ph/9506413.
- [108] G. Burgio, F. Di Renzo, G. Marchesini, and E. Onofri, Phys. Lett. B **422**, 219 (1998), hep-ph/9706209.
- [109] R. Horsley, P. E. Rakow, and G. Schierholz, Nucl. Phys. B Proc. Suppl. **106**, 870 (2002), hep-lat/0110210.
- [110] Y. Meurice, Phys. Rev. D **74**, 096005 (2006), hep-lat/0609005.
- [111] T. Lee, Phys. Rev. D **82**, 114021 (2010), 1003.0231.
- [112] G. S. Bali, C. Bauer, and A. Pineda, Phys. Rev. Lett. **113**, 092001 (2014), 1403.6477.
- [113] S. Necco and R. Sommer, Nucl. Phys. B **622**, 328 (2002), hep-lat/0108008.
- [114] G. Boyd *et al.*, Nucl. Phys. B **469**, 419 (1996), hep-lat/9602007.
- [115] L. Del Debbio, F. Di Renzo, and G. Filaci, Eur. Phys. J. C **78**, 974 (2018), 1807.09518.
- [116] C. Peset, A. Pineda, and J. Segovia, JHEP **09**, 167 (2018), 1806.05197.
- [117] A. V. Manohar and M. B. Wise, *Heavy Quark Physics* (Cambridge University Press, 2000).
- [118] C. Ayala, G. Cvetič, and A. Pineda, JHEP **09**, 045 (2014), 1407.2128.
- [119] C. Ayala, G. Cvetič, and A. Pineda, J. Phys. Conf. Ser. **762**, 012063 (2016), 1606.01741.
- [120] Particle Data Group, M. Tanabashi *et al.*, Phys. Rev. D **98**, 030001 (2018).
- [121] Fermilab Lattice, MILC, TUMQCD, A. Bazavov *et al.*, Phys. Rev. D **98**, 054517 (2018), 1802.04248.
- [122] A. Pineda, JHEP **06**, 022 (2001), hep-ph/0105008.

- [123] I. I. Y. Bigi, M. A. Shifman, N. G. Uraltsev, and A. I. Vainshtein, Phys. Rev. D **50**, 2234 (1994), hep-ph/9402360.
- [124] M. Beneke, Phys. Lett. B **434**, 115 (1998), hep-ph/9804241.
- [125] T. Lee, JHEP **10**, 044 (2003), hep-ph/0304185.
- [126] T. Lee, Phys. Rev. D **67**, 014020 (2003), hep-ph/0210032.
- [127] T. Lee, Phys. Rev. D **73**, 054505 (2006), hep-ph/0511238.
- [128] TUMQCD, N. Brambilla, J. Komijani, A. S. Kronfeld, and A. Vairo, Phys. Rev. D **97**, 034503 (2018), 1712.04983.
- [129] J. Komijani, JHEP **08**, 062 (2017), 1701.00347.
- [130] T. Lee, Phys. Rev. D **56**, 1091 (1997), hep-th/9611010.
- [131] A. H. Hoang *et al.*, JHEP **04**, 003 (2018), 1704.01580.
- [132] C. Bauer, G. S. Bali, and A. Pineda, Phys. Rev. Lett. **108**, 242002 (2012), 1111.3946.
- [133] M. Beneke, P. Marquard, P. Nason, and M. Steinhauser, Phys. Lett. B **775**, 63 (2017), 1605.03609.
- [134] A. Pineda, (2017), 1704.05095.
- [135] G. S. Bali, C. Bauer, and A. Pineda, PoS **LATTICE2011**, 222 (2011), 1111.6158.
- [136] L. D. McLerran and B. Svetitsky, Phys. Rev. D **24**, 450 (1981).
- [137] A. Duncan *et al.*, Phys. Rev. D **51**, 5101 (1995), hep-lat/9407025.
- [138] APE, C. R. Allton *et al.*, Nucl. Phys. B Proc. Suppl. **42**, 385 (1995), hep-lat/9502013.
- [139] UKQCD, A. K. Ewing *et al.*, Phys. Rev. D **54**, 3526 (1996), hep-lat/9508030.
- [140] ATLAS, CDF, CMS, D0, (2014), 1403.4427.
- [141] CMS, V. Khachatryan *et al.*, Phys. Rev. D **93**, 072004 (2016), 1509.04044.
- [142] ATLAS, M. Aaboud *et al.*, Phys. Lett. B **761**, 350 (2016), 1606.02179.
- [143] A. H. Hoang, C. Lepenik, and M. Preisser, JHEP **09**, 099 (2017), 1706.08526.
- [144] G. Corcella, Front. in Phys. **7**, 54 (2019), 1903.06574.
- [145] A. S. Kronfeld, Phys. Rev. D **58**, 051501 (1998), hep-ph/9805215.
- [146] N. Gray, D. J. Broadhurst, W. Grafe, and K. Schilcher, Z. Phys. C **48**, 673 (1990).
- [147] S. Bekavac, A. Grozin, D. Seidel, and M. Steinhauser, JHEP **10**, 006 (2007), 0708.1729.
- [148] M. Neubert, Phys. Lett. B **393**, 110 (1997), hep-ph/9610471.

- [149] P. Marquard, A. V. Smirnov, V. A. Smirnov, and M. Steinhauser, *Phys. Rev. Lett.* **114**, 142002 (2015), 1502.01030.
- [150] M. Cheng *et al.*, *Phys. Rev. D* **77**, 014511 (2008), 0710.0354.
- [151] A. Bazavov *et al.*, *Phys. Rev. D* **86**, 114031 (2012), 1205.6155.
- [152] JLQCD, T. Kaneko *et al.*, *PoS LATTICE2013*, 125 (2014), 1311.6941.
- [153] A. Bazavov *et al.*, *Phys. Rev. D* **90**, 074038 (2014), 1407.8437, [Erratum: *Phys.Rev.D* 101, 119902 (2020)].
- [154] A. Bazavov, P. Petreczky, and J. H. Weber, *Phys. Rev. D* **97**, 014510 (2018), 1710.05024.
- [155] TUMQCD, A. Bazavov, N. Brambilla, P. Petreczky, A. Vairo, and J. H. Weber, *Phys. Rev. D* **98**, 054511 (2018), 1804.10600.
- [156] F. Karbstein, M. Wagner, and M. Weber, *Phys. Rev. D* **98**, 114506 (2018), 1804.10909.
- [157] J. H. Weber, A. Bazavov, and P. Petreczky, *PoS Confinement2018*, 166 (2019), 1811.12902.
- [158] TUMQCD, A. Bazavov *et al.*, *Phys. Rev. D* **100**, 114511 (2019), 1907.11747.
- [159] W. Fischler, *Nucl. Phys. B* **129**, 157 (1977).
- [160] Y. Schroder, *Phys. Lett. B* **447**, 321 (1999), hep-ph/9812205.
- [161] N. Brambilla, A. Pineda, J. Soto, and A. Vairo, *Phys. Rev. D* **60**, 091502 (1999), hep-ph/9903355.
- [162] S. G. Gorishnii, A. L. Kataev, and S. A. Larin, *Phys. Lett. B* **273**, 141 (1991), [Erratum: *Phys.Lett.B* 275, 512 (1992), Erratum: *Phys.Lett.B* 341, 448 (1995)].
- [163] A. V. Smirnov, V. A. Smirnov, and M. Steinhauser, *Phys. Lett. B* **668**, 293 (2008), 0809.1927.
- [164] C. Anzai, Y. Kiyo, and Y. Sumino, *Phys. Rev. Lett.* **104**, 112003 (2010), 0911.4335.
- [165] A. V. Smirnov, V. A. Smirnov, and M. Steinhauser, *Phys. Rev. Lett.* **104**, 112002 (2010), 0911.4742.
- [166] A. Pineda and J. Soto, *Phys. Lett. B* **495**, 323 (2000), hep-ph/0007197.
- [167] N. Brambilla, A. Vairo, X. Garcia i Tormo, and J. Soto, *Phys. Rev. D* **80**, 034016 (2009), 0906.1390.
- [168] A. Pineda and M. Stahlhofen, *Phys. Rev. D* **84**, 034016 (2011), 1105.4356.
- [169] N. Brambilla, X. Garcia i Tormo, J. Soto, and A. Vairo, *Phys. Lett. B* **647**, 185 (2007), hep-ph/0610143.
- [170] A. Pineda, *Phys. Rev. D* **84**, 014012 (2011), 1101.3269.
- [171] R. N. Lee, A. V. Smirnov, V. A. Smirnov, and M. Steinhauser, *Phys. Rev. D* **94**, 054029 (2016), 1608.02603.
- [172] A. Pineda, *J. Phys. G* **29**, 371 (2003), hep-ph/0208031.
- [173] S. Necco and R. Sommer, *Phys. Lett. B* **523**, 135 (2001), hep-ph/0109093.
- [174] S. Recksiegel and Y. Sumino, *Phys. Rev. D* **65**, 054018 (2002), hep-ph/0109122.

- [175] N. Brambilla, X. Garcia i Tormo, J. Soto, and A. Vairo, *Phys. Rev. Lett.* **105**, 212001 (2010), 1006.2066, [Erratum: *Phys.Rev.Lett.* 108, 269903 (2012)].
- [176] H. Takaura, T. Kaneko, Y. Kiyo, and Y. Sumino, *Phys. Lett. B* **789**, 598 (2019), 1808.01632.
- [177] H. Takaura, T. Kaneko, Y. Kiyo, and Y. Sumino, *JHEP* **04**, 155 (2019), 1808.01643.
- [178] C. Ayala, X. Lobregat, and A. Pineda, *JHEP* **09**, 016 (2020), 2005.12301.
- [179] A. Pineda and J. Soto, *Nucl. Phys. B Proc. Suppl.* **64**, 428 (1998), hep-ph/9707481.
- [180] N. Brambilla, A. Pineda, J. Soto, and A. Vairo, *Nucl. Phys. B* **566**, 275 (2000), hep-ph/9907240.
- [181] T. Appelquist, M. Dine, and I. J. Muzinich, *Phys. Lett. B* **69**, 231 (1977).
- [182] T. Appelquist, M. Dine, and I. J. Muzinich, *Phys. Rev. D* **17**, 2074 (1978).
- [183] Y. Sumino and H. Takaura, *JHEP* **05**, 116 (2020), 2001.00770.
- [184] T. Lee, *Phys. Lett. B* **462**, 1 (1999), hep-ph/9908225.
- [185] T. van Ritbergen, J. Vermaseren, and S. Larin, *Phys. Lett. B* **400**, 379 (1997), hep-ph/9701390.
- [186] P. Baikov, K. Chetyrkin, and J. Kühn, *Phys. Rev. Lett.* **118**, 082002 (2017), 1606.08659.
- [187] V. Mateu and P. G. Ortega, *JHEP* **01**, 122 (2018), 1711.05755.
- [188] F. Herren and M. Steinhauser, *Comput. Phys. Commun.* **224**, 333 (2018), 1703.03751.
- [189] Flavour Lattice Averaging Group, S. Aoki *et al.*, *Eur. Phys. J. C* **80**, 113 (2020), 1902.08191.
- [190] M. Beneke and V. M. Braun, *Phys. Lett. B* **348**, 513 (1995), hep-ph/9411229.
- [191] D. J. Broadhurst, *Z. Phys. C* **58**, 339 (1993).
- [192] H. Takaura, *JHEP* **10**, 039 (2020), 2002.00428.
- [193] R. Tarrach, *Nucl. Phys.* **B183**, 384 (1981).
- [194] K. G. Chetyrkin and M. Steinhauser, *Phys. Rev. Lett.* **83**, 4001 (1999), hep-ph/9907509.
- [195] K. G. Chetyrkin and M. Steinhauser, *Nucl. Phys.* **B573**, 617 (2000), hep-ph/9911434.
- [196] K. Melnikov and T. v. Ritbergen, *Phys. Lett.* **B482**, 99 (2000), hep-ph/9912391.
- [197] P. Marquard, L. Mihaila, J. H. Piclum, and M. Steinhauser, *Nucl. Phys.* **B773**, 1 (2007), hep-ph/0702185.
- [198] P. Marquard, A. V. Smirnov, V. A. Smirnov, M. Steinhauser, and D. Wellmann, *Phys. Rev.* **D94**, 074025 (2016), 1606.06754.
- [199] N. Brambilla, A. Pineda, J. Soto, and A. Vairo, *Rev. Mod. Phys.* **77**, 1423 (2005), hep-ph/0410047.
- [200] A. Pineda, *Prog. Part. Nucl. Phys.* **67**, 735 (2012), 1111.0165.
- [201] W. E. Caswell and G. P. Lepage, *Phys. Lett. B* **167**, 437 (1986).

Acknowledgements

First and foremost, I want to express my deepest gratitude to Antonio Pineda for everything he has done for me during these years. He gave me an incredible opportunity, and has been absolutely instrumental in making this project flourish. Working under his guidance has been a very enriching experience, and I owe him a lot.

I also want to thank César Ayala for all these years of close collaboration, and all the time we have spent together which has always been great.

IFAE has changed a lot since I first arrived. People have come and gone, and working here has allowed me to meet very interesting people. I have very good memories of the many lunches with almost daily discussions about physics with the old guard of the theory division Ph.D. students: Clara, Marc, Marc, Mateo, Matteo, Sergi and Thibaud, and with those that started more or less with me: Bernat, Dani, Dirk, Lindber, Ramon, Rudin and Victor. A special mention goes to Dani and Rudin for collaborating with me in that first paper that we published. I also want to thank the students of the experimental group, whom I had the chance to (finally) get to know at the end of my time here, as well as the newer faces around: Alex, César, Clara, Daniele, Giulia, Jan, Judit, Laura, Manuel, Marcel and Marco.

To those outside IFAE that have made my life so much better: Anna, Cora, Fidel, Iñigo, Jordi, Kai, Mel, Mischa, Raul, Sandra, Silvia and Silvia. You guys made Barcelona a great place to live in.

I also want to thank Rafel Escribano for the great experience of being teaching assistant with him, and for all the thrashings he gave me at squash. I am very grateful too to Gunnar Bali for his warm hospitality during my stay in Regensburg.

Nire senitartekoei, zuen laguntza gabe ez nintzelako honaino iritsiko. Eskerrik asko.

And finally, thank you Elia for being the most amazing person I have ever met.